

LIBRARY SCREENING AND FOCUSED MULTIOMICS OF ANTIBACTERIAL ACTION
ON VAMCOMYCIN-RESISTANT *ENTEROCOCCUS FAECIUM*

A DISSERTATION IN
Pharmaceutical Sciences
and
Chemistry

Presented to the Faculty of the University of
Missouri-Kansas City in partial fulfillment of
the requirements for the degree

DOCTOR OF PHILOSOPHY

by

SHIVANI GARGVANSHI

M.Sc., Banasthali University, 2013
B.Sc, Banasthali University, 2011

Kansas City, Missouri
2023

© 2023

SHIVANI GARGVANSHI

ALL RIGHTS RESERVED

LIBRARY SCREENING AND FOCUSED MULTIOMICS OF ANTIBACTERIAL ACTION
ON VAMCOMYCIN-RESISTANT *ENTEROCOCCUS FAECIUM*

Shivani Gargvanshi, Candidate for the Doctor of Philosophy Degree

University of Missouri-Kansas City, 2023

ABSTRACT

Antimicrobial resistance is a major public health threat, and there is an urgent need for new strategies to address this issue. In a gram-positive bacteria, the peptidoglycan layer is thick as compared to gram negatives and is made up of peptide like polysaccharide chains. This peptidoglycan layer is a target for many antibiotics to inhibit bacteria. *Enterococcus* species are gram-positive bacteria of the intestine in humans and animals that can lead to problematic infections of the gastrointestinal tract and the soft tissues. Vancomycin has been one of most important agents for the treatment of gram-positive bacterial infections. The emergence and spread of vancomycin resistance has become a serious public health issue and vancomycin resistant bacteria are world's highest priority pathogen according to WHO. Resistance in VanA-type vancomycin-resistant *Enterococcus faecium* (VREfm) is due to an inducible gene cassette encoding seven proteins (*vanRSHAXYZ*). This provides for an alternative peptidoglycan (PG) biosynthesis pathway whereby D-Alanine-D-Alanine is replaced by D-Alanine-D-Lactate (Lac), to which vancomycin cannot bind effectively. While the general features of this resistance mechanism are well known, the details of the choreography between vancomycin exposure, *vanA* gene induction, and changes in the normal and alternative pathway intermediate levels have not been described previously.

Part I of my dissertation describes quantifying the cytoplasmic levels of normal and alternative pathway PG intermediates in VanA-type VRE *faecium* (VREfm) by liquid chromatography-tandem mass spectrometry before and after vancomycin exposure and to correlate these changes with changes in *vanA* operon mRNA levels measured by real-time quantitative PCR (RT-qPCR). Normal pathway intermediates in VREfm predominate in the absence of vancomycin, with low basal levels of alternative pathway intermediates. RT-qPCR demonstrated that *vanA* operon mRNA transcript levels increase rapidly after exposure, reaching maximal levels in 15 minutes. To resolve the effect of increased *van* operon protein expression on PG metabolite levels, linezolid was used to block protein biosynthesis. Surprisingly, linezolid dramatically reduced PG intermediate levels when used alone. When used in combination with vancomycin, linezolid only modestly reduced alternative UDP-linked PG intermediate levels, indicating substantial alternative pathway presence before vancomycin exposure. Comparison of PG intermediate levels between VRE *faecium*, vancomycin-sensitive *Enterococcus faecium*, and methicillin-resistant *Staphylococcus aureus* after vancomycin exposure demonstrated substantial differences between *S. aureus* and *E. faecium*.

Part II of my thesis describes developing a two-dimensional chemical compound library screening strategy. The first screening was done using an FDA approved drug library that was screened against vancomycin-resistant *Enterococcus faecium* (VREfm) in both its original (unmetabolized; UM) and its microsome metabolized (pre-metabolized; PM) forms, and in the absence and presence of vancomycin. This allows the identification of agents with active metabolites and agents that can act synergistically with the resistant-to-antibiotic. 2 x 2 experimental design library screening was also done using NCI diversity set V against both methicillin-resistant *Staphylococcus aureus* (MRSA) in absence and presence of cefoxitin and

against VRE *faecium* in absence and presence of vancomycin. The synergistic combinations of all the actives obtained after the screen can be used for in-vitro studies in future as it helps in the reduction the dose when combined. This can help in minimizing the side effects of high concentrations of drugs.

Part III of my dissertation describes experiments like active versus active where the active hits obtained after screening results were further combined to look for synergistic and antagonistic combinations. The other experiment was to look at the mechanism of action of various drugs against VRE faecium. As previously described, many resistant genes are involved in the resistance pathway of VREfm. When VREfm was treated with these antibiotics, the resistance genes were induced which showed the presence of resistance in VRE *faecium*. Therefore, gene induction was observed using both low ($1/4^{\text{th}}$ x MIC) and high (4x MIC) of an antibiotic. Furthermore, mutagenesis study was also done using MRSA. In this study, mutants of MRSA were generated on resistant antibiotic plates. It was followed by the extraction of genomic DNA which was later used to study whole genome sequence of MRSA. This study helped us to identify the mutation causing genes. This experiment can further be used for VRE *faecium* and gram-negatives.

APPROVAL PAGE

The faculty listed below, appointed by the Dean of School of Graduate Studies have examined a thesis titled “Library Screening and Focused Multiomics of Antibacterial Action on Vancomycin-Resistant *Enterococci faecium*,” presented by Shivani Gargvanshi, candidate for the Doctor of Philosophy degree, and certify that in their opinion it is worth of acceptance.

Supervisory Committee

Dr. William Gutheil, Ph.D., Committee Chair

Division of Pharmacology and Pharmaceutical Sciences

Dr. Gerald Wyckoff, Ph.D.

Division of Pharmacology and Pharmaceutical Sciences

Dr. Simon Friedman, Ph.D.

Division of Pharmacology and Pharmaceutical Sciences

Dr. Mridul Mukherji, Ph.D.

Division of Pharmacology and Pharmaceutical Sciences

Dr. Keith Buszek, Ph.D.

Department of Chemistry

TABLE OF CONTENTS

ABSTRACT.....	iii
TABLE OF CONTENTS.....	vii
LIST OF ILLUSTRATIONS	xvii
LIST OF TABLES	xxv
ACKNOWLEDGEMENTS	xxvii
PART I: FOCUSED METABOLOMICS, PROTEOMICS AND TRANSCRIPTOMICS OF VANA-TYPE VAMCOMYCIN RESISTANT <i>ENTEROCOCCUS FAECIUM</i>	
1. INTRODUCTION AND LITERATURE REVIEW	
1.1 Bacteria	1
1.2 Bacterial classification	2
1.3 Vancomycin-resistant <i>Enterococci</i> (VRE)	3
1.4 VanA and VanB type vancomycin-resistant <i>Enterococci</i>	4
1.5 Other types of Van resistance in vancomycin-resistant <i>Enterococci</i>	5
1.6 Antibiotics for treatment of vancomycin-resistant <i>Enterococci</i>	6
1.7 Bacterial peptidoglycan layer	6
1.8 Cell wall biosynthesis in bacteria	7
1.9 Resistance pathway in vancomycin-resistant <i>Enterococci</i>	13
1.10 Nucleosides in bacteria	16
1.11 Bacterial proteomics	17
1.12 Bacterial metabolomics.....	17

2. EFFECT OF VANCOMYCIN ON CYTOPLASMIC PEPTIDOGLYCAN INTERMEDIATES AND VAN OPERON mRNA LEVELS IN VANA-TYPE VANCOMYCIN RESISTANT *ENTEROCOCCUS FAECIUM*

2.1 Introduction and Rationale.....	19
2.2 Material and Methods	22
2.2.1 General	22
2.2.2 UDP-linked intermediates standard preparation from methicillin-resistant <i>Staphylococcus Aureus</i> (MRSA)	24
2.2.3 Purification of novel UDP-linked intermediates from vancomycin-resistant <i>Enterococcus faecium</i> for use as standards.....	25
2.2.4 Ion-pairing (IP) LC-MS/MS based quantification of UDP-lined intermediates.....	26
2.2.5 Amine and amino acid quantification	26
2.2.6 LC-MS/MS method development for nucleotides.....	27
2.2.7 Comparison of centrifugation vs filtration for metabolite extraction	27
2.2.8 Comparison of metabolite extraction and amino acid derivatization at 15 and 90 min	29
2.2.9 Standard growth and metabolite extraction procedure for VRE <i>faecium</i> vancomycin exposure experiment	30
2.2.10 Experimental procedure for long-term vancomycin exposure.....	30
2.2.11 Time dependence of cytoplasmic cell wall biosynthesis intermediate levels in VRE <i>faecium</i> after vancomycin exposure	31
2.2.12 Time dependence of VanA mRNA levels in VREfm after vancomycin exposure.....	31
2.2.13 Vancomycin concentration dependence of VRE <i>faecium</i> mRNA levels.....	32
2.2.14 Minimal inhibitory concentration (MIC) determination of linezolid, rifaximin and	

oritavancin	33
2.2.15 Effect of linezolid on vancomycin associated metabolite pool level changes	33
2.2.16 Effect of linezolid and rifaximin on vancomycin associated mRNA level changes..	34
2.2.17 Whole cell protein isolation from VRE <i>faecium</i>	34
2.3 Results and discussion	35
2.3.1 LC-MS/MS method development.....	35
2.3.2 LC-MS/MS method development for nucleotides.....	38
2.3.3 Comparison of sample preparation by centrifugation vs filtration for metabolite analysis	39
2.3.4 Survey of vancomycin effects on cell wall biosynthesis intermediates in VREfm	39
2.3.5 Detailed summary of survey of vancomycin effects on cell wall intermediates in VRE <i>faecium</i> results	39
2.3.6 Time course results from both VRE <i>faecium</i> and VSE <i>faecium</i>	43
2.3.7 Time dependence of vancomycin effect on metabolite pools in VRE <i>faecium</i>	44
2.3.8 Growth curve of VRE <i>faecium</i>	46
2.3.9 Time dependence of VanA gene induction.....	47
2.3.10 Vancomycin concentration dependence on VRE <i>faecium</i> metabolite and mRNA response	47
2.3.11 Effect of protein biosynthesis inhibition (linezolid) on metabolite levels after vancomycin exposure	49
2.3.12 Effect of linezolid, vancomycin and rifaximin on mRNA gene pool levels.....	50
2.3.13 Comparison of metabolite extraction and amino acid derivatization after 15 and 90 minutes	51

2.3.14 Proteomics on vancomycin-resistant <i>Enterococcus faecium</i>	54
2.4 Conclusion	55
Part II: CHEMICAL LIBRARY SCREENING FOR NEW ANTIBACTERIAL DRUG DISCOVERY	
3. INTRODUCTION AND LITERATURE REVIEW	
3.1 Methicillin-resistant <i>Staphylococcus aureus</i>	60
3.2 Pathophysiology of methicillin-resistant <i>Staphylococcus aureus</i>	61
3.3 Antibiotic resistance in methicillin-resistant <i>Staphylococcus aureus</i>	62
3.4 Challenges in antibacterial discovery	63
3.5 Drug discovery	65
3.6 Chemical library screening	69
3.7 Drug metabolism	71
3.8 Drug metabolite identification	72
3.9 Minimal inhibitory concentrations	74
3.10 Synergy and antagonism	75
3.11 Spectrum of activity	78
3.12 Thymidine folate biosynthesis inhibitors	80
4. LIBRARY SCREENING FOR SYNERGISTIC COMBINATIONS OF FDA-APPROVED DRUGS AND METABOLITES WITH VANCOMYCIN AGAINST VANA-TYPE VANCOMYCIN-RESISTANT <i>ENTEROCOCCUS FAECIUM</i>	
4.1 Introduction and Rationale	82
4.2 Materials and Methods	83
4.2.1 General	83

4.2.2 UM/PM vs +/- vancomycin library screen against VRE <i>faecium</i>	84
4.2.3 Hit picking and minimum inhibitory concentration determination	84
4.2.4 Different VRE strains stock preparation and CFU/mL determination	85
4.2.5 Spectrum of activity of VRE hits.....	86
4.2.6 Checkerboard assay to confirm synergy	87
4.2.7 Large scale metabolism of mupirocin.....	87
4.3 Results and Discussion	88
4.3.1 Library screening preparation and workflow.....	89
4.3.2 Library screening results.....	92
4.3.3 Optimization of VRE <i>faecium</i> fluorescence/absorbance	96
4.3.4 Spectrum of activity.....	124
4.3.5 Mupirocin activity after metabolism.....	125
4.3.6 Synergistic combination between vancomycin and FDA VRE <i>faecium</i> hits	127
4.3.7 Optimization of checkerboard experiment.....	129
4.4 Conclusion	131
5. SCREENING THE NCI DIVERSITY SET V FOR ANTI-MRSA ACTIVITY:	
CEFOXITIN SYNERGY AND LC-MS/MS CONFIRMATION OF FOLATE/THYMIDINE	
BIOSYNTHESIS INHIBITION	
5.1 Introduction and Rationale.....	132
5.2 Materials and Methods.....	133
5.2.1 General	133
5.2.2 In vitro microsomal metabolism to provide pre-metabolized library	134
5.2.3 UM/PM vs +/- cefoxitin library screen against MRSA	135

5.2.4 Hit picking and minimum inhibitory concentration determination	136
5.2.5 Checkerboard assay to confirm synergy with cefoxitin	136
5.2.6 +/- Thymidine counter screen and LC-MS/MS confirmation for folate biosynthesis inhibitors	137
5.2.7 Spectrum of activity	138
5.3 Results and Discussions	138
5.3.1 Library screening and hit minimal inhibitory concentration determination	138
5.3.2 Comparative minimal inhibitory concentration analysis to identify agents synergistic with cefoxitin.....	151
5.3.3 Checkerboard analysis	152
5.3.4 Identification and confirmation of folate/thymidine biosynthesis inhibitors.....	153
5.3.5 Spectrum of activity	157
5.4 Conclusion	158
6. SCREENING THE NCI DIVERSITY SET V APPROVED DRUGS AND METABOLITES WITH VANCOMYCIN AGAINST VANA-TYPE VANCOMYCIN- RESISTANT <i>ENTEROCOCCUS FAECIUM</i>	
6.1 Introduction and Rationale.....	159
6.2 Materials and Methods.....	161
6.2.1 General.....	161
6.2.2 In vitro microsomal metabolism to provide pre-metabolized library	161
6.2.3 UM/PM vs +/- vancomycin library screen against VRE <i>faecium</i>	162
6.2.4 Hit picking and minimum inhibitory concentration determination	163
6.2.5 Checkerboard assay to confirm synergy with vancomycin	164

6.2.6 Spectrum of activity against MRSA strains and <i>E. coli</i>	164
6.2.7 Spectrum of activity against VRE strains	164
6.2.8 -/+ Thymidine counter screen for folate biosynthesis inhibitors	165
6.3 Results and Discussion	165
6.3.1 Library screening and hit minimal inhibitory concentration determination	165
6.3.2 Comparative minimal inhibitory concentration analysis to identify agents synergistic with vancomycin.....	166
6.3.3 Checkerboard analysis	167
6.3.4 Identification of folate/thymidine biosynthesis inhibitors	168
6.3.5 Spectrum of activity	168
6.4 Conclusion	169
Part III: DRUG INTERACTIONS AND WHOLE GENOME SEQUENCING OF RESISTANT BACTERIA	
7. INTRODUCTION AND LITERATURE REVIEW	
7.1 Mechanism of action of antibiotics.....	171
7.2 Antibiotics targeting bacterial cell wall	172
7.2.1 Protein biosynthesis inhibitors.....	173
7.2.2 DNA replication inhibitors	175
7.2.3 Inhibitors for folic acid metabolism.....	175
7.3 Mutation in bacteria	176
7.4 Frequency of resistance in bacteria.....	177
7.5 Role of DNA in bacteria	178
7.6 Whole genome sequencing in bacteria	179

7.7 RNA induction in bacteria	181
8. TWO-DIMENSIONAL SCREEN OF ACTIVE VERSUS ACTIVE	
8.1 Introduction and Rationale.....	183
8.2 Materials and Methods.....	184
8.2.1 General	184
8.2.2 Determination of minimum inhibitory concentration of all actives from FDA and NCI screen against VRE <i>faecium</i> in 384 well plate	184
8.2.3 Determination of MICS of all actives from FDA and NCI screen against VRE <i>faecium</i> in 96 well plates	185
8.2.4 Active vs Active experiment in a 384 well plate	186
8.3 Results and Discussion	187
8.3.1 2-dimensional approach of active vs actives for synergy	187
8.3.2 MICs of actives in 384 well plate for FDA compounds	188
8.3.3 MICs of actives in 384 well plate for NCI compounds	189
8.3.4 MICs of actives from FDA and NCI screen in 96 well plate.....	190
8.3.5 FDA active vs FDA active synergistic combinations.....	191
8.3.6 NCI active vs NCI active synergistic combinations	192
8.3.7 FDA active vs NCI active synergistic combinations	193
8.4 Conclusion	194
9. MECHANISM OF ACTION OF DIFFERENT ANTIBIOTICS AGAINST VANA-TYPE VANCOMYCIN-RESISTANT <i>ENTEROCOCCI FAECIUM</i>	
9.1 Introduction and Rationale.....	196
9.2 Material and Methods	197

9.2.1 General	197
9.2.2 Minimal inhibitory concentrations of various drugs against VanA-type clinical <i>faecium</i> strain and ATCC 0787	198
9.2.3 Effect of different antibiotics on VRE <i>faecium</i> mRNA level changes at 1/4th x Minimum inhibitory concentration	199
9.2.4 Effect of different antibiotics on VRE <i>faecium</i> mRNA level changes at 4 x MIC....	200
9.3 Results and Discussion	200
9.3.1 Determination of minimum inhibitory concentration using two different VanA-type strains of VRE i.e., VRE clinical <i>faecium</i> strain and ATCC 0787	200
9.3.2 Effect of antibiotics on mRNA level at 1/4th x MIC.....	202
9.3.3 Effect of antibiotics on mRNA level at 4 x MIC	202
9.4 Conclusion	204
10. FREQUENCY OF RESISTANCE DETERMINATION AND WHOLE GENOME SEQUENCING OF METHICILLIN-RESISTANT <i>STAPHYLOCOCCUS AUREUS</i>	
10.1 Introduction and Rationale.....	205
10.2 Material and Methods	207
10.2.1 General	207
10.2.2 MIC determination of antibiotics to make mutant MRSA	207
10.2.3 -/+ Thymidine counter screen for folate/thymidine biosynthesis inhibitors	207
10.2.4 Preparation of resistant antibiotic agar plates at 4x MIC of antibiotic	208
10.2.5 Preparation of different concentrations of resistant antibiotic MH agar plates	208
10.2.6 Serial dilution and plating at 4x MIC	209
10.2.7 Serial dilution and plating at various MICs	209

10.2.8 Genomic DNA isolation from mutant colonies	210
10.3 Results and Discussion	211
10.3.1 +/- Thymidine MICs	211
10.3.2 Preparation of different MICs of antibiotic agar plate and mutation results	212
10.3.3 Genomic DNA isolation optimization	216
10.4 Conclusion	216
GENERAL CONCLUSION	218
APPENDIX.....	226
REFERENCES	228
VITA.....	258

LIST OF ILLUSTRATIONS

Figure	Page
Figure 1- Bacteria and bacterial morphology ²⁶¹	1
Figure 2 - Classification of bacteria by their shapes ²⁶²	2
Figure 3 - Structural difference between gram-positive and gram-negative bacteria ³	3
Figure 4 - Vancomycin-resistant <i>Enterococci</i> ⁷	4
Figure 5 - Peptidoglycan layer composed of cross-linked chains of peptidoglycan monomers ¹⁷	7
Figure 6 - First stage of bacterial cell wall biosynthesis ¹⁹	9
Figure 7 - Second stage of bacterial cell wall biosynthesis ¹⁹	10
Figure 8 - Third stage of bacterial cell wall biosynthesis ¹⁹	11
Figure 9 - Bacterial cell wall biosynthesis of a gram-positive bacteria ²⁶³	13
Figure 10 - Mechanism of resistance in vancomycin-resistant <i>Enterococci</i> ⁶	14
Figure 11 - Signal transduction mechanism of VanRS ²⁵	15
Figure 12 - Genes involved in VRE resistance pathway ²⁷	16
Figure 13 - Various steps involved in bacterial study ³¹	18
Figure 14 - Generic PG biosynthesis process in gram-positive bacteria. In <i>E. faecium</i> a D-iAsp “bridging” residue is added to the amino group of L-Lys ⁵⁶ GlcN, glucosamine; GlcNAc, N-acetylglucosamine (NAG); GlcNAc-1P, N-acetylglucosamine-1-phosphate; PEP, phosphoenolpyruvate; AEK, L-Ala-γ-D-Glu-L-Lys	20
Figure 15 - VanA-type resistance gene cluster ⁴⁶	20
Figure 16 - Alternative cell wall biosynthesis pathway in VanA-type resistance	21

Figure 17- LC-MS/MS chromatograms of VanA-type VRE specific cytoplasmic UDP cell wall intermediates. UDP-Penta included for reference.....	37
Figure 18 - LC-MS/MS representation of AXP and UXP peaks.....	38
Figure 19 - Time courses of VREfm PG intermediates (same data as Figure 20) and VSEfm PG intermediates plotted as fold changes vs their t_0 values (t_0 values in Table 5). The x-axis is plotted in a semi-square root form to expand early time points for easier visualization.	43
Figure 20 - Time course of VREfm PG intermediates in response to added vancomycin plotted as fold changes versus time zero values (shown in Table 5). UDP sum is the sum of all UDP-linked intermediates DADA, D-Alanine-D-Alanine; DADL, D-Alanine-D-Lactate.	45
Figure 21 - Growth curves of VREfm with and without vancomycin. The blue curve represents the control VREfm with no vancomycin and the orange curve represents VREfm with added vancomycin	46
Figure 22 - Time course of the effect of vancomycin (16 $\mu\text{g/mL}$) on RT-qPCR determined mRNA levels in VREfm. Data is presented as mean \pm SE (n = 3)	47
Figure 23 - Fold changes (relative to no-vancomycin control) in key VREfm PG intermediate levels after 15-min exposure to different vancomycin concentration (n = 4), shown with a semilogarithmic y axis.	48
Figure 24 - Corresponding fold changes in mRNA levels (n = 4).....	49
Figure 25 - Fold changes (relative to no vancomycin control) in key VREfm PG intermediate levels after 15-min exposure to vancomycin (Vm) and/or linezolid (n = 3), shown with a semilogarithmic y axis.....	50
Figure 26 - Corresponding fold changes in mRNA levels (n = 4).....	51

Figure 27 - Comparison of metabolite extraction at 90 mins and at 15 mins incubation time. The figure above shows metabolites extracted at 90 mins and the figure below shows metabolites extracted at 15 mins. Y axis represents the fold change.....	52
Figure 28 - Comparison between amino acid derivatized samples after 90 and 15 mins. The figure above shows amino acid derivatization after 90 mins of incubation and the figure below shows amino acid derivatization after 15 mins of incubation	53
Figure 29 - Volcano plots showing the resistant genes (in red) upregulated 16-fold	54
Figure 30 - Methicillin-resistant <i>Staphylococcus aureus</i> ⁷⁶	60
Figure 31 - Stages of <i>Staphylococcus aureus</i> infection ⁷²	61
Figure 32 - Bacterial targets of antibiotics active against MRSA ⁸⁵	63
Figure 33 - Drug discovery challenges ⁹²	65
Figure 34 - Eras in drug discovery ⁹⁷	66
Figure 35 - Workflow of high-throughput screening ¹⁰²	70
Figure 36 - Top-down approach	70
Figure 37 - Pathways for drug metabolism ¹⁰⁶	72
Figure 38 - Various techniques for drug metabolite identification ¹¹²	74
Figure 39 - Interpretation of MIC results ¹¹⁴	75
Figure 40 - Synergy checkerboard assay ¹²⁰	76
Figure 41 - Representation of synergy, additive and antagonistic effect ¹²¹	77
Figure 42 - Shows the isobolograms for checkerboard ¹¹⁹	78
Figure 43 - Spectrum of activity of various drugs against different pathogens ¹²⁴	79
Figure 44 - Outline of folate metabolism ¹²⁴	81

Figure 45 - THF is directly involved in the synthesis of dTMP through the regulation of pabA gene ¹²⁴	81
Figure 46 - Replication and metabolism of un-metabolized and pre-metabolized library in presence of human liver microsomes.....	90
Figure 47 - Describes how each 96 well plate is replicated in a 384 well plate. The figure above represents 4 different 96 well plates and the figure below represent a 384 well plate.	91
Figure 48 - Represents library screen and the blue dot represents hits. These hits were used to make a merged hit list.....	92
Figure 49 - MICs were determined twice for all the hits that gave MIC below 100 μ M. The blue dot represents hits. The yellow dots represent UM drugs and grey dot represents PM drugs	93
Figure 50 - MICs were determined in triplicate for all the hits that gave MIC ≤ 25 μ M. The blue dots represent MICs of hits. The yellow dots represent UM library drugs and the grey dot represents PM drugs.....	94
Figure 51 - Shows MICs for the hits in Matlab. MICs represented in blue.....	95
Figure 52 - This image represents a cutoff between growth and no growth after screening the library with VRE <i>faecium</i> . Orange represents no growth of bacteria (actives) and the yellow represents growth of bacteria (inactives) with a cutoff at -0.1	95
Figure 53 - Figure above represents resazurin salt that is a blue dye which when added to the bacteria undergoes reduction process and is used to distinguish between growth (pink color) and no growth (blue color) in bacteria. The figure below represents how resazurin salt helps in predicting a cut off between active and inactives.	96
Figure 54 - Pattern of 384 well plate after 2 hours of incubation at fluorescence 530/600....	97

Figure 55 - Pattern of 384 well plate after 4 hours of incubation at fluorescence 530/600....	97
Figure 56 - Plates read at absorption value 590 nm.....	98
Figure 57 - Plates read at absorption ration 460/610 after 2 hours of incubation at 35 °C	98
Figure 58 - Plates read at absorption ration 460/610 after 4 hours of incubation at 35 °C. ...	98
Figure 59 - Plate read using absorbance values at 570 nm - 460 nm.....	99
Figure 60 - Shows A) 96 well plate after addition of VREfm. B) 96 well plate after immediate addition of resazurin dye. C) 96 well plate after 2 hours of incubation at 35 °C	99
Figure 61 - Chemical structure of mupirocin.....	126
Figure 62 - Fractions of metabolized mupirocin were collected after preparative HPLC and screened against VRE <i>faecium</i> . Wells D1, D2 and D3 shows activity and these three fractions were injected into LC-MS/MS to check the metabolite activity.	126
Figure 63 - Checkerboard experiment in 96 well plate.....	128
Figure 64 - Checkerboard assay results (isobolograms) for combinations of vancomycin with potentially synergistic agents. Isobolograms for combinations of vancomycin (y-axes) with other agents (x-axes). The dashed line in the isobolograms is for the no interaction (additive MICs) curve	128
Figure 65 - Checkerboard experiment with a diagonal pattern ²⁶⁷	129
Figure 66 - Checkerboard experiment with 8x MIC of vancomycin (Vm)	129
Figure 67 - Checkerboard experiment with 4x MIC of vancomycin (Vm)	130
Figure 68 - No difference was observed when water or DMSO were used as a solvent.....	131
Figure 69 - Checkerboard assay results as isobolograms for combinations of cefoxitin with celastrol, porfiromycine, 4-quinazolinediamine (4-QDA), and teniposide against MRSA (ATCC 43300). The dashed line in the isobolograms is for the no interaction	

(additive MICs) curve. MICs for other agents alone as given in Table 14.	152
Figure 70 - Structure of active compounds from Table 14.	154
Figure 71 - Fold-changes in the levels of ATP and dTTP upon exposure to 4x MIC of different agents for 15 min relative to an untreated control	156
Figure 72 - Checkerboard assay results as isobolograms for combinations of vancomycin with celastrol, 4-quinazolinediamine (4-QDA), and Streptovaricin against VREfm. The dashed line in the isobolograms is for the no interaction (additive MICs) curve. MICs for other agents alone as given in Table 20.	168
Figure 73 - Mechanism of action of antibiotics ²⁰⁰	172
Figure 74 - Mechanism of action of beta-lactams antibiotics ²⁰²	173
Figure 75 - Protein biosynthesis inhibition with different antibiotics ²⁰²	174
Figure 76 - Resistance in bacteria using antibiotics ²¹²	177
Figure 77 - Frequency of resistance experimental protocol ¹¹⁴	178
Figure 78 - Workflow for bacterial whole genome sequencing ²¹⁷	181
Figure 79 - Workflow for active vs active 2D screen. The diagonal line gives 1/2x MICs of drugs The blue wells represent no bacterial growth wells, and the pink well represents growth.	187
Figure 80 - 384 well plate with FDA active MICs.	188
Figure 81 - 384 well plate with NCI active MICs	189
Figure 82 - MICs of FDA actives in duplicates.....	190
Figure 83 - MICs of NCI actives in duplicates.	190
Figure 84 - FDA active vs FDA actives in a 384 well plate.	191
Figure 85 - NCI active vs NCI active in a 384 well plate.....	193

Figure 86 - FDA (column) active vs NCI (row) actives in a 384 well plate.....	194
Figure 87 - Resistant genes involved in the resistance pathway of VRE <i>faecium</i>	197
Figure 88 - Fold changes in gene levels showing teicoplanin and vancomycin resistance at 1/4 th x MIC.....	202
Figure 89 - Action of bacitracin on bacterial peptidoglycan layer ²⁵¹	203
Figure 90 - Fold changes in gene levels showing teicoplanin, vancomycin, doxycycline and oritavancin induces resistance genes at 4x MIC.	204
Figure 91 - Workflow for bacterial whole-genome sequencing ²⁶⁰	206
Figure 92 - MH plates with different MIC of Trimethoprim, Floxuridine and Gemcitabine	208
Figure 93 - Serial dilution in steps of 20 from 2 ml of high MRSA cell density.	209
Figure 94 - Various dilutions of MRSA plated on different MIC MH agar plates.....	210
Figure 95 - Workflow of bacterial whole genome sequencing ²⁶¹	211
Figure 96 - Various dilutions of MRSA plated on different Floxuridine MIC MH agar plates. Each MIC plate made in quadruplicates and plated with dilution starting at 20 ¹ ,20 ² , 20 ³ , 20 ⁴ in a clockwise direction (Starting from the highest to the lowest concentration of dilution).....	213
Figure 96 - Various dilutions of MRSA plated on different Gemcitabine MIC MH agar plates. Each MIC plate made in quadruplicates and plated with dilution starting at 20 ¹ ,20 ² , 20 ³ , 20 ⁴ in a clockwise direction (Starting from the highest to the lowest concentration of dilution).....	214
Figure 96 - Various dilutions of MRSA plated on different Trimethoprim MIC MH agar plates. Each MIC plate made in quadruplicates and plated with dilution starting at 20 ¹ ,20 ² , 20 ³ ,	

20⁴ in a clockwise direction (Starting from the highest to the lowest concentration of dilution).....215

Figure 99 - 7 different control plates were made and plated with 7 dilutions of MRSA.

Only of the control plates with colonies is shown.....216

LIST OF TABLES

Table	Page
Table 1 - Vancomycin-resistant <i>Enterococci</i> resistance types and minimal inhibitory concentrations ⁴	5
Table 2 - Primers used for RT-qPCR of VanA mRNA transcripts.....	23
Table 3 - Parameters for AXP and UXP	27
Table 4 - Summary of optimized parameters and sensitivities for negative mode IP-LC-MS/MS detection of UDP-linked intermediates in VRE.....	36
Table 5 - Effect of vancomycin (Vm) exposure on cytoplasmic PG intermediates in VSE and VRE and comparison with MRSA	42
Table 6 - Drugs and their targets, with their mode of actions ⁹⁷	67
Table 7 - FICI and interpretation ¹¹⁹	78
Table 8 - ATCC VRE strains and cfu/mL	86
Table 9 - FDA library anti-VRE <i>faecium</i> hit MICs (Min_MIC ≤ 12.5 μM)	100
Table 10 - List of actives (validated min_MIC < 100 μM) from library screening against VRE (clinical) (UM/PM vs +/- 16 μg/mL vancomycin) ranked by lowest minimum MIC. NA = no activity.....	101
Table 11 - All the inactive drugs screened against VRE <i>faecium</i>	102
Table 12 - Spectra of activity (UM-Vm) against VRE (MICs in μM).	125
Table 13 - Spectra of activity of (doxifluridine (DFUR), floxuridine, 5'-fluorouracil) against VRE (MIC in μM)	125
Table 14 - MICs (μM) for top 14 NCI Diversity Set V compounds against MRSA (ATCC #43300). UM = original unmetabolized library compounds, PM = human liver microsome	

metabolized compounds (nominal MICs). -Cef = in the absence of cefoxitin, +Cef = in the presence of 8 mg/L cefoxitin	139
Table 15 - List of active compounds (validated MIC \leq 100 μ M) from NCI Diversity Set V library screening against MRSA (ATCC 43300) (UM/PM vs $-/+$ 8 μ g mL $^{-1}$ Cefoxitin) ranked by lowest minimum MIC	140
Table 16 - List of inactive compounds (MIC $>$ 100 μ M) from library screening against MRSA (ATCC 43300).	142
Table 17 - MICs (μ M) for the top NCI Diversity Set V compounds against MRSA (ATCC #43300) in the absence and presence of 4 μ M of thymidine.	155
Table 18 - Retention time (tR) and MS/MS parameters for ATP and dTTP quantification.	156
Table 19 - Spectrum of activity of NCI compounds (MIC in μ M).....	157
Table 20 - NCI library anti-VRE <i>faecium</i> hit MICs (Min_MIC \leq 25 μ M)	166
Table 21 - All FDA active hits with MICs in μ M.	188
Table 22 - All NCI hits with MICs in μ M	189
Table 23 - FDA active vs FDA active synergistic combinations	192
Table 24 - NCI active vs NCI active synergistic combinations	193
Table 25 - FDA active vs NCI active synergistic combinations.	194
Table 26 - Primers used for RT-qPCR of VanA mRNA transcripts	198
Table 27 - Antibiotics and MICs against different VRE strains.....	201
Table 28 - Shows MICs of FDA and NCI screened compounds against MRSA	212

ACKNOWLEDGEMENTS

Writing a thesis has been a long and arduous journey, and I would like to express my heartfelt gratitude to the many people who have supported me throughout my Ph.D. Your support, encouragement, and kindness have meant the world to me and helped me through the ups and downs of this process.

First and foremost, I would like to thank my thesis supervisor, Dr. William Gutheil, for his unwavering support, invaluable guidance, encouragement, and patience throughout my Ph.D. He has been my rock throughout this journey, providing me with the inspiration and motivation I needed to keep going, even when the going got tough. A biology student like me, who knew nothing about bioanalytical work, can now teach other students how to use bioanalytical instruments, all because of Dr. Gutheil. I am thankful to Dr. Gutheil for believing in me. I am thankful for his constructive feedback, insightful comments, and expertise in the field, which have been instrumental in shaping the direction of this thesis. I am genuinely grateful for his mentorship and inspiration. Without him, it would have not been possible for me to start and finish new and exciting projects.

I also want to express my gratitude to the members of my Ph.D. committee for their valuable feedback, suggestions, and guidance. Their expertise and insights have helped me refine my research questions and methodology and have contributed significantly to the quality of this thesis. I would like to thank Dr. Gerald Wyckoff, for being an amazing chair of the Pharmacy department, for being there with us and helping us in every way possible. His suggestions and quick responses helped the students, including me. Recently, I also got a chance to collaborate

with him on a project and I am grateful to him for helping and guiding me as an excellent mentor. I would like to thank Dr. Simon Friedman, whom I have known not only as a phenomenal medicinal chemistry professor but also as a kind and a humble person. Dr. Friedman taught me the value of discipline, respectfulness, and punctuality. I cannot thank him enough for making medicinal chemistry easy for me to understand and most importantly, helping me to become a better person. I also want to thank Dr. Mridul Mukherji, for helping and supporting me throughout my Ph.D. life. I remember an instance, where I was facing difficulty in extracting genomic DNA from a gram-positive bacteria. Dr. Mukherji stepped in and helped me until I got my desired experimental result. I am grateful to him for always being there to help, guide and motivate me. Lastly, I am grateful for having Dr. Keith Buszek on my Ph.D. supervisory committee and for being the friendliest professor at UMKC. Dr. Buszek's way of teaching is simple and easy to understand. Learning Chemistry from him was so much fun during his classes. I am always thankful for his motivation and encouragement.

I would also like to thank the Dean of the Pharmacy School, Dr. Russell Melchert for helping the students. I am deeply grateful to UMKC School of Pharmacy for providing me with the resources and facilities necessary for carrying out this research. I am also, thankful to the faculty and staff members of the school for always helping and supporting me. A big thank you to my senior lab members, Dr. Navid Ayon, Dr. Amar Deep Sharma for their constant support and my colleagues, Gioia and Niharika for being my friends and a source of motivation.

To the friends, both old and new, thank you for your understanding, support, and encouragement. Your kindness and support have helped me through the tough times and made the good times even better. I feel so lucky to have you all in my life. A special thank you to 'my

people' Prajakta, Sameer and Melody, who I know would support me in any step of life and pick me up every time I'll fall. I would also like to thank my close friends, Mayank, Aishwarya, Anupama, Aditya, Vaishali, Nitish, Rachna, Pratik, Raj, Akshay, Deya, Dan, Todd, Chloe, Nick, Lauren, and Jackie for their friendship. An extra special thanks to the very special people Drinnan, Vidit, Krishna, and Bhagyesh for their support and for all the fun times together. I would also like to thank Chayan, Aninda, Sharon Breashers, Sharon Self, Joyce, and Jeannie for their support.

Last, but not the least, to my parents, I want to thank you for being your daughter. I want to express my deepest gratitude for your love and unwavering support. Your sacrifices and encouragement have made this journey possible, and I could not have done it without you. Thank you for always believing in me and for being my biggest cheerleader.

In conclusion, I want to express my deepest gratitude to all those who have helped me along the way. Your support, encouragement, and kindness have meant the world to me, and I could not have done it without you. Thank you for being a part of my journey and for making it all worthwhile.

With gratitude,

Shivani

Dedicated To My Wonderful and Loving Parents

Mr. Ajay Singh and Dr. Kalpana Singh

PART I: FOCUSED METABOLOMICS, PROTEOMICS AND TRANSCRIPTOMICS OF
VANA-TYPE VANCOMYCIN-RESISTANT *ENTEROCOCCUS FAECIUM*

CHAPTER 1

1. INTRODUCTION AND LITERATURE REVIEW

1.1 Bacteria

Bacteria are the first form of life that existed on Earth. They are single-celled organisms and prokaryotes meaning they lack a nucleus and other membrane-bound organelles. Their genetic material is in the form of a single circular DNA and is found in the cytoplasm. Bacteria also contain small circular DNA molecules called plasmids, which can be exchanged between two bacterial cells. Bacterial species are metabolically active and reproduce by a process called binary fission. Some bacteria undergo horizontal gene transfer that leads to increased genetic diversity and antibiotic resistance. They are relatively simple organisms and are highly adaptable and sophisticated. However, in the medical world, they are a significant threat for various diseases. Bacteria are everywhere and have the flexibility to adapt to changing environments. They survive in free-living forms or live inside a host. Studying bacteria is crucial for understanding fundamental biological processes and human health.¹ Figure 1 shows bacterial morphology.

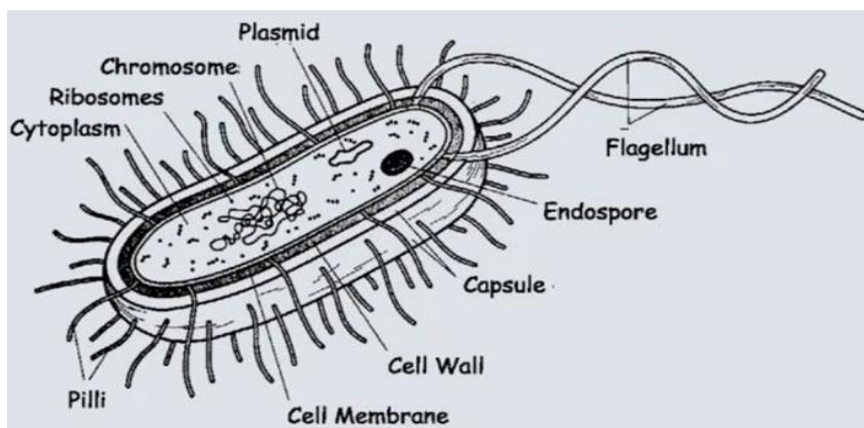


Figure 1 - Bacteria and bacterial morphology²⁶¹

1.2 Bacterial classification

Bacteria can be classified based on shape, growth conditions, cell wall structure, and aerobic and anaerobic growth preference. Some common shapes among bacteria include cocci (spherical), spirilla (spiral-shaped), and bacilli (rod-shaped). Figure 2 shows different shapes of bacteria. However, bacteria are mainly classified into two fundamental categories, gram-positive bacteria and gram-negative. This classification is based on the structure of the bacterial cell wall. Gram-positive bacteria are surrounded by a thick layer of cell wall which is known as a monoderm. Gram-negative bacteria are surrounded by a comparatively thinner cell wall with an outer membrane made up of lipopolysaccharides and are known as diderms. Gram-positive and gram-negative bacteria can be distinguished by gram staining which was developed in 1884 by the Danish bacteriologist Hans Christian Gram.² The difference between gram-positive and gram-negative bacteria is shown in Figure 3.

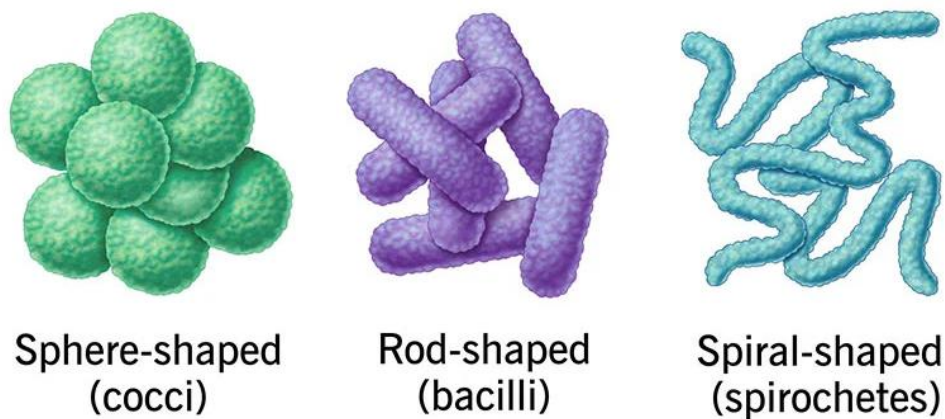


Figure 2 - Classification of bacteria by their shapes²⁶²

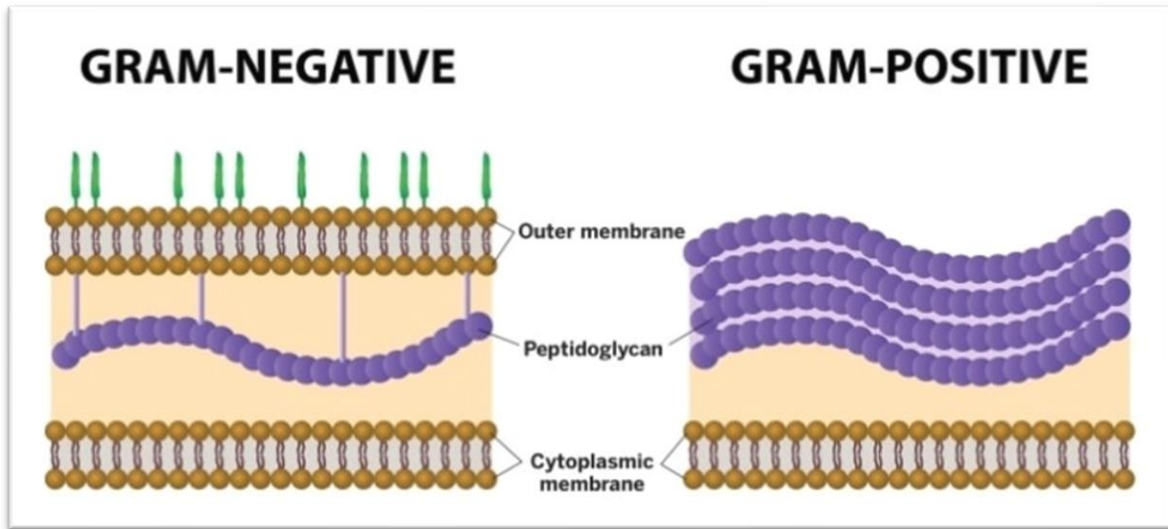


Figure 3 - Structural difference between gram-positive and gram-negative bacteria ³

1.3 Vancomycin-Resistant *Enterococci* (VRE)

Vancomycin-resistant *Enterococci* (VRE) were first identified in the mid-1980s. They are a group of antibiotic-resistant bacteria that belong to the genus *Enterococcus*. Due to their rapid spread, it became a significant concern in Europe and the United States ⁴ This bacteria is classified as a gram-positive bacteria. VRE is critical to medical and public health because it causes multidrug-resistant infections. These species constitute an essential part of intestinal microbiota in healthy humans and animals. VRE can survive at elevated temperatures and high salt concentrations and resist chemical stress. People primarily at risk of getting VRE infection have been previously treated with long duration of antibiotics. VRE targets people with compromised immune systems, especially patients in intensive care units or patients suffering from cancer ⁵ It also causes infections in people who have undergone surgery or have medical devices inserted into their bodies. The most common way VRE can spread is through person-to-person contact via contaminated hands and through contaminated equipment or surfaces. The clinical manifestation

of VRE includes endocarditis, urinary tract infection, intra-abdominal and pelvic infections, septic arthritis, and bacteremia^{5 6}



Figure 4 - Vancomycin-resistant *Enterococci*⁷

1.4 VanA and VanB type vancomycin-resistant *Enterococci*

VRE phenotypes are defined based on the expression of vancomycin-related virulence and resistance factors. Among all the *Enterococcus* species identified, only few are responsible for most human infections. Among the phenotypes, VanA, VanB, and VanC can confer high levels of resistance to vancomycin and teicoplanin and therefore are of the most clinical importance⁸. However, VanA-type of resistance appears more virulent among the three phenotypes. VanA-type resistance typically involves strains of *Enterococcus faecium*, which accounts for 5 to 15 % of all clinical infections and was isolated from patients in England and France in 1986. VanB-type resistance involves strains of *Enterococcus faecalis* that account for 80 to 90 % of all the infections and was recovered from a patient in Missouri in 1987⁹. VanA-type is resistant to both vancomycin

64 µg/ml and teicoplanin 16-51 µg/ml. Whereas, VanB-type shows vancomycin resistance 8 µg/ml and is sensitive to teicoplanin.

1.5 Other types of Van resistance in vancomycin-resistant *Enterococci*

VanC-type of resistance is found in *E. casseliflavus*, *E. flavescens* and *E. gallinarum*. VanC is inducible with vancomycin at 8-32 µg/ml but sensitive to teicoplanin at 0.5 µg/ml. However, the transmission in this type of resistance cannot pass from one person to the other, unlike that of VanA and VanB- type resistance^{10 11} There is another type of resistance known as VanD type that has a vanD gene which is a ligase gene and is comparable to both vanA and vanB gene. Resistance against vancomycin for this gene is 128 µg/ml, and against teicoplanin is 4 µg/ml. Moreover, the amino acid sequence of VanD-type shows 67% homology to VanA-type genes. Another most recently discovered resistance gene, VanE-type, shows resistance to low concentrations of vancomycin 16 µg/ml but is susceptible to teicoplanin 0.5 µg/ml. MICs for Van types are shown in Table 1.

Table 1 - Vancomycin-resistant *Enterococci* resistance types and minimal inhibitory concentrations⁴

Characteristic	Phenotype				
	VanA	VanB	VanC	VanD	VanE
Vancomycin MIC (µg/ml)	64->1,000	4-1,024	2-32	128	16
Teicoplanin MIC (µg/ml)	16-512	≤0.5	≤0.5	4	0.5
Most frequent enterococcal species	<i>E. faecium</i> , <i>E. faecalis</i>	<i>E. faecium</i> , <i>E. faecalis</i>	<i>E. gallinarum</i> , <i>E. casseliflavus</i> , <i>E. flavescens</i>	<i>E. faecium</i>	<i>E. faecalis</i>
Genetic determinant	Acquired	Acquired	Intrinsic	Acquired	Acquired
Transferable	Yes	Yes	No	No	No

1.6 Antibiotics for treatment of vancomycin-resistant *Enterococci*

Enterococci have developed a variety of mechanisms of resistance towards many antibiotics like beta-lactams, tetracyclines, quinolones, aminoglycosides, and vancomycin (glycopeptide). It has penicillin-binding proteins with a low affinity towards beta-lactams and decreased cellular permeability to other antibiotics. Antibiotic treatment of VRE depends on the type of infection and drug susceptibility of organisms. Most *E. faecium* species are highly resistant to beta-lactams and aminoglycosides.⁵ Conventional antimicrobial treatment options include doxycycline, high-dose ampicillin, chloramphenicol, bacitracin, novobiocin, and nitrofurantoin. Two recently approved novel antibiotics are quinupristin/dalfopristin and linezolid against *E. faecium*. Moreover, investigational antimicrobials include daptomycin, oritavancin, and tigecycline¹²

1.7 Bacterial peptidoglycan layer

Peptidoglycan (PG) layer, also known as murein, is a polymeric macromolecule consisting of linear glycan strands attached by a peptide bridges. This layer is polymerized on the exterior side of the cytoplasmic membrane. It forms a mesh-like closed layer known as a sacculus. It provides physical strength to the cell envelope and is the target for many antibiotics¹³ This layer continuously undergoes remodeling due to bacterial cell growth and division. The PG layer is made of glycan chains with alternating units of N-acetylglucosamine (NAG) and N-acetylmuramic acid (NAM), cross-linked together via intermediate peptide bridges as shown in Figure 5. These peptide bridges are composed of various amino acids and differ between bacterial species. However, developing the PG layer is a complex process involving multiple enzymes that synthesize the glycan chains and peptide bridges. Inhibition of PG biosynthesis can lead to

bacterial death, and their regulation becomes critical for the survival of bacteria^{14 15} Only few of the enzymes in the PG biosynthesis pathway have been targeted by current antibiotics. Therefore, PG biosynthesis is a promising target for new antibacterial drug development¹⁵

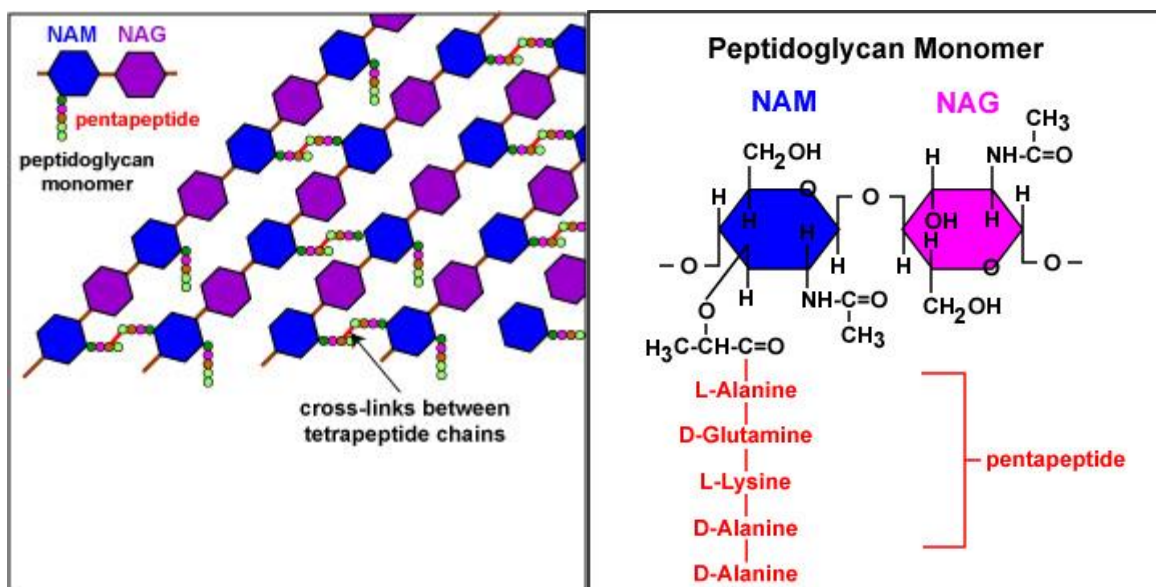


Figure 5 - Peptidoglycan layer composed of cross-linked chains of peptidoglycan monomers¹⁷

1.8 Cell wall biosynthesis in bacteria

Bacterial cell wall is a complex structure made up of peptidoglycan, lipids, and proteins. This process is a highly coordinated process which involves multiple enzymes, regulatory factors, and transporters. Cell wall synthesis occurs in three different compartments of bacteria. The cytoplasm, the cytoplasmic membrane, and the periplasmic space¹⁶ The synthesis starts in the cytoplasm with the synthesis of nucleotide precursor, such as UDP-N-acetylglucosamine UDP-GlcNAc which is synthesized from fructose-6-phosphate by Glm enzymes and UDP-N-acetylmuramyl-pentapeptide (UDP-MurNAc), which is synthesized by Mur enzymes (MurA, MurB, MurC, MurD, MurE and MurF) using UDP-GlcNAc as a starting material.

The phase involves 7 steps:

- a. Biosynthesis of glucosamine from fructose-6-phosphate and glutamine.
- b. N-acetyl-glucosamine-6-phosphate formed by the transfer of acetyl-group by Acetyl CoA
- c. Isomerization of N-acetyl-glucosamine-6-phosphate to acetyl-glucosamine-1-phosphate
- d. N-acetyl-glucosamine-1-phosphate acquires UDP component from UTP and forms UDP-N-acetylglucosamine (UDP-NAG) thereby releasing an inorganic pyrophosphate
- e. Addition of lactyl group to UDP-N-acetylglucosamine to form UDP-N-acetyl muramic acid (UDP-NAM)
- f. Addition of phosphoenolpyruvate to UDP-NAM to synthesize UDP-enol pyruvate derivative
- g. Addition of 5 amino acids including key amine intermediate D-Alanine-D-Alanine to UDP-Mur-L-Alanine-D-Glutamine-L-Lysine-D-Alanine-D-Alanine (UDP Penta or UDP MurNAc pentapeptide). These steps are synthesized by enzymes MurZ, MurA, MurF ¹⁸ as shown in Figure 6

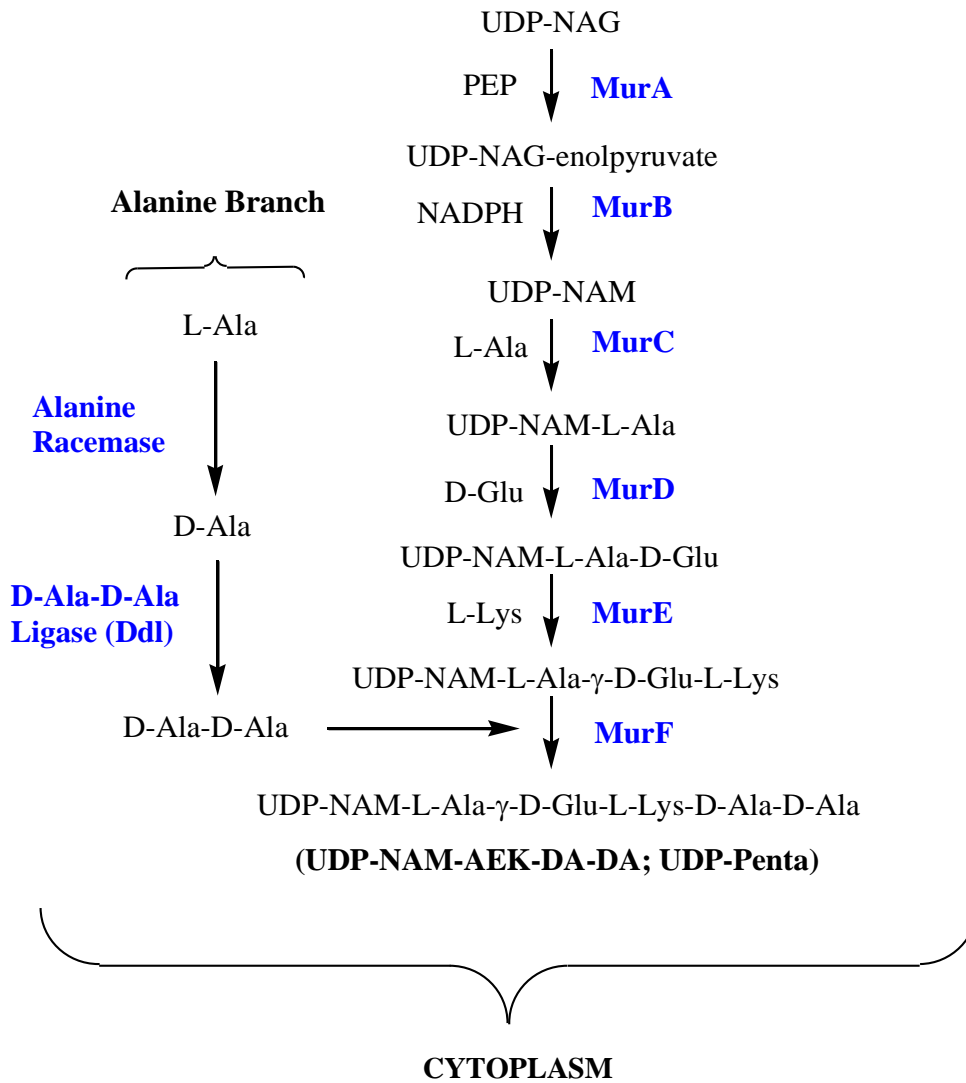


Figure 6 - First stage of bacterial cell wall biosynthesis¹⁹

2. Lipid I biosynthesis occurs in the presence of enzymes MraY and MurG by an association of undecaprenol-phosphate (a 55-carbon-containing compound) and UDP-Penta. Then N-acetyl glucosamine (NAG) is added to Lipid I to form β-(1,4) linked NAG-NAM pentapeptide (Lipid II) in the presence of MurF enzyme¹⁹ as shown in Figure 7.

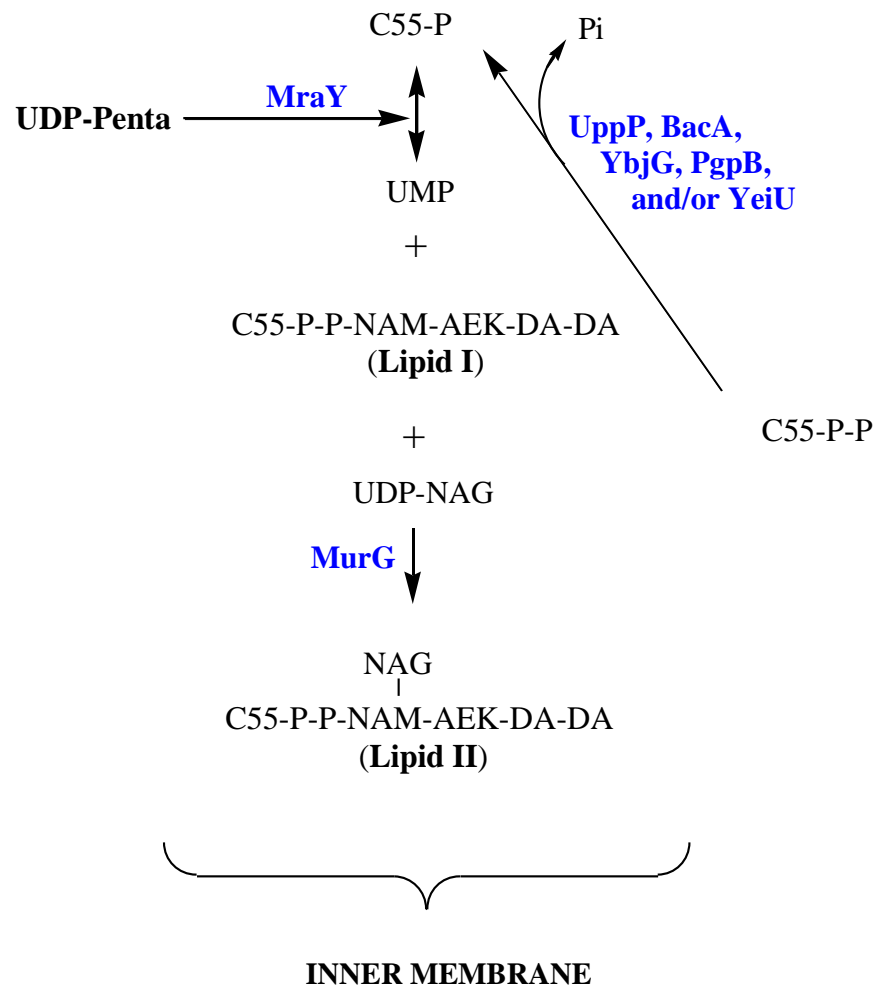


Figure 7 - Second stage of bacterial cell wall biosynthesis¹⁹

3. This is the last step where lipid I traverse the cell membrane and project outside the cell membrane to cell exterior in the presence of transglycosylase and penicillin binding protein. Transglycosylase catalyzes lipid II association with the growing peptidoglycan and penicillin binding proteins crosslink the peptidoglycan across the cell wall²¹ as shown in Figure 8.

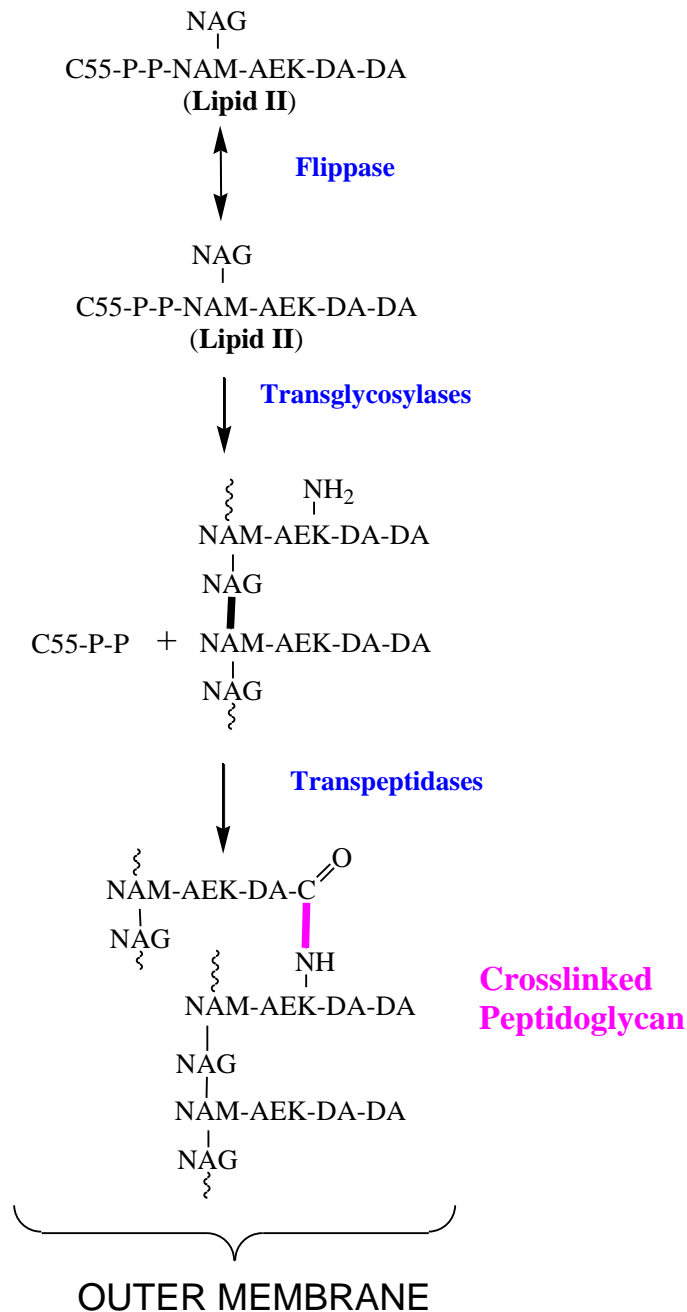


Figure 8 - Third stage of bacterial cell wall biosynthesis¹⁹

Cytoplasmic synthesis of precursors: The first step in PG synthesis involves formation of lipid linked disaccharides pentapeptide intermediates known as lipid II. This process begins with the synthesis of peptidoglycan monomers amino sugars N-acetylglucosamine (NAG) and N-

acetylmuramic acid (NAM) which are joined together by help of transglycosylase enzymes. Transpeptidase enzymes are responsible for cross-linking the chains to provide strength to the bacterial cell wall and enable the bacteria to prevent osmotic lysis. There is a pentapeptide chain which is linked to NAM moiety of bacterial cell wall. This pentapeptide chain is made up of amino acids L-alanine, D-glutamine, L-lysine and two D-alanines. The peptide cross-link forms by formation of a short peptide interbridge consisting of 5 glycines. The biosynthesis of peptidoglycan monomers NAM and NAG occurs in bacterial cytoplasm where they attach to a membrane carrier molecule called bactoprenol. This carrier molecule is responsible for transporting peptidoglycan monomers across the cytoplasmic membrane and work with the bacterial enzymes to insert each monomer into an existing PG enabling bacterial growth via binary fission. As soon as the monomers are inserted, glycosidic bonds help to link these monomers into the growing PG. These long sugar chains are then joined to the other long sugar chain by means of peptide cross-links between peptides coming off from the NAM monomer as shown in Figure 9.

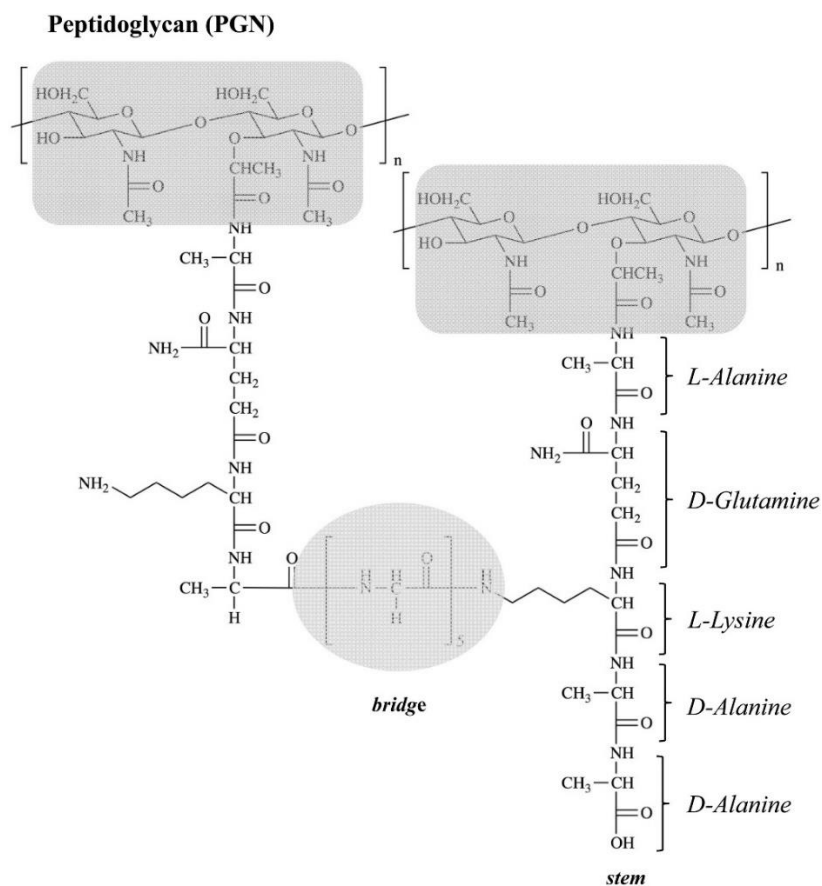


Figure 9 - Bacterial cell wall biosynthesis of a gram-positive bacteria²⁶³

1.9 Resistance pathway in vancomycin-resistant *Enterococci*

Widespread antibiotic resistance among bacteria is a major threat that needs urgent care. Hundreds and thousands of deaths each year are caused by VRE. *Enterococci* is recognized as a major hospital-acquired pathogen because of their natural resistance to a plethora of antibiotics²² Resistance in VRE can be induced by glycopeptides, vancomycin, teicoplanin, ristocetin, and avoparcin and by nonglycopeptides such as bacitracin, robenidine, and polymyxin B. VanA-type resistance is mediated by transposon T1546 elements that are 11 kb mobile genetic element and is located chromosomally or in plasmids. This transposon codes nine polypeptides involved in vancomycin resistance. Under normal conditions in VRE, two molecules of D-Alanine are linked

together by a ligase enzyme to form D-Alanine-D-Alanine, which is added to UDP-N-acetylmuramyl-tripeptide to form UDP-N-acetylmuramyl-pentapeptide. Vancomycin has a high affinity for the D-Alanine-D-Alanine termini of the pentapeptide chain, thereby blocking the growth of the peptidoglycan chain as shown in Figure 10.

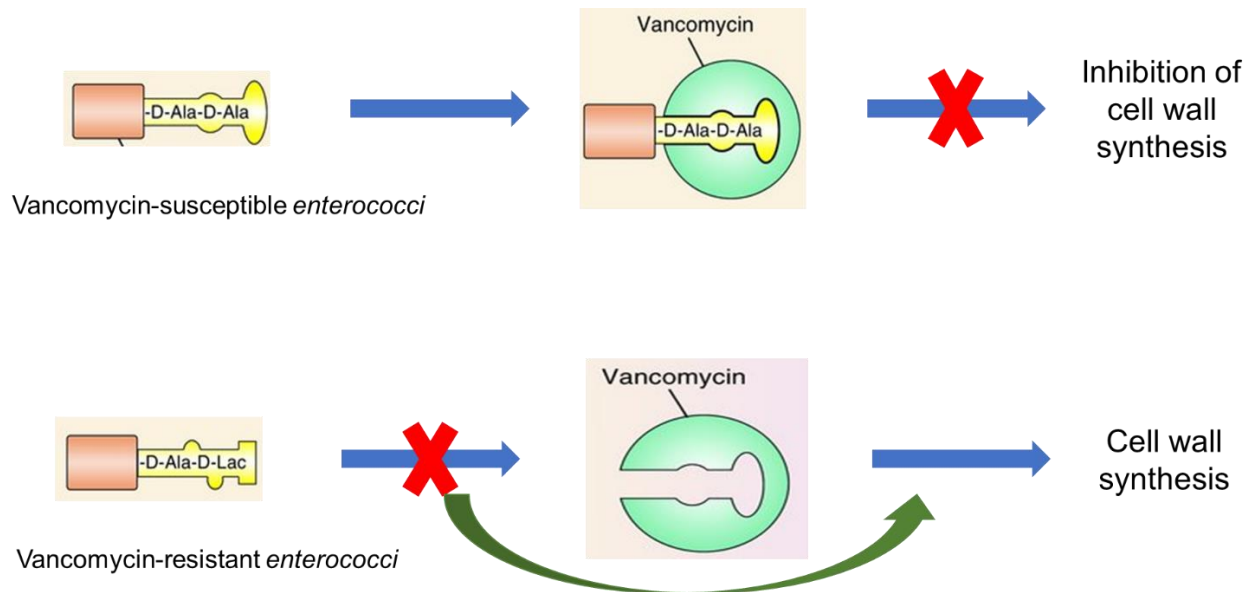


Figure 10 - Mechanism of resistance in vancomycin-resistant *Enterococci* ⁶

However, in the case of a resistant VRE substitution of D-Ala-D-Ala with D-Ala-D-Lac is the job of the nine *vanA* resistance gene located on transposon (Tn1546) of *E. faecium*. Expression of these genes results in the synthesis of D-Alanine-D-Lactate. Vancomycin shows a lower affinity towards D-Alanine-D-Lactate. Each gene's role in synthesizing resistant pathway is as follows.

VanR and VanS are two regulatory proteins that regulate the transcription of *vanHAX*. VanS is a membrane-associated sensor that contains a histidine residue that gets phosphorylated when it detects glycopeptides in the culture medium. After the activation of VanS, VanR acts as

transcriptional activator by accepting phosphoryl group on the aspartate residue. This allows VanS to control the level of expression of VanR. This phosphorylated VanR activates cotranscription of *vanH*, *vanA*, *vanX*, *vanY*, genes and thus leads to resistance in VRE²⁵ In the absence of a vancomycin signal, VanS removes the phosphoryl group from VanR, down-regulating expression of the resistance genes as shown in Figure 11.

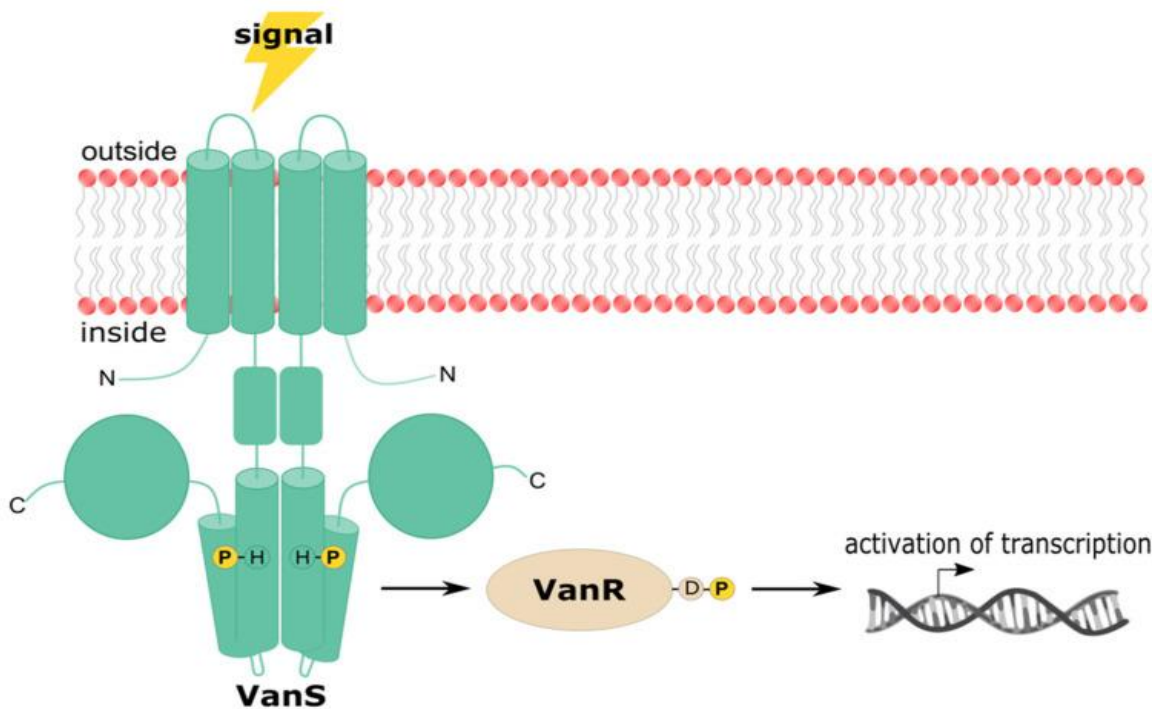


Figure 11 - Signal transduction mechanism of VanRS²⁵

VanA protein is a ligase that helps in ligating D-Alanine-D-Lactate²³ VanH is a D-hydroxy acid dehydrogenase that synthesizes D-lactate for the resistant pathway²⁴ VanX protein is a D,D-dipeptidase that hydrolyzes the D-Alanine-D-Alanine dipeptide in pentapeptide chain. VanY is a D-D-carboxypeptidase that cleaves terminal D-Alanine from UDP Pentapeptide. VanZ is of unknown function²⁶

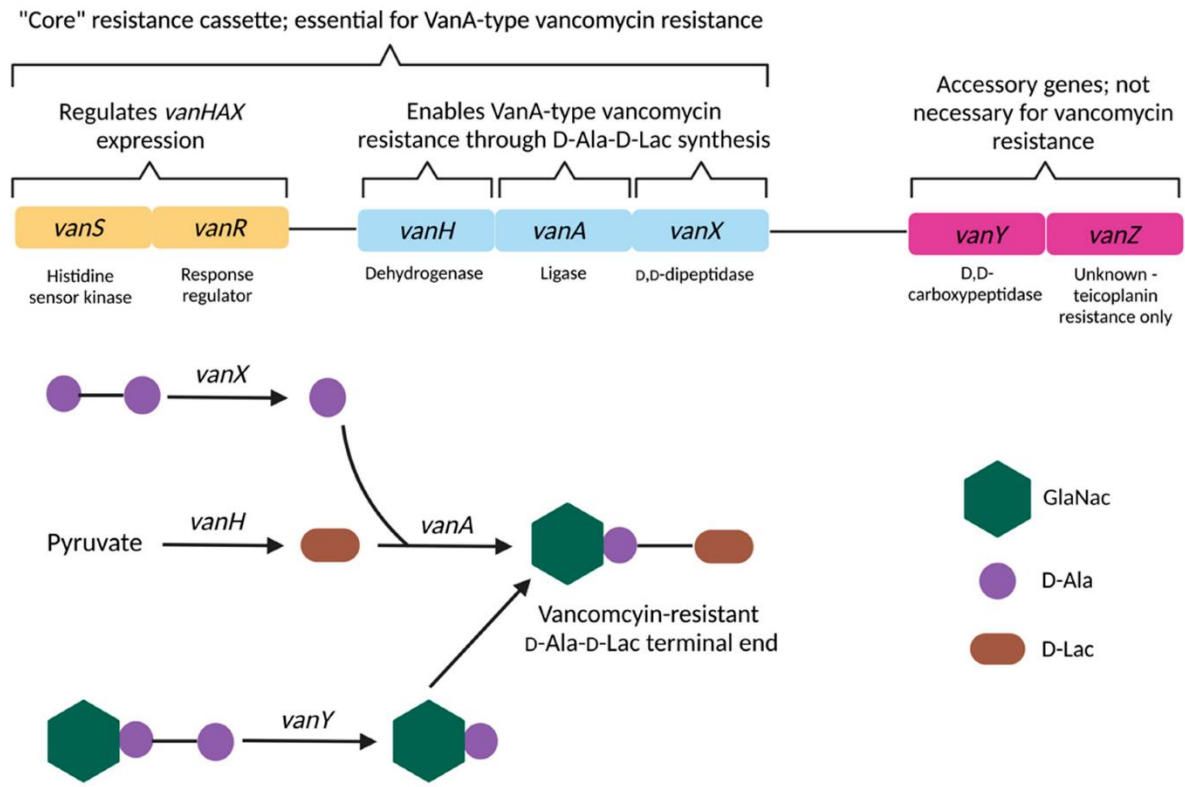


Figure 12 - Genes involved in VRE resistance pathway²⁷

1.10 Nucleosides in bacteria

Nucleosides are precursors to nucleotides and are formed by combining a nitrogenous base (adenine, guanine, cytosine, thymine, and uracil) with a sugar molecule (ribose or deoxyribose) and a phosphate group. In case of bacteria, nucleosides play an important role, such as nucleotide synthesis, which is crucial for building DNA and RNA. Nucleosides can be phosphorylated to nucleotides which can be used for DNA replication, transcription, and translation. A few nucleosides like adenosine are also involved in cellular energy metabolism. Bacteria can recycle nucleosides from degraded DNA and RNA molecules and conserve energy and resources to

synthesize new nucleotides. Nucleoside analogs have also been developed to act as an antibacterial agent. Nucleosides can participate in signal transduction pathways that help bacteria to respond to changes in the environment²⁸

1.11 Bacterial proteomics

Proteomics is the study of proteins, protein structure, function, and interaction with an organism. However, in the case of bacteria, proteomics is a powerful tool for understanding bacterial biology, which involves bacterial growth, survival, reproduction, and adaptation. Proteomics can help to identify proteins that contribute to bacterial pathogenicity, antibiotic resistance mechanisms and understand the function of uncharacterized proteins and their role in bacterial physiology. Proteomics can also help to study protein-protein interactions, post-translational modification, host-pathogen interactions, biomarker discovery and can help in identifying key enzymes and pathways in bacterial metabolism²⁹

1.12 Bacterial metabolomics

Metabolomics is a system biology technique that mainly focuses on comprehensive profiling and analysis of metabolites. Metabolites are small molecules that are cellular metabolism's building blocks and products. This technique helps researchers to gain valuable insight related to the functional state of organisms and the interaction between different organisms. However, in context to bacteria, this technique is used to study the pathogenesis interaction between different species and physiology. Metabolomics is a powerful tool to provide insights into bacterial metabolic pathways, regulation, and their response to stress conditions. Metabolomics can also study metabolites involved in virulence and host immune response. Bacterial metabolism

involves the following steps: sample preparation, metabolite extraction, analysis using mass spectrometry, data processing and interpretation via various methods like liquid chromatography mass spectrometry and, gas chromatography-mass spectrometry. Metabolomics is useful for the development of novel antibiotics that can target resistant bacteria³⁰

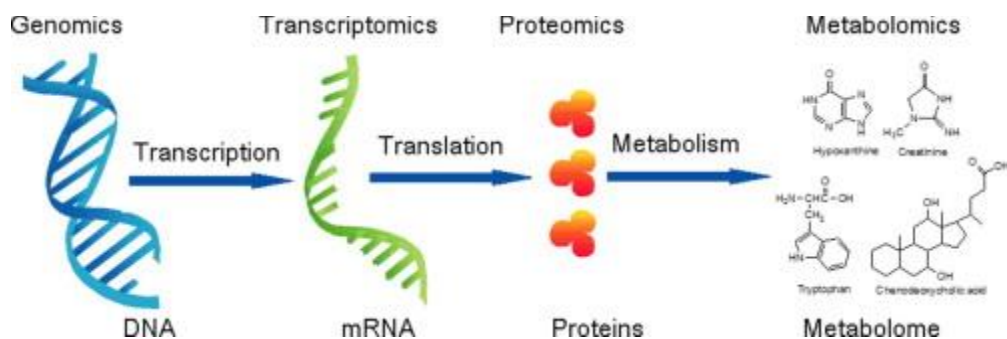


Figure 13 - Various steps involved in bacterial study³¹

CHAPTER 2

2. EFFECT OF VANCOMYCIN ON CYTOPLASMIC PEPTIDOGLYCAN INTERMEDIATES AND VAN OPERON mRNA LEVELS IN VANA-TYPE VANCOMYCIN-RESISTANT *ENTEROCOCCUS FAECIUM*

2.1 Introduction and Rationale

VREfm is highly resistance to vancomycin due to the presence of a vancomycin resistance gene cassette. Exposure to vancomycin induces the expression of genes in this cassette, which encode for enzymes that provide for an alternative peptidoglycan biosynthesis pathway. In VanA-type resistance these alternative pathway enzymes replace the D-Alanine-D-Alanine terminus of normal PG intermediates with D-Alanine-D-Lactate terminated intermediates, to which vancomycin cannot bind. While the general features of this resistance mechanism are well known, the details of the choreography between vancomycin exposure, VanA gene induction, and changes in the normal and alternative pathway intermediate levels has not been described previously. This study comprehensively explores how VREfm responds to vancomycin exposure at the mRNA and peptidoglycan intermediate levels. Vancomycin is an important agent for the treatment of gram-positive bacterial infections resistant to other antibacterial agents, including vancomycin sensitive *enterococcal* (VSE) and MRSA infections^{32 33 34} Vancomycin resistance in *enterococci* is a serious public health issue given the general resistance of these organism to alternative agents^{32 35 36 37 38 39} Vancomycin acts by binding to D-Alanine-D-Alanine moieties in peptidoglycan (PG) precursors on the outer leaf of the cell membrane and blocking cell wall biosynthesis (CWB)^{40 41 42} as shown in Figures 14,15,16.

VanH is a dehydrogenase that produces D-Lactate from pyruvate, and VanA is a D-Alanine-D-Lactate ligase that links D-Lactate to D-Alanine^{43 47} VanX is a zinc dipeptidase that cleaves D-Alanine-D-Alanine^{48 49} VanY is a DD-carboxypeptidase that cleaves the terminal D-Alanine residue from UDP-Penta^{44 47} as shown in Figure 16.

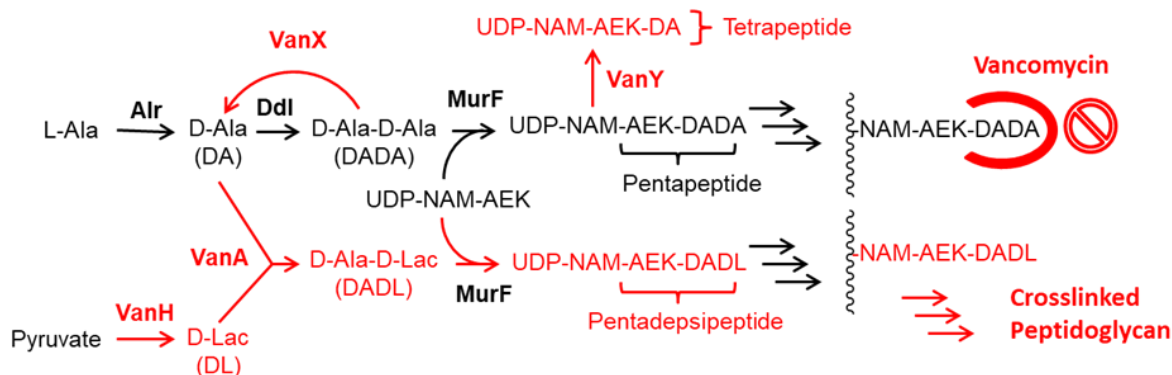


Figure 16 - Alternative cell wall biosynthesis pathway in VanA-type resistance

VanR and VanS are regulatory proteins involved in induction of vancomycin resistance⁵⁰. The function of the VanZ protein in VanA-type resistance to vancomycin is unknown, but it confers increased resistance to teicoplanin, a homolog of vancomycin^{51 52}. An essential aspect of vancomycin resistance in *Enterococci* is the shift from the vancomycin naive state – with cell wall biosynthesis based on normal D-Alanine-D-Alanine based cell wall intermediates, to the vancomycin exposed state – using alternative cell wall intermediates^{46 52} as shown in Figure 16. This shift is poorly understood at the metabolite level, in part due to the lack of methods for the quantification of these PG intermediates. The cytoplasmic UDP-linked intermediates unique to *E. faecium* VanA-type VRE (VREfm) resistance pathways are⁵³:

UDP-NAM-L-Ala- γ -D-Glu-L-Lys-D-Ala-D-Lac (UDP-Pentadepsi),
 UDP-NAM-L-Ala- γ -D-Glu-L-Lys-D-Ala (UDP-Tetra),
 UDP-NAM-L-Ala- γ -D-Glu-L-Lys-(β -D-Asp)-D-Ala-D-Ala (UDP-Penta-D-isoAsp),
 UDP-NAM-L-Ala- γ -D-Glu-L-Lys-(β -D-Asp)-D-Ala-D-Lac (UDP-Pentadepsi-D-isoAsp),
 UDP-NAM-L-Ala- γ -D-Glu-L-Lys-(β -D-Asp)-D-Ala (UDP-Tetra-D-isoAsp).

This list contains several D-iAsp containing PG intermediates. D-iAsp, subsequently α -amidated^{54 55}, acts as a bridging residue for PG crosslinking reactions in *E. faecium*⁵⁶ It is preferentially added to the Lipid I PG intermediate, but with addition to UDP-Penta and UDP-Pentadepsi intermediates observed in cells targeted with late stage CWB inhibitors⁵³ In recent studies, we have developed LC-MS/MS based quantification methods for cytoplasmic UDP-linked intermediates,^{20 57 58} and amine intermediates (L-Alanine, D-Alanine, D-Alanine-D-Alanine) in *S. aureus*^{59 60 61}, and D-Alanine-D-Lactate in VRE⁶¹. In this study, these methods are extended to the unique UDP-linked intermediates in VanA-type VREfm and used to characterize how these metabolites respond to vancomycin exposure. To further support these observations, transcriptomic studies of VanA-gene mRNA transcript levels were also performed using RT-qPCR.

2.2 Materials and Methods

2.2.1 General

VanA-type vancomycin resistant *Enterococcus faecium* (VREfm) was a clinical isolate provided by Dr. Betty Herndon (University of Missouri-Kansas City, School of Medicine). VSE was obtained from American Type Culture Collection (ATCC #BAA-2127). D-Alanine, L-Alanine, D-Alanine-D-Alanine, ¹³C-D-Alanine, UDP-glucuronic acid (UDP-GlcA), vancomycin,

hemin, and triethylamine were from Millipore Sigma. N,N-dimethylhexylamine (DMHA) was from Alfa Aesar. Other materials and reagents were generally as described previously^{20 57 61} VRE growth media consisting of brain heart infusion (BHI) (37.5 g/L), hemin (10 µg/mL), and NAD⁺ (10 µg/mL), was prepared following standard procedures. The forward and reverse primers for the vanH, vanA, vanX, vanY and vanZ genes were from Integrated DNA Technologies (IDT) (Table 2).

Table 2 - Primers used for RT-qPCR of VanA mRNA transcripts.

Gene	Primer	Sequence (5' – 3')
VanH	F	CGATAATTAACGCCAACGTG
	R	ATTCACACCGGCTCTCTTC
VanA	F	TAATTGAGCAGGCTGTTTCG
	R	TACTGCAGCCTGATTGGTC
VanX	F	GATTGCTTCTATGGGACGGT
	R	CAGTTCGGTCAATATTGGGA
VanY	F	ATGCTTGGAATAACGGGTTC
	R	CCATATATTCCTCGAGAACG
VanZ	F	TTGGAGCGACAGACATAACA
	R	TGATTCATATGCTTATTGCT
16S	F	GTCAGCTCGTGTCTGAGAT
	R	GAGTGCCCAACTGAATGATG

F – Forward primer, R – Reverse primer.

DEPC treated water was from Ambion, TRIzol max bacterial RNA isolation kit and iTaq Universal SYBR Green PCR kit were from Life technologies and Bio-Rad respectively. qPCR was performed on a Bio-Rad CFX Connect Real Time System. Bacterial cell densities were determined by absorbance at 600 nm in a Biomate 3 spectrophotometer. Centrifugations were performed on a

Sorvall RT6000 centrifuge, Beckman Coulter Avanti Tm J-251 centrifuge, or an Eppendorf 5424 microcentrifuge. Marfey's reagent (1-fluoro-2,4-dinitrophenyl-L-5-alanine amide) was from Novabiochem (a division of EMD Chemicals). LC-MS/MS analyses were performed on an AB Sciex 3200 QTrap mass spectrometer coupled to a Shimadzu UFLC system using electrospray ionization (ESI) and run with Analyst v1.4.2 software (Sciex).

2.2.2 UDP-linked intermediates standard preparation from methicillin-resistant *Staphylococcus aureus* (MRSA)

From an overnight methicillin-resistant *Staphylococcus aureus* primary culture, a 2 L secondary culture was set up at 0.05 OD. At 0.5 OD₆₀₀ 64 µg/mL of cycloserine was added to extract UDP-Mono, UDP-Di and UDP-Tri and 16 µg/mL of vancomycin was added to extract UDP-Penta. After the addition of antibiotics, the cells were grown with good agitation for 90 mins at 35 °C. The samples were then transferred on ice, and the cells pelleted by centrifugation at 3000 g at 4 °C for 20 mins. Supernatants were discarded, the cells washed twice by resuspending in 30 mL of ice-cold 0.9% saline and re-pelleting. After resuspending pellet in 0.9% saline, the cells were resuspended in 120 mL of the first extraction solvent (80% methanol, 20% water, 0.1% formic acid). Magnetic bead was used to resuspend the cells and the samples were kept on ice for 5-15 minutes, the cell debris pelleted at 3000g at 4 °C for 20 mins, and the supernatants collected into previously chilled 250 mL glass flask on ice. The pellets were then extracted a second time with 120 mL of the same extraction buffer. After 5 min on ice the samples were centrifuged again at 3000 g at 4 °C for 20 mins, and the second sample extraction supernatant removed and combined with the first sample extraction supernatant. This double extraction protocol maximizes analyte recovery and reduces variation. To this analyte was then added ice-cold pure water and the sample

was evaporated with the help of rotary vap to evaporate large amount of solvent. The extracts were frozen overnight in -80 °C, and then dried in a speedvac under strong vacuum (<50 µmHg). The dried samples were then dissolved in 2 mL of 3.5% acetonitrile/24 mM DMHA and were split into 1 mL each and stored at -20 °C prior to analysis. With 1 mL of the sample, ion exchange chromatography was done to clean the sample and collect different elute of various concentration. The other 1 mL sample was run on preparative HPLC to collect fractions. The collected fractions were analyzed on LC-MS/MS using flow injection analysis (FIA) method. FIA helped in identifying the UDPs present in each fraction. The fractions which showed UDP were later freeze-dried, dissolved in 3.5% acetonitrile/24 mM DMHA and ran on a C18 column to check for UDP standard purity. The fractions were later combined to make VREfm external standard.

2.2.3 Purification of the novel UDP-linked intermediates from vancomycin-resistant *Enterococcus faecium* for use as standards

The alternative PG biosynthesis pathway in VanA-type VREfm uses several unique UDP-linked intermediates as shown in Figure 14. Several of these intermediates were purified from vancomycin (64 µg/mL) treated VREfm cultures by preparative ion-pairing RP-HPLC as described previously for the isolation of the normal pathway UDP-linked intermediates from *S. aureus*⁵⁶ This provided purified samples of UDP-Pentadepsi, UDP-Pentadepsi-D-iAsp, and UDP-Tetra. These purified intermediates were used to optimize MS/MS parameters for their detection and quantification shown in Table 4, Figure. 18, and these detection parameters combined with those for normal CWB pathway intermediates^{19 26} to provide a comprehensive method for both normal and alternative pathway UDP-linked intermediates in VREfm. Two unique VREfm UDP-linked intermediates (UDP-Penta-D-iAsp and UDP-Tetra-D-iAsp) were too low in abundance for

purification, and for these intermediates the MS/MS detection parameters for UDP-Penta and UDP-Tetra, respectively, were used.

2.2.4 Ion pairing (IP)-LC-MS/MS based quantification of UDP-linked intermediates

Analytical separations were performed on a Nucleodur 100-3 C18 125x2 mm column (Macherey–Nagel) at 300 μ L/min. Mobile phases were: A - 10 mM formic acid in water, B - 10 mM formic acid in 70:30 acetonitrile/water, C - 10 mM formic acid in acetonitrile, and D - 160 mM DMHA in water adjusted to pH 3.0 with formic acid. The optimized elution gradient was 5% channel D throughout (to provide 8 mM DMHA in the chromatography solvent stream), with 80% A and 15% B initially. After sample injection a linear gradient to 75% A and 20% B over 10 min was used to elute analytes. MS/MS detection settings for normal CWB pathway UDP-linked intermediates were as reported previously⁵⁷, and as given in Table 4 for the VanA-type resistance specific UDP-linked intermediates. Intracellular analyte concentrations were determined using purified UDP-linked intermediates as external standards, and intracellular concentrations calculated using a culture to cell-dry-weight (CDW) conversion factor of 533 mg CDW (L culture)⁻¹ OD₆₀₀-1, and an internal cell volume of 2 μ L/(mg dry cells), which were determined as described previously²⁰

2.2.5 Amine and amino acid quantification

Amino acids from bacterial extracts were diluted 5-fold with pure water, derivatized with Marfey's reagent, and quantified by LC-MS/MS analysis in negative mode as described in detail elsewhere^{59 60 61 62}

2.2.6 LC-MS/MS method development for nucleotides

We also built a method to detect cytoplasmic levels of AXP (AMP, ADP, ATP) and UXPs (UMP, UDP, UTP) in VREfm. 100 μ M standard solutions of AXP and UXPs were made in HPLC grade water and were used for optimizing MS/MS detection by infusion using the automated optimization feature of Analysts 1.6.2. The most intense fragment mass was chosen for detection. These AXP & UXPs channels were then included in the VRE metabolite method for LC-MS/MS quantitative evaluation of UDP-linked intermediates, and a standard mix (20 μ M) was analyzed with these samples to allow exact quantification. UDP-linked intermediates were quantified by LC-MS/MS using ion-pairing HPLC coupled with negative mode MS/MS detection.

Table 3 - Parameters for AXP and UXP.

Note: DP, declustering potential; EP, entrance potential; CEP, collision cell entrance potential; CE, collision energy; For each parent ion (Q1), one most intense product ion (Q3) was optimized for detection

Nucleotides	Q1	Q3	DP (V)	EP (V)	CE (V)
UMP	323.0	79	-60	-6	-38
UDP	402.0	158.9	-65	-3.5	-32
UTP	482.0	158.9	-60	-6	-38
AMP	346.0	79	-60	-4	-58
ADP	426.0	158.9	-65	-3.5	-36
ATP	506.0	158.9	-60	-3	-44

2.2.7 Comparison of centrifugation vs filtration for metabolite extraction

Bacterial cells for metabolomics studies can be collected either by filtration or centrifugation, with advantages and disadvantages for each. A comparison of these two approaches for VREfm was made to determine which strategy would be the best, as described previously for *S. aureus*²⁰ For filtration-based metabolite extraction, VREfm cultures were chilled on ice, and 10 mL samples filtered through 47 mm diameter 0.2 μ m nylon membrane filters. Filters were quickly

washed twice with 5 mL ice-cold 0.9% saline and transferred to 15 mL centrifuge tubes containing 3 mL of ice-cold methanol/ water/ formic acid (66:33:1) with 100 μM $^{13}\text{C}_3\text{-D-Ala}$ and 10 μM UDP-GlcA as internal standards. Samples were kept on ice for 5 min with regular vortexing, centrifuged at 3000 g at 4 °C for 20 mins, and the supernatants collected. Filters and cell pellets were then extracted a second time with 2 mL of 67% methanol/water without any added internal standards, centrifuged at 3000 g at 4 °C for 20 mins, and the second supernatants combined with the first. To the combined supernatants was added 2 mL of HPLC grade water, which allowed the samples to be frozen prior to vacuum drying. The extracts were frozen at -80 °C, dried in a vacuum centrifuge under strong vacuum (<50 μmHg), and dissolved in 100 μl of 3.5% acetonitrile/24 mM DMHA/water. This level of DMHA in the samples facilitates UDP-linked intermediate binding to the C18 column for chromatographic analysis.

For centrifugation-based metabolite extraction, quadruplicate samples of 40 mL from each culture flask were transferred into chilled 50 mL centrifuge tubes on ice, and the cells pelleted by centrifugation at 3000g at 4 °C for 20 mins. Supernatants were discarded, the cells washed once by resuspending in 1 mL of ice-cold 0.9% saline and re-pelleting. Washed cells were resuspended in 1 mL of ice-cold 0.9% saline, and metabolites extracted by adding 4 mL of the first extraction solvent (80% methanol with 100 μM $^{13}\text{C}_3\text{-D-Ala}$ and 10 μM UDP-GlcA as internal standards).

These samples were kept on ice for 5-15 minutes, the cell debris pelleted at 3000g at 4 °C for 20 mins, and the supernatants collected into previously chilled 15 mL centrifuge tubes on ice. The pellets were then extracted a second time with 2 mL of the second extraction solvent (67% methanol/water without any internal standards added), using vortexing and pipetting to resuspend the samples. After 5 min on ice the samples were centrifuged again at 3000g at 4 °C for 20 mins, and the second sample extraction supernatants removed and combined with the first sample

extraction supernatants. This double extraction protocol maximizes both analyte and internal standard recovery and reduces variation. To the combined extracts 2 mL ice-cold pure water is added to allow it to freeze at -80 °C, the extracts were frozen in -80 °C, and then dried in a speedvac under strong vacuum (<50 µmHg). The dried samples were then dissolved in 100 µl of 3.5% acetonitrile/24 mM DMHA and stored at -20 °C prior to analysis. Centrifugation gave slightly higher levels of recovered metabolites as compared to filtration (~10% overall, data not shown). Since centrifugation is also more convenient, the remaining studies were performed using the centrifugation-based cell collection and extraction approach.

2.2.8 Comparison of metabolite extraction and amino acid derivatization at 15 mins and 90 mins

A 20 ml saturated overnight VRE *faecium* primary culture was grown in VRE media and used to inoculate 1300 mL of VRE media in a baffled 2 L flask (secondary culture) to an optical density at 600 nm (OD₆₀₀) of 0.05. The cells were grown with good agitation at 35 °C (doubling time of 45 min). When the secondary culture reached an optical density OD₆₀₀ of 0.5, 160 mL portions were transferred into separate 500 ml baffled flasks. Different concentrations of vancomycin were added to these flasks except for one which was the no vancomycin control, and one flask was incubated with shaking for 15 mins and the other flask was incubated with shaking for 90 mins, respectively. Flasks were then rapidly chilled in an ice slush bath, and the samples from individual flasks were collected in quadruplicate and stored on ice for up to 15 min prior to centrifugations and processing for metabolite extraction, as described above. Samples were analyzed for UDP-linked intermediates as described previously⁵⁸ with the expanded set of LC-MS parameters for the alternative UDP-linked intermediates found in VREfm described above and for

amine and amino acid intermediates using the Marfey's derivatization-based approach with negative mode-based detection also as described previously^{61 62}

2.2.9 Standard growth and metabolite extraction procedure for VRE *faecium* vancomycin exposure experiments

A 20 ml saturated overnight VREfm primary culture was grown in VRE media and used to inoculate 1300 mL of VRE media in a baffled 2 L flask (secondary culture) to an optical density at 600 nm (OD₆₀₀) of 0.05. The cells were grown with good agitation at 35 °C (doubling time of 45 min). When the secondary culture reached an optical density OD₆₀₀ of 0.5, 160 mL portions were transferred into separate 500 ml baffled flasks. Different concentrations of vancomycin were added to these flasks except for one which was the no vancomycin control, and the flasks were incubated with shaking for an appropriate time. Flasks were then rapidly chilled in an ice slush bath, and the samples from individual flasks were collected in quadruplicate and stored on ice for up to 15 min prior to centrifugations and processing for metabolite extraction, as described above. Samples were analyzed for UDP-linked intermediates as described previously⁵⁸ with the expanded set of LC-MS parameters for the alternative UDP-linked intermediates found in VREfm described above, and for amine and amino acid intermediates using the Marfey's derivatization-based approach with negative mode-based detection also as described previously^{61 62} This constituted a single experiment, which was replicated on separate days to provide three to four replications.

2.2.10 Experimental procedure for long-term vancomycin exposure

A 20 mL saturated primary culture of VRE was grown in VRE media with 16 µg/mL vancomycin. This primary culture was used to inoculate fresh 100 mL VRE media with 16 µg/mL

vancomycin in a baffled flask (secondary culture). The culture was grown with good agitation at 35 °C (doubling time of 45 min). When the secondary culture reached an optical density at OD₆₀₀ of 0.5, triplicate samples of 15 mL were collected, and the cells collected and extracted for LC-MS analysis as described above.

2.2.11 Time dependence of cytoplasmic cell wall biosynthesis intermediate levels in VRE *faecium* after vancomycin exposure

This experiment was performed following the standard growth procedure described above. Cells were grown in the secondary culture (no vancomycin) to mid log phase (0.5 OD₆₀₀) and vancomycin (16 µg/mL) added. At regular time intervals (0, 1, 2, 3, 4, 5, 10, 20, 40, 60, 90, 120, 180 and 240 min) triplicate samples of 15 mL were collected by centrifugation and prepared for analysis as described above.

2.2.12 Time dependence of VanA mRNA levels in VRE *faecium* after vancomycin exposure

A 20 ml saturated overnight VREfm culture was grown in VRE media and was used to inoculate 500 mL of VRE media to an OD₆₀₀ of 0.05. When the secondary culture reached an OD₆₀₀ of 0.5, 16 µg/mL vancomycin was added to the flasks. Quadruplicate samples of 10 mL were collected at different time points after vancomycin addition (1, 15, 45, and 180 min, 18hr), and chilled and stored on ice prior to mRNA extraction. A sample was also collected immediately prior to vancomycin addition as the control (t=0) sample. mRNA was extracted from these samples using the TRIzol max bacterial RNA isolation kit following the manufacturer's protocol (ThermoFischer Scientific). The quality and concentration of mRNA was determined using a Nanodrop instrument (ThermoFischer Scientific). RNA (100 ng) was then used as the template in

quantitative RT-PCR (RT-qPCR) with primer pairs (Table 2) designed to amplify internal regions of VanH, VanA, VanX, VanY and VanZ⁷¹ RT-qPCR was performed with the comparative Ct method. Measurements were performed on a Bio-Rad CFX Connect Real Time system. RT-qPCR reactions cycles were: 10 seconds at 50 °C, 5 minutes at 95 °C, 30 seconds at 94 °C, 30 seconds at 53.2 °C, 30 seconds at 72 °C (for 45 cycles), and 30 seconds at 25 °C. The gene expression was internally normalized to 16S ribosomal gene. After obtaining initial results, mRNA levels were adjusted to give threshold cycle (Ct) values of 18-29. Ct values were used to calculate the fold change (FC) of Van gene expression between control and vancomycin treated cultures using the following formula:

$$FC = 2^{-(\Delta\Delta C_T)} \quad \dots \text{(Equation 1)}$$

where,

$$\Delta\Delta C_T = [C_{T(Sample)} - C_{T(16S_Sample)}] - [C_{T(Control)} - C_{T(16S_Control)}] \quad \dots \text{(Equation 2)}$$

The relative fold changes in VanA gene mRNA levels between control and vancomycin exposed time course samples from three completely independent experiments were determined, and the independent experiment mean, and standard errors reported.

2.2.13 Vancomycin concentration dependence of VRE *faecium* mRNA levels

Primary and secondary cultures were grown following the standard growth protocol. When the secondary culture reached an OD₆₀₀ of 0.5, 50 mL aliquots were transferred to 250 mL baffled flasks and various concentrations of vancomycin (0.0625, 0.125, 1, 4, 16, and 64 µg/mL) added. A no vancomycin control flask was also included. The cultures were grown for 15 minutes, and

quadruplicate samples of 10 mL were collected on ice. mRNA was isolated and quantified as described above. This experiment was repeated in pentaplicate.

2.2.14 Minimal inhibitory concentration (MIC) determination of linezolid, rifaximin and oritavancin

Minimal inhibitory concentrations (MIC) were determined by adding 2 μ L samples of 0.5 mM stock of linezolid, rifaximin and oritavancin into the first columns of 384 well plates. These samples were then serially diluted in steps of two across the plates with DMSO using an Integra Viaflo Assist automated multichannel pipettor. The last column was left blank for control (DMSO only). These plates were frozen at -80 °C and dried under strong vacuum as described above. To each well in each set was added 20 μ L VRE growth medium containing 4000 cfu VREfm. This provided MIC plates with 50 μ M as the highest test agent concentration. Plates were incubated for 48 h at 35 °C. Fresh VRE growth medium (10 μ L) was added to the wells of these four sets of plates, followed by incubation for 2 h at 35 °C to restart active cell growth. To the wells of these plates was then added 10 μ L of 100 μ g mL⁻¹ resazurin^{145 146 147} The plates were incubated for another 2 h at 35 °C, and the A610 - A450 absorbance difference measured as described above. All MICs were determined at least in triplicate to ensure reproducibility.

2.2.15 Effect of linezolid on vancomycin associated metabolite pool level changes

Primary and secondary cultures were grown following the standard growth protocol. When the secondary culture reached an OD₆₀₀ of 0.5, 50 mL portions were transferred into separate 250 mL baffled flasks. Different antibiotics and their combinations (vancomycin (64 μ g/mL), linezolid (8 μ g/mL, 4×MIC), vancomycin + linezolid) were added to these flasks at 4 times the MIC. A no

antibiotic flask was also included. The flasks were incubated at 35 °C with shaking for 15 minutes and 10 mL Samples from individual flasks were collected in quadruplicate and processed for metabolite analysis as described above.

2.2.16 Effect of linezolid and rifaximin on vancomycin associated mRNA level changes.

Primary and secondary cultures were grown following the standard growth protocol. When the secondary culture reached an OD₆₀₀ of 0.5, 50 mL portions were transferred into separate 250 ml baffled flasks. Different antibiotics and their combinations (vancomycin, linezolid, rifaximin, vancomycin + linezolid and vancomycin + rifaximin) were added to these flasks at 4 times the MIC. A no antibiotic flask was also included as control. The flasks were incubated at 35 °C with shaking for 15 minutes. 10 mL samples from individual flasks were collected in quadruplicate and processed for metabolite analysis as described above.

2.2.17 Whole cell protein isolation from VRE *faecium*

Two separate 20 ml saturated overnight VREfm primary cultures with and without vancomycin were grown in VRE media. This primary culture was used to inoculate 50 mL of VRE media with and without vancomycin in a baffled 250 mL flask (secondary culture) to an optical density at 600 nm (OD₆₀₀) of 0.05. The cells were grown with good agitation at 35 °C (doubling time of 45 min). When the secondary culture reached an optical density OD₆₀₀ of 0.5, 10 mL from each culture flask were transferred into chilled 50 mL centrifuge tubes on ice, and the cells were pelleted by centrifugation at 3000 g at 4 °C for 20 mins. Supernatants were discarded, and the cells were washed twice by resuspending with 5 mL of phosphate buffer saline and re-pelleting. Washed cells were resuspended in 5 mL of lysis buffer (7 M urea, 4% w/v CHAPS, and 50 mM DTT) with

protease inhibitors. RNase and DNase were also added to the lysis buffer. Both with and without vancomycin samples were incubated at 4 °C for 1 hour on a rocker shaker. The tubes were then sonicated at an amplitude of 30% with an interval of 3 seconds for 5 mins. The cells were then pelleted at 12000 rpm at 4 °C for 40 mins, and the supernatants collected into previously chilled 15 mL centrifuge tubes on ice. The protein concentration was measured using nanodrop. The samples were later sent to the proteomics facility at UMKC School of Biological Sciences, where they were run on Waters Orbitrap.

2.3 Results and Discussion

2.3.1 LC-MS/MS method development.

In prior studies, the normal cell wall biosynthesis (CWB) pathway cytoplasmic intermediates in *S. aureus* were preparatively purified and LC-MS/MS methods for their quantification in bacterial extracts developed⁵⁷ These normal CWB pathway intermediates are shared by vancomycin-sensitive *Enterococcus faecium* (VSEfm) and VREfm. VREfm also has several additional unique vancomycin resistance associated intermediates as shown in Figure 16⁵³ Several of these intermediates (UDP-Pentadepsi, UDP-Tetra, UDP-Pentadepsi-D-iAsp) were preparatively purified from vancomycin treated VREfm cultures and were used to optimize their LC-MS/MS quantification as shown in Table 4 following previously described methods⁵⁷ UDP Tetra-D-iAsp and UDP-Penta-D-iAsp lacked sufficient concentration for purification, and their LC-MS/MS quantification parameters were adopted from UDP-Tetra and UDP-Penta respectively. LC-MS/MS chromatograms are shown in Figure 17. Serial dilutions of these intermediates in water and VREfm extract were linear over a detection range of 0.2 – 2000 pmol with no apparent

matrix effects, as observed in prior studies for the UDP-linked intermediates from *S. aureus*⁵⁷ (data not shown).

Table 4 - Summary of optimized parameters and sensitivities for negative mode IP-LC-MS/MS detection of UDP-linked intermediates in VRE.

	t_r (min) ^a	Q1	Q3	DP (V)	EP (V)	CE (V) ^b	AU/pmol	LOD (fmol) ^c
UDP-Penta	12.1	1148.3	403.0	-140	-10	-60	3970	80
UDP-Penta-D-iAsp^d	17.5	1263.3	403.0	-140	-10	-60	3970	80
UDP-Pentadepsi	15.5	1149.3	403.0	-120	-10	-62	4120	70
UDP-Pentadepsi-D-iAsp	20.5	1264.3	403.0	-100	-8	-45	2450	180
UDP-Tetra	11.0	1077.3	403.0	-125	-12	-56	3550	89
UDP-Tetra-D-iAsp^e	13.10	1192.3	403.0	-125	-12	-56	3550	89

^a t_r chromatographic retention time; Q1, quadrupole 1 m/z for analyte precursor ion; Q3, quadrupole 3 m/z for analyte fragment ion; AU, area units; CE, collision energy; DP, declustering potential; EP, entrance potential; LOD, lower limit of detection

^b For all ions: Collision cell entrance potential = -8 V; Collisionally activated dissociation gas level, arbitrary units = medium; Source temperature = 600 °C; Curtain gas setting = 30 psi; GS1 = 70 psi; GS2 = 20 psi.

^c Lower limits of quantification (LLOQs) were 3.3x the LOD for a particular analyte.

^d UDP-Penta-D-iAsp MS/MS detection values were obtained from UDP-Penta.

^e UDP-Tetra-D-iAsp MS/MS detection values were obtained from UDP-Tetra.

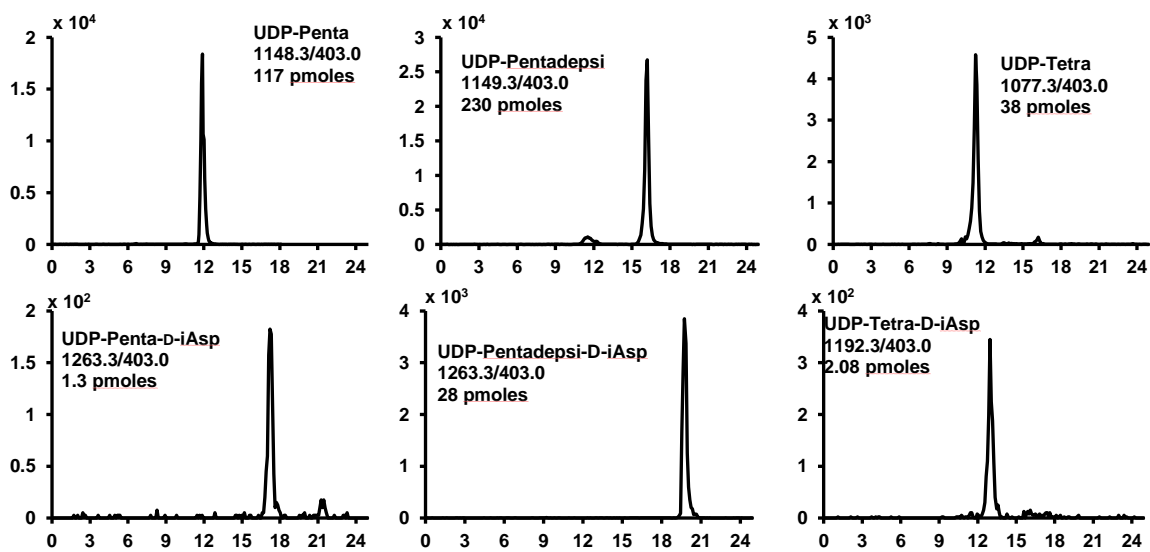
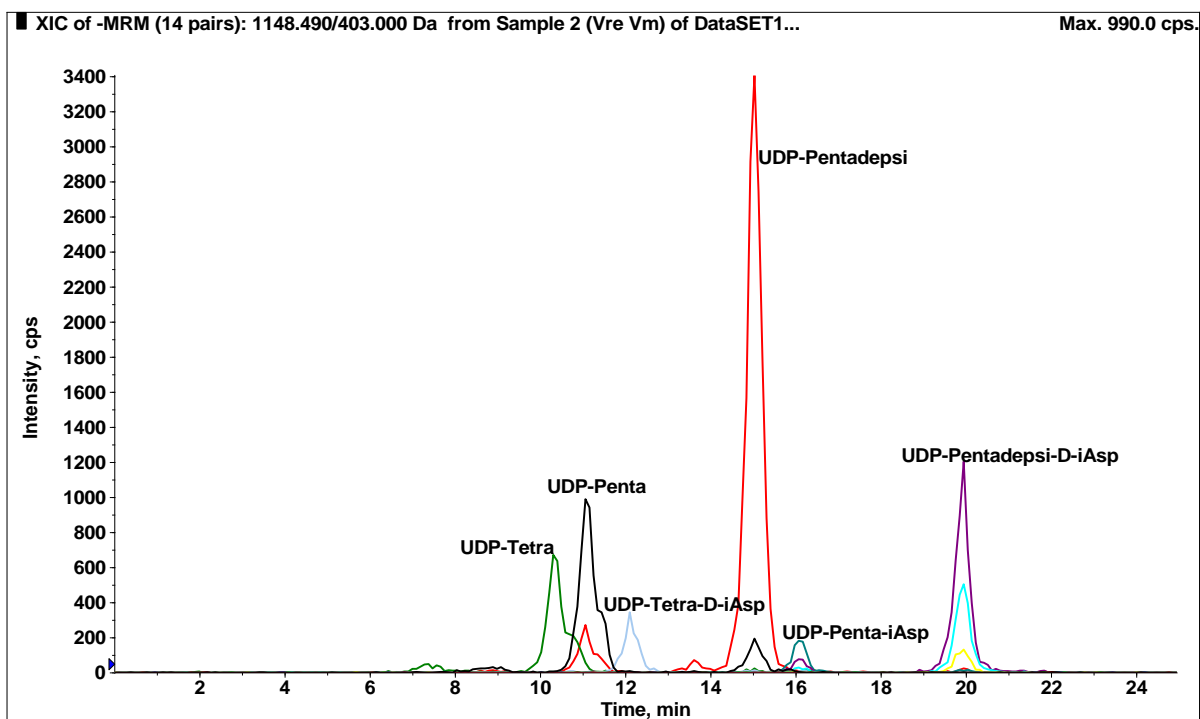


Figure 17 - LC-MS/MS chromatograms of VanA-type VREfm specific cytoplasmic UDP cell wall intermediates. UDP-Penta included for reference.

2.3.2 LC-MS/MS method development for nucleotides

100 μ M of each nucleotide was infused in Quadrupole 3200 and the highest intensity peaks were selected to build the method. Figure 18 shows the UV and chromatographs of the LC-MS/MS method developed.

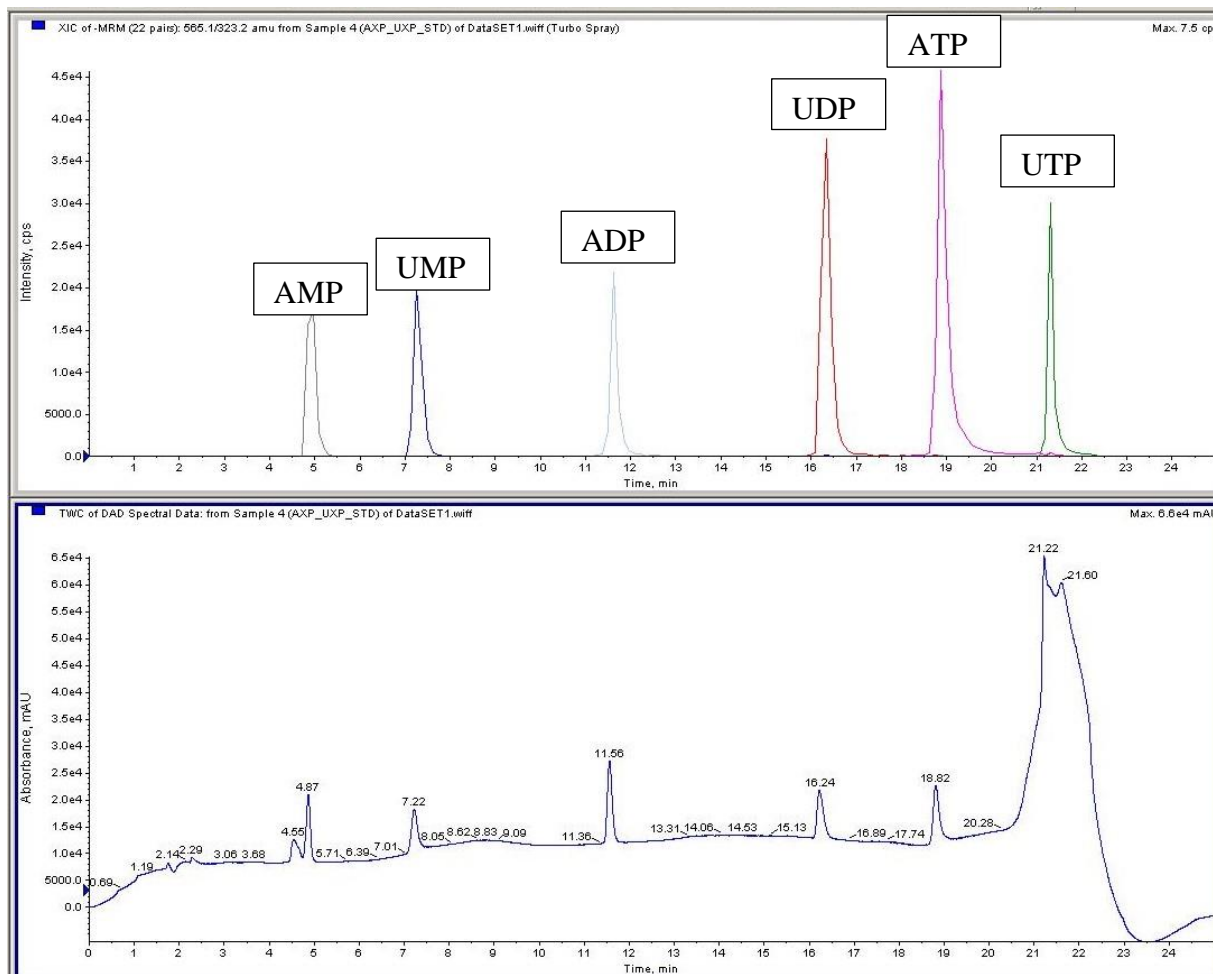


Figure 18 - LC-MS/MS representation of AXP and UXP peaks

2.3.3 Comparison of sample preparation by centrifugation vs. filtration for metabolite analysis

Two different protocols for VREfm cytoplasmic intermediate isolation and extraction – filtration and centrifugation – were compared²⁰ Centrifugation showed slightly improved metabolite recovery (~10%, data not shown) and was therefore used for the remainder of this study.

2.3.4 Survey of vancomycin effects on cell wall biosynthesis intermediates in *E. faecium*

Data from VSEfm-/ +Vm and VREfm-/ +Vm (Vm for vancomycin) are presented in Table 5. Values from MRSA-/ +Vm are also included for comparison⁵⁸ Several detailed comparisons can be made based on this data. Overall, VSEfm behaves very differently than MRSA in its response to vancomycin. UDP-linked intermediate levels increased remarkably in MRSA+90, whereas VSEfm+90 shows only a modest overall increase in UDP-linked metabolite levels, indicating fundamental differences between *E. faecalis* and MRSA PG biosynthesis pathways. A major difference between VSEfm+90 and VREfm+90 is that VRE+90 shows a much lower level of UDP-Penta accumulation. In contrast UDP-Sum (total UDP-linked intermediate pool level) is nearly the same between VSE+90 and VRE+90. The total level of UDP-linked intermediates (UDP-Sum) in VREfm+18 is similar to VREfm-Vm, indicating a complete return to normal levels of these key intermediates after prolonged vancomycin exposure.

2.3.5 Detailed summary of survey of vancomycin effects on CWB intermediates in *E. faecium* results (Table 5)

VSEfm-Vm vs VREfm-Vm: The UDP-linked PG pathway intermediate profiles of VSEfm-Vm and VREfm-Vm have similar (+/-3-fold) levels of normal (i.e., not VanA resistance related) UDP-linked pathway intermediates. UDP-Sum (the sum of all UDP-linked intermediate

concentrations) is also similar in these control samples. Most PG related amines included in this study also show similar levels between VSEfm-Vm and VREfm-Vm, except for D-Ala-D-Ala, which is notably lower in VREfm-Vm than in VSEfm-Vm. MRSA-Vm shows higher amino acid levels than VSEfm-Vm and VREfm-Vm.

MRSA+90 vs VSEfm+90: After vancomycin treatment for 90 minutes, substantial changes in metabolite levels are apparent. As reported previously⁵⁸, MRSA+90 shows a dramatic increase in total UDP-linked metabolites (UDP-Sum) – particularly of the terminal cytoplasmic intermediate UDP-Penta – due to continued synthesis of UDP-linked intermediates and their accumulation. VSEfm+90 in contrast shows a decrease in early UDP-linked intermediates, and only a relatively modest increase in UDP-Penta and UDP-Sum, indicating that entry into the pathway is restricted in VSE in the presence of vancomycin, and possibly that turnover of pathway intermediates continues at a reduced rate. Amines levels are also decreased in VSEfm+90.

VREfm-Vm vs VREfm+90: In VREfm+90, most normal intermediate levels are close to their VREfm-Vm values, except UDP-Penta, which is modestly higher. Substantially increased levels of VanA-type resistance UDP intermediates are apparent in VREfm+90 – particularly UDP-Pentadepsi, UDP-Tetra, and D-Alanine-D-Lactate, which are the key intermediates for vancomycin resistance in VanA-type VREfm as shown in Figure 14. UDP-Pentadepsi, synthesized from D-Alanine-D-Lactate, is the replacement for UDP-Penta in VanA-type resistance, and UDP-Tetra is the degradation product of UDP-Penta in VanA-type resistance. D-Alanine-D-Alanine is decreased modestly.

VREfm+18 vs VREfm+18 & VREfm+Vm: After extended (18 hr) vancomycin exposure (VREfm+18), the normal UDP-linked metabolite levels have partially returned towards VREfm-Vm levels compared to VREfm+90 except for UDP-Penta, which is lower in VREfm+18 than in

either the VREfm-Vm or VREfm+90. D-Alanine-D-Alanine levels are also low in VREfm+18. The unique VanA-type resistance UDP-linked intermediate levels have also dropped from their 90 min exposure levels. UDP-Sum is nearly the same in VFRfm+18 as in VREfm-vancomycin. These data indicate that, upon vancomycin exposure, VREfm shows an initial accumulation of both normal and alternative UDP-linked pathway intermediates, followed by a partial return of normal intermediates to their -Vm levels and a drop in the alternative intermediate levels from the higher values observed in VREfm+90. The level of the D-isoAsp containing intermediates is small and only detectable in vancomycin treated VREfm samples and appear unlikely to play a significant role in PG biosynthesis in VREfm.

Table 5 - Effect of vancomycin (Vm) exposure on cytoplasmic PG intermediates in VSE and VRE and comparison with MRSA

	VSE		VRE			MRSA	
	-Vm	+Vm (90 min)	-Vm	+Vm (90 min)	+Vm (18 hrs)	-Vm	+Vm (90 min)
UDP-Linked Intermediates (μM)^{a,b}							
UDP-NAG	940 (20)	290 (20)	590 (40)	510 (30)	470 (30)	740 (60)	77 (10)
UDP-NAM	1130 (60)	740 (50)	480 (20)	740 (20)	320 (30)	1250 (60)	5200 (900)
UDP-Mono	113 (2)	7.2 (0.5)	80 (10)	63 (4)	35 (1)	81 (7)	2900 (500)
UDP-Di	55 (6)	4.3 (1.5)	95 (8)	24 (2)	47.8 (0.4)	32 (6)	110 (50)
UDP-Tri	30 (5)	97 (7)	48 (7)	43 (1)	26 (4)	10 (2)	35 (8)
UDP-Penta	590 (20)	2280 (120)	356 (8)	900 (40)	190 (90)	260 (30)	62000 (2000)
UDP-Pentadepsi	ND	ND	13.4 (0.4)	730 (10)	290 (50)	ND	ND
UDP-Tetra	ND	ND	15.6 (0.4)	774 (6)	44 (5)	ND	ND
UDP-Penta-D-iAsp	ND	ND	ND	ND	1.3 (0.2)	ND	ND
UDP-Pentadepsi-D-iAsp	ND	ND	13.2 (0.9)	46 (2)	27 (2)	ND	ND
UDP-Tetra-D-iAsp	ND	ND	ND	ND	2.1 (0.1)	ND	ND
UDP-Sum	2860 (60)	3500 (200)	1470 (130)	3820 (30)	1460 (60)	2380 (90)	71000 (1900)
Amino Acid and D-Ala-D-Ala Intermediates (mM)							
L-Ala	52 (8)	17.4 (0.6)	29 (2)	20.1 (0.8)	15.2 (0.9)	67 (7)	64 (7)
D-Ala	26 (3)	5.2 (0.2)	22 (2)	12 (3)	11 (1)	48 (8)	46 (16)
D-Ala-D-Ala	2.8 (0.4)	0.3 (0.1)	0.71 (0.05)	0.4 (0.1)	0.12 (0.07)	0.9 (0.3)	17 (2)
D-Ala-D-Lac	ND	ND	0.11 (0.01)	2.8 (0.1)	2.1 (0.3)	ND	ND
L-Glu	126 (9)	24.2 (0.6)	81 (3)	95 (2)	57 (9)	250 (30)	210 (30)
D-Glu	10.7 (0.2)	4.7 (0.7)	17.6 (0.3)	51 (9)	49 (2)	200 (40)	230 (50)
L-Lys	11.1 (1.2)	4.1 (0.4)	11.8 (0.5)	21 (1)	12.6 (0.6)	64 (5)	79 (3)
L-Asp	38 (4)	9.3 (0.2)	18.3 (0.4)	21 (2)	22 (3)	96 (11)	15 (8)
D-Asp	22 (3)	5 (1)	14 (1)	25.1 (0.5)	15.7 (0.2)	63 (9)	15 (4)
^a UDP-enolpyruvate levels were not detectable (<0.5 μM).							
^b ND = Not detectable.							

2.3.6 Time course results from both VRE *faecium* and VSE *faecium*

Time course results from both VREfm and VSEfm were plotted on a “semi-square root” x-axis to expand early time course changes.

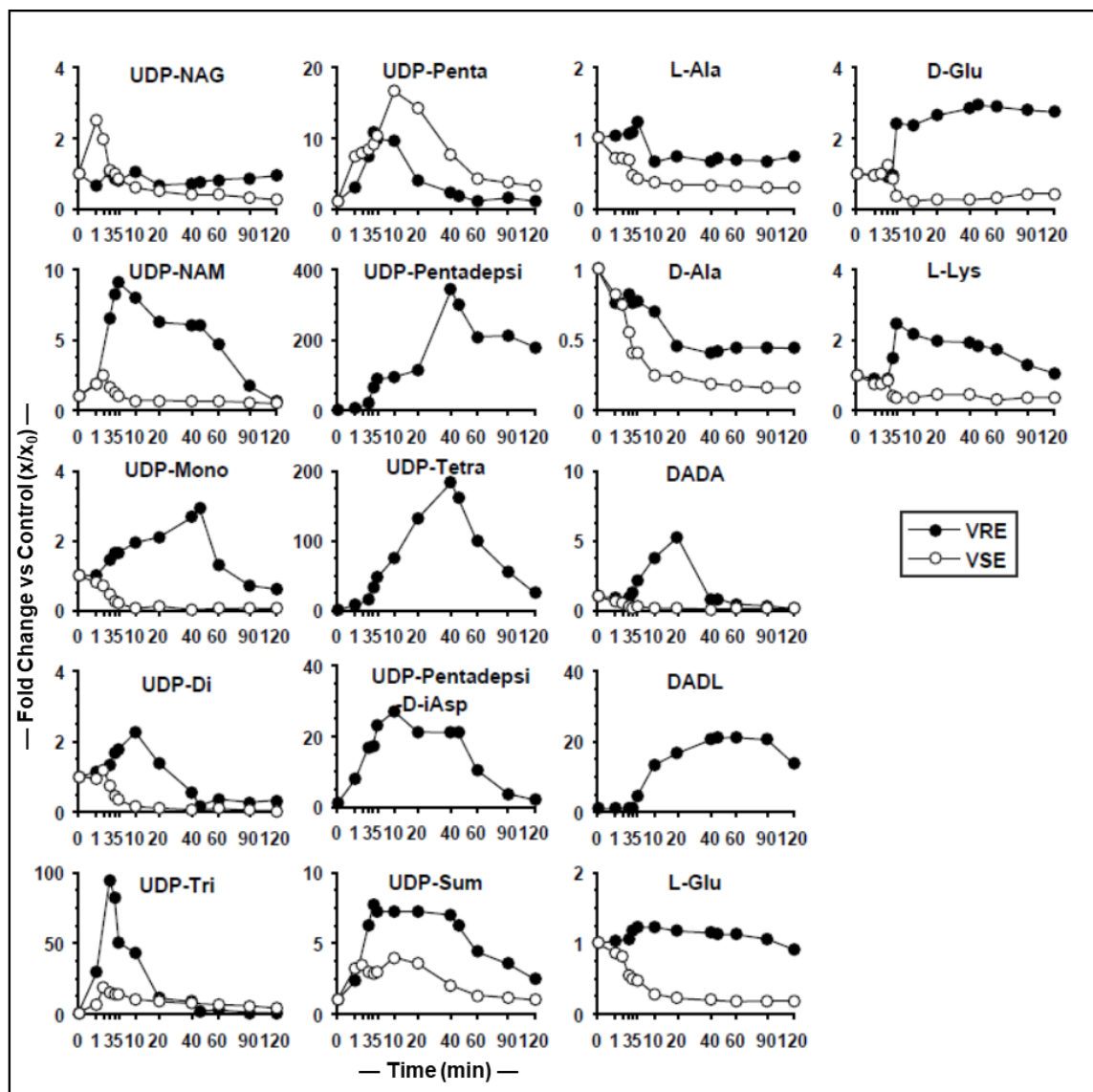


Figure 19 - Time courses of VREfm PG intermediates (same data as Figure 20), and VSEfm PG intermediates plotted as fold changes vs their t_0 values (t_0 values in Table 5).

The x-axis is plotted in a semi-square root form to expand early time points for easier visualization.

2.3.7 Time dependence of vancomycin effect on metabolite pools in *VRE faecium*

A time course experiment was performed to determine the rates at which PG intermediate levels change in VREfm upon vancomycin exposure as shown in Figure 20, and in VSEfm as shown in Figure. 19. This data shown in Figure 20 reveals that most normal pathway VREfm PG metabolite levels change rapidly in response to vancomycin exposure. UDP-NAM, UDP-Tri, and UDP-Penta peaked at 10-to-100-fold of their $t=0$ levels in 3-10 min, and then decreased back towards their $t=0$ levels. UDP-Tri shows the largest fold increase since its uninhibited level is low (37 μM) and rises to nearly as high as UDP-Penta (1080 μM for peak UDP-Tri vs 1150 μM for peak UDP-Penta). D-Alanine-D-Alanine increases and spikes at a 5-fold increase at 20 min (3800 μM) quite a bit lower (fold change wise) and slower than most of the normal UDP-linked intermediates, and then rapidly drops to a low level. Key alternative UDP-linked PG pathway intermediates (UDP-Pentadepsi, UDP-Tetra, and D-Alanine-D-Lactate) peaked at 20-to-400-fold their $t=0$ levels at 30-45 min (peak levels of 4450, 2550 and 2850 μM respectively). UDP-Pentadepsi – the replacement for UDP-Penta in the alternative pathway – then plateaus at around a 200-fold increase. D-Alanine-D-Lactate plateaus at a 15-to-20-fold increase, whereas UDP-Tetra continues to decline towards its $t=0$ level. Interestingly, the D-Alanine-D-Lactate level appears to show a distinct lag before beginning to increase at 5 min. UDP-Sum shows a sharp initial rise in level peaking at 4 min, and then gradually decreasing over the next two hours. The rise of UDP-Sum is linear for 4 min after vancomycin exposure, with a slope of 2800 $\mu\text{M}/\text{min}$. This represents a minimum value for the flux of metabolites through this pathway prior to vancomycin addition. Using this same approach, MRSA was found to have a flux of 1475 $\mu\text{M}/\text{min}$ ⁵⁸ The doubling times of MRSA and VREfm under geometrical growth conditions are nearly the same (~40 min), and

the source of this difference in flux is presently unknown. UDP-Sum then plateaus until 40 min before gradually decreasing.

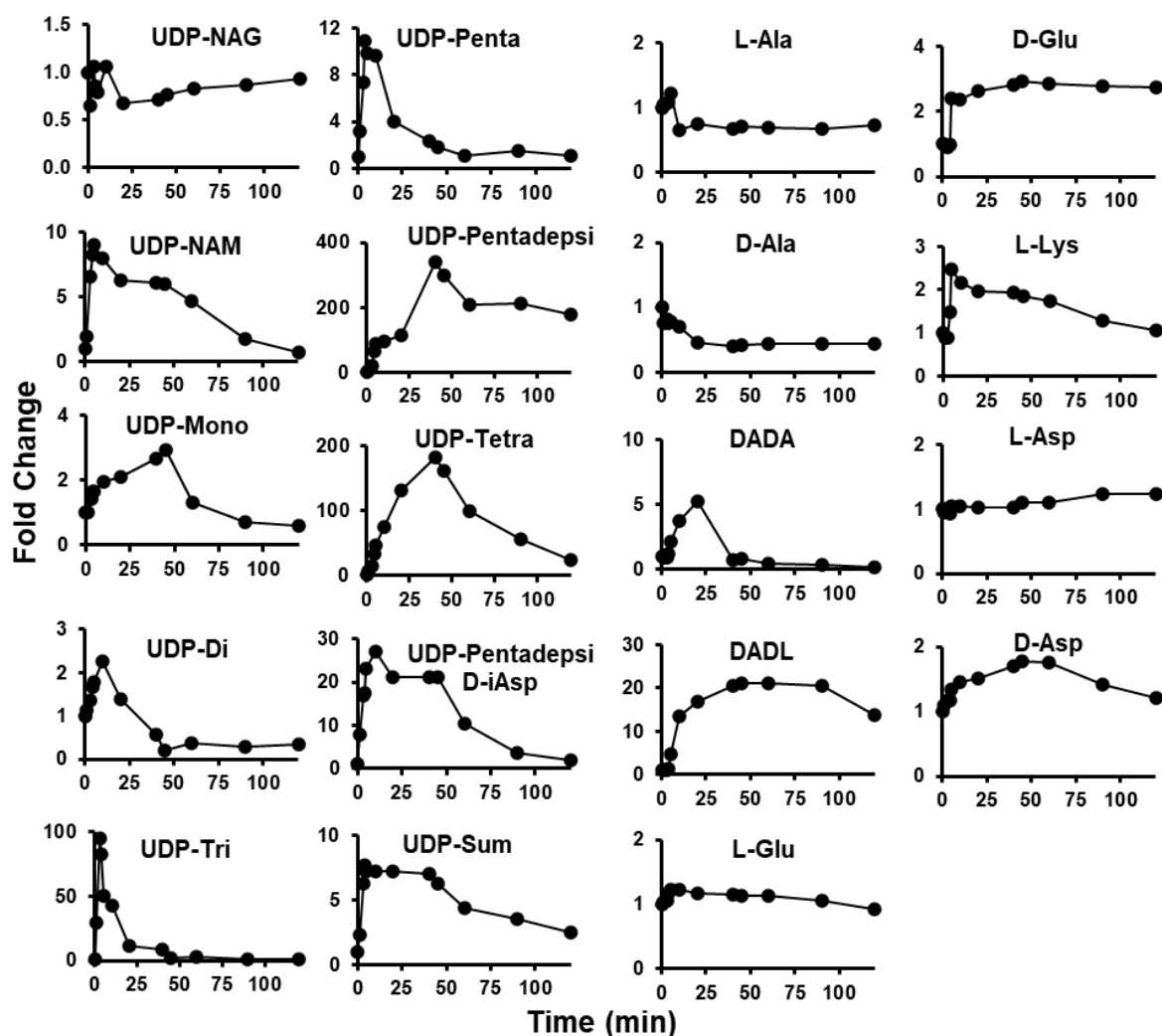


Figure 20 - Time course of VREfm PG intermediates in response to added vancomycin (16 $\mu\text{g/ml}$ added at a culture OD_{600} of 0.5), plotted as fold changes versus the time zero values (shown in Table 5). UDP sum is the sum of all UDP-linked intermediates DADA, D-Alanine-D-Alanine; DADL, D-Alanine-D-Lactate.

2.3.8 Growth curve of *VRE faecium*

We plotted growth curve of VREfm in absence and presence of 16 µg/mL vancomycin which is the subMIC of vancomycin against VREfm. The growth was observed for 500 mins. The doubling time for VREfm is 45 minutes. We observed that after adding vancomycin the growth of VREfm with added vancomycin was slow as compared to the control VREfm without vancomycin. The bacteria continued to grow thereby proving that VREfm is resistant towards vancomycin. The growth pattern of VREfm with and without vancomycin is shown in Figure 21.

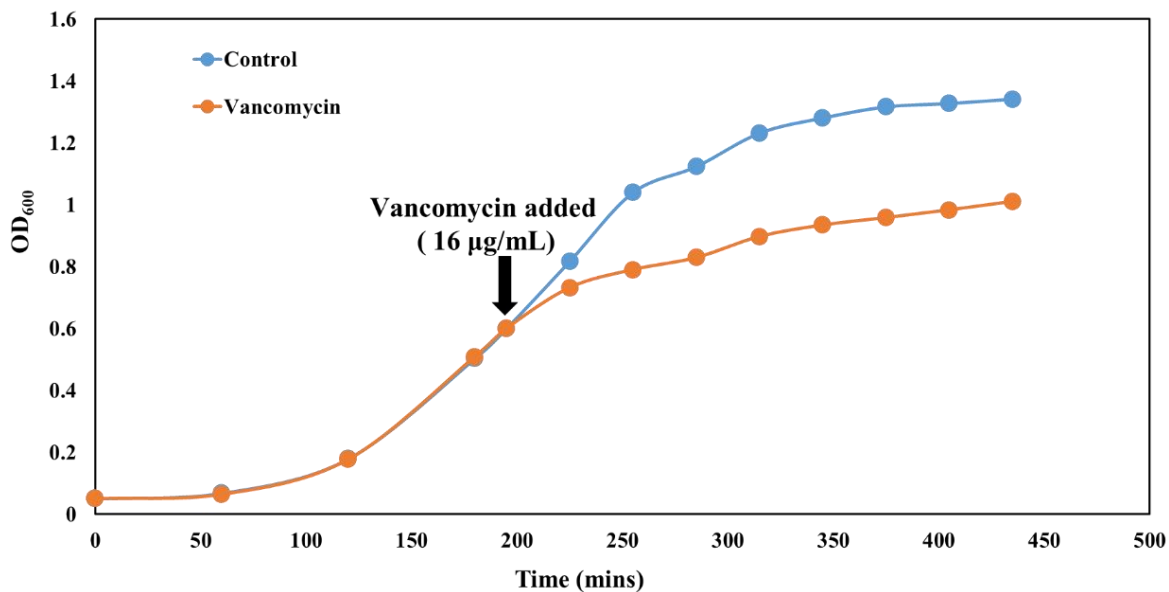


Figure 21- Growth curve of VREfm with and without vancomycin. The blue curve represents the control VREfm with no vancomycin and the orange curve represents VREfm with added vancomycin.

2.3.9 Time dependence of VanA gene induction

To assess the time dependence of VanA gene, RT-qPCR was used to quantitatively amplify VanA-type mRNA transcripts for VanH, VanA, VanX, VanY and VanZ proteins as a function of time after vancomycin exposure as shown in Figure 22. The response was rapid, as evident in the 1 min samples (collected immediately after vancomycin addition) – which show a definite increase over control samples (collected immediately prior to vancomycin addition). mRNA levels peaked within 15 min after vancomycin exposure, and then decreased over time. These observations are consistent with prior studies^{63 64 65}

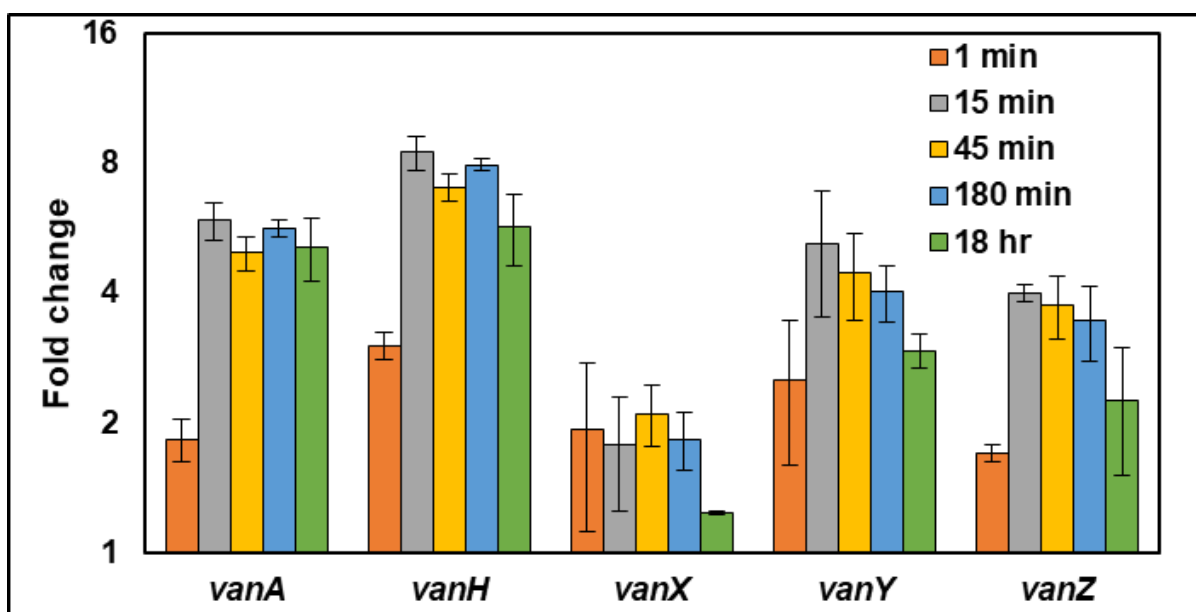


Figure 22 - Time course of the effect of vancomycin (16 µg/mL) on RT-qPCR determined mRNA levels in VREfm. Data is presented as mean ± SE (n = 3)

2.3.10 Vancomycin concentration dependence of VRE *faecium* metabolite and mRNA response

The effect of various concentrations of vancomycin on PG metabolite and mRNA levels after a 15 min exposure was also assessed shown in Figures 23 and 24. The midpoint for the effect

of vancomycin on the key PG metabolites (UDP-Penta, UDP-Pentadepsi, D-Alanine-D-Alanine) and mRNA levels was 1-4 $\mu\text{g/mL}$ vancomycin, and possibly higher (4-16 $\mu\text{g/mL}$) for mVanX, Y, and Z. The effect of increasing vancomycin was generally monotonic for most of these intermediates, except for D-Alanine-D-Alanine, which initially decreased at low vancomycin concentration and then approached normal levels at higher vancomycin concentration. Late-stage intermediates (UDP-Tri, -Penta, -Tetra, and -Pentadepsi) and D-Alanine-D-Lactate all increased substantially in response to increasing vancomycin concentration.

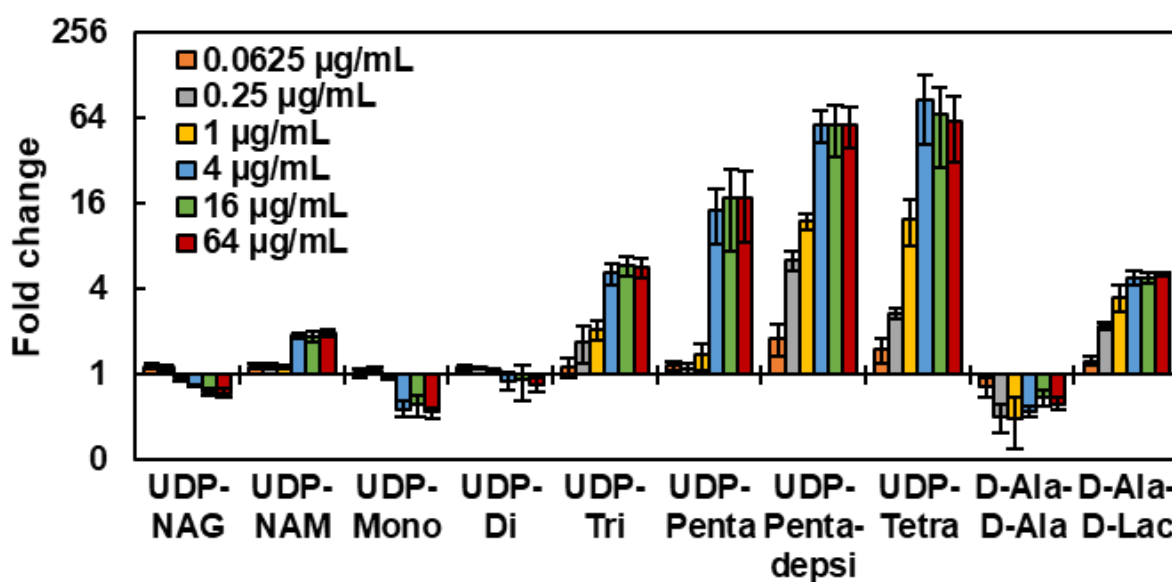


Figure 23 - Fold changes (relative to no-vancomycin control) in key VREfm PG intermediate levels after 15-min exposure to different vancomycin concentration ($n = 4$), shown with a semilogarithmic y axis.

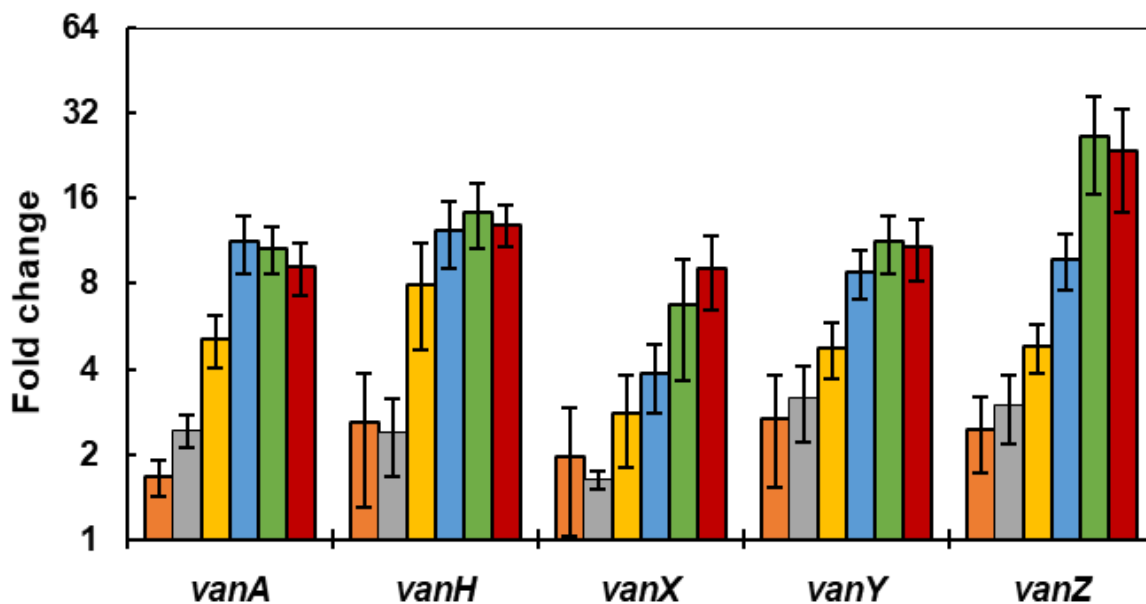


Figure 24 - Corresponding fold changes in mRNA levels (n = 4)

2.3.11 Effect of protein biosynthesis inhibition (linezolid) on metabolite levels after vancomycin exposure

To disentangle the effect of gene induction on metabolite levels in VREfm after vancomycin exposure, linezolid – a protein biosynthesis inhibitor effective against VREfm, was employed as shown in Figure 25. Linezolid alone increased UDP-NAG levels, and decreased later stage intermediates (UDP-Penta, UDP-Tetra, and UDP-Pentadepsi).

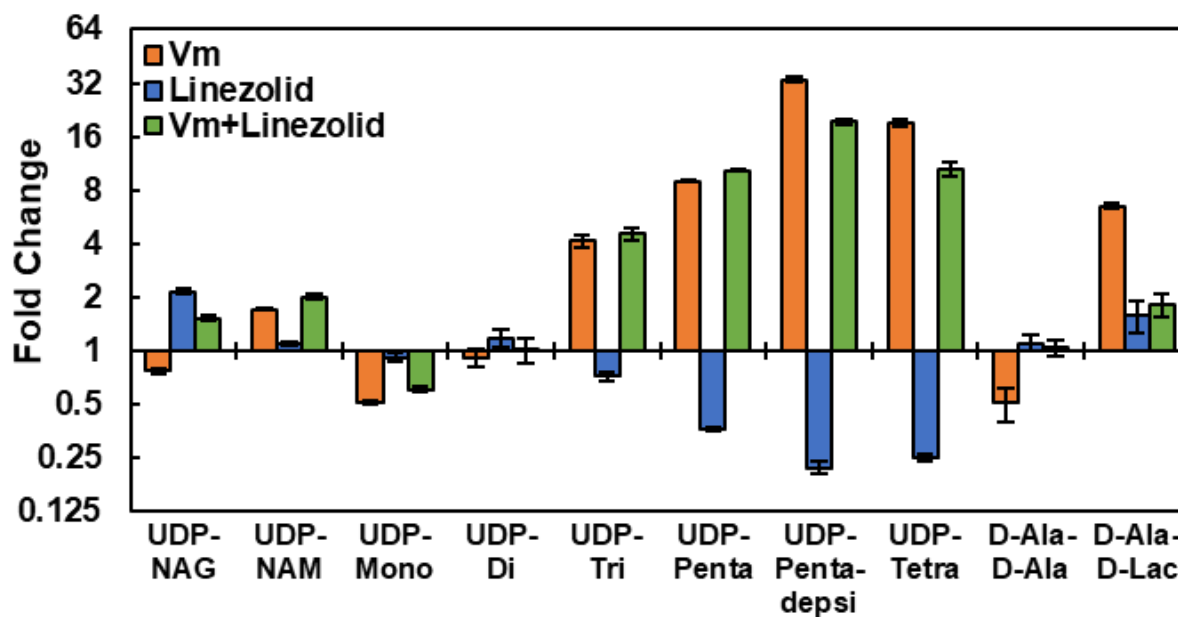


Figure 25 - Fold changes (relative to no vancomycin control) in key VREfm PG intermediate levels after 15-min exposure to vancomycin (Vm) and/or linezolid (n = 3), shown with a semilogarithmic y axis.

2.3.12 Effect of linezolid, vancomycin and rifaximin on mRNA gene pool levels

Figure 26 shows the difference in the mRNA level of each antibiotic and their combination with vancomycin. Vancomycin when combined with linezolid or rifaximin is showing induction of resistance gene van (A H Y Z). However, there is less induction seen in case of gene vanX. The antibiotics alone are not inducing the genes as compared to combinations.

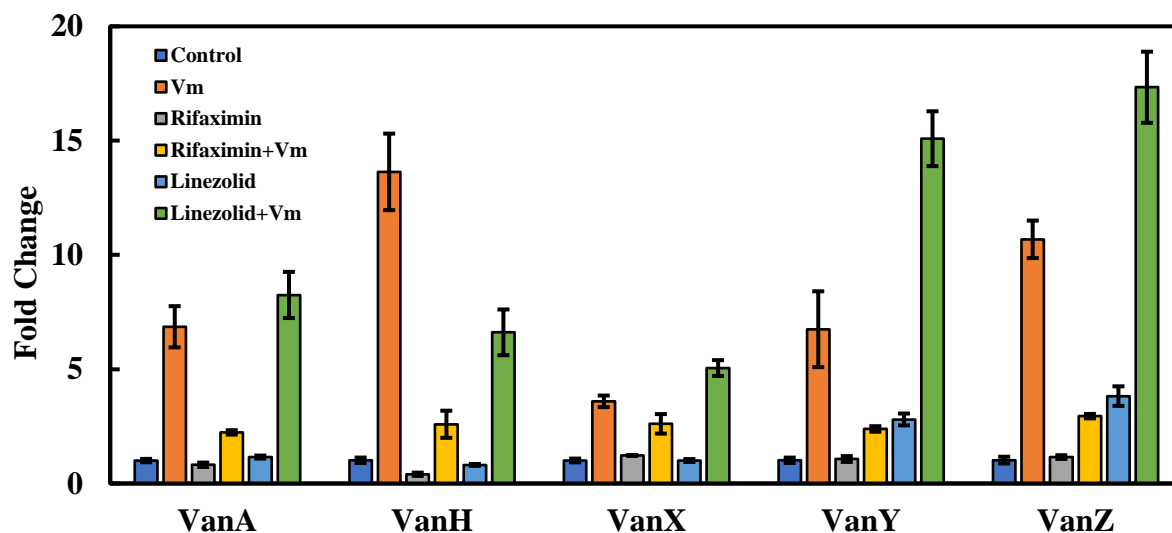


Figure 26 - Corresponding fold changes in mRNA levels (n = 4)

2.3.13 Comparison of metabolite extraction and amino acid derivatization after 15 and 90 mins.

UDP metabolites were extracted after both 15- and 90-min incubation period with different concentration of vancomycin. It was observed that both early metabolites like UDP-NAG, UDP-NAM, UDP-Mono and UDP Di, and late-stage metabolites like UDP-Tri, UDP-Tetra, UDP-Penta and UDP-Pentadepsi in VREfm showed better yield at 15 minutes than those at 90 mins. After this observation, 15 minutes were used as an incubation time after adding the antibiotics for all the experiments. The same observation was made after running the amino acid derivatized samples on LC-MS/MS. The comparison between both the time is shown in Figures 27 and 28.

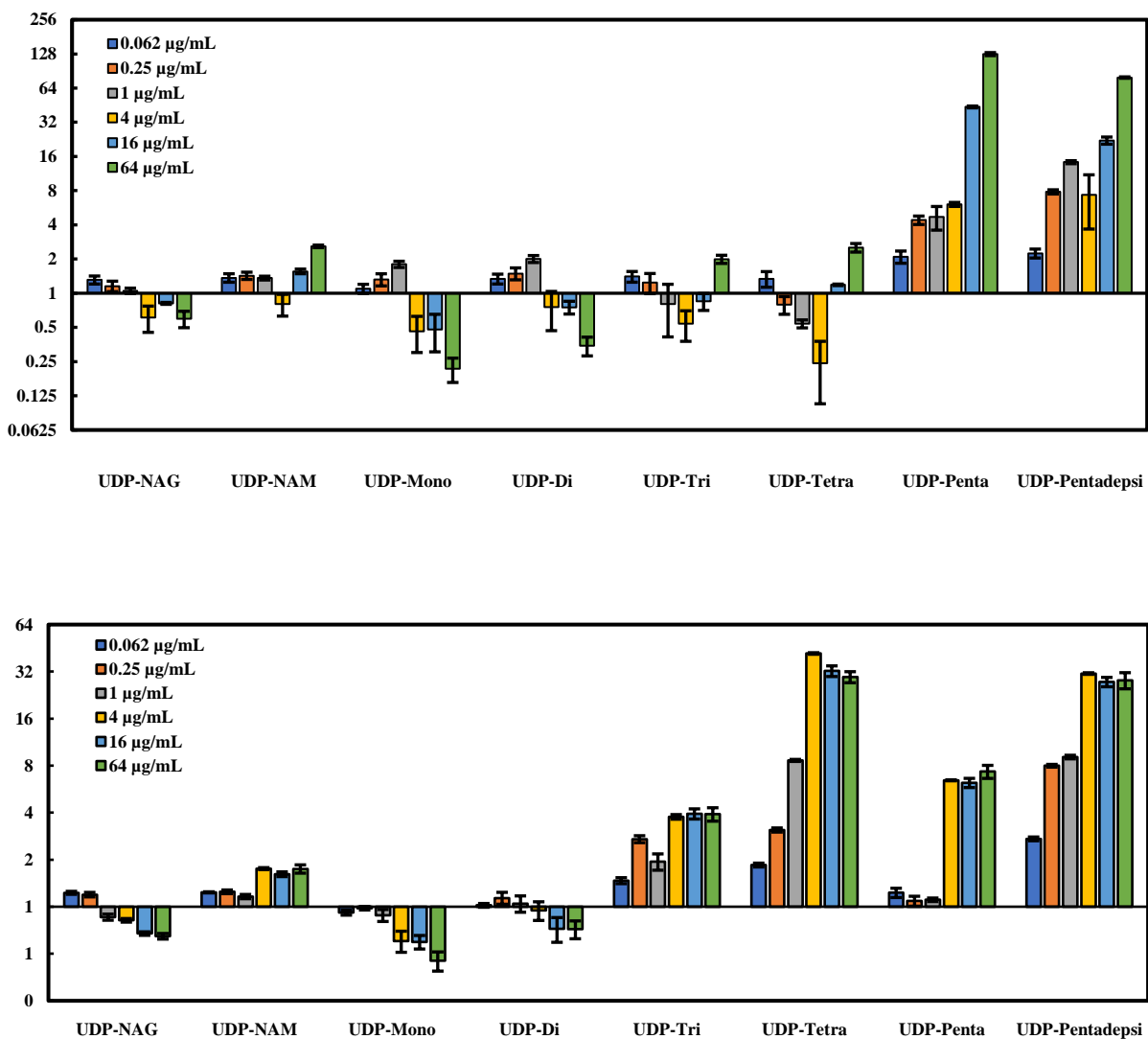


Figure 27 - Comparison of metabolite extraction at 90- and 15-mins incubation time. The figure above shows metabolites extracted at 90 mins and the figure below shows metabolites extracted at 15 mins. Y axis represents fold change.

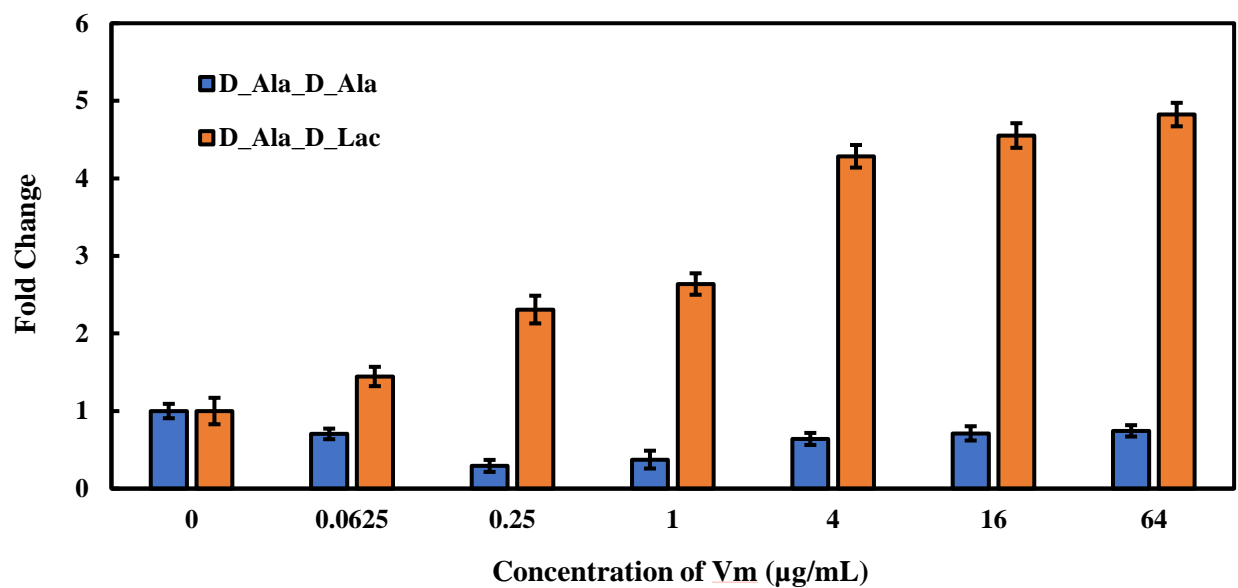
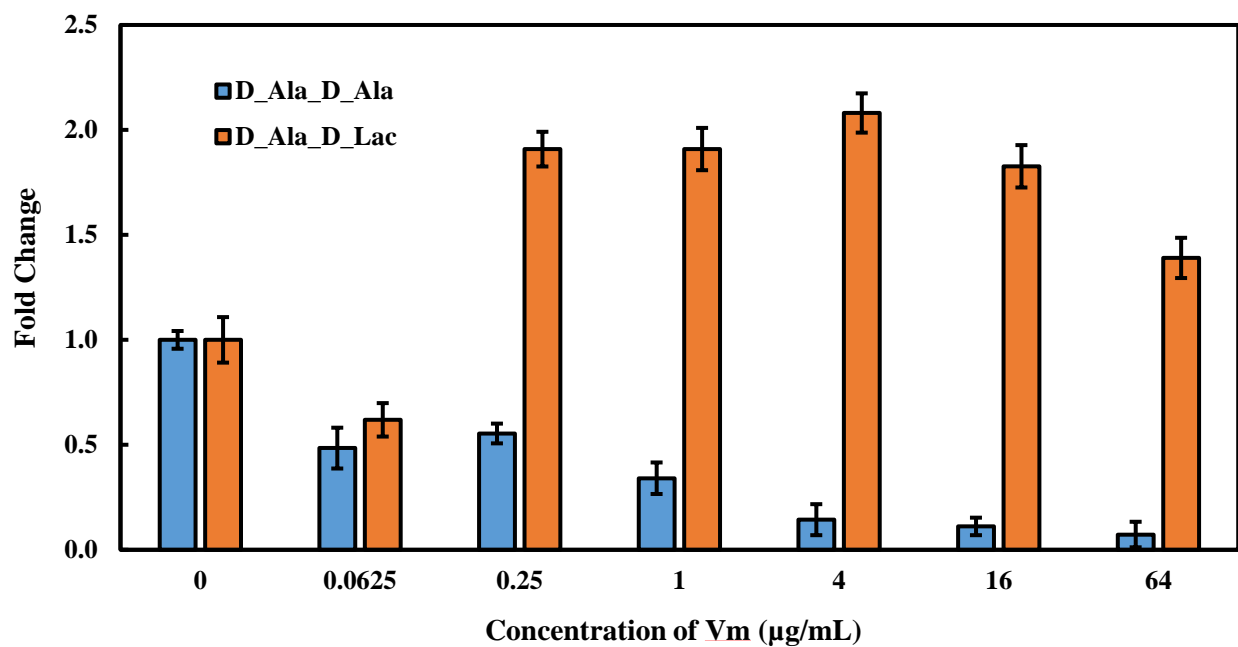


Figure 28 - Comparison between amino acid derivatized samples after 90 and 15 mins. The figure above shows amino acid derivatization after 90 mins of incubation and the figure below shows amino acid derivatization after 15 mins of incubation.

2.3.14 Proteomics on vancomycin-resistant *Enterococcus faecium*

After the protein isolation, VREfm peptides were made. These peptides were run on Waters Orbitrap. After the peptide study in VREfm, we observed that the crucial van genes required by VREfm to form a resistance alternate pathway in presence of vancomycin shows a 16-fold difference as compared to no vancomycin treated samples. Figure 29 shows all the resistance genes in red which are upregulated 16-fold after vancomycin exposure. Volcano plot is plotted by subtracting the control sample from vancomycin treated sample.

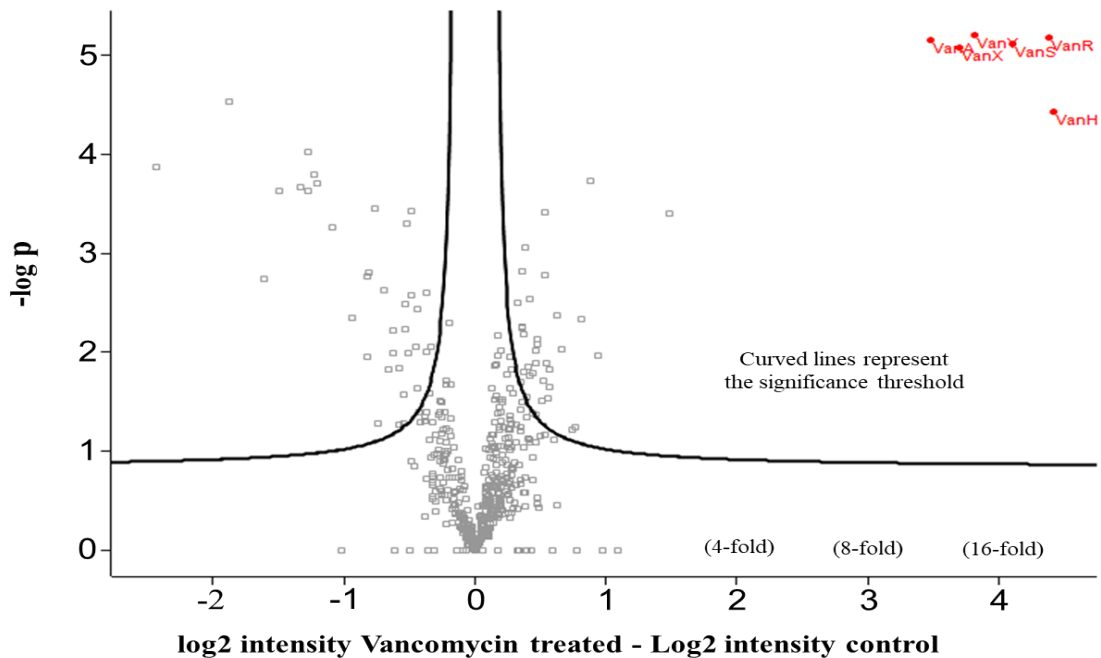


Figure 29 - Volcano plot showing the resistant genes (in red) upregulated 16-fold.

2.4 Conclusion

Bacterial peptidoglycan (PG) biosynthesis is the target of many important antibacterial agents^{66 67} VREfm is particularly problematic given its resistance to vancomycin and most other commonly used antibacterial agents^{39 68 69} Vancomycin resistance in VRE is due to the presence of gene cassettes that encode for alternative PG biosynthetic pathways⁴⁶ The most common of these clinically is VanA-type resistance in which D-Alanine-D-Alanine is replaced with D-Alanine-D-Lactate as shown in Figures 14, 15 and 16. The goal of this study was to investigate how cytoplasmic PG intermediate levels in VanA-type VREfm respond to vancomycin exposure, and to compare this response to MRSA and VSEfm. The first step in this study was to extend LC-MS/MS assays for the normal PG pathway intermediates developed previously^{58 59 60 61 62} to the unique intermediates responsible for vancomycin resistance in VREfm shown in Figures 14, 15 and 16. Purification of several of these intermediates from VREfm and ion pairing LC-MS/MS method development was straightforward based on these prior studies shown in Figure 18 and Table 4. Since vancomycin resistance involves induction of the alternative PG biosynthesis pathway, RT-qPCR was also used to provide complimentary data on the levels of VanA-type mRNA transcripts.

PG intermediate levels were first determined in both VSEfm and VREfm before and after vancomycin exposure shown in Table 5. Previously reported values from MRSA are also included for comparison⁵⁸ Several significant features are apparent. VSEfm shows much less vancomycin exposure associated UDP-linked intermediate accumulation (UDP-Sum) than MRSA, demonstrating a substantial difference in this pathway between VSEfm and MRSA. In VSEfm, the substantial reduction in early intermediates indicates reduced entry into the pathway is partially or wholly responsible for this effect. Continuing turnover of PG metabolites may also contribute

to this observation. In VREfm, both normal and alternative pathway intermediates accumulate substantially after a 90 min vancomycin exposure. After extended vancomycin exposure, levels of both normal and alternative pathway intermediates drop considerably. Somewhat unexpectedly, UDP-Penta – the normal pathway terminal PG intermediate – was only reduced to about ½ the no vancomycin level, equivalent to 2/3rds the level of UDP-Pentadepsi – the analogous vancomycin resistance pathway intermediate. An early study of VanA-type resistance in *E. faecalis* (VREfs) found a high UDP-Pentadepsi:UDP-Penta ratio of about 98:2 associated with a vancomycin MIC of 256 µg/mL⁵², whereas in this study a ratio of about 60:40 was observed with an MIC for vancomycin of 512 µg/mL. This observation indicates that a complete shift from D-Alanine-D-Alanine to D-Alanine-D-Lactate based intermediates is not required for high-level vancomycin resistance.

D-isoAsp containing intermediates have been identified in *E. faecium* in prior studies^{53 56 70}. These intermediates (UDP-Penta-D-iAsp, UDP-Pentadepsi-D-iAsp and UDP-Tetra-D-iAsp) were observed in VREfm shown in Table 5 but were undetectable in VSEfm. The step at which D-Asp is added to nascent PG has been unclear. Indications are that it is preferentially added to the Lipid I PG intermediates, but with addition to UDP-Penta and UDP-Pentadepsi intermediates observed in cells targeted with late stage CWB inhibitors⁵³. The results observed here are consistent with and support this interpretation.

Time course experiments for VREfm metabolite levels shown in Figure 20 and mRNA levels shown in Figure 22 were then performed. Similar data for VSEfm, overlaid with the VREfm data, is shown in Figure 19 using a semi-square root x-axis to expand and highlight early changes in metabolite levels. A key observation in VREfm is that normal pathway intermediates generally respond rapidly to Vm exposure – peaking in 3-5 min, whereas alternative pathway

intermediates peak around 30-45 min. PG intermediates in VSEfm initially respond similarly to VREfm, but then begin to drop relative to VREfm after 3-5 min, except for UDP-Penta in VSEfm which increases more dramatically than in VREfm. This indicates that the PG pathway is more completely blocked in VSEfm than in VREfm, which is as expected. These observations also indicate that entry into the UDP-linked intermediate part of this pathway is substantially reduced in VSEfm relative to VREfm after vancomycin exposure. Similar time course experiments in MRSA show a continuous increase in UDP-Penta and UDP-Sum accumulation for up to 120 minutes after vancomycin exposure⁵⁸, in stark contrast to VSEfm and VREfm which show accumulation to a peak level between 5-20 minutes shown in Figures 20 and 19, and then decreasing levels of these intermediates. These observations indicate that the entry into the UDP-linked intermediate part of this pathway is down regulated in *E. faecium* in response to vancomycin exposure, in contrast to MRSA in which UDP-linked intermediates accumulate unabated in response to vancomycin exposure.

A time course of mRNA transcript levels for key *vanA* genes was also performed shown in Figure 22 mRNA levels rose quickly, showing a significant jump even at one minute and reaching a plateau within 15 minutes. This time frame precedes that over which alternative pathway intermediates (UDP-Pentadepsi, UDP-Tetra, and D-Alanine-D-Lactate) rise to maximum levels and then began to decrease as shown in Figure 20. It is also noted that there was a noticeable lag in D-Alanine-D-Lactate, UDP-Pentadepsi, and UDP-Tetra profiles shown in Figure 19.

The effect of vancomycin concentration on metabolite and mRNA levels was also assessed after 15 min exposure shown in Figures 23 and 24. A midpoint for effect on metabolite levels was 0.25-1 $\mu\text{g/mL}$, whereas the midpoint for effect on mRNA levels appeared slightly higher at 1-4 $\mu\text{g/mL}$. The maximal effect on metabolite levels was at 4 $\mu\text{g/mL}$, whereas for mRNA it was at 16

μg/mL. UDP-Penta shows a sudden transition from -Vm levels to +Vm levels at 4 μg/mL. Most other metabolites show a monotonic shift to the +Vm state.

To assess the role of gene induction in the observed metabolite pool changes, an experiment using linezolid to block new protein biosynthesis was performed as shown in Figure 25. Somewhat surprisingly, linezolid in the absence of vancomycin suppressed later UDP linked intermediate levels (UDP-Penta, -Pentadepsi, and -Tetra), increased the UDP-NAG level, and had no significant effects on D-Alanine-D-Alanine or UDP-Tri levels. This indicates that one of the enzymes in this pathway (MurA-E) may have a relatively short half-life, with activity loss contributing the lower observed later metabolite levels, and modest accumulation of the upstream UDP-NAG intermediate. Combination of linezolid with vancomycin resulted in a nearly identical metabolite level change pattern as observed with vancomycin alone. This observation indicates that basal alternative pathway enzyme levels are sufficient for a substantial shift towards the vancomycin induced state even in the absence of new protein biosynthesis. Exceptions to this observation are apparent for D-Alanine-D-Alanine and D-Alanine-D-Lactate, indicating that for these intermediates the shift to the vancomycin induced state is dependent on new protein biosynthesis.

PART II: CHEMICAL LIBRARY SCREENING FOR NEW ANTIBACTERIAL DRUG
DISCOVERY

CHAPTER 3

3. INTRODUCTION AND LITERATURE REVIEW

3.1 Methicillin-resistant *Staphylococcus aureus*

Methicillin-resistant *Staphylococcus aureus* (MRSA) first emerged in England in 1961 and has disseminated globally²⁶⁴ MRSA was responsible for many outbreaks and became known as healthcare-associated MRSA. It has become a leading cause of bacterial infection in the community and the health care system⁷² It is associated with high rates of mortality and morbidity. It is a gram-positive bacteria that is non-motile cocci as shown in Figure 30. *Staphylococcus* genus has a lot of species and subspecies, but *S. aureus* is the most clinically relevant strain^{73 74} It is usually found in the human microbiota. With a disruption in the mucosal and cutaneous barrier, for instance, in chronic skin conditions, this bacteria enters the underlying tissue and bloodstream. Patients with compromised immune systems and invasive medical devices are also at a high risk of getting MRSA infection⁷⁵ The drug methicillin was widely used, but due to its increased toxicity, it has been largely replaced by other penicillins. MRSA can cause various infections, such as endocarditis, pneumonia, soft tissue infections and bloodstream infections.

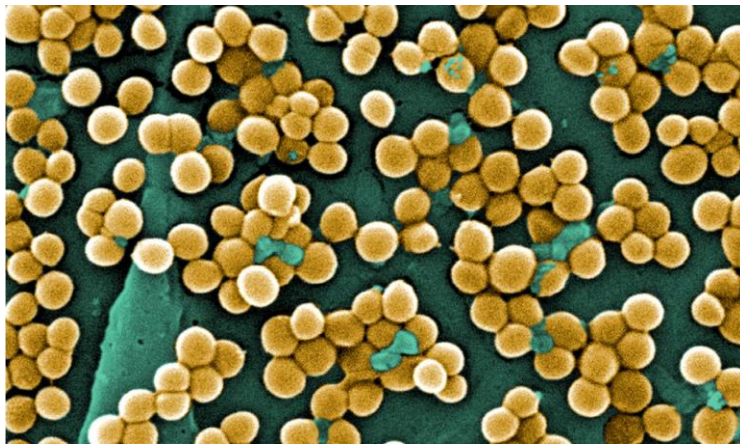


Figure 30 - Methicillin resistant *Staphylococcus aureus*⁷⁶

3.2 Pathophysiology of methicillin resistant *Staphylococcus aureus*

The contamination of MRSA can develop due to the colonization of the bacteria, and the leading site for the infection is the nose. However, colonization can also occur in the throat and perineum^{77 78} When we talk about colonization of MRSA, 15% is permanent colonization, where the infection stays in the body. In contrast, intermittent infection is about 70%, where the infection comes and spontaneously gets cleared. However, 15% of patients are non-carrier of this infection, which means that they never get MRSA infection⁷⁹ MRSA has several virulence factors, which include host cell-damaging, adhesive, and immunomodulatory molecules and such virulence factors vary between clones⁸⁰ The initiation of infection in bacteria starts when the bacteria transfers itself from the nose to the other wounded part of the skin as depicted in Figure 31. The surface proteins on MRSA help the bacteria attach and multiply in the wounded tissue and this starts a local inflammation in the tissues^{81 82}

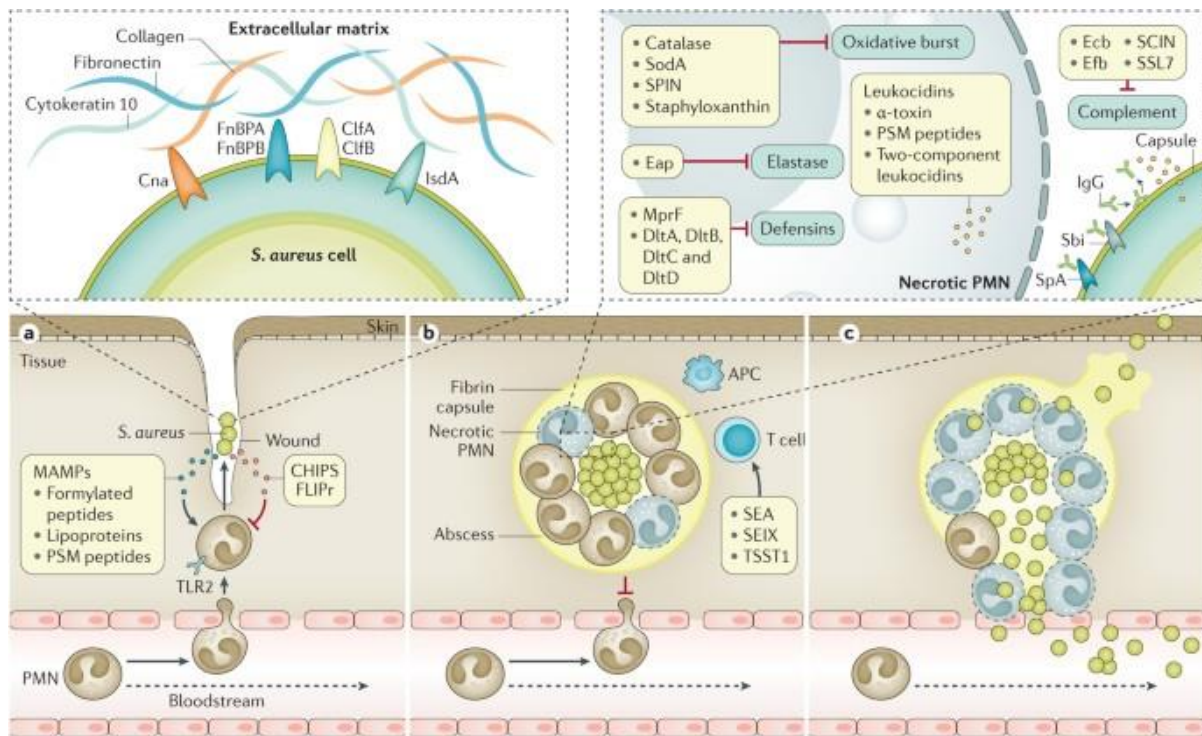


Figure 31 - Stages of *Staphylococcus aureus* infection⁷²

3.3 Antibiotic resistance in methicillin-resistant *Staphylococcus aureus*

Widespread use and misuse of antibiotics have led to the development of resistance in many bacterial species. People with MRSA colonization, for instance (presence of bacteria in the body that do not cause a host immune response, clinical signs, cellular damage, or any symptoms of infection) are prone to the risk of MRSA infection and are a source of person-to-person contact transmission. The spread of MRSA occurs via two mechanisms 1) acquisition of SCCmec gene by methicillin-sensitive *S. aureus* and 2) spread of resistant clones to both human and pathogenic strains⁷² By 1960, MRSA acquired SCCmec complex by several multidrug-resistant strains which showed resistant towards penicillin, tetracycline, streptomycin, and erythromycin⁸³ This made MRSA resistant towards most of the β -lactam family of antibiotics. There are twelve known SCCmec, among which Type I, II, and III are large SCCmec elements responsible for resistance to several antibiotic classes. They are mostly found in healthcare-associated MRSA. Some smaller SSCmec, such as type IV, and V are found in community-acquired MRSA. All SCCmec types consist of *mecA* that encodes for penicillin-binding proteins 2a (PBP2a) a peptidoglycan transpeptidase enzyme that cross-links the peptidoglycan in the bacterial cell wall. Beta-lactam family of antibiotics like penicillin and methicillin bind to the active site of PBP and prevent cell wall formation. PBP2a shows low affinity towards beta-lactam antibiotics. MRSA can produce modified PBP that no longer allows beta-lactams to bind to them. There is a second way in which MRSA can acquire resistance: the efflux pumps. These pumps are proteins that help remove antibiotics from the bacterial system before they start affecting it. When these efflux proteins overexpress, it leads to resistance in MRSA⁸⁴ Resistance in MRSA is acquired through mutations, horizontal gene transfer, and gene amplification. However, horizontal gene transfer is a critical cause of bacteria gaining resistance by acquiring new genetic material. This process can occur

through the transfer of transposons and plasmids between MRSA strains. Figure 32 shows the antibiotic targets against MRSA.

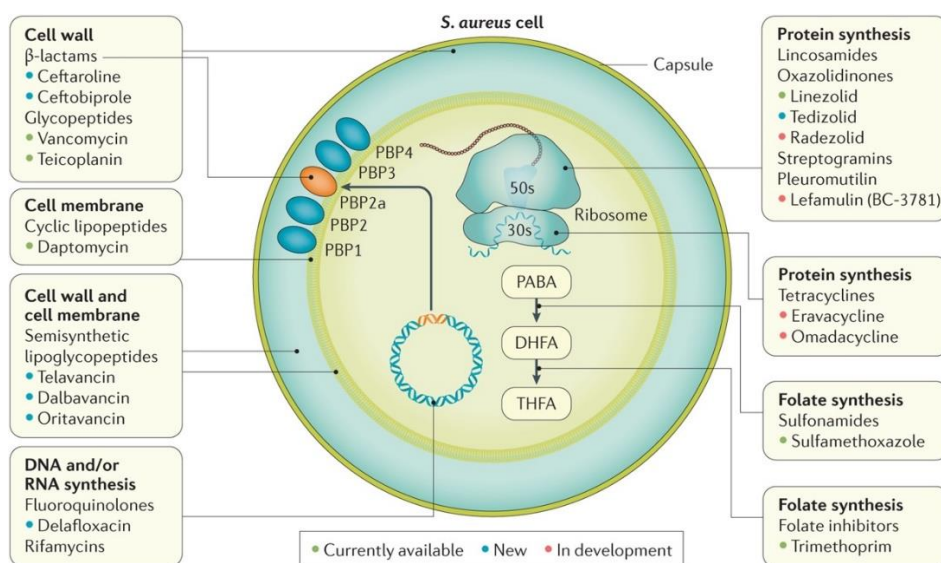


Figure 32 - Bacterial targets of antibiotics active against MRSA⁸⁵

3.4 Challenges in antibacterial discovery

Irrespective of the molecular target of the drug and chemical class, resistance has evolved towards several antibiotics ever placed in clinical practice⁸⁶ The earliest antibiotics were first identified by Alexander Fleming (penicillin) and Selman Waksman (streptomycin) in academic laboratories⁸⁷ After the Second World War, commercialization of penicillin and streptomycin began. Big pharmaceutical companies like Bristol, Merck, Abbott, Pfizer, Roche, and Glaxo became leaders in antibiotic drug development and maintained research on such drugs for decades⁸⁸ However, the discovery of new antibacterial agents is becoming crucial because of the resistance developing in the bacteria against a particular drug.

Antibiotic resistance is the ability of bacteria to resist the effect of antibiotics and therefore rendering them ineffective. Such resistance takes place when there is prolonged use of an antibiotic in patients. It also occurs due to genetic mutations, gene transfer between the bacteria allowing them to survive in the presence of an antibiotic. This increasing prevalence is becoming crucial and therefore highlights the need for the development of new antibiotics⁸⁹

Another major challenge in antibacterial discovery is the need for understanding of the mechanism of action of bacterial machinery and infection. Bacteria are ubiquitous and have diverse and complex biological systems that enables the bacteria to survive in various environments. To understand the mechanism of their growth and survival, one needs to understand the process and identify new targets for antibacterial drugs, which is a challenging task. Moreover, bacteria survive inside a host, which makes it difficult to target them with antibacterials⁹⁰ High cost of antibacterial drugs also adds to significant challenges in antibacterial discovery. Regulatory challenges are also another hurdle in antibacterial discovery. Such a process is complex and requires clinical trials and approval by regulatory bodies like FDA. This approval process is complicated due to the emergence of antibiotic resistance that requires additional clinical trials to demonstrate the efficacy of new antibiotics⁹¹ Furthermore, technical challenges are also a significant cause in antibacterial discovery that involves difficulty targeting bacterial pathogens while leaving the host's cell intact. Antibacterial drugs should target only the bacteria and not the host cell because this might lead to harmful side effects. New antibiotic drug development also requires knowledge and understanding of microbiology, biology, and chemistry⁹¹ Lastly, financial incentive absence for drug development plays a critical role in antibacterial drug discovery. This process has led to a decline in drug development leading to many infectious diseases without

proper treatment. Therefore, antibacterial drug discovery is a challenging and complex area of research. The difficulties in drug discovery are shown in Figure 33.

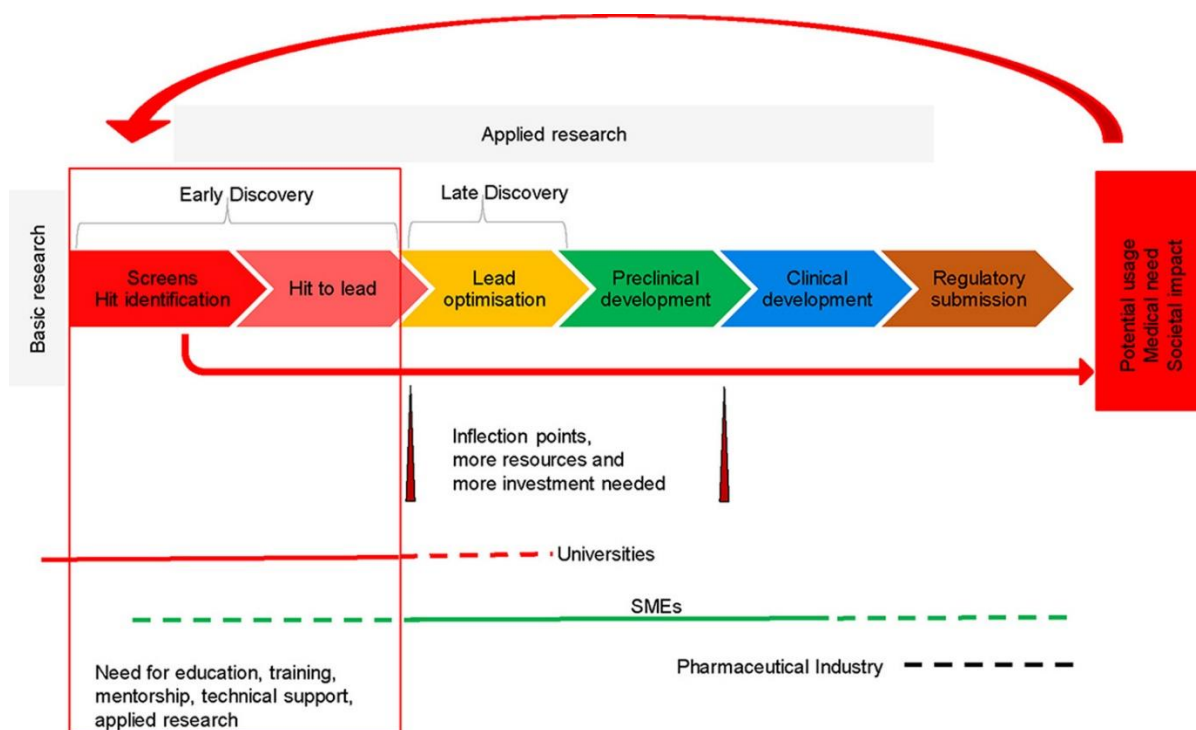


Figure 33 - Drug discovery challenges⁹²

3.5 Drug discovery

The modern era of antibiotics started when penicillin was discovered by Sir Alexander Fleming in 1928⁹³ Since that time, antibiotics have saved millions of lives and transformed modern medicine⁹⁴ as shown in Figure 34. Penicillin was a successful antibiotic that controlled many bacterial infections during World War II shortly by enabling effective control against infections caused by gram-positive pathogens such as *Staphylococcus*, *Streptococcus* and *Mycobacterium tuberculosis*. However, shortly after its demand, Penicillin resistance became a major clinical problem^{95 96}

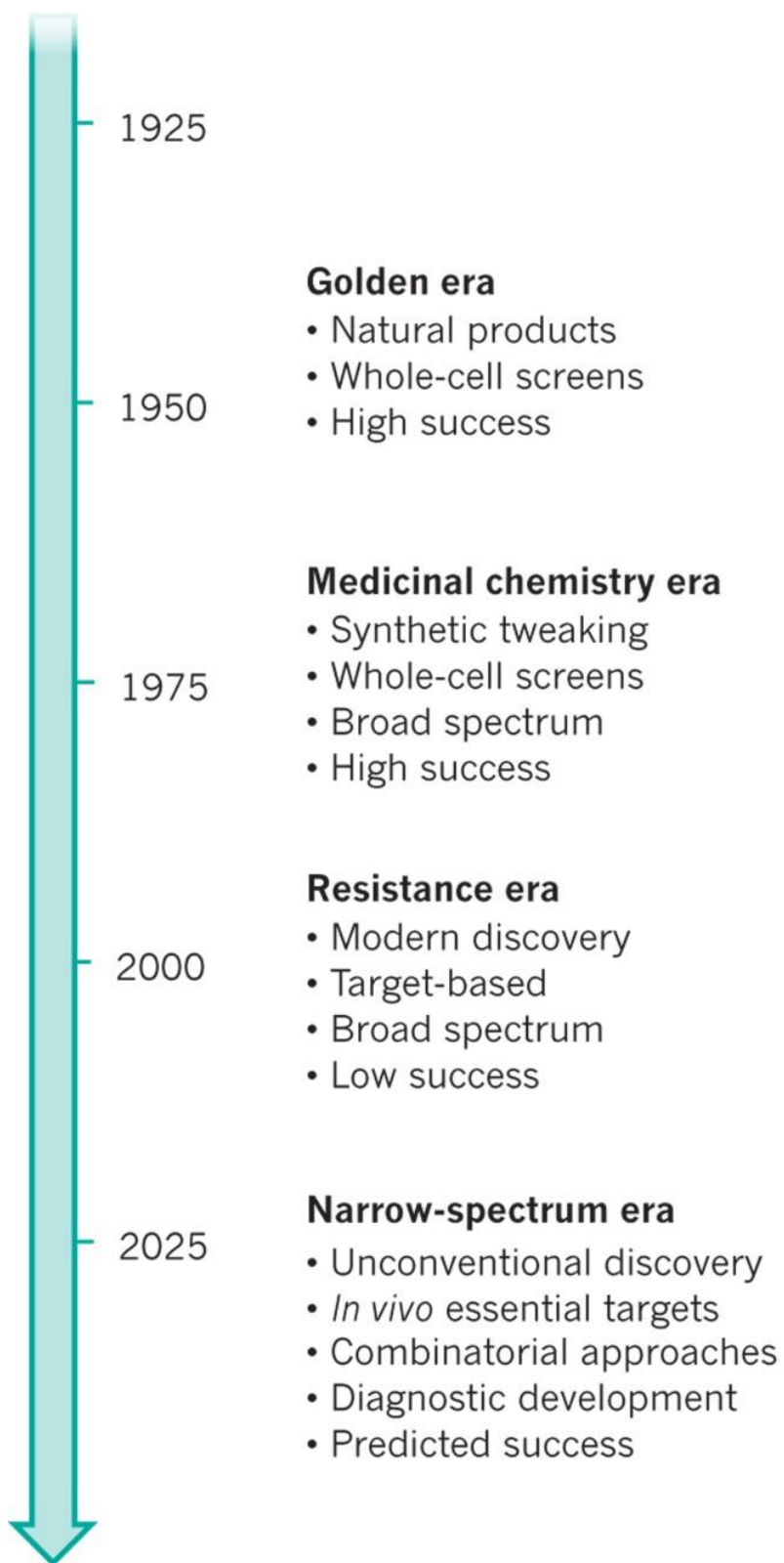


Figure 34 – Eras in drug discovery⁹⁷

Table 6 – Drugs and their targets with their mode of actions⁹⁷

Chemical class	Target	Mode of action	Examples
Sulfonamides*	Folate synthesis	Bacteriostatic	Sulfanilamide Penicillins Cephalosporins
β -Lactams†	Cell-wall synthesis	Bacteriocidal	Carbapenems Spectinomycin Kanamycin
Aminoglycosides†	Protein synthesis	Bacteriocidal	Neomycin Tetracycline
Tetracyclines†	Protein synthesis	Bacteriostatic	Doxycycline
Chloramphenicols†	Protein synthesis	Bacteriostatic	Chloramphenicol Erythromycin
Macrolides†	Protein synthesis	Bacteriostatic	Clarithromycin Vancomycin
Glycopeptides†	Cell-wall synthesis	Bacteriocidal	Teicoplanin
Oxazolidinones*	Protein synthesis	Bacteriostatic	Linezolid
Ansamycins†	RNA synthesis	Bacteriocidal	Rifamycin
Quinolones†	DNA synthesis	Bacteriocidal	Ciprofloxacin
Streptogramins†	Protein synthesis	Bacteriocidal	Pristinamycin

1. *Synthetic chemical
2. †Natural product

The antibiotic resistome, which is also known as the global collection of microbial resistance genes in the microbial world and is found in the environment and samples, is genetically diverse and widespread throughout the environment^{98 99} The use of many antibiotics has caused

multidrug resistance and is eroding the ability to curb various kind of infections. Synthetic molecules were the first antimicrobial agents discovered by screening libraries of chemicals in dyes. It was assumed that the screening would develop metabolites of bacteria and fungi and could be used to treat infection in humans with minimal toxic side effects. Sir Selman Waksman who also discovered streptomycin used soil-dwelling bacteria to produce metabolites. This process was later known as Waksman platform⁹⁷. This screening process led to the discovery of many antimicrobials. However, this screening process did not help identify new and effective antibiotics because of the pharmacological and toxicological effects of the metabolites produced. Along with this the resistance through horizontal gene transfer was also becoming a problem. This issue gave rise to the era of screening. Medicinal chemistry involved a synthetic version of natural metabolite and improved the application of antibiotics by increasing antimicrobial spectrum and lower doses⁹⁷

As our understanding of pathogenesis and molecular mechanism of drug action continues to improve progress is expected in the field of drug discovery. After medicinal chemistry drug's success came a new scaffold that began in the 1960s and lasted until the 1990s. This involved various innovative drug discovery approaches involving manipulations of recombinant DNA to produce desired proteins and high throughput screening of chemical libraries. Along with this the computing revolutions made it much easier to handle large sets of data. There have been recent advances that have led to the improvement and success of drug discovery. These advances are artificial intelligence and machine learning, high-throughput screening technologies, and structural biology such as X-ray crystallography and cryo-electron microscopy.

3.6 Chemical library screening

Chemical library screening (CLS) is a widely used approach in drug discovery. High throughput screening (HTS) is one such approach that has gained popularity over the years and is now a standard method for antibacterial drug discovery as shown in Figure 36. This process involves screening and assaying many drugs against a specific target. The libraries can be protein, chemical, peptide, or genomic libraries. The main purpose of HTS is to accelerate drug discovery by screening many drugs in a short period. It can also be used to characterize toxicological, metabolic, and pharmacokinetic data about new drugs leading to cost reduction. The screening process involves target selection that is involved in a disease or a biological process of interest. This target can be an enzyme or a receptor. The second step involves library preparation, where the compounds are added to a microtiter plate. Step third involves an assay development that measures the activity of the target molecule in the presence of a chemical library. Step fourth involves screening the library to identify compounds that interact with the target molecule. We obtain hits at this step. Positive hits are further evaluated to determine their pharmacological properties, potency, or selectivity¹⁰⁰ The final step involves hit validation which involves retesting the compounds in the assay and verifying their activity. The advantages of HTS include a) This automated system allows rapid screening of large libraries. Initially, 96 well plates were used, but these plates are now replaced by higher density microplates with 1536 wells per plate. The working volume of the compound is from 2.5 μ l to 10 μ l¹⁰¹ Therefore, it is possible to screen 10,000 compounds per day with the help of HTS b) Chemical libraries may include compounds of diverse chemical properties and structures c) it is a cost-effective approach to drug discovery.

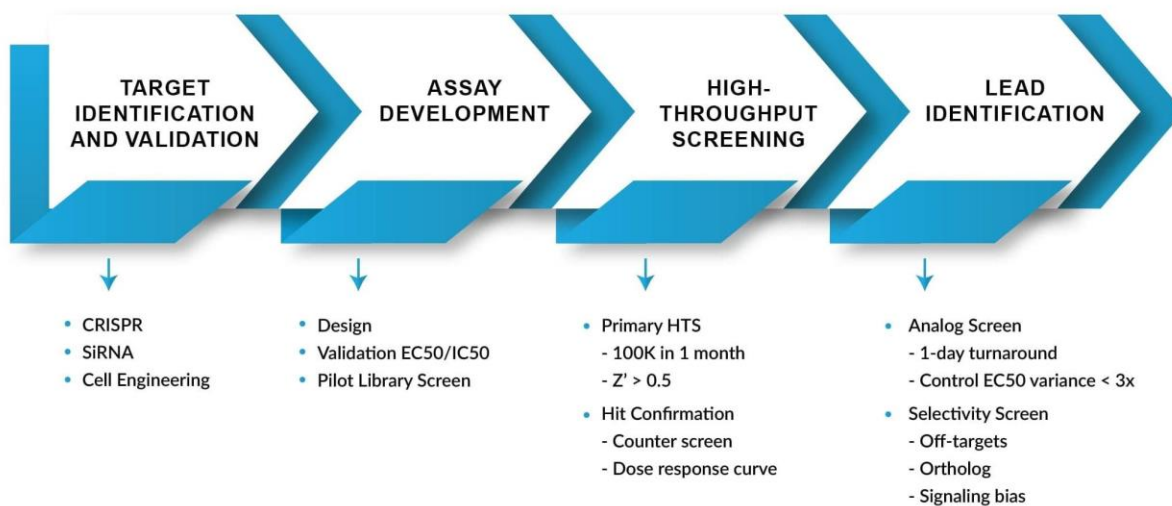


Figure 35 - Workflow of high-throughput screening¹⁰²

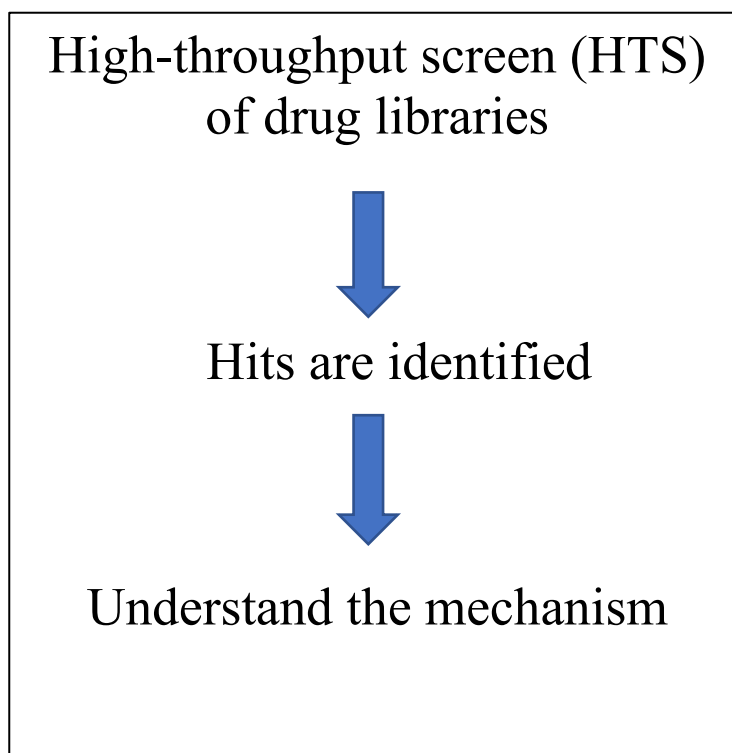


Figure 36 - Top-down approach

HTS as depicted in Figure 35 is one of the most commonly used technologies in pharmaceutical and biotechnology industries due to its potential offering of information-rich results, which started as an empirical drug discovery approach but, with the advent of automation and system biology approaches, are now also being used for different downstream application for lead optimization¹⁰³

3.7 Drug metabolism

Drug metabolism is a critical step in pharmacology and is responsible for the transformation of drugs inside the body. According to the definition, drug metabolism is a process of transformation or chemical modification of a xenobiotic substance or a drug by the body to help eliminate from the body. This process occurs in the presence of various enzymes and pathways that combine to convert the drug into its metabolite that can be easily excreted from the body. The main site for drug metabolism is the liver but other organs, such as the intestines, kidneys, and lungs can also metabolize drugs. Figure 37 shows all the pathways for drug metabolism. Two types of enzymes are involved in drug metabolism: Phase I and Phase II. Phase I metabolism involves reactions like oxidation, hydrolysis, and reduction. Cytochrome P450 (CYP) enzymes play a crucial role in phase I metabolism by oxidizing many drugs, toxins, and endogenous compounds. These enzymes are a group of hemoproteins located in the liver cells endoplasmic reticulum and have high specificity towards a substrate. Different isoforms of CYPs metabolize different drugs. Phase II metabolism involves the conjugation of Phase I metabolite with endogenous molecules like sulfate, glutathione, and glucuronic acid. This process helps to increase the water solubility of the metabolite. Some examples of phase II reactions involve sulfation, glucuronidation, methylation, and acetylation. Drug metabolism is influenced by many factors such as age, gender,

drug interaction, disease, and genetic variability¹⁰⁴ The use of in vitro systems in drug metabolism has become crucial throughout drug discovery. The advantages include reducing the use of live animals, speed and investigating the metabolic disposition of a compound¹⁰⁵

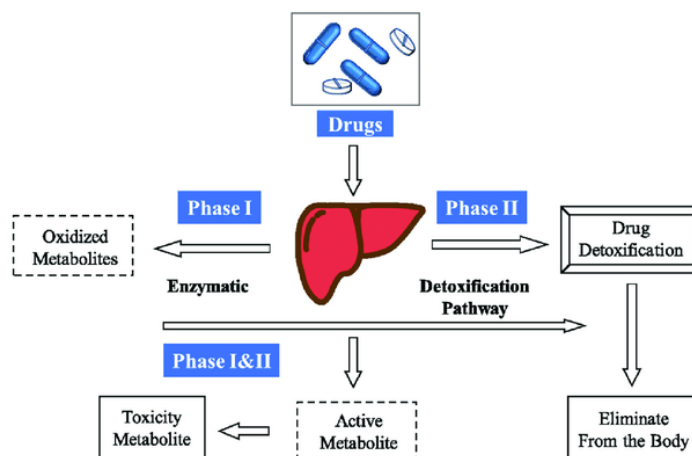


Figure 37 - Pathways for drug metabolism¹⁰⁶

3.8 Drug metabolite identification

Many analytical techniques that have developed an automated high-throughput techniques to identify complete or almost complete coverage of a genome and proteome. However, the chemical diversity of a metabolome is complex and broad, and the analytical tools need to isolate and identify chemically different compounds. Therefore, metabolomics requires different analytical techniques such as HPLC, GC, LC-MS, GC-MS, NMR^{107 108 109} as shown in figure 38. Metabolomics is not even close to automation or high-throughput data generation due to its complexity, and the most difficulty is to identify the complex metabolites. The computational and spectral databases are also insufficient to identify a metabolite therefore, metabolite identification becomes slow and almost incomplete. Compound identification is why high-resolution

chromatographic and spectroscopic methods have become so popular in chemistry research laboratories worldwide. Metabolite identification can be of two types. When we look for a specific metabolite, or class of metabolites, this type of selective metabolite identification is called targeted metabolomics. The other type is untargeted metabolomics. All the metabolites in the samples are studied irrespective of chemical class or character. However, untargeted metabolomics still does not get a complete picture of all the metabolites present in an organism. 5000 metabolites that exist as commercially available including 1100 core metabolites, 1200 US-approved FDA drugs and 1300 approved food additives, and 1500 phytochemical metabolites¹¹⁰ Drug metabolite identification requires several steps including sample preparation, separation, detection, and characterization. The metabolites can be extracted from various biological fluids and tissues like urine, plasma, blood and, microsomes. The methods involved in metabolite quantification are liquid chromatography, gas chromatography, mass spectrometry, nuclear magnetic resonance (NMR), and high-resolution imaging techniques like MALDI-TOF. The first step is sample preparation which involves isolating metabolites from biological samples. After the sample preparation, the sample is separated with the help of chromatography which separates it based on size, polarity, and charge. The next step involves metabolite detection using various detectors like UV-visible, mass spectrometry, and NMR. Among all these techniques, mass spectrometry is the most used technique due to its specificity and high sensitivity. In the last step, metabolites are characterized by MS/MS, NMR and high-resolution imaging where MS/MS provides the structural information on metabolites and high-resolution imaging like MALDI-TOF shows the spatial localization of metabolites in tissues¹¹¹

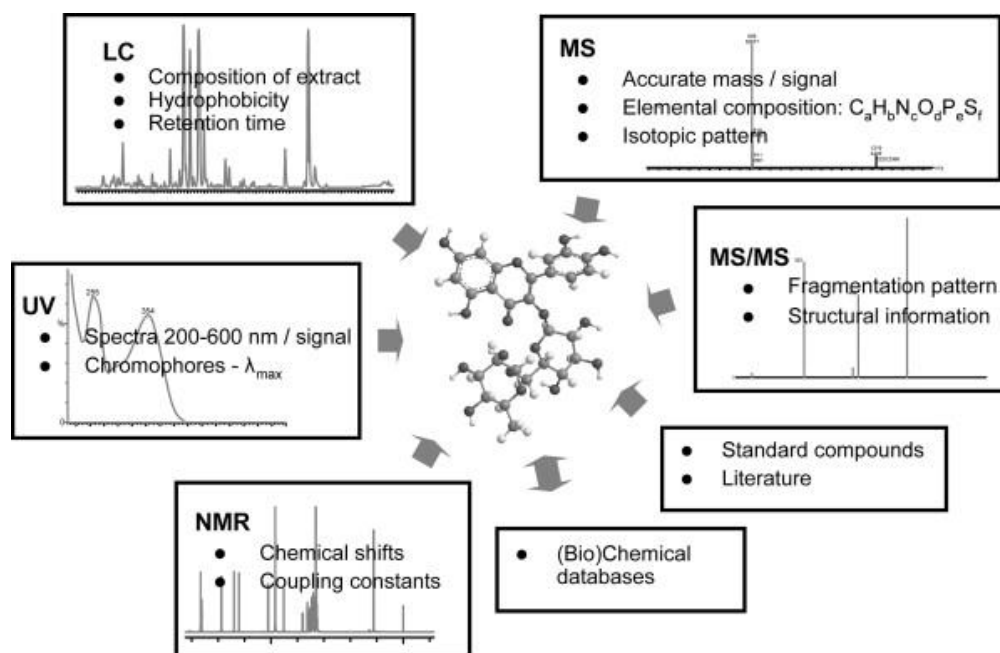


Figure 38 - Various techniques for drug metabolite identification¹¹²

3.9 Minimal inhibitory concentrations

Minimal inhibitory concentration, also known as MIC, is the lowest concentration of a drug at which it inhibits the growth of a microorganism. It is a crucial tool for selecting an appropriate antimicrobial agent against a microorganism and is expressed in mg/L or (μ g/mL). It is a critical parameter to determine the resistance or susceptibility of bacteria against antibacterial agents. We use MICs to measure the potency of an antibacterial drug against a bacterial species. Serial dilutions of the drug can determine MICs in the growth medium in which the organism grows or by gradient methods where strips are impregnated with a predefined drug concentration. This culture is incubated, and the MIC is determined as the lowest concentration at which the growth of microorganism is inhibited. MICs are used to monitor the emergence of resistance and to guide the selection of antibacterial drugs in clinical laboratories. The lower the MIC, the more effective

the drug is against the microorganism. MICs are essential to determine not just the potency of a drug but also to determine the optimal dosing regimen against bacteria. Therefore, the MIC value is the best available parameter to determine the significance and effectiveness of an antimicrobial drug against bacterial strains¹¹³ Figure 39 shows how the MIC is predicted in a 96 well plate.

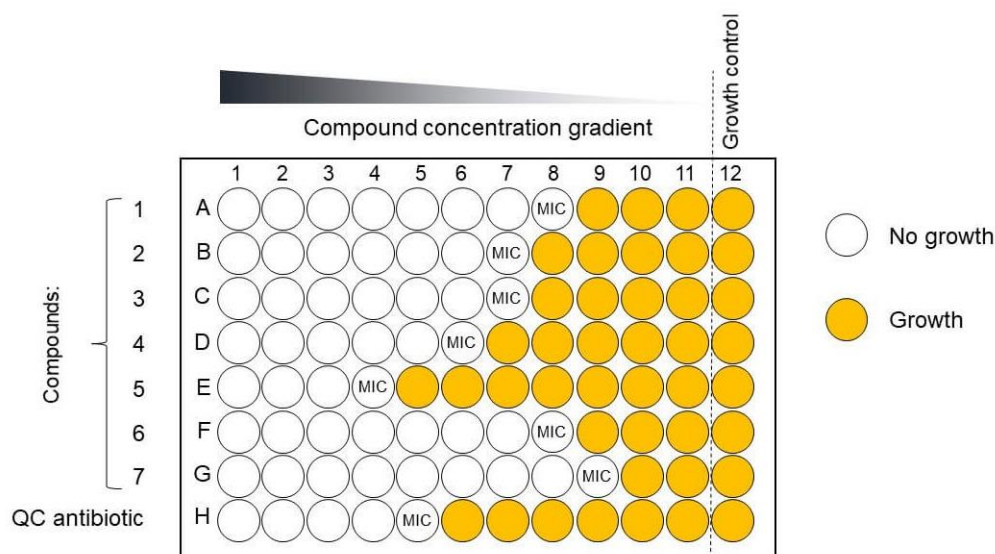


Figure 39 - Interpretation of MIC results¹¹⁴

3.10 Synergy and antagonism

The study involving interactive interactions between molecules is ancient. In the case of antimicrobial drugs, two or more combinations of drugs are often tested in vitro, which leads to positive interaction inhibiting the growth of bacteria. Synergy in relation to medicine and pharmacology is defined when two or more drugs work in combination, which is greater than the additive effect of the same. Many diseases require a cocktail or mixtures of drugs, which is the case in cancer treatment. This process maximizes the therapeutic effect of the drugs while minimizing the side effects^{115 116} If two drugs are combined then the lower dose of each drug could be used for fewer side effects while still providing the desired outcome. There is another concept

called the additive effect or the noninteraction or inertism. This method is considered as the baseline effect for synergy detection and is expected from the combination of drugs when there is the absence of synergy¹¹⁷ Synergy is defined as a combined effect and is greater than the additive effect and is also known as superadditivity. On the other hand, antagonism is a term opposite to synergy and occurs when the combined effect of two drugs is less than additivity. Figure 42 and table Table 7 shows the isobologram and the interpretation of MICS. It has an adverse scenario as it plays no role in the therapeutic effect. Antagonism is also known as subadditivity¹¹⁸ One of the models used to measure such interpretation is known as the checkerboard experiment. In this process, a two-dimensional array of serial dilution of two drugs is used, and a fractional inhibitory concentration (FIC) index is calculated as shown in Figure 40. FIC has gained popularity because this method has been used in many journals and publications as a solid technique to figure out synergy and antagonism between drugs. The formula to calculate FIC is:

$$FIC\ index = \left(\frac{MIC\ of\ drug\ 1\ in\ presence\ of\ drug\ 2}{MIC_{Drug1}} \right) + \left(\frac{MIC\ of\ drug\ 2\ in\ presence\ of\ drug\ 1}{MIC_{Drug2}} \right)$$

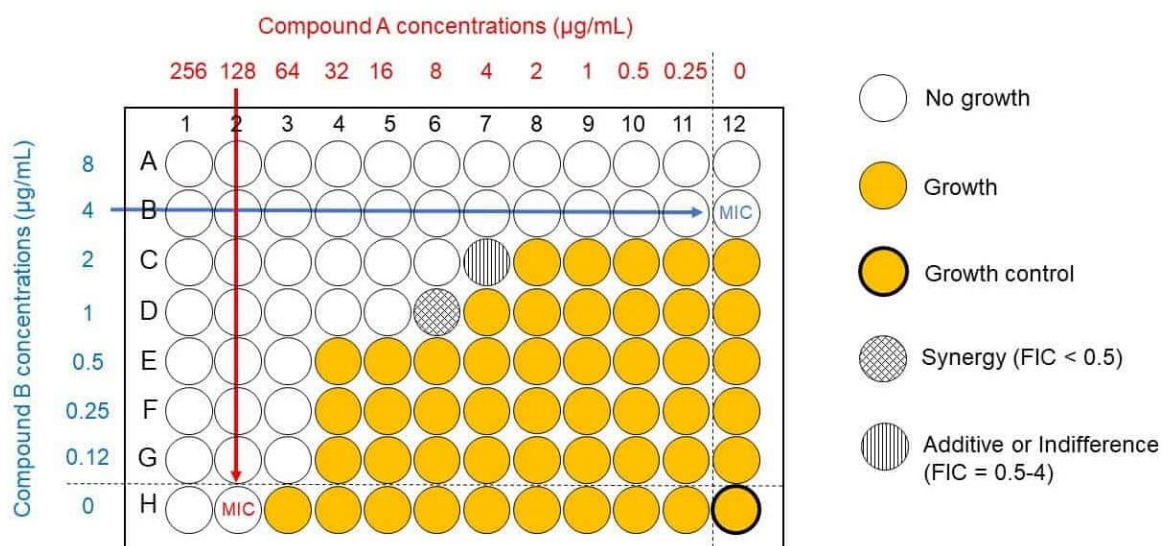


Figure 40 – Synergy checkerboard assay¹²⁰

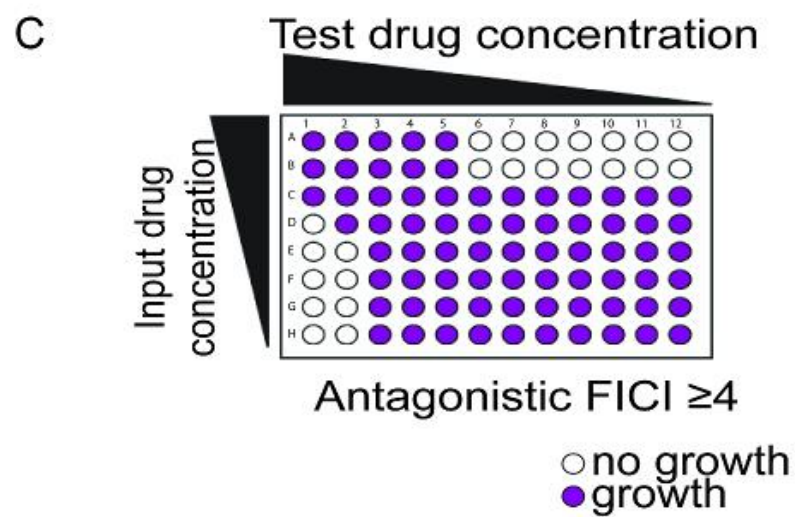
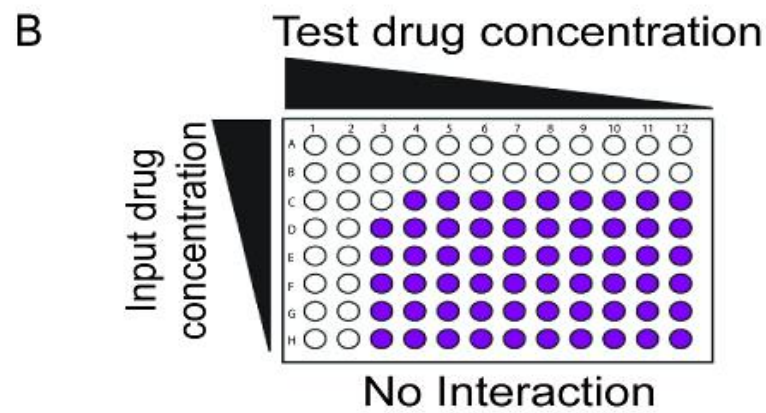
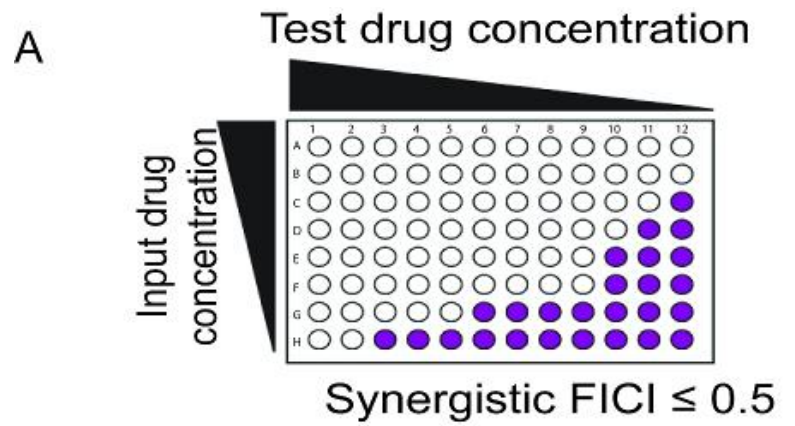


Figure 41 - Representation of synergistic, additive and antagonistic effect¹²¹

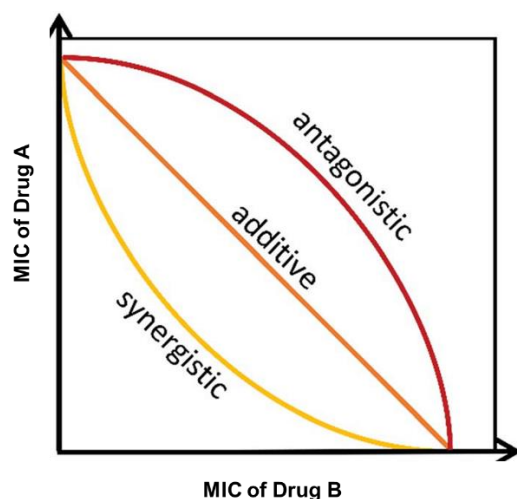


Table 7- FICI and its interpretation	
FICI	Interpretation
< 0.5	Synergy
0.5 – 1.0	Additive
1.0 – 4.0	Indifference
> 4.0	Antagonism

Figure 42 – Shows the isobolograms for checkerboard and Table 7 represents the FICI of all interpretations¹¹⁹

3.11 Spectrum of activity

Spectrum of activity is a term that is commonly used in pharmacology, biochemistry, and microbiology. This term refers to the range of effectiveness a specific antibacterial drug has toward different bacterial species. Therefore, it is crucial to understand the effect of the spectrum of activity for the appropriate selection and use of antimicrobial agents in clinical practice and research. Spectrum of activity can be classified into three main categories:

In a narrow spectrum, antimicrobials with a narrow spectrum of activity are effective against a limited group of microorganisms, mainly targeting gram-positive or gram-negative

bacteria. Examples of narrow-spectrum drugs are penicillin, fidaxomicin, sarecycline, erythromycin, and clindamycin. The second category is broad-spectrum which includes all the drugs that can target both gram-positive and gram-negative bacteria. Broad-spectrum drugs include amoxicillin, ampicillin, doxycycline, chloramphenicol, ciprofloxacin, and imipenem. The third category is the extended spectrum, where the drugs have an even broader range of activity because they are effective against a wide variety of bacteria, including those resistant to antibiotics. Few factors affect the spectrum of activity. Those factors include a drug's chemical structure which allows them to target specific microorganisms by penetrating their cell wall efficiently. Second, is the resistance mechanism by microorganisms, which narrows the spectrum of activity of the drug. The third factor includes the mechanism of action of the drug. Therefore, the spectrum of activity is helpful in the appropriate selection of drugs against a specific infection, avoiding resistance by using broad-spectrum drugs instead of narrow-spectrum drugs and minimizing side effects by using drugs with a narrow spectrum of activity reducing the potential for side effects and disruption of the normal microbiota of the body^{122 123} Figure 43 represents the antibiotic sensitivity view.

Gram Positive Cocci			Gram Negative Bacilli			Anaerobes
MRSA	MSSA	Streptococci	E.coli, Klebsiella	Pseudomonas	ESCAPPM*	
		Penicillin	Proteus			
		Amoxycillin				
		Flucloxacillin				
		Cephazolin				
		Clindamycin				Clindamycin
Rifampicin/Fusidic Acid						
		Vancomycin/Teicoplanin, Linezolid, Daptomycin				Metronidazole
			Trimethoprim			
			Ciprofloxacin			
			Gentamicin/Tobramycin, Aztreonam			
			Moxifloxacin			Moxifloxacin
			Cefuroxime			
			Ceftriaxone			
			Ceftazidime			
			Cefepime			

Figure 43 - Spectrum of activity of various drugs against different pathogens¹²⁴

3.12 Thymidine folate biosynthesis inhibitors

To escape from the immune system attack *Staphylococcus aureus*, hide inside macrophages¹²⁵ MRSA proliferation relies on dTMP synthesis which requires tetrahydrofolate (THF). THF is a reduced bioactive form of folate. Hence, THF from folate metabolism plays a vital role in nucleotide synthesis pathway¹²⁶ Folate metabolism is a process that involves several metabolic pathways and biochemical mechanisms that promote de novo purine and thymidylate synthesis, methionine cycle and conversion of glycine and serine in cytoplasm and mitochondria Figure 44 ¹²⁷ This pathway starts when the reaction is catalyzed by serine hydroxymethyl transferase in which the serine gets converted to glycine and serine molecule donates one carbon unit. Folic acid is an essential cofactor for various cellular processes like DNA, RNA, and protein synthesis. Folate cannot be synthesized de novo in humans and thus should be obtained from the diet²⁶⁵ However, bacteria can synthesize their folic acid through a series of enzymatic reactions. This difference leads to the involvement of folate biosynthesis inhibitors that can act and stop the process of folate biosynthesis. The main targets for folate biosynthesis inhibitors are two key enzymes in the pathway called dihydrofolate reductase (DHFR) and dihydropteroate synthase (DHPS). DHFR catalyzes the conversion of dihydrofolate to tetrahydrofolate, while DHPS catalyzes the condensation of para-aminobenzoic acid (pABA) and dihydropteridine pyrophosphate to form dihydropteroate. By inhibiting these enzymes folate biosynthesis inhibitors stop the biosynthesis of THF, which leads to the unavailability of essential cofactors and thus leads to cell death. Some of the folate biosynthesis inhibitors are trimethoprim which inhibits DHFR and sulfonamides, which are structural analogs of pABA and competitively inhibit DHPS as shown in Figure 45.

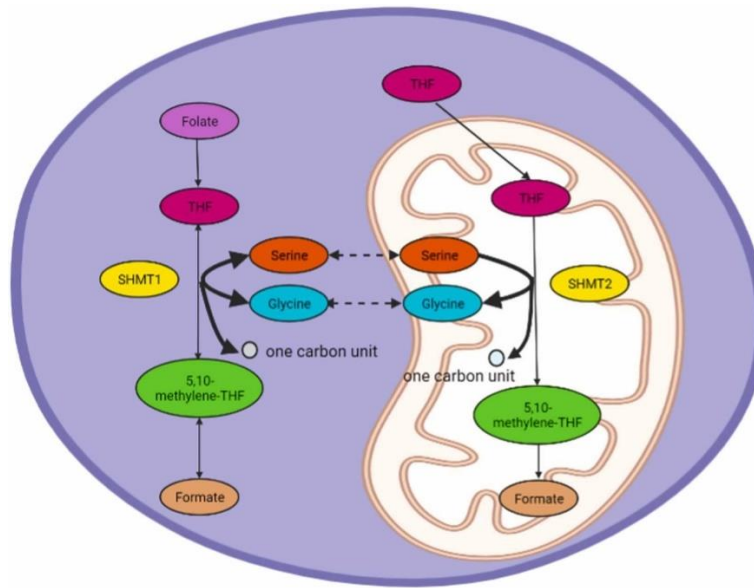


Figure 44 - Outline of folate metabolism¹²⁴

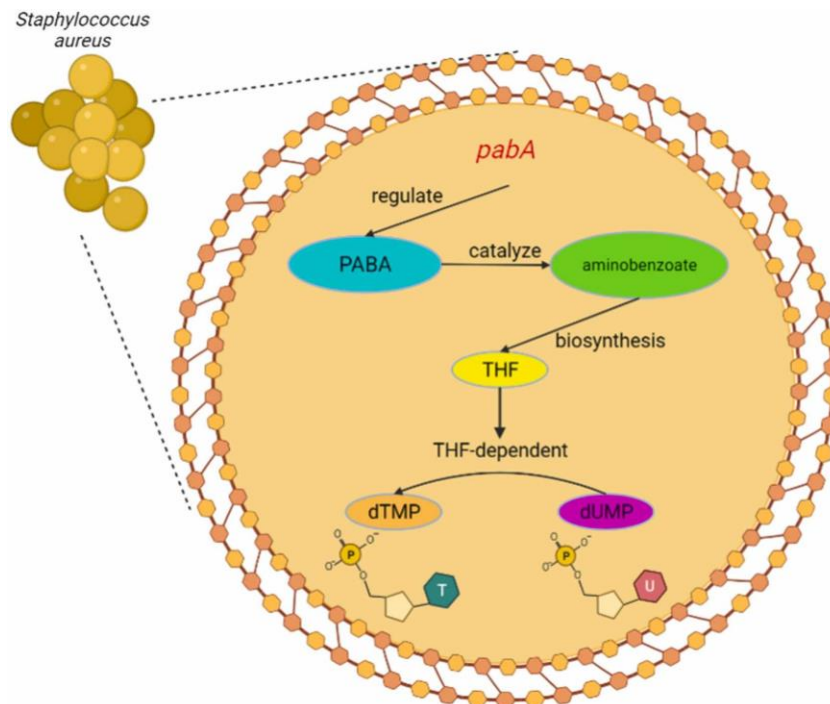


Figure 45 - THF is directly involved in the synthesis of dTMP through the regulation of *pabA* gene¹²⁴

CHAPTER 4

4. LIBRARY SCREENING FOR SYNERGISTIC COMBINATIONS OF FDA APPROVED DRUGS AND METABOLITES WITH VANCOMYCIN AGAINST VANA-TYPE VANCOMYCIN-RESISTANT *ENTEROCOCCUS FAECIUM*

4.1 Introduction and Rationale

Pathogenic bacteria are becoming increasingly drug resistant, with some now virtually untreatable^{68 129 130 131} There has concurrently been a lack of new antibacterial agents identified over the last thirty years to counter this threat^{68 131 132} *Enterococcus* spp. are gram-positive commensal bacteria of the intestine in humans and animals that can cause problematic infections of the GI tract and soft tissues^{35 67 133 134} Vancomycin (Vm) is one of the most important agents for the treatment of G+ bacterial infections resistant to most other antibacterial agents, including vancomycin- sensitive *Enterococcal* (VSE) and MRSA infections^{32 33 34} The emergence and spread of vancomycin-resistant *Enterococcus* spp. (VRE) is a serious public health issue given the lack of alternatives for these organisms and their increasing resistance to currently used agents^{32 35 39 67} VRE is a therefore WHO high priority pathogen for new agent development¹³⁵

Chemical compound library screening is a core approach for the discovery of new bioactive agents, including for antibacterial activity. However, large untargeted (whole cell) and targeted (individual protein) library screening efforts have given overall disappointing results^{136 137} An alternative to large library screens are smaller scale efforts with high value libraries such as FDA approved drug library screening, which has become a popular strategy for “drug repurposing”¹³⁸ This strategy can reveal novel new activities of FDA approved drugs, which provides a potentially greatly shortened path to clinical application. Another strategy to counter anti-microbial resistance

is to identify agents that can act synergistically with or restore the activity of another antibiotic¹³¹
¹³⁹ ¹⁴⁰ Many drugs are also known to have active metabolites ¹⁴¹ ¹⁴² Comparative screening of the
un-metabolized (UM) and pre-metabolized (PM) libraries allows agents with increased
antibacterial activity to be identified for deconvolution and active metabolite identification, as
recently demonstrated using a human liver microsome metabolized FDA approved drug library¹⁴³
In a prior study we have demonstrated an approach in which FDA approved drug library screening
is performed with both FDA approved drugs and their metabolites, and simultaneously in the
absence and presence of a resistant-to-antibiotic¹⁴³ This allows intrinsically active agents, agents
with active metabolites, and agents synergistic with the resistant-to-antibiotic to be identified in a
single screen. In this study this approach was used to screen an FDA approved library in its
original (un-met; UM) and human microsome metabolized (pre-met; PM) versions against VREfm
in the absence and presence of sub-MIC levels of vancomycin (-/+Vm) (2x2 library screening
design).

4.2 Materials and Methods

4.2.1 General

The reagents and materials used in this study were as described previously¹⁴³ Bacterial
strains were obtained from American Type Culture Collection (ATCC; Manasas, VA) and the
Biodefense and Emerging Infections Research Resources Repository (BEI; Manasas, VA). The
bacterial strain used for library screening was a VanA-type vancomycin resistant *Enterococcus*
faecium (VREfm) clinical strain. Other bacterial strains used in this study were as indicated in the
appropriate tables. UM and PM working library plates including control antibiotics and control
microsomal metabolism substrates were prepared as described previously¹⁴³ at 0.5 mM. VRE

growth medium consisted of brain heart infusion (37.5 g/L), hemin (10 mg/L), and NAD⁺ (10 mg/L).

4.2.2 UM/PM vs +/- Vancomycin library screen against VRE *faecium*

Four sets of library screening plates were prepared for the following screens: UM-Vm, UM+Vm PM-Vm, PM+Vm. Two sets of UM plates and two set of PM plates were first prepared from working library samples (2 μ L @ 0.5 mM of working library samples per well) in 384 well Corning microtiter plates (catalog 3680) using a Biomek 3000 liquid handling workstation. Plates were frozen at -80 °C and dried under strong vacuum (<50 μ mHg) in a Genevac Quatro centrifugal concentrator. To each well in each set was added 20 μ L of VRE growth medium containing 4000 cfu VRE and containing either no Vm for -Vm screens, or +16 μ g mL⁻¹ Vm ($\leq 1/16 \times$ MIC) for +Vm screens. These additions were performed using an Integra Viaflo Assist automated multichannel pipette (Hudson, NH) in a Labconco (Kansas City, MO) BSL-2 biosafety cabinet. Plates were incubated for 48 h at 35 °C. Fresh VRE growth medium (10 μ L) was added to the wells of these four sets of plates, followed by incubation for 2 h at 35 °C to restart active cell growth. To the wells of these plates was then added 10 μ L of 100 μ g mL⁻¹ resazurin (sodium salt)^{145 146 147} The plates were incubated for another 2 h at 35 °C, and the A610 - A450 absorbance difference (Promega Technical Bulletin TB317) measured in a Molecular Devices SpectraMax M5 multimode microplate reader (San Jose, CA).

4.2.3 Hit picking and minimum inhibitory concentration determination

Library screening data was processed and analyzed using homemade Matlab® scripts (The Mathworks, Natick, MA). Based on the values for known active and inactive antibacterial agent

controls, a cut-off value between active and inactive compounds was selected and lists of active wells in each screening set (UM-Vm, UM+Vm, PM-Vm, PM+Vm) generated. These lists were merged to give a pooled hit list. Rows were added to this pooled hit list to include known active and inactive antibiotics containing wells as controls. MICs were determined by hit picking 2 μ L samples from both UM and PM working plates (two sets from each) into the first columns of 384 well plates (four sets total, for UM-Vm, UM+Vm, PM-Vm and PM+Vm MIC determinations). These samples were then serially diluted in steps of two across the plates with DMSO using an Integra Viaflo Assist automated multichannel pipettor. The last column was left blank (DMSO only). These plates were frozen at -80 °C and dried under strong vacuum as described above. To each well in each set was added 20 μ L VRE growth medium containing 4000 cfu VREfm and containing either no Vm for -Vm MICs or 16 μ g mL⁻¹ Vm for +Vm MICs. (This provided MIC plates with 50 μ M as the highest test agent concentration.) Plates were incubated for 48 h at 35 °C. Fresh VRE growth medium (10 μ L) was added to the wells of these four sets of plates, followed by incubation for 2 h at 35 °C to restart active cell growth. To the wells of these plates was then added 10 μ L of 100 μ g mL⁻¹ resazurin^{145 146 147} The plates were incubated for another 2 h at 35 °C, and the A610 - A450 absorbance difference measured as described above. MICs were determined using a cutoff midway between known active and inactive samples. All MICs were determined at least in triplicate, and at least in quadruplicate for MIC_{min} \leq 25 μ M to ensure reproducibility.

4.2.4 Different VRE strains stock preparation and CFU/mL determination

Brain heart infusion agar plates were prepared by mixing 3.7 gms of BHI and 1.5 gms of agar. An overnight primary culture was used to set up a secondary culture at 0.05 OD. When the

OD₆₀₀ of secondary culture reached 0.5 OD, 1:100 stock was made from the secondary culture. To make 1:100 stock, 300 µL of secondary culture was added in 30 mL fresh BHI media to which 6 mL of 100% glycerol was already added. This glycerol culture mix was used to make aliquots of 100 µL on ice in 2 mL autoclaved eppendorf tubes and were later stored at -80 °C. Next day, one of the stocks was used to determine the colony forming unit (cfu/mL) of the strain. Serial dilution of the stock was done, and these dilutions were plated separately on BHI agar plates. The plates were incubated overnight at 35 °C and colonies were counted the next day to determine the cfu/mL of the stock. A panel of VRE strains were ordered from American type cell culture (ATCC). The stocks were made, and the cfu/mL was determined for all the strains. Table 8 below list all the strains with their cfu/mL.

Table 8 - ATCC VRE strains and cfu/mL

Strains	Cfu/ mL
<i>Enterococcus faecium</i>	
BAA-2317	4.55x10 ⁻⁸
BAA-2318	8.40x10 ⁻⁸
ATCC 51575	1.7x10 ⁻⁸
<i>Enterococcus faecalis</i>	
BAA-2365	5.10x10 ⁻⁸
ATCC 700802	5.8x10 ⁻⁸
BAA-49532	7.25x10 ⁻⁸
BAA-49533	1x10 ⁻⁸

4.2.5 Spectrum of activity of VRE hits

MICs were determined against a panel of VRE_{fm} and VRE_{fa} strains as shown in Table 12. Plates were prepared by serial dilution of compounds in DMSO across 384 well plates and drying under high vacuum as described above.

4.2.6 Checkerboard assays to confirm synergy

Checkerboard assays¹⁴⁸ were performed to confirm synergy for prospective synergistic agents. Checkerboard assays were performed in 96 well plates from DMSO compound stocks and dried under vacuum similarly to the MIC determinations described above. To these plates was added 100 μ L VRE growth medium containing 4000 cfu VRE to each well, and plates incubated for 48 h at 35 °C. Fresh VRE growth medium (50 μ L) was added, plates incubated at 35 °C for 2 h, 50 μ L of 100 μ g mL⁻¹ resazurin added, plates incubated an additional 2 h, and the resazurin absorbance difference measured as described above. All checkerboard assays were performed at least in triplicate and averaged.

4.2.7 Large scale metabolism of mupirocin

Mupirocin demonstrated significant antibacterial activity only after metabolism as shown in Table 9. To identify its active metabolite(s), a scaled-up metabolism reaction was performed on 1 mL of 10 mM mupirocin. This 10 mM stock of mupirocin is added to 15 mL falcon tube and frozen in -80 °C and later freeze dried in a Genevac Quatro centrifugal concentrator. To the dried samples 500 μ L of 20% acetonitrile was added and incubated with shaking at 37 °C. This solution was later metabolized using the reaction mixture as described¹⁴³ To this reaction mixture was then added 4 mL 80% ice-cold isopropanol/200 mM acetic acid, the sample mixed well, and microsome debris pelleted at 4000g for 30 min at 4 °C. The supernatant was collected, and the pellet re-extracted with 2 mL 67% isopropanol/200 mM acetic acid. Supernatant was collected and combined with the first supernatant. The combined extracts were frozen at -80 °C and dried in a Genevac Quatro centrifugal concentrator. The residue was dissolved in 0.4 mL of 3% acetonitrile/97% 10 mM ammonium acetate and syringe filtered to make a sample for semi-

preparative HPLC. The sample was purified by semi-preparative HPLC on a Kromasil C18 column (3.0 × 150 mm, 5 µm particle size, catalog # K08670646). Fractions were collected at 1 min intervals in a 96 well microtiter plate (MidSci, catalog # TP92096). The flow rate was 250 µL min⁻¹ and the purification gradient was: 3% B for 0–5 min, 3–13% B for 5–65 min, 13–100% B for 65–75 min; solvent A = 10 mM ammonium acetate pH 6.5, solvent B = 30% solvent A with 70% acetonitrile, and solvent C = 100% acetonitrile¹⁴³

4.3 Results and Discussion

While there has been some progress in the development of new antibacterial agents to combat the emergence and spread of antimicrobial resistance (AMR) in pathogenic bacteria, there has been an overall lack of new antibacterial agents of novel mechanism and without established resistance mechanisms developed in the last several decades^{131 144 149 150 151} Novel new agents are therefore urgently needed. Another approach to combating AMR is the identification of effective synergistic agent combinations, particularly from the repertoire of existing antibacterial agents^{139 148 152 153} Such synergistic agent combinations have enhanced activity against targeted organisms and can also reduce the emergence and spread of resistance. Both new agent identification and the identification of new synergistic agent combinations are potential pathways to addressing the problem of AMR. The development and demonstration of compact and effective approaches that can perform both types of screens simultaneously would be of obvious utility for efforts to address AMR.

In a prior study we demonstrated in MRSA how a two-dimensional screening strategy comparing an un-met (UM) vs pre-met (PM) FDA library screen combined with a -/+ resistant-to-antibiotic screen could enhance the ability to identify new agents and new synergistic

combinations¹⁴³ Focusing this approach on an FDA approved drug library offers the potential of identifying novel antibacterial activities in FDA approved drugs and FDA approved drug metabolites, and to identify novel synergistic drug combinations, all features demonstrated previously¹⁴³ The rationale for this strategy is to perform screening replication under somewhat different but informative conditions. Screening of the PM library allows FDA approved drugs with active metabolites to be identified, and screening in the absence and presence of a resistant-to-antibiotic allows agents acting synergistically with the resistant-to-antibiotic to be identified.

4.3.1 Library screening preparation and workflow

The original library was replicated twice. One for the un-metabolized drugs and the other for pre-metabolized drugs. The UM library was reconstituted in DMSO, and the final concentration made was to 0.5 mM. The PM library drug plate was metabolized in presence of human liver microsomes, extracted, dried, and reconstituted in DMSO with a final concentration of 0.5 mM. Figure 46 describes the workflow of FDA-approved drug library replication and metabolism. Figure 47 describes how the library is replicated from original 96 well plates to working 384 well plates.

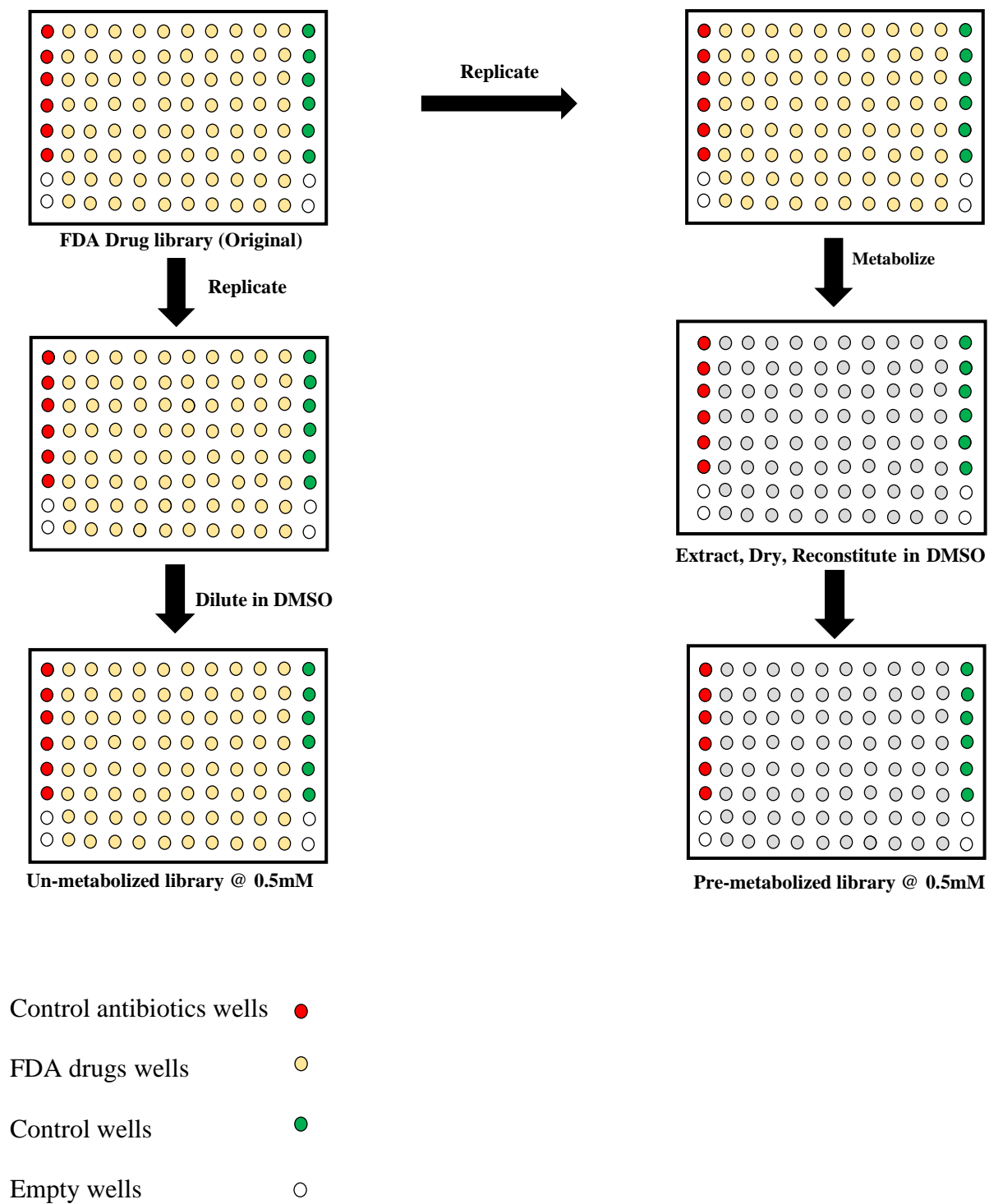


Figure 46 - Replication and metabolism of Un-metabolized and Pre-metabolized library in presence of human liver microsomes.

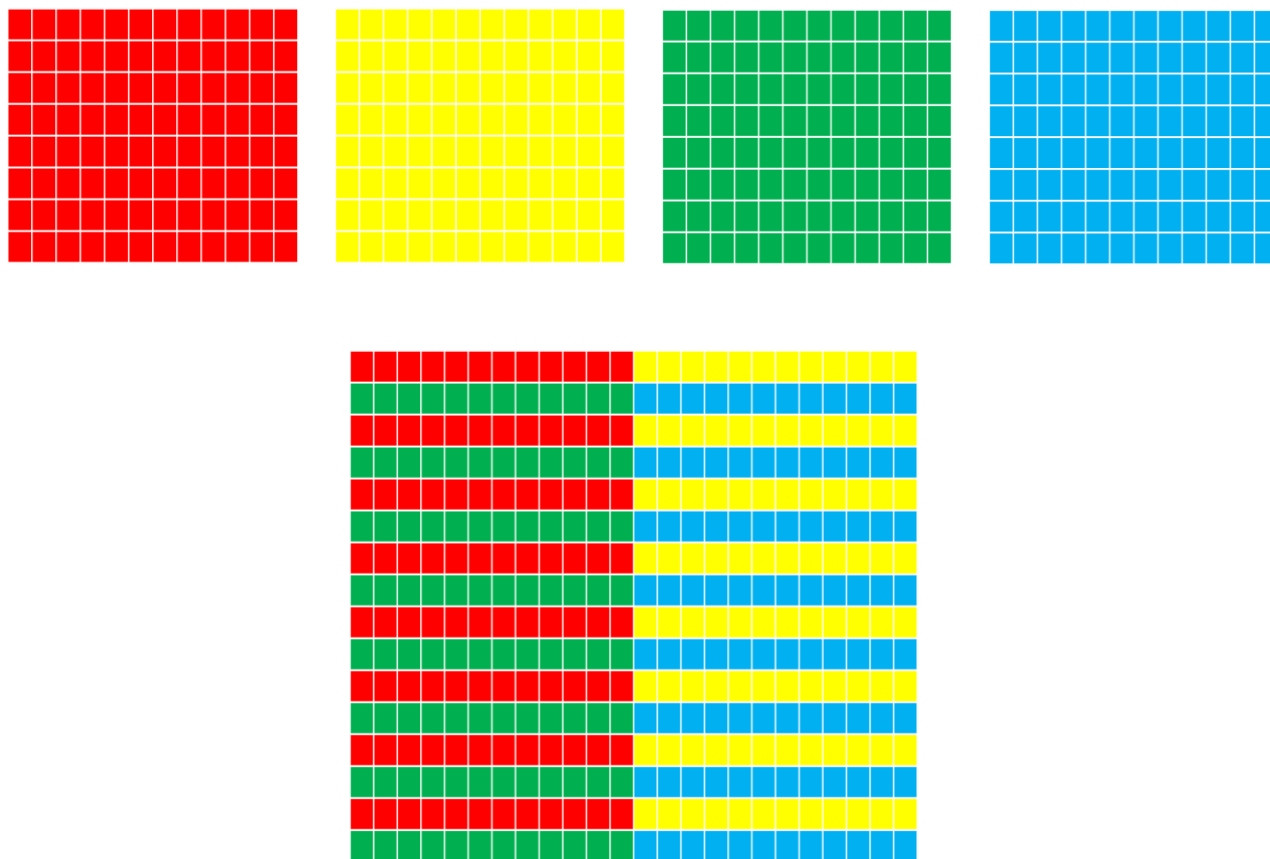


Figure 47 - Describes how each 96 well plate is replicated in a 384 well plate. The figure above represents 4 different 96 well plates and the figure below represent a 384 well plate.

4.3.2 Library screening results

In this study this effort was extended to a vancomycin-resistant *Enterococcus faecium* strain in the absence and presence of vancomycin. Library screens were performed at 50 μ M of the library compounds and in the absence and presence of 16 μ g/mL vancomycin (1/8xMIC).

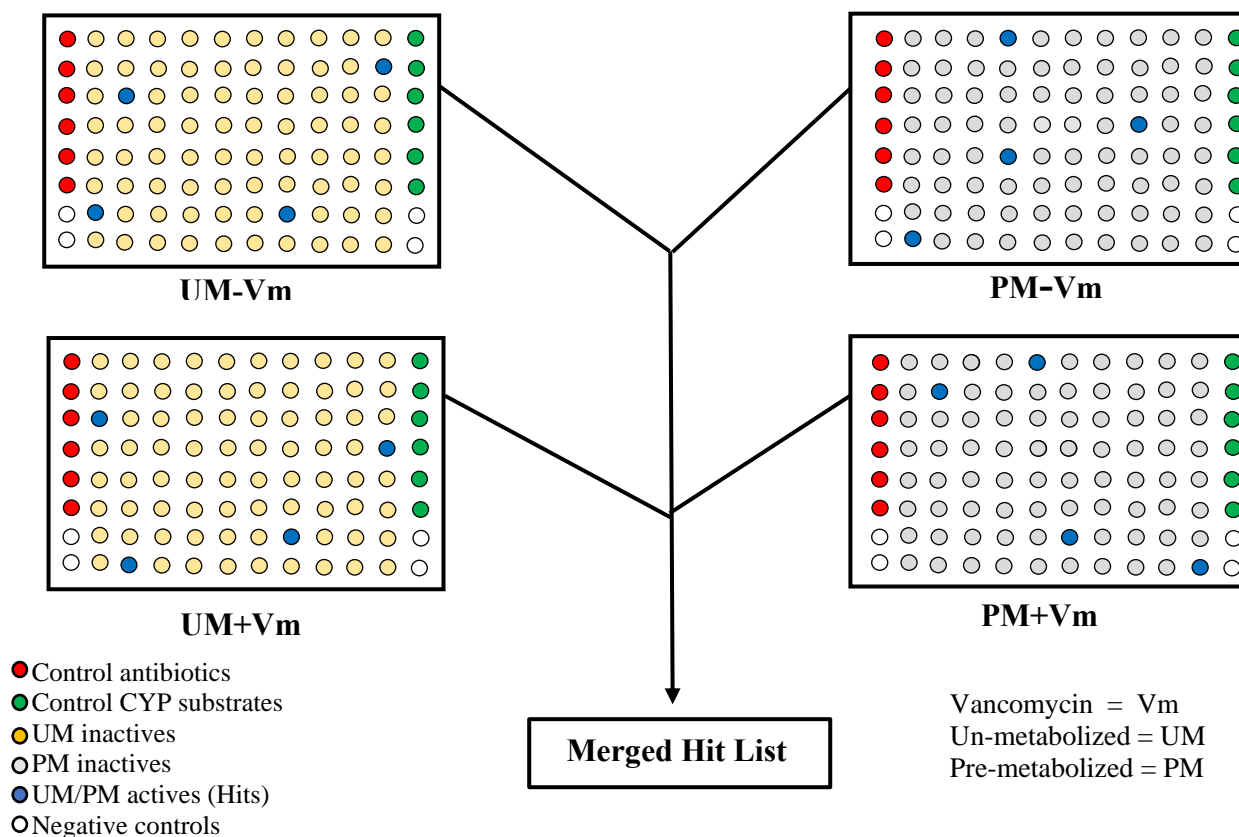


Figure 48 - Represents library screen and the blue dot represents hits. These hits were used to make a merged hit list.

Following library screening a merged hit list was made as shown in Figure 48, in which any compound that gave a hit (was active) under any of the four screening conditions (UM-Vm, UM+Vm, PM-Vm, and PM+Vm) was included in the list. MICs for all the compounds in this

pooled hit list were then determined under all four screening conditions to give a preliminary table of MICs. Figure 49 shows MICs determined twice for all the hits with $\text{MIC} \leq 100 \mu\text{M}$.

MICs for compounds that gave a minimum MIC over all four tested conditions of $\leq 25 \mu\text{M}$ were then determined at least in triplicate as shown in Figure 50. The results for agents with an $\text{MIC}_{\text{min}} \leq 12.5$ (under all 4 test conditions) are summarized in Table 9. A complete list of all active and inactive agents is provided in Tables 10 and 11 respectively.

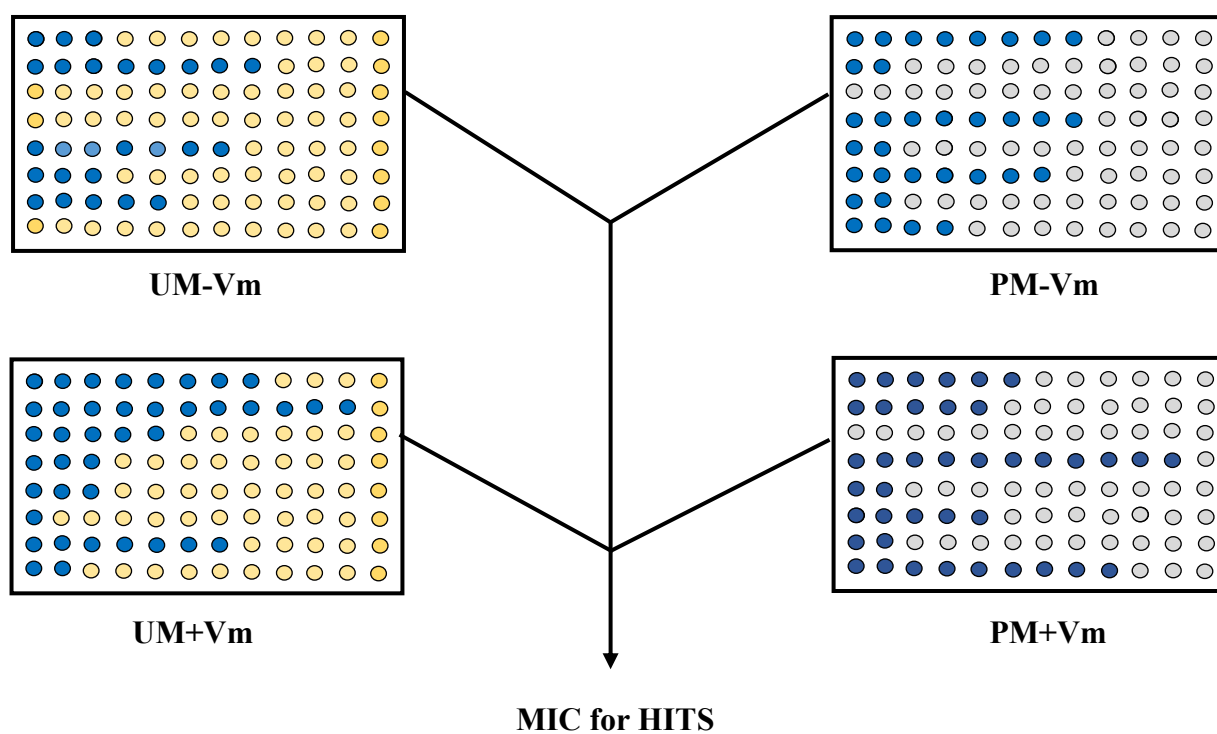


Figure 49 - MICs were determined twice for all the hits with $\text{MIC} \leq 100 \mu\text{M}$. The blue dot represents hits. The yellow dots represent UM drugs, and grey dot represents PM drugs.

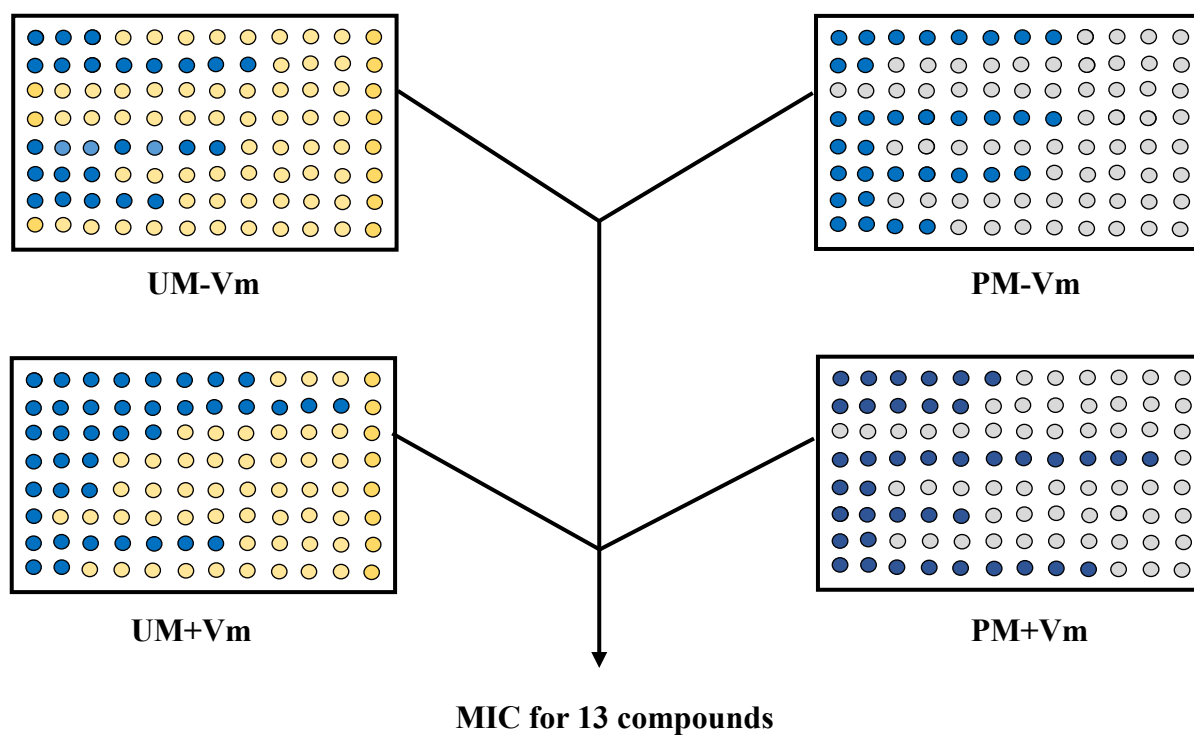


Figure 50 - MICs were determined in triplicate for all the hits that gave $\text{MIC} \leq 25 \mu\text{M}$. The blue dots represent hits. The yellow dots represent UM drugs, and grey dot represent PM drugs.

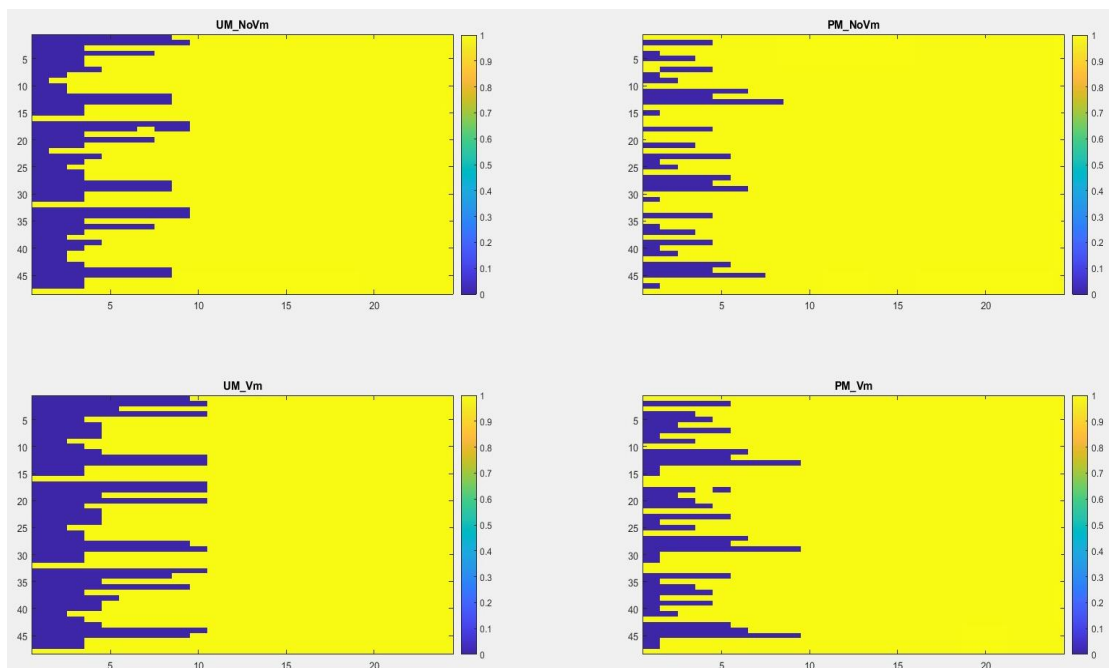


Figure 51 - Shows MICs for the hits in Matlab. MICs represented in blue.

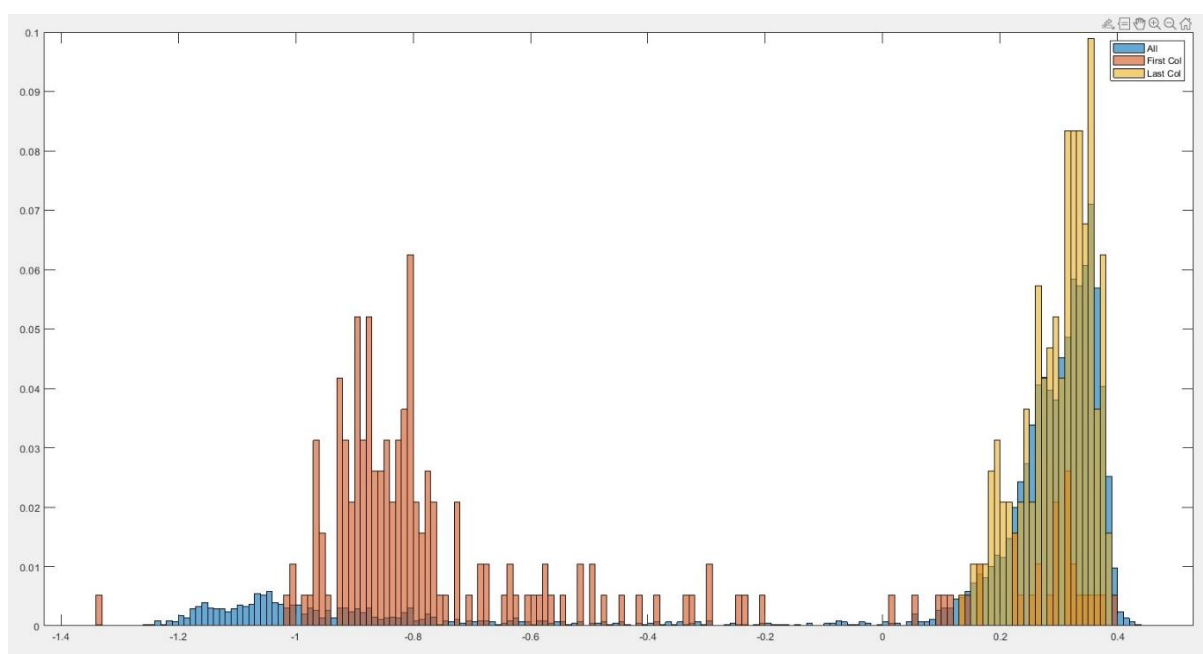


Figure 52 - This image represents a cutoff between growth and no growth after screening the library with VRE *faecium*. Orange represents no growth of bacteria (actives) and yellow represents growth of bacteria (inactives) with a cutoff at -0.1.

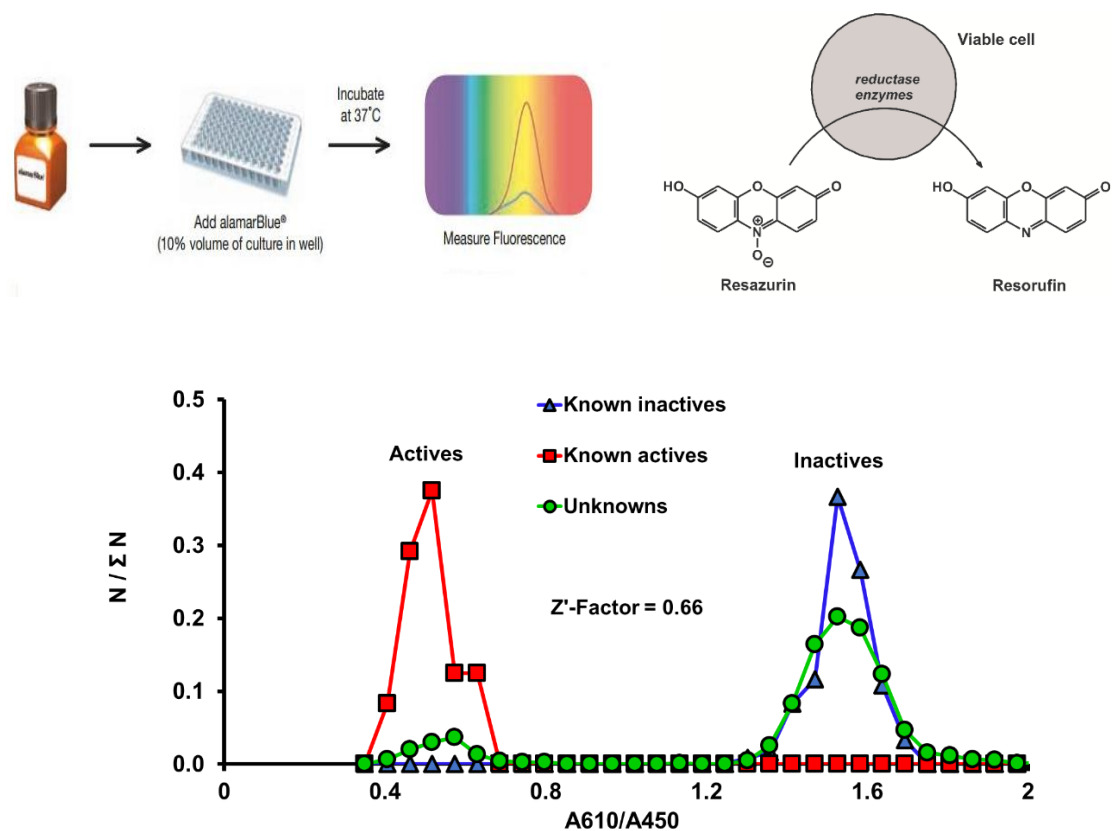


Figure 53 - Figure above shows resazurin salt that is a blue dye which when added to the bacteria undergoes reduction process and is used to distinguish between growth (pink color) and no growth (blue color) in bacteria. The figure below represents how resazurin salt helps in predicting a cut off between active and inactives.

4.3.3 Optimization of VRE *faecium* fluorescence/absorbance.

After the addition of resazurin blue, a blue colored dye, we were unable to obtain clear distinction between the growth (pink) and no growth (blue) in VREfm well. Therefore, we tried optimizing the experiments to get better results. We first tried reading the plate after 2 hours of incubation at 35°C using fluorescence at 530/600. The incubation time did not yield us good result; therefore, we extended the incubation time to 4 hours. However, 4 hours fluorescence did not give

a clear distinction pattern between growth and no growth wells as well. Figure 54 shows results after 2 hours of incubation. Figure 55 shows results after 4 hours incubation.

2744.2	4333.2	4644.4	4155.5	4132.5	4387.7	4131.6	4181.9	4178.5	4406.7	4329.8	4722.0	3588.2	3705.3	4535.2	4081.4	4071.1	4322.8	3733.0	4513.1	3252.5	4417.3	4310.8	4706.1
2842.9	4495.6	4512.9	4835.9	3972.6	5041.8	4065.7	3639.6	4194.9	1831.1	4344.3	5008.9	4338.5	3207.1	2175.9	4538.0	4508.2	3762.9	4406.4	5035.4	3872.7	4681.2	4632.1	4112.8
5289.4	5417.9	3581.2	3593.8	3149.5	4218.2	3967.8	4000.2	4176.3	5062.4	7097.0	4614.8	8277.7	4810.2	4675.2	4553.8	3536.1	4417.4	4332.6	5112.6	3519.9	4563.1	4100.4	4217.8
3878.5	3873.5	2391.6	4055.1	3768.5	4713.5	3595.2	3878.7	4624.7	4454.5	5097.5	4862.3	7121.3	5076.2	4718.7	4391.6	2409.1	4271.2	2283.1	4390.4	3512.5	4929.0	4647.3	4257.1
2727.4	4118.7	3851.3	3773.9	5117.3	3933.5	3955.4	4018.4	4329.0	4167.4	4488.1	4021.7	4524.2	4235.0	5290.8	2486.6	4186.1	4787.2	3910.7	4138.2	3619.0	4288.8	3910.9	3694.8
2912.3	3784.5	4558.3	5249.4	4225.3	5138.3	4233.4	6654.9	4312.4	4696.5	4792.7	4607.2	4419.5	4719.1	2590.9	4577.4	4336.5	4765.6	7006.7	4573.7	3324.8	3957.3	4214.1	4049.9
1848.4	2148.4	3741.1	3865.2	4159.9	4773.2	3929.2	3925.6	3635.8	3750.9	4425.7	4285.2	2727.7	3503.8	5582.8	4081.4	5034.0	4612.8	3585.6	4109.9	3425.7	3737.2	3988.3	4447.1
1903.8	3879.4	4840.7	3980.2	4963.0	4000.5	3833.9	3887.8	5058.5	4173.7	3158.7	4725.6	1990.8	4891.2	4397.3	4406.6	2214.9	2378.5	3820.8	4406.0	3162.6	4398.8	4138.7	3889.9
2737.3	4329.0	4259.2	3797.1	4334.3	4235.5	4110.7	4406.1	3459.3	4120.5	4242.3	4344.8	4023.3	4435.9	4415.4	4505.2	4330.1	4719.5	2287.4	4039.2	3282.1	3594.4	3805.8	3917.2
2581.8	4178.6	4006.7	4255.3	3648.8	4548.5	3043.6	4119.0	4146.2	3567.2	5820.1	4419.0	2935.9	3791.6	3763.2	3415.0	3989.8	3536.8	3717.4	3782.7	2745.2	3342.4	3558.9	3754.8
2076.2	4051.5	3087.9	4094.7	4260.8	4127.6	4642.8	3399.4	3327.8	3564.3	4402.5	3839.8	2092.5	3269.6	4021.6	4036.1	3846.0	3992.7	3525.9	4070.8	3101.2	3739.1	3884.3	3428.8
2455.4	4122.4	4009.0	4520.6	3992.6	3386.3	3374.6	2222.2	4017.3	4031.4	4070.0	4360.5	2348.0	4147.3	2388.1	4502.5	4878.9	2526.2	3946.0	4145.0	2999.4	3819.7	3790.8	3323.0
2708.6	4525.9	3337.6	3463.4	3903.8	4437.1	3921.6	4112.1	3480.7	3695.9	3543.3	4056.4	3819.7	4043.4	4114.7	4031.8	4063.6	5981.4	4162.9	3703.4	3127.7	3923.2	3876.3	3772.0
2357.9	5546.6	3409.5	9042.5	4880.5	7728.4	3869.0	3814.2	4151.5	3624.6	4284.6	4284.6	3364.6	2354.6	3122.8	9377.4	4373.0	4428.3	3335.8	4403.8	3347.6	3168.7	4094.0	3530.3
2221.5	4404.9	3612.5	3094.6	2235.8	3680.6	3444.4	4970.9	8362.3	4111.2	3821.0	3459.9	3385.5	4783.2	4340.9	3932.0	4401.3	4810.8	3419.6	4440.5	3370.6	2480.0	3378.1	3683.5
7425.3	3829.0	4152.9	3906.9	4158.3	5542.6	3608.8	3349.0	4059.0	3705.4	3331.8	4052.3	3468.0	3830.9	3875.3	5259.4	4159.7	3770.8	3821.2	4039.8	5065.0	4071.1	3681.9	3575.4

Figure 54 - Pattern of 384 well plate after 2 hours of incubation at fluorescence 530/600

2566.6	4030.1	4473.4	3961.2	3888.3	4186.6	3894.3	3837.1	3928.5	4118.4	4173.8	4250.7	3183.0	3110.8	4357.5	3773.4	3928.7	4142.2	3479.9	4167.9	3146.1	4053.8	3954.8	4095.5
2697.1	4141.1	4342.3	4482.1	3619.5	4731.2	3887.2	3611.1	3781.0	2032.5	4170.4	4589.9	3781.7	2845.5	2416.7	4372.1	4219.2	3452.9	4096.4	4591.9	3664.1	4335.1	4412.4	3839.8
4907.4	5065.2	2944.8	3052.8	2648.7	3712.5	3759.2	3668.0	4012.9	5052.6	8189.2	4255.5	8240.1	4593.4	4509.8	4340.3	3323.9	4109.0	4051.3	4571.9	3349.2	4148.4	3669.8	3963.6
3386.9	3539.3	2697.3	3739.1	3230.8	4468.8	3310.5	3648.2	4436.9	4252.8	4637.0	4683.8	7027.6	4713.3	4434.7	4180.8	2647.6	4012.9	2525.5	4091.1	3317.2	4316.4	4479.5	3935.0
2629.3	3700.1	3549.8	3451.1	4311.5	4276.9	3683.1	3689.5	3958.9	3845.9	4083.3	3551.1	3869.9	3842.4	4823.3	2651.1	3978.2	4229.7	3543.8	3767.7	3384.9	3991.4	3674.4	3361.2
2712.0	3985.9	3998.4	4986.7	3786.4	5053.9	3990.0	6555.6	4036.0	4393.9	4629.8	4274.4	2545.5	4194.5	2813.0	4353.9	4942.2	4678.2	6901.2	4044.9	2926.6	3565.4	3896.6	3652.8
2053.4	1769.8	3398.9	3584.4	3788.4	4459.1	3596.7	3603.8	3276.1	3308.0	3939.9	3855.0	2360.1	3264.2	5327.9	3766.9	4571.3	4068.1	3365.5	3805.6	3212.3	3376.6	3575.1	4036.9
2161.0	4087.4	4571.8	3634.4	4625.7	3674.5	3440.6	3429.2	4776.8	3872.1	3416.3	4519.0	2124.3	4639.0	4043.9	4012.7	2416.4	2659.7	3535.8	4115.9	2945.5	4301.9	3889.9	3445.4
2430.4	4471.8	4002.5	3487.6	4072.6	3974.9	3891.2	4137.4	3294.0	3880.4	3996.8	4045.4	3646.7	4158.0	4264.0	4218.7	4130.7	4383.0	2458.0	3650.6	2934.5	3199.9	3454.6	3460.9
2348.7	3847.3	3546.3	3937.4	3238.8	4128.7	2805.8	3841.0	3881.4	3297.0	6399.7	4364.2	2532.8	3523.7	3433.4	3065.0	3732.8	3266.9	3374.4	3495.3	2389.0	2984.0	3258.0	3337.2
2370.4	3602.0	2816.1	3833.1	3975.0	3857.7	4185.8	3047.6	3025.4	3266.5	4145.7	3598.3	2243.3	3146.9	3342.1	3866.3	3601.1	3735.4	3131.5	3627.8	2902.0	3478.3	3555.0	2932.7
2821.4	3719.4	3466.0	4201.5	3740.6	2951.9	2967.5	2416.3	3620.6	3786.2	3801.7	4048.8	2507.2	3973.6	2618.6	4113.6	4639.5	2774.3	3719.8	3888.6	2883.4	3494.3	3485.9	2935.7
2476.8	4302.2	2667.6	3210.9	3552.7	4214.5	3606.4	3796.9	3227.1	3453.1	3281.8	3839.2	3473.6	3712.7	3764.6	3763.3	3852.7	5971.8	3873.7	3425.8	2964.6	3635.9	3517.2	3326.6
2190.2	4930.5	2841.4	3667.6	8386.1	4669.5	2435.4	3558.0	3512.6	3732.4	3235.3	3879.5	3039.7	2599.4	2863.1	9820.0	4031.9	4186.1	3068.9	3908.6	3135.6	2788.0	3786.5	3217.1
2039.3	4064.6	3289.9	2540.2	1828.9	3306.3	3139.7	4669.2	8176.4	3904.7	3286.8	3055.2	3085.3	4216.4	3842.8	3601.4	4133.6	4245.5	3082.3	3934.3	3160.1	2779.6	3158.1	3275.9
2219.0	3395.7	3891.9	3572.8	3790.8	5264.0	3185.5	3006.5	3760.2	3332.8	3004.1	3715.9	3204.4	3470.1	3595.7	4805.6	4026.4	3504.2	3486.3	3609.2	4899.2	3715.8	3412.9	3232.5

Figure 55 - Pattern of 384 well plate after 4 hours of incubation at fluorescence 530/600

Further optimization was done using absorbance for reading the plates to get a better separation between growth and no growth of bacteria. 590 nm was the absorption value used to read the plates. However, 590 nm did not provide a better distinction between growth and no growth. Figure 56 represents results at absorption value 590 nm.

0.19	0.33	0.17	0.46	0.31	0.28	0.30	0.29	0.31	0.30	0.30	0.27	0.19	0.31	0.28	0.28	0.25	0.32	0.26	0.32	0.24	0.43	0.39	0.45
0.28	0.37	0.35	0.32	0.31	0.34	0.31	0.29	0.27	0.36	0.29	0.27	0.26	0.26	0.05	0.29	0.24	0.37	0.27	0.32	0.35	0.36	0.39	0.40
0.30	0.35	0.32	0.31	0.34	0.34	0.34	0.15	0.36	0.25	0.33	0.28	0.21	0.30	0.31	0.37	0.26	0.33	0.27	0.29	0.29	0.30	0.43	0.36
0.34	0.43	0.09	0.35	0.40	0.36	0.29	0.36	0.38	0.08	0.29	0.38	0.27	0.34	0.36	0.27	0.25	0.32	0.18	0.45	0.44	0.27	0.50	0.50
0.28	0.38	0.35	0.32	0.05	0.05	0.33	0.34	0.29	0.36	0.38	0.33	0.25	0.36	0.38	0.05	0.37	0.38	0.35	0.35	0.34	0.55	0.51	0.55
0.34	0.50	0.08	0.34	0.24	0.34	0.40	0.17	0.41	0.42	0.43	0.43	0.33	0.45	0.17	0.46	0.48	0.48	0.21	0.50	0.52	0.52	0.54	0.57
0.26	0.48	0.51	0.47	0.45	0.46	0.44	0.43	0.34	0.37	0.39	0.40	0.05	0.41	0.12	0.47	0.54	0.45	0.53	0.52	0.53	0.54	0.57	0.60
0.17	0.56	0.40	0.52	0.42	0.42	0.47	0.40	0.45	0.47	0.06	0.45	0.18	0.48	0.51	0.51	0.21	0.23	0.56	0.56	0.59	0.61	0.62	0.67
0.44	0.43	0.43	0.41	0.44	0.45	0.48	0.46	0.49	0.47	0.50	0.47	0.49	0.51	0.55	0.54	0.56	0.56	0.24	0.59	0.63	0.64	0.64	0.58
0.55	0.53	0.32	0.59	0.53	0.56	0.52	0.53	0.59	0.51	0.17	0.42	0.49	0.56	1.06	0.55	0.63	0.46	0.49	0.62	0.59	0.60	0.66	0.61
0.05	0.61	0.57	0.58	0.48	0.49	0.60	0.57	0.27	0.60	0.54	0.41	0.06	0.57	0.59	0.55	0.55	0.60	0.60	0.61	0.62	0.69	0.63	0.64
0.11	0.52	0.55	0.52	0.64	0.48	0.51	0.16	0.45	0.60	0.57	0.66	0.41	0.69	0.32	0.71	0.64	0.35	0.76	0.75	0.75	0.76	0.82	0.61
0.52	0.48	0.49	0.49	0.60	0.57	0.60	0.58	0.57	0.64	0.58	0.74	0.82	0.79	0.88	0.75	0.70	0.39	0.74	0.72	0.75	0.77	0.78	0.78
0.60	0.06	0.64	0.50	0.12	0.63	0.59	0.57	0.59	0.62	0.54	0.64	0.66	0.18	0.71	0.21	0.56	0.53	0.72	0.72	0.70	0.75	0.74	0.75
0.59	0.47	0.64	0.47	0.56	0.52	0.62	0.57	0.24	0.57	0.60	0.61	0.59	0.69	0.72	0.70	0.72	0.54	0.68	0.72	0.74	0.37	0.75	0.76
0.60	0.29	0.71	0.53	0.75	0.44	0.59	0.43	0.62	0.60	0.58	0.61	0.61	0.77	0.60	0.50	0.12	0.74	0.60	0.51	0.14	0.76	0.72	0.71

Figure 56 - Plates read at absorption value 590 nm.

Furthermore, plates were later read using absorption value at 460/610 after 2 and 4 hours of incubation respectively. This absorption ratio failed to provide an optimum result and is shown in Figures 57 and 58.

0.60	0.92	0.69	1.15	1.07	1.12	1.17	0.96	1.18	1.17	1.18	0.81	0.99	0.91	1.17	1.31	1.24	1.31	0.73	1.27	1.27	1.26	0.94	1.19
0.50	0.92	1.09	1.17	0.76	1.18	1.20	1.03	0.78	0.71	1.24	1.16	0.98	1.12	0.67	1.22	1.11	1.31	1.13	1.27	0.95	0.98	0.99	1.15
0.43	0.82	0.89	1.11	1.03	0.87	1.18	1.12	1.03	1.24	0.74	0.86	0.81	1.11	1.17	1.20	1.19	1.21	1.19	0.99	0.93	1.28	1.20	1.16
0.53	0.90	0.33	0.79	1.12	1.22	0.86	1.14	1.19	1.15	1.15	1.19	1.03	1.16	1.15	1.14	0.57	1.12	0.95	1.26	1.12	1.00	1.11	1.13
0.62	0.98	1.06	0.82	0.71	0.55	1.07	1.12	1.01	1.19	1.21	1.16	1.02	1.18	1.12	0.50	1.11	1.10	1.17	1.22	1.11	1.25	1.09	1.16
0.58	1.09	1.33	1.06	0.94	0.93	1.21	1.09	1.16	1.25	1.24	1.26	0.98	1.29	0.83	1.28	0.81	1.34	0.94	1.31	1.19	1.29	1.22	1.18
0.49	0.85	1.09	0.99	1.02	0.98	1.08	1.16	1.09	1.19	1.08	1.18	0.45	1.01	0.84	1.22	1.10	1.01	1.35	1.37	1.26	1.20	1.10	1.16
0.57	1.13	1.04	1.12	1.12	1.16	1.12	1.13	1.08	1.26	1.14	1.29	0.86	1.25	1.23	1.28	0.67	0.91	1.21	1.21	1.16	1.30	1.15	1.15
0.97	1.05	1.11	1.21	1.17	1.25	1.20	1.29	1.19	1.25	1.24	1.22	1.17	1.27	1.17	1.31	1.21	1.32	0.68	1.31	1.15	1.21	1.14	1.15
1.03	1.12	0.93	1.01	1.14	1.02	1.22	1.31	1.30	1.28	1.19	1.29	1.21	1.30	1.36	1.35	1.33	1.32	1.37	1.27	1.35	1.33	1.27	1.00
0.57	1.05	1.07	1.05	1.21	1.25	1.18	1.07	1.16	1.16	1.28	1.28	0.77	1.14	1.20	1.34	1.33	1.35	1.09	1.04	1.11	1.08	1.27	1.00
0.54	1.03	1.03	1.08	1.21	1.16	1.11	0.87	1.08	1.30	1.21	1.23	0.62	1.04	0.56	1.03	1.06	0.47	1.16	1.24	1.11	1.21	1.21	1.10
1.08	1.06	1.02	0.99	1.16	1.10	1.31	1.29	1.23	1.24	1.07	1.30	1.18	1.22	1.21	1.24	1.18	1.06	1.11	1.33	1.08	1.18	1.19	1.12
0.99	0.76	1.04	1.04	0.73	1.09	1.11	1.06	1.09	1.07	1.05	1.06	1.12	0.47	1.07	0.62	1.04	0.88	1.06	1.11	1.04	1.11	1.10	1.14
0.91	1.04	0.97	1.04	0.94	1.15	1.06	1.09	1.03	1.07	1.02	1.22	1.09	1.05	1.07	1.17	1.12	1.06	1.07	1.13	1.06	0.44	1.13	1.00
1.01	1.00	1.10	1.02	1.04	1.04	1.04	1.16	1.14	1.15	1.06	1.16	1.07	1.16	1.01	1.12	0.87	1.11	1.07	1.18	0.61	1.06	1.06	1.09

Figure 57 - Plates read at absorption ratio 460/610 after 2 hours of incubation at 35 °C

0.57	0.84	0.61	1.02	0.94	1.02	1.07	0.89	1.07	1.09	1.09	0.78	0.90	0.82	1.09	1.18	1.12	1.17	0.71	1.13	1.17	1.15	0.91	1.07
0.48	0.85	1.02	1.14	0.77	1.15	1.11	0.98	0.69	0.60	1.17	1.11	0.88	1.06	0.56	1.15	1.04	1.23	1.01	1.16	0.91	0.95	0.94	1.08
0.40	0.84	0.81	1.06	0.97	0.87	1.11	1.04	1.02	1.25	0.75	0.82	0.73	1.12	1.15	1.17	1.10	1.14	1.07	0.94	0.90	1.19	1.11	1.10
0.49	0.82	0.32	0.75	1.05	1.19	0.83	1.08	1.14	1.13	1.09	1.16	0.95	1.13	1.13	1.10	0.50	1.07	0.69	1.17	1.08	0.95	1.04	1.07
0.58	0.91	1.02	0.77	0.63	0.52	1.02	1.05	1.00	1.14	1.15	1.08	0.97	1.10	1.08	0.49	1.06	1.02	1.09	1.13	1.07	1.17	1.07	1.05
0.55	1.03	1.30	1.03	0.91	0.94	1.15	0.98	1.09	1.18	1.23	1.20	1.03	1.21	0.65	1.21	0.69	1.26	0.81	1.22	1.13	1.18	1.14	1.10
0.44	0.74	1.00	0.95	0.96	0.97	1.04	1.10	1.06	1.11	1.06	1.11	0.43	0.96	0.89	1.13	1.05	0.96	1.29	1.29	1.20	1.10	1.03	1.08
0.51	1.06	1.00	1.06	1.09	1.10	1.06	1.07	1.06	1.22	1.02	1.27	0.72	1.20	1.13	1.22	0.60	0.74	1.13	1.13	1.12	1.25	1.09	1.08
0.85	0.97	1.06	1.14	1.12	1.21	1.15	1.26	1.16	1.22	1.20	1.19	1.12	1.21	1.11	1.24	1.16	1.25	0.60	1.21	1.11	1.14	1.07	1.04
0.93	1.04	0.87	0.98	1.11	0.98	1.20	1.27	1.27	1.24	1.11	1.26	1.16	1.25	1.26	1.30	1.29	1.27	1.25	1.30	1.21	1.27	1.27	1.22
0.51	0.93	0.97	1.01	1.21	1.21	1.14	1.03	1.12	1.13	1.29	1.23	0.70	1.09	1.13	1.28	1.26	1.29	1.02	0.96	1.09	1.02	1.21	0.88
0.51	0.95	0.99	1.07	1.20	1.12	1.07	0.76	1.05	1.27	1.17	1.18	0.61	1.01	0.55	0.99	1.02	0.49	1.11	1.18	1.09	1.15	1.13	1.01
1.00	1.02	0.97	0.95	1.14	1.10	1.23	1.26	1.21	1.22	1.10	1.31	1.13	1.18	1.14	1.19	1.13	1.08	1.07	1.27	1.06	1.12	1.10	1.07
0.88	0.67	0.97	0.99	0.71	1.08	1.09	1.01	1.08	1.04	1.02	1.04	1.08	0.47	1.02	0.63	1.01	0.89	1.01	1.05	1.02	1.05	1.08	1.10
0.90	0.98	0.95	0.98	0.87	1.10	1.02	1.05	1.00	1.02	0.96	1.16	1.05	0.98	1.02	1.11	1.08	1.01	1.02	1.07	1.04	0.47	1.09	0.99
0.97	0.94	1.05	0.97	0.99	1.02	1.03	1.14	1.07	1.09	1.00	1.10	1.02	1.11	1.00	1.07	0.91	1.08	1.05	1.14	0.64	1.03	1.04	1.09

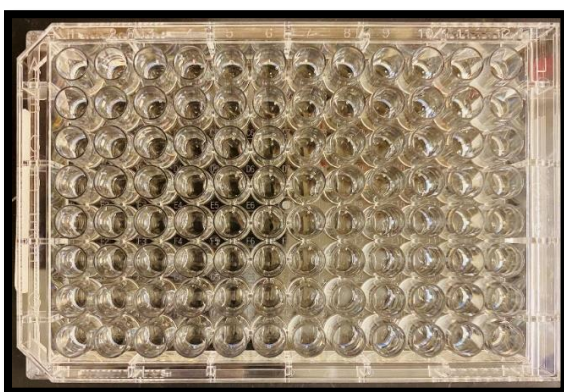
Figure 58 - Plates read at absorption ratio 460/610 after 4 hours of incubation at 35 °C

We optimized VREfm plates using absorbance subtraction values 570 - 460 nm that provided clear difference between growth (pink) and no growth (blue) wells in a 384 well plate.

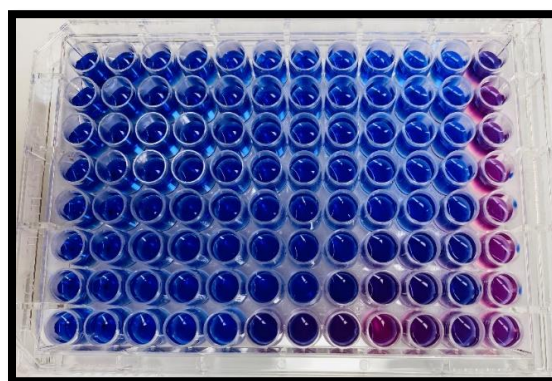
These values were later changed to 610 nm - 450 nm for better optimization. This value was further used for all the experiments. Figure 59 represents the difference between the active and the inactive wells using absorption value 570 - 460 nm.

-0.20	-0.40	-0.35	-0.40	-0.39	-0.39	-0.41	-0.42	-0.42	-0.38	-0.40	-0.42	-0.29	-0.36	-0.38	-0.27	-0.35	-0.35	-0.25	-0.18	-0.15	-0.41	-0.34	-0.21
-0.27	-0.35	-0.39	-0.39	-0.39	-0.27	-0.22	-0.26	-0.39	0.99	-0.34	-0.20	-0.21	-0.28	-0.25	-0.32	-0.45	-0.41	-0.33	-0.33	-0.29	-0.24	-0.31	-0.21
-0.34	-0.27	-0.23	-0.35	-0.37	-0.36	-0.32	-0.24	-0.23	-0.14	-0.28	-0.23	-0.17	-0.18	-0.32	-0.21	-0.34	-0.32	-0.22	-0.21	-0.21	-0.26	-0.27	-0.20
-0.37	-0.38	0.67	-0.40	-0.39	-0.40	-0.39	-0.41	-0.40	-0.43	-0.41	-0.35	-0.38	-0.40	-0.41	-0.40	-0.20	-0.40	0.82	-0.38	-0.33	-0.41	-0.37	-0.35
-0.29	-0.38	-0.40	-0.39	0.81	0.87	-0.26	-0.39	-0.20	-0.39	-0.38	-0.28	-0.30	-0.42	-0.32	0.70	-0.38	-0.34	-0.17	-0.35	-0.33	-0.15	-0.19	-0.19
-0.32	-0.24	-0.37	-0.18	-0.37	-0.24	-0.40	-0.33	-0.33	-0.21	-0.34	-0.14	-0.30	-0.19	-0.15	-0.23	-0.35	-0.20	-0.26	-0.20	-0.29	-0.23	-0.29	-0.21
-0.33	-0.37	-0.35	-0.39	-0.39	-0.40	-0.35	-0.40	-0.29	-0.34	-0.40	-0.20	-0.38	-0.40	-0.35	-0.24	-0.40	-0.38	-0.40	-0.36	-0.40	-0.32	-0.33	-0.22
-0.35	-0.38	-0.41	-0.39	-0.38	-0.39	-0.39	-0.40	-0.35	-0.37	0.23	-0.39	-0.29	-0.37	-0.32	-0.36	-0.32	0.71	-0.27	-0.37	-0.32	-0.45	-0.34	-0.32
-0.28	-0.39	-0.39	-0.33	-0.25	-0.28	-0.39	-0.34	-0.26	-0.17	-0.11	-0.36	-0.18	-0.34	-0.40	-0.26	-0.31	-0.28	0.37	-0.30	-0.09	-0.31	-0.37	-0.23
-0.28	-0.32	-0.35	-0.44	-0.40	-0.29	-0.28	-0.42	-0.13	-0.15	-0.02	-0.12	-0.07	-0.12	-0.08	-0.09	-0.08	-0.11	-0.08	-0.18	-0.18	-0.16	-0.09	-0.27
0.74	-0.39	-0.40	-0.41	-0.42	-0.34	-0.04	-0.44	-0.31	-0.35	-0.30	-0.37	0.67	-0.38	-0.32	-0.37	-0.34	-0.37	-0.33	-0.34	-0.26	-0.36	-0.28	-0.29
0.75	-0.35	-0.32	-0.35	-0.35	-0.34	-0.25	0.23	-0.24	-0.31	-0.24	-0.25	0.64	-0.30	0.66	-0.31	-0.15	0.72	-0.08	-0.31	-0.10	-0.34	-0.10	-0.18
-0.29	-0.36	-0.33	-0.36	-0.38	-0.35	-0.31	-0.29	-0.34	-0.26	-0.32	-0.18	-0.07	-0.12	-0.22	-0.10	-0.29	-0.18	-0.32	-0.19	-0.06	-0.28	-0.26	-0.28
-0.30	-0.30	-0.30	-0.35	-0.08	-0.35	-0.30	-0.41	-0.27	-0.36	-0.27	-0.31	-0.28	-0.16	-0.22	-0.29	-0.36	-0.38	-0.08	-0.15	-0.32	-0.28	-0.24	-0.22
-0.34	-0.39	-0.34	-0.41	-0.36	-0.32	-0.33	-0.32	-0.24	-0.27	-0.23	-0.33	-0.30	-0.33	-0.33	-0.29	-0.24	-0.25	-0.22	-0.27	-0.29	0.79	-0.26	-0.35
-0.36	-0.25	-0.27	-0.28	-0.25	-0.24	-0.26	-0.31	-0.31	-0.29	-0.32	-0.13	-0.28	-0.34	-0.25	-0.21	-0.23	-0.13	-0.19	-0.23	-0.19	-0.12	-0.22	-0.23

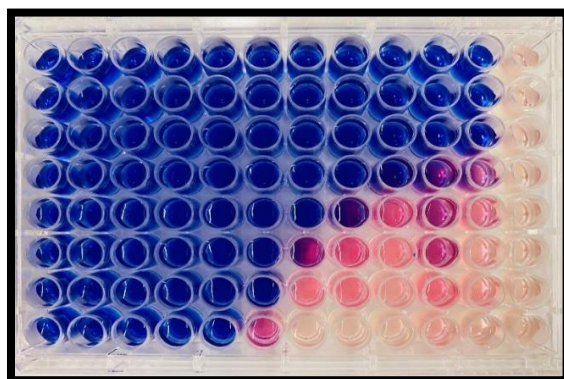
Figure 59 - Plate read using absorbance values 570 nm - 460 nm.



A



B



C

Figure 60 - Shows A) 96 well plate after addition of VREfm. B) 96 well plate after immediate addition of resazurin dye. C) 96 well plate after 2 hours incubation at 35 °C

Table 9 - FDA library anti-VREfm hit MICs (Min_MIC ≤ 12.5 μ M).

Compound	UM MICs (μ M)		PM MICs (μ M)		Min_MIC	L2 _(UM/PM-Vm) ^a	AL2 _(UM/PM) ^b	L2 _(UM-/ +Vm) ^c	AL2 _(-/ +Vm) ^d
	-Vm	+Vm	-Vm	+Vm					
Rifampin	0.1	2.4×10^{-2}	12.5	12.5	2.4×10^{-2}	-7	-8	2	1
Rifapentine	0.2	2.4×10^{-2}	25	12.5	2.4×10^{-2}	-7	-8	3	2
Retapamulin	0.2	4.9×10^{-2}	3.1	1.6	4.9×10^{-2}	-4	-4.5	2	1.5
Rifaximin	0.39	4.9×10^{-2}	50	50	4.9×10^{-2}	-7	-8.5	3	1.5
Rifabutin	0.2	9.8×10^{-2}	25	6.25	9.8×10^{-2}	-7	-6.5	1	1.5
Valnemulin	0.39	9.8×10^{-2}	0.2	9.8×10^{-2}	9.8×10^{-2}	1	0.5	2	1.5
Gemcitabine	0.78	0.2	25	25	0.2	-5	-6	2	1
Mupirocin	3.1	0.78	0.78	0.39	0.39	2	1.5	2	1.5
Closantel	1.6	1.6	12.5	12.5	1.6	-3	-3	0	0
Novobiocin	3.1	1.6	3.1	3.1	1.6	0	-0.5	1	0.5
Fidaxomicin	12.5	6.25	100	100	6.25	-3	-3.5	1	0.5
Florfenicol	25	25	12.5	6.25	6.25	1	1.5	0	0.5
Linezolid	3.1	1.6	6.25	6.25	6.25	-1	-1.5	1	0.5

^a $L2_{(UM/PM-Vm)} = \log_2 \left(\frac{UM-Vm}{PM-Vm} \right)$. ^b $AL2_{(UM/PM)} = \text{Avg}(\log_2 \left(\frac{UM-Vm}{PM-Vm} \right), \log_2 \left(\frac{UM+Vm}{PM+Vm} \right))$.

^c $L2_{(UM-/ +Vm)} = \log_2 \left(\frac{UM-Vm}{UM+Vm} \right)$. ^d $AL2_{(-/ +Vm)} = \text{Avg}(\log_2 \left(\frac{UM-Vm}{UM+Vm} \right), \log_2 \left(\frac{PM-Vm}{PM+Vm} \right))$.

Table 10 - List of actives (validated min_MIC < 100 μ M) from library screening against VREfm (clinical) (UM/PM vs +/- 16 μ g/mL vancomycin) ranked by lowest minimum MIC. NA = no activity.

Compound	CAS_Number	UM MICs (μ M)		PM MICs (μ M)		Min_MIC
		-Vm	+Vm	-Vm	+Vm	
Retapamulin	224452-66-8	0.10	4.9E-2	3.1	1.6	4.9E-2
Valnemulin	133868-46-9	0.39	9.8E-2	0.20	9.8E-2	9.8E-2
Mupirocin	12650-69-0	3.1	0.78	0.78	0.39	0.39
Rifapentine	61379-65-5	0.2	2.4E-2	25	12.5	2.4E-2
Novobiocin	1476-53-5	3.1	1.6	3.1	3.1	1.60
Fidaxomicin	873857-62-6	12.5	6.25	NA	NA	6.25
Closantel	57808-65-8	1.6	1.6	12.5	12.5	1.60
Florfenicol	73231-34-2	25	25	12.5	6.25	6.25
Cetrimonium Bromide	57-09-0	12.5	12.5	NA	NA	12.5
Linezolid	165800-03-3	3.1	1.6	6.25	6.25	1.60
Rifampin	13292-46-1	0.10	2.4E-2	12.5	12.5	2.4E-2
Rifaximin	80621-81-4	0.39	4.9E-2	50	50	4.9E-2
Gemcitabine	95058-81-4	0.78	0.20	25	25	0.20
Rifabutin	72559-06-9	0.20	9.8E-2	25	6.25	9.8E-2
Cetylpyridinium Chloride	123-03-5	50	25	NA	NA	25
Daunorubicin	23541-50-6	50	25	NA	NA	25
Methacycline	3963-95-9	50	25	NA	NA	25
Sitafloxacin	163253-35-8	25	25	NA	NA	25
Thiamphenicol	15318-45-3	50	50	25	25	25
Balofloxacin	127294-70-6	NA	NA	50	50	50
Benzethonium chloride	121-54-0	50	50	NA	NA	50
Candesartan cilexetil	145040-37-5	NA	50	NA	NA	50
Clomifene citrate (Serophene)	50-41-9	NA	50	NA	NA	50
Domiphen Bromide	538-71-6	50	50	NA	NA	50
Doxorubicin	25316-40-9	NA	50	NA	NA	50
Dronedaron HCl (Multaq)	141625-93-6	50	50	NA	NA	50
Epirubicin HCl	56390-09-1	NA	50	NA	NA	50
Gatifloxacin	112811-59-3	NA	NA	50	50	50
Idarubicin	57852-57-0	NA	50	NA	NA	50
Moxifloxacin	186826-86-8	NA	NA	50	NA	50
Otilonium Bromide	26095-59-0	50	50	NA	NA	50
Penfluridol	26864-56-2	NA	50	NA	NA	50
Tamoxifen	54965-24-1	50	50	NA	NA	50
Terfenadine	50679-08-8	NA	50	NA	NA	50

Table 11 - All the inactive drugs screened against VREfm.

9-Aminoacridine	90-45-9
Abitrexate	59-05-2
Acipimox	51037-30-0
Adrucil	51-21-8
Cinacalcet	364782-34-3
Amoxicillin	26787-78-0
Amoxicillin	34642-77-8
Azlocillin	37091-65-9
Bacitracin	1405-87-4
Bazedoxifene	198480-56-7
Benzbromarone	3562-84-3
Bifonazole	60628-96-8
Brinzolamide	138890-62-7
Caspofungin	179463-17-3
Celecoxib	169590-42-5
Chlorprothixene	113-59-7
Clorsulon	60200-06-8
Clotrimazole	23593-75-1
Crizotinib	877399-52-5
Curcumin	458-37-7
Diclazuril	101831-37-2
Diethylstilbestrol	56-53-1
Duloxetine	136434-34-9
Econazole	24169-02-6
Elvitegravir	697761-98-1
Ethoxzolamide	452-35-7
Famotidine	76824-35-6
Fosaprepitant	265121-04-8
Isoconazole	24168-96-5
Ivacaftor	873054-44-5
Licofelone	156897-06-2
Miconazole	22916-47-8
Miconazole	22832-87-7
Mitoxantrone	70476-82-3
Nadifloxacin	124858-35-1
Nebivolol	152520-56-4
Nifuroxazide	965-52-6
Oxethazaine	126-27-2
Oxytetracycline	6153-64-6
Pitavastatin	147526-32-7

Ponatinib	943319-70-8
Pralatrexate	146464-95-1
Prochlorperazine	84-02-6
Pyrithione	13463-41-7
Sertraline	79559-97-0
Sulconazole	82382-23-8
Telmisartan	144701-48-4
Teriflunomide	108605-62-5
Tetracycline	64-75-5
Ticagrelor	274693-27-5
Tioconazole	65899-73-2
Tolfenamic	13710-19-5
Trifluoperazine	440-17-5
Trifluridine	70-00-8
Trimethoprim	738-70-5
Verteporfin	129497-78-5
Zafirlukast	107753-78-6
Axitinib	319460-85-0
Lapatinib	388082-77-7
Vandetanib	443913-73-3
Anastrozole	120511-73-1
Cladribine	4291-63-8
Bendamustine	3543-75-7
Etoposide	33419-42-0
Vincristine	2068-78-2
Posaconazole	171228-49-2
Altretamine	645-05-6
Camptothecin	7689-03-4
Megestrol	595-33-5
Felbamate	25451-15-4
Ivermectin	70288-86-7
Doripenem	364622-82-2
Mosapride	112885-42-4
Stavudine	3056-17-5
Alfuzosin	81403-68-1
Tizanidine	64461-82-1
Atazanavir	229975-97-7
Alprostadil	745-65-3
Pimobendan	74150-27-9
Olmesartan	144689-63-4
Silodosin	160970-54-7
Ethinyl	57-63-6
Amphotericin	1397-89-3

Ketorolac	74103-07-4
Enalaprilat	84680-54-6
Aminoglutethimide	125-84-8
Sulfanilamide	63-74-1
Desonide	638-94-8
Deferasirox	201530-41-8
Indomethacin	53-86-1
Mesna	19767-45-4
Esomeprazole	161973-10-0
Suprofen	40828-46-4
Oxytetracycline	79-57-2
Betaxolol	63659-19-8
Albendazole	54029-12-8
Afatinib	439081-18-2
Lenalidomide	191732-72-6
Vorinostat	149647-78-9
Docetaxel	114977-28-5
Aprepitant	170729-80-3
Decitabine	2353-33-5
Nelarabine	121032-29-9
Evista	82640-04-8
Agomelatine	138112-76-2
Prasugrel	150322-43-3
Amisulpride	71675-85-9
Carmofur	61422-45-5
Mercaptopurine	50-44-2
Fluconazole	86386-73-4
Ketoconazole	65277-42-1
Gestodene	60282-87-3
Nafamostat	82956-11-4
Tenofovir	202138-50-9
Clopidogrel	120202-66-6
Topiramate	97240-79-4
Marbofloxacin	115550-35-1
Fludarabine	21679-14-1
Tadalafil	171596-29-5
Pomalidomide	19171-19-8
Cefdinir	91832-40-5
Riluzole	1744-22-5
Naproxen	26159-34-2
Ibuprofen	15687-27-1
Adenosine	58-61-7
Dofetilide	115256-11-6

Aminophylline	317-34-0
Betamethasone	5593-20-4
Didanosine	69655-05-6
Piroxicam	36322-90-4
Terbinafine	91161-71-6
Methocarbamol	532-03-6
Niacin	59-67-6
Pyrazinamide	98-96-4
Simvastatin	79902-63-9
Acyclovir	59277-89-3
Proparacaine	5875-06-9
Chloroxine	773-76-2
Pefloxacin	70458-95-6
Bortezomib	179324-69-7
Nilotinib	641571-10-0
Masitinib	790299-79-5
Paclitaxel	33069-62-4
Bicalutamide	90357-06-5
Dutasteride	164656-23-9
Bleomycin	9041-93-4
Leflunomide	75706-12-6
Ramelteon	196597-26-9
Aniracetam	72432-10-1
Cetirizine	83881-52-1
Streptozotocin	18883-66-4
Flumazenil	78755-81-4
Lansoprazole	103577-45-3
Drospirenone	67392-87-4
Omeprazole	73590-58-6
Tenofovir	147127-20-6
Ranolazine	95635-56-6
Tranilast	53902-12-8
Cyclosporine	79217-60-0
Tazarotene	118292-40-3
Risperidone	106266-06-2
Nitazoxanide	55981-09-4
Amprenavir	161814-49-9
Zolmitriptan	139264-17-8
Isradipine	75695-93-1
Amorolfine	78613-38-4
Betapar	1247-42-3
Divalproex	76584-70-8
Levonorgestrel	797-63-7

Prednisolone	50-24-8
Nimodipine	66085-59-4
Quetiapine	111974-72-2
Ethionamide	536-33-4
Ramipril	87333-19-5
Nifedipine	21829-25-4
Pranlukast	103177-37-3
Lomustine	13010-47-4
Metoprolol	392-17-7
Bosutinib	380843-75-4
Pazopanib	635702-64-6
Capecitabine	154361-50-9
Fulvestrant	129453-61-8
Melatonin	73-31-4
Clofarabine	123318-82-1
Fludarabine	75607-67-9
Enzalutamide	915087-33-1
Artemisinin	63968-64-9
Cilnidipine	132203-70-4
Dexamethasone	50-02-2
Fluoxetine	56296-78-7
Levetiracetam	102767-28-2
Ruxolitinib	941678-49-5
Ondansetron	99614-01-4
Tigecycline	220620-09-7
Repaglinide	135062-02-1
Venlafaxine	99300-78-4
Calcitriol	32222-06-3
Betamethasone	378-44-9
Natamycin	7681-93-8
Sulfasalazine	599-79-1
Rizatriptan	145202-66-0
Sulfameter	651-06-9
Triamcinolone	76-25-5
Albendazole	54965-21-8
Telbivudine	3424-98-4
Estrone	53-16-7
Chloramphenicol	56-75-7
Betamethasone	2152-44-5
Emtricitabine	143491-57-0
Glipizide	29094-61-9
Gemfibrozil	25812-30-0
Nisoldipine	63675-72-9

Fenofibrate	49562-28-9
Amiloride	2016-88-8
Oxfendazole	53716-50-0
Chenodeoxycholic	474-25-9
Dasatinib	302962-49-8
Rapamycin	53123-88-9
Vismodegib	879085-55-9
Cisplatin	15663-27-1
Thalidomide	50-35-1
Bisoprolol	104344-23-2
Dacarbazine	4342-03-4
Topotecan	119413-54-6
Dienogest	65928-58-7
Asenapine	65576-45-6
Cilostazol	73963-72-1
Doxazosin	77883-43-3
Fluvoxamine	61718-82-9
Lidocaine	137-58-6
Isotretinoin	4759-48-2
Oxcarbazepine	28721-07-5
Trilostane	13647-35-3
Rolipram	61413-54-5
Voriconazole	137234-62-9
Doxercalciferol	54573-75-0
Mycophenolate	128794-94-5
Telaprevir	402957-28-2
Candesartan	139481-59-7
Pyridostigmine	101-26-8
Prilocaine	721-50-6
Orlistat	96829-58-2
Chlorothiazide	58-94-6
Monobenzene	103-16-2
Flucytosine	2022-85-7
Flurbiprofen	51543-39-6
Praziquantel	55268-74-1
Progesterone	57-83-0
Glyburide	10238-21-8
Indapamide	26807-65-8
Thiabendazole	148-79-8
Oxybutynin	5633-20-5
Beta Carotene	7235-40-7
Azacitidine	320-67-2
Ranolazine	95635-55-5

Amlodipine	111470-99-6
Carvedilol	72956-09-3
Cimetidine	51481-61-9
Diltiazem	33286-22-5
Erlotinib	183319-69-9
Sorafenib	475207-59-1
Cabozantinib	849217-68-1
Valproic	1069-66-5
Exemestane	107868-30-4
Dexrazoxane	149003-01-0
2-Methoxyestradiol	362-07-2
Entecavir	209216-23-9
Vemurafenib	918504-65-1
Benazepril	86541-74-4
Floxuridine	50-91-9
Edaravone	89-25-8
Loratadine	79794-75-5
Lopinavir	192725-17-0
Pizotifen	5189-11-7
Vecuronium	50700-72-6
Sildenafil	171599-83-0
Zileuton	111406-87-2
Alfacalcidol	41294-56-8
Cephalexin	15686-71-2
Saxagliptin	361442-04-8
Apixaban	503612-47-3
Methimazole	60-56-0
Darunavir	635728-49-3
Allopurinol	315-30-0
Ursodiol	128-13-2
Tretinoin	302-79-4
Trichlormethiazide	133-67-5
Disulfiram	97-77-8
Busulfan	55-98-1
Lamivudine	134678-17-4
Adefovir	142340-99-6
Mitotane	53-19-0
Guaifenesin	93-14-1
Enoxacin	74011-58-8
Cefditoren	117467-28-4
Vidarabine	5536-17-4
Ranitidine	66357-59-3
Chlorpheniramine	113-92-8

Atracurium	64228-81-5
Clemastine	14976-57-9
Diphenhydramine	147-24-0
Gefitinib	184475-35-2
Sunitinib	341031-54-7
Everolimus	159351-69-6
Regorafenib	755037-03-7
Finasteride	98319-26-7
Letrozole	112809-51-5
Nepafenac	78281-72-8
Acarbose	56180-94-0
Budesonide	51333-22-3
Ftorafur	17902-23-7
Etodolac	41340-25-4
Genistein	446-72-0
Losartan	124750-99-8
Meropenem	96036-03-2
Resveratrol	501-36-0
Bimatoprost	155206-00-1
Sumatriptan	103628-48-4
Ziprasidone	122883-93-6
Iloperidone	133454-47-4
Dyphylline	479-18-5
Febuxostat	144060-53-7
Reserpine	50-55-5
Metolazone	17560-51-9
Prednisone	53-03-2
Nitrofurazone	59-87-0
Phenylbutazone	50-33-9
Loteprednol	82034-46-6
Mesalamine	89-57-6
Carbamazepine	298-46-4
Hydrochlorothiazide	58-93-5
Zalcitabine	7481-89-2
Methylprednisolone	83-43-2
Sulfadiazine	68-35-9
Acadesine	2627-69-2
Fenoprofen	34597-40-5
Butoconazole	64872-77-1
Dapoxetine	129938-20-1
Imatinib	220127-57-1
Temsirolimus	162635-04-3
Malotilate	59937-28-9

Ritonavir	155213-67-5
Irinotecan	97682-44-5
Oxaliplatin	61825-94-3
Methazolastone	85622-93-1
Rufinamide	106308-44-5
Adapalene	106685-40-9
Bumetanide	28395-03-1
Ifosfamide	3778-73-2
Etomidate	33125-97-2
Glimepiride	93479-97-1
Acitretin	55079-83-9
Mianserin	21535-47-7
Rocuronium	119302-91-9
Tianeptine	30123-17-2
Zonisamide	68291-97-4
Naratriptan	143388-64-1
Aztreonam	78110-38-0
Furosemide	54-31-9
Cefoperazone	62893-19-0
Acetylcysteine	616-91-1
Erythromycin	114-07-8
Ketoprofen	22071-15-4
Ezetimibe	163222-33-1
Aminocaproic	60-32-2
Ipratropium	22254-24-6
Hydrocortisone	50-23-7
Estradiol	50-28-2
Azathioprine	446-86-6
Meloxicam	71125-38-7
Nevirapine	129618-40-2
Teniposide	29767-20-2
Acetylcholine	60-31-1
Erdosteine	84611-23-4
Azithromycin	83905-01-5
Daidzein	486-66-8
Valaciclovir	124832-27-5
Ganciclovir	82410-32-0
Carbidopa	28860-95-9
Diclofenac	15307-79-6
Pregnenolone	145-13-1
Triamcinolone	124-94-7
Sulfamethizole	144-82-1
Nicorandil	65141-46-0

Propylthiouracil	51-52-5
Pramipexole	191217-81-9
Ginkgolide	15291-75-5
Lornoxicam	70374-39-9
Terazosin	70024-40-7
Argatroban	74863-84-6
Ambrisentan	177036-94-1
Imidapril	89371-37-9
Roflumilast	162401-32-3
Irinotecan	136572-09-3
Nalidixic	389-08-2
Genipin	6902-77-8
Bethanechol	590-63-6
Famciclovir	104227-87-4
Manidipine	89226-50-6
Olanzapine	132539-06-1
Racecadotril	81110-73-8
Vardenafil	330808-88-3
Acetanilide	103-84-4
Sulbactam	69388-84-7
Dimethyl Fumarate	624-49-7
Acemetacin	53164-05-9
Cobicistat	1004316-88-4
Aspirin	50-78-2
Fenoprofen	71720-56-4
Rofecoxib	162011-90-7
Medetomidine	86347-15-1
Etravirine	269055-15-4
Vitamin C	50-81-7
Sulfamethazine	57-68-1
Roxatidine	93793-83-0
Valsartan	137862-53-4
Avobenzone	70356-09-1
Sulfamethoxazole	723-46-6
Nystatin	1400-61-9
Sulbactam	68373-14-8
Fluticasone	80474-14-2
Suplatast	94055-76-2
Phentolamine	65-28-1
Captopril	62571-86-2
Bromhexine	611-75-6
Mecarbinat	15574-49-9
Trimebutine	39133-31-8

Bexarotene	153559-49-0
Lapatinib	231277-92-2
Dextrose	50-99-7
Apatinib	811803-05-1
Ammonium	1407-03-0
Geniposidic	27741-01-1
Chlorpromazine	69-09-0
Fenbendazole	43210-67-9
Milrinone	78415-72-2
Olopatadine	140462-76-6
Ribavirin	36791-04-5
Xylazine	23076-35-9
Ciclopirox	29342-05-0
Clomipramine	17321-77-6
Azelastine	79307-93-0
Cloxacillin	7081-44-9
Xylometazoline	1218-35-5
Miglitol	72432-03-2
Tioxolone	4991-65-5
Arecoline	300-08-3
Carbazochrome	51460-26-5
Niflumic	4394-00-7
Linagliptin	668270-12-0
Cinepazide	26328-04-1
Diclofenac Potassium	15307-81-0
Ulipristal	159811-51-5
Sulfathiazole	72-14-0
Sodium	54-21-7
Protionamide	14222-60-7
Dipyridamole	58-32-2
Amlodipine	88150-42-9
Sulfisoxazole	127-69-5
Isoniazid	54-85-3
Meglumine	6284-40-8
Lacidipine	103890-78-4
Mirtazapine	85650-52-8
Uridine	58-96-8
Nimesulide	51803-78-2
Lovastatin	75330-75-5
Rosiglitazone	302543-62-0
Ivabradine	148849-67-6
Temocapril	110221-44-8
Cisatracurium	96946-42-8

Xylose	25990-60-7
Dabigatran	211915-06-9
TAME	901-47-3
D-Mannitol	69-65-8
Tolbutamide	64-77-7
Clindamycin	21462-39-5
Fluocinolone	67-73-2
Oxymetazoline	2315-02-8
Rosiglitazone	155141-29-0
Maprotiline	10347-81-6
Dopamine	62-31-7
Phenformin	834-28-6
5-Aminolevulinic	5451-09-2
Phenacetin	62-44-2
Pioglitazone	111025-46-8
Dehydroepiandrosterone	53-43-0
Noradrenaline	108341-18-0
Rivaroxaban	366789-02-8
Ciclopirox	41621-49-2
Bindarit	130641-38-2
Azilsartan	147403-03-0
Diclofenac	78213-16-8
Indacaterol	753498-25-8
Oxybutynin	1508-65-2
Methylthiouracil	56-04-2
Idoxuridine	54-42-2
Hydroxyurea	127-07-1
Metronidazole	443-48-1
Crystal violet	548-62-9
Levofloxacin	100986-85-4
Pranoprofen	52549-17-4
Aripiprazole	129722-12-9
Benidipine	91599-74-5
Flunarizine	30484-77-6
Dyclonine	536-43-6
Cytidine	65-46-3
Tiopronin	1953-02-2
Atorvastatin	134523-03-8
Rivastigmine	129101-54-8
Gabexate	56974-61-9
Mestranol	72-33-3
Tebipenem	161715-24-8
Eltrombopag	496775-62-3

Sorbitol	50-70-4
Levosimendan	141505-33-1
Clonidine	4205-91-8
Gallamine	65-29-2
Moroxydine	3160-91-6
Ozagrel	82571-53-7
Roxithromycin	80214-83-1
Naphazoline	550-99-2
Ritodrine	23239-51-2
Ceftiofur	103980-44-5
Clarithromycin	81103-11-9
Isoprenaline	51-30-9
Zidovudine	30516-87-1
Tolvaptan	150683-30-0
Idebenone	58186-27-9
Ibrutinib	936563-96-1
Paroxetine	78246-49-8
Rimonabant	168273-06-1
Vildagliptin	274901-16-5
Naloxone	357-08-4
2-Thiouracil	141-90-2
Ornidazole	16773-42-5
Methenamine	100-97-0
Sparfloxacin	110871-86-8
Potassium	7681-11-0
Flutamide	13311-84-7
Haloperidol	52-86-8
Enalapril	76095-16-4
Sulphadimethoxine	122-11-2
Methscopolamine	155-41-9
Maraviroc	376348-65-1
Formoterol	43229-80-7
Fenticonazole	73151-29-8
Memantine	41100-52-1
Orphenadrine	4682-36-4
Dexmedetomidine	145108-58-3
Rasagiline	161735-79-1
Conivaptan	168626-94-6
Naftopidil	57149-07-2
Rosuvastatin	147098-20-2
Esomeprazole	161796-78-7
Cephalomannine	71610-00-9
Amantadine	665-66-7

Clozapine	5786-21-0
Imatinib	152459-95-5
Mycophenolic	24280-93-1
Pancuronium	15500-66-0
Scopolamine	114-49-8
Epinephrine	51-42-3
Scopine	498-45-3
Rosiglitazone	122320-73-4
Medroxyprogesterone	71-58-9
Quinapril	82586-55-8
Pramiracetam	68497-62-1
Mifepristone	84371-65-3
Nilvadipine	75530-68-6
Zanamivir	139110-80-8
Cabazitaxel	183133-96-2
Solifenacin	242478-38-2
Moguisteine	119637-67-1
Dexamethasone	1177-87-3
Milnacipran	101152-94-7
Felodipine	72509-76-3
Tropisetron	105826-92-4
Fluvastatin	93957-55-2
Phenindione	83-12-5
Menadione	58-27-5
Rimantadine	13392-28-4
Amiodarone	19774-82-4
Raltegravir	518048-05-0
Chlormezanone	80-77-3
Rebamipide	90098-04-7
Cyproheptadine	969-33-5
Gimeracil	103766-25-2
Lafutidine	118288-08-7
Moexipril	82586-52-5
Betaxolol	659-18-7
Naltrexone	16676-29-2
Ibutilide	122647-32-9
S-(+)-Rolipram	85416-73-5
Aliskiren	173334-58-2
Fesoterodine	286930-03-8
10-Deacetylbaecatin-III	32981-86-5
Amfebutamone	31677-93-7
Pramipexole	104632-26-0
Itraconazole	84625-61-6

Nateglinide	105816-04-4
Phenoxybenzamine	63-92-3
Sotalol	959-24-0
L-Adrenaline	51-43-4
Tiotropium	139404-48-1
Terbinafine	78628-80-5
Phenylephrine	61-76-7
Clindamycin	25507-04-4
Buflomedil	35543-24-9
Dabrafenib	1195765-45-7
Zaltoprofen	74711-43-6
Bufexamac	2438-72-4
Pravastatin	81131-70-6
Azelnidipine	123524-52-7
Dexmedetomidine	113775-47-6
Darifenacin	133099-07-7
Deflazacort	14484-47-0
Nicotinamide	98-92-0
Alibendol	26750-81-2
Methoxsalen	298-81-7
Primidone	125-33-7
Adenine	2922-28-3
Pyrimethamine	58-14-0
Ketotifen	34580-14-8
Epalrestat	82159-09-9
Doxifluridine	3094-09-5
Cyclophosphamide	6055-19-2
Moxonidine	75438-57-2
Cleviprex	167221-71-8
Detomidine	90038-01-0
Levosulpiride	23672-07-3
Probucol	23288-49-5
Desmethyl Erlotinib	183320-51-6
Artemether	71963-77-4
Paeoniflorin	23180-57-6
Benserazide	14919-77-8
Domperidone	57808-66-9
Lincomycin	859-18-7
Nitrendipine	39562-70-4
Propafenone	34183-22-7
Spectinomycin	21736-83-4
Phenytoin	630-93-3
Trospium	10405-02-4

Cortisone	50-04-4
Prednisolone	52-21-1
Clobetasol	25122-46-7
L-Thyroxine	51-48-9
Fluocinonide	356-12-7
Clindamycin	18323-44-9
Pazopanib	444731-52-6
Lamotrigine	84057-84-1
Bepotastine	190786-44-8
Alverine	5560-59-8
Beclomethasone	5534-09-8
Pidotimod	121808-62-6
Biotin	58-85-5
Tripelennamine	154-69-8
Nizatidine	76963-41-2
Vitamin	68-19-9
Tropicamide	1508-75-4
Irsogladine	57381-26-7
Nefiracetam	77191-36-7
Mometasone	83919-23-7
Sulindac	38194-50-2
Urapidil	64887-14-5
Aspartame	22839-47-0
Pioglitazone	112529-15-4
Tolnaftate	2398-96-1
Ozagrel	78712-43-3
Adiphenine	50-42-0
Almotriptan	181183-52-8
Flunixin	42461-84-7
Arbidol	131707-23-8
Atropine	5908-99-6
DAPT	208255-80-5
DL-Carnitine	461-05-2
Geniposide	24512-63-8
Bupivacaine	18010-40-7
Estriol	50-27-1
Loperamide	34552-83-5
Quinine	6119-47-7
Tenoxicam	59804-37-4
Phenytoin	57-41-0
Secnidazole	3366-95-8
Tolterodine	124937-52-6
Amiloride	17440-83-4

Tetracaine	136-47-0
Brompheniramine	980-71-2
Gliclazide	21187-98-4
Lonidamine	50264-69-2
Carfilzomib	868540-17-4
PMSF	329-98-6
Azilsartan	863031-21-4
Atovaquone	95233-18-4
Pyridoxine	58-56-0
Sulfamerazine	127-79-7
Entacapone	130929-57-6
Estradiol	979-32-8
Benztropine	132-17-2
Carbenicillin	4800-94-6
Azacyclonol	115-46-8
Moclobemide	71320-77-9
Desloratadine	100643-71-8
Probenecid	57-66-9
Vitamin	50-14-6
toltrazuril	69004-03-1
Vitamin	67-97-0
Lomerizine	101477-54-7
Droperidol	548-73-2
Deoxyarbutin	53936-56-4
Amfenac	61618-27-7
Doxofylline	69975-86-6
1-Hexadecanol	36653-82-4
Penciclovir	39809-25-1
Chlorquinaldol	72-80-0
Benzocaine	94-09-7
Pilocarpine	54-71-7
Meclofenamate	6385-02-0
Diphenylpyraline	132-18-3
Metaraminol	33402-03-8
Procyclidine	1508-76-5
Noscapine	912-60-7
Acetarstone	97-44-9
Oxeladin	52432-72-1
Tacrolimus	104987-11-3
Articaine	23964-57-0
Altrenogest	850-52-2
Flumequine	42835-25-6
Reboxetine	98769-84-7

Pergolide	66104-23-2
Hyoscyamine	101-31-5
Procaine	51-05-8
Doxapram	7081-53-0
Pheniramine	132-20-7
Spiroinolactone	52-01-7
Escitalopram	219861-08-2
Propranolol	318-98-9
Levobetaxolol	116209-55-3
Dydrogesterone	152-62-5
Clofazimine	2030-63-9
Clorprenaline	6933-90-0
Benzydamine	132-69-4
Sulfaguanidine	57-67-0
Tiratricol	51-24-1
Azaguanine-8	134-58-7
Furaltadone	3759-92-0
Montelukast	151767-02-1
Piperacillin	59703-84-3
Nithiamide	140-40-9
Deoxycorticosterone	56-47-3
Disopyramide	22059-60-5
Meticrane	1084-65-7
Ractopamine	90274-24-1
Phenothrin	26002-80-2
Mepenzolate	76-90-4
Bephenium	3818-50-6
Pasiniazid	2066-89-9
Pimecrolimus	137071-32-0
Gliquidone	33342-05-1
Ampicillin	69-52-3
Amitriptyline	549-18-8
Triflusal	322-79-2
Lithocholic	434-13-9
Cyclamic	100-88-9
Homatropine	80-49-9
Dibucaine	61-12-1
Estradiol	313-06-4
Guanabenz	23256-50-0
Mequinol	150-76-5
Loxapine	27833-64-3
Dexlansoprazole	138530-94-6
Dicloxacillin	13412-64-1

Carprofen	53716-49-7
Ethamsylate	2624-44-4
Chlorpropamide	94-20-2
Trometamol	77-86-1
Broxyquinoline	521-74-4
Isosorbide	652-67-5
Dirithromycin	62013-04-1
Mevastatin	73573-88-3
Zoxazolamine	61-80-3
Serotonin	153-98-0
Moxalactam	64953-12-4
Phthalylsulfacetamide	131-69-1
Aceclidine	6109-70-2
Brucine	652154-10-4
Butenafine	101827-46-7
Anagrelide	58579-51-4
Adrenalone	62-13-5
Ethambutol	1070-11-7
Ouabain	630-60-4
Homatropine	51-56-9
Methazolamide	554-57-4
Bisacodyl	30652-11-0
Methyclothiazide	135-07-9
tinidazole	19387-91-8
Mefenamic	61-68-7
Flumethasone	2135-17-3
Esmolol	81161-17-3
Triclabendazole	68786-66-3
Dropropizine	17692-31-8
Chlorzoxazone	95-25-0
Cyromazine	66215-27-8
Uracil	66-22-8
Salicylanilide	87-17-2
Ethacridine	6402-23-9
Dibenzothiophene	132-65-0
Sucralose	56038-13-2
Mexiletine	5370-01-4
Phenazopyridine	136-40-3
Sodium	134-03-2
Anisotropine	80-50-2
Famprofazone	22881-35-2
Nalmefene	58895-64-0
Tacrine	1684-40-8

Carbenoxolone	7421-40-1
Imipramine	113-52-0
Camylofin	54-30-8
Procodazole	23249-97-0
Mepivacaine	1722-62-9
Antipyrine	60-80-0
Azatadine	3978-86-7
Catharanthine	2468-21-5
Pentamidine	140-64-7
Allylthiourea	109-57-9
Hydroxyzine	2192-20-3
norethindrone	68-22-4
Carbimazole	22232-54-8
Ropivacaine	98717-15-8
Guanidine	50-01-1
Halobetasol	66852-54-8
Voglibose	83480-29-9
Isovaleramide	541-46-8
Amprolium	137-88-2
Bezafibrate	41859-67-0
Climbazole	38083-17-9
Sasapyrine	552-94-3
Bemegride	64-65-3
Cysteamine	156-57-0
Primaquine	63-45-6
Vinorelbine	125317-39-7
Benzthiazide	91-33-8
Isoetharine	7279-75-6
Nialamide	51-12-7
Pimozide	2062-78-4
Nicotine	65-31-6
Proadifen	62-68-0
Clofoctol	37693-01-9
Sodium	94-16-6
Ethynodiol	297-76-7
Atomoxetine	82248-59-7
(+,-)-Octopamine	770-05-8
Meptazinol	59263-76-2
Mirabegron	223673-61-8
Avanafil	330784-47-9
Flavoxate	3717-88-2
olsalazine	6054-98-4
Bextra	181695-72-7

Sodium Nitroprusside	14402-89-2
Decamethonium	541-22-0
triamterene	396-01-0
Fenspiride	5053-08-7
Eprosartan	144143-96-4
Penicillin	69-57-8
Coumarin	91-64-5
Mezlocillin	42057-22-7
Cyclandelate	456-59-7
Aminothiazole	96-50-4
Clofibric	882-09-7
Liothyronine	55-06-1
Fluorometholone	3801-06-7
Cepharanthine	481-49-2
Rotigotine	99755-59-6
Calcium	17140-60-2
Mepiroxol	6968-72-5
Carbachol	51-83-2
Pridinol	6856-31-1
Pyrilamine	59-33-6
Diperodon	537-12-2
Trimipramine	521-78-8
Sertaconazole	99592-39-9
Betahistine	5579-84-0
Ropinirole	91374-20-8
Fexofenadine	153439-40-8
Acebutolol	34381-68-5
Sodium	10040-45-6
Aclidinium	320345-99-1
nafcillin	7177-50-6
valganciclovir	175865-59-5
Erythromycin	1264-62-6
Aminosalicylate	133-10-8
sulfacetamide	127-56-0
Pramoxine	637-58-1
Diminazene	908-54-3
Tilmicosin	108050-54-0
Azithromycin	117772-70-0
Benzoic	65-85-0
Choline	67-48-1
Nicardipine	54527-84-3
Cinchophen	132-60-5
Antazoline	2508-72-7

Chromocarb	4940-39-0
Azaperone	1649-18-9
Oxybuprocaine	5987-82-6
Bergapten	484-20-8
Nelfinavir	159989-65-8
Carbadox	6804-07-5
Mesoridazine	32672-69-8
Pentoxifylline	6493-05-6
Tolmetin	64490-92-2
Triflupromazine	1098-60-8
Difloxacin	91296-86-5
Isoxicam	34552-84-6
Vinblastine	143-67-9
Tylosin	74610-55-2
Amidopyrine	58-15-1
Ampiroxicam	99464-64-9
Tolcapone	134308-13-7
Diphemanil	62-97-5
tetrahydrozoline	522-48-5
Nabumetone	42924-53-8
Ronidazole	7681-76-7
Sodium	7632-00-0
Spiramycin	8025-81-8
Difluprednate	23674-86-4
Troxipide	30751-05-4
Ampicillin	7177-48-2
Betamipron	3440-28-6
Tolperisone	3644-61-9
Chlorocresol	59-50-7
Bosentan	147536-97-8
Oxaprozin	21256-18-8
Doxylamine	562-10-7
Ospemifene	128607-22-7
Ceftazidime	78439-06-2
Metaproterenol	5874-97-5
Piromidic	19562-30-2
Glafenine	65513-72-6
Dicyclomine	67-92-5
Fosfomycin	78964-85-9
Nifenazone	2139-47-1
Tofacitinib	540737-29-9

Several assessments and comparisons are possible using Table 9 MIC data¹⁴³ The first is to assess for interesting intrinsically active agents as revealed by examining the UM-Vm data in Table 9. Most of the agents listed in the UM-Vm column are well known antibacterial agents except for gemcitabine and closantel. Closantel is a veterinary antiparasitic drug that has previously been identified as having anti-MRSA and anti-VRE activity^{154 155 156 157} Gemcitabine has also previously been identified as having anti-MRSA activity^{158 159}, including in our own efforts¹⁴³, but its anti-VRE activity appears novel.

4.3.4 Spectrum of activity

The spectrum of activity of several of the better agents from Table 9 were determined against a panel of VRE isolates (both *E. faecium* (VREfm) and *E. faecalis* (VREfa)), in which gemcitabine demonstrated activity against all tested VRE strains with a median MIC of 0.78 μ M as shown in Table 12, but at higher MICs than against a panel of MRSA strains where the median MIC was 0.049 μ M. Several other nucleoside analogs were also tested for activity against these same VRE strains as shown in Table 13, but these did not exhibit the same broad anti-VRE activity as gemcitabine or as several of these same agents exhibited against MRSA¹⁴³ Gemcitabine and similar agents may have some potential for further development as anti-VRE and anti-MRSA agents.

Table 12 - Spectra of activity (UM-Vm) against VRE (MICs in μM).

Compound	VREfm (Clinical) ^a	VREfm (BAA-2317) ^b	VREfm (BAA-2318)	VREfm (BAA-2365)	VREfa (49532)	VREfa (49533)	VREfa (51575)	VREfa (700802)
Rifampin	0.1	NA ^c	0.39	1.6	6.25	6.25	6.25	6.25
Retapamulin	0.2	9.8×10^{-2}	9.8×10^{-2}	NA	NA	NA	NA	NA
Rifabutin	0.2	NA	0.78	3.1	25	25	25	25
Rifapentine	0.2	NA	1.6	3.1	6.25	6.25	6.25	12.5
Rifaximin	0.39	50	25	1.6	1.6	1.6	3.1	1.6
Valnemulin	0.39	0.39	0.39	NA	NA	NA	NA	NA
Gemcitabine	0.78	0.39	2.4×10^{-2}	0.78	1.6	1.6	0.78	3.1

^a Values from Table 9.^b American Type Culture Collection (ATCC) catalog numbers in parentheses.^c NA – Not active at 50 μM , the highest concentration used in these MIC determinations.Table 13 - Spectra of activity of (doxifluridine (DFUR), floxuridine, 5'-fluorouracil) against VRE (MIC, μM).

Compound	VREfm (Clinical)	VREfm (BAA-2317) ^a	VREfm (BAA-2318)	VREfa (BAA-2365)	VREfa (49532)	VREfa (49533)	VREfa (51575)	VREfa (700802)
DFUR	NA ^b	NA	NA	NA	NA	NA	50	NA
floxuridine	NA	NA	NA	3.1	25	50	6.25	50
5-fluorouracil	NA	NA	NA	3.1	25	25	12.5	50

^a American Type Culture Collection (ATCC) catalog numbers in parentheses.^b NA – Not active at 50 μM , the highest concentration used in these MIC determinations.

4.3.5 Mupirocin activity after metabolism

The second assessment is to compare Table 9 MICs to identify agents with increased activity after metabolism, indicative of more active metabolites. Nearly all drugs are transformed into at least one metabolite, and such metabolites frequently have distinct biological activities¹⁴¹

¹⁴² Our prior study demonstrated the potential of a UM vs PM library screen to identify active drug metabolites¹⁴³ The effect of microsomal metabolism on compound activity against VREfm is highlighted in Table 9 in the L2(UM/PM-Vm) and the AL2(UM/PM) columns. Values of L2(UM/PM-Vm) ≥ 2 (i.e., 4-fold reduction in MIC) are highlighted in red and indicate substantially increase potency (lower MIC) after metabolism. Only mupirocin met this standard after metabolism as shown in Table 9, suggesting the possibility of an active metabolite. However, no active metabolite was identified. While library metabolism was useful in identifying novel anti-

MRSA compounds¹⁴³, it was not successful when applied to VREfm. The metabolite of mupirocin is called monic acid A. Figure 61 shows the chemical structure of mupirocin. Figure 62 shows mupirocin preparative HPLC fractions collected and screened with VREfm after large scale metabolism.

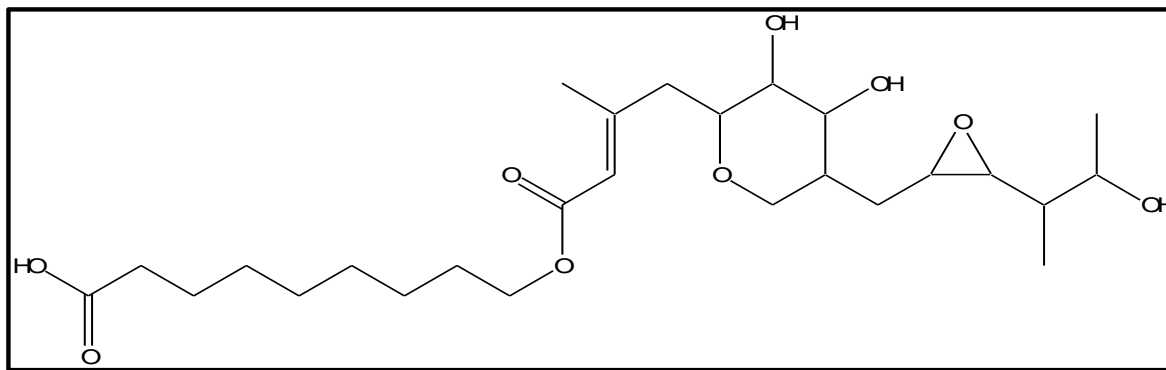


Figure 61- Chemical structure of Mupirocin

	1	2	3	4	5	6	7	8	9	10	11	12
A	0.57	0.62	0.58	0.70	0.66	0.65	0.64	0.67	0.67	0.67	0.71	0.83
B	0.53	0.73	0.64	0.70	0.71	0.68	0.69	0.66	0.66	0.68	0.67	0.82
C	0.52	0.55	0.61	0.64	0.66	0.69	0.60	0.61	0.46	0.64	0.73	0.83
D	0.15	0.11	0.12	0.35	0.66	0.70	0.59	0.62	0.64	0.69	0.68	0.76
E	0.50	0.64	0.63	0.68	0.66	0.63	0.59	0.60	0.59	0.60	0.59	0.73
F	0.54	0.62	0.64	0.65	0.67	0.61	0.58	0.58	0.60	0.60	0.55	0.62
G	0.58	0.65	0.61	0.68	0.69	0.61	0.64	0.63	0.70	0.67	0.66	0.64
H	0.60	0.65	0.66	0.67	0.70	0.66	0.66	0.77	0.75	0.75	0.80	0.80

Figure 62 - Fractions of metabolized mupirocin were collected after preparative HPLC and screened against VREfm. Wells D1, D2 and D3 shows activity and these three fractions were injected into LC-MS/MS to check metabolite activity.

4.3.6 Synergistic combinations between vancomycin and FDA VRE *faecium* hits

The third assessment from Table 9 data are comparisons to reveal possible synergistic agent combinations with vancomycin shown in Table 9; L2(UM-/ +Vm) and AL2(-/+Vm) columns. This identified nine potential synergistic combinations with vancomycin: rifabutin, rifampin, rifaximin, valnemulin, linezolid, mupirocin, retapamulin, rifapentine and gemcitabine. Checkerboard assays of these revealed significant synergies ($\Sigma\text{FIC}_{\text{min}} \leq 0.5$) for eight of these (except gemcitabine) as shown in Figures, 64 a, b, c, d, e, f, g and h respectively. Since several of these were rifamycins, synergy for rifabutin was also tested for and confirmed as shown in Figure 64 a. The observation of synergy of several rifamycins – RNA biosynthesis inhibitors - with vancomycin is interesting and has not been observed previously to the best of our knowledge. Both pleuromutilin (retapamulin and valnemulin) protein biosynthesis inhibitors also demonstrated synergy with vancomycin as shown in Figures 64 g and c respectively. A checkerboard assay was also performed between linezolid and vancomycin to determine if protein biosynthesis inhibitors were generally synergistic with vancomycin, and this was also confirmed shown in Figure 64 e. Mupirocin, an Ile-tRNA biosynthesis inhibitor which induces (p)ppGpp biosynthesis (stringent response)^{160 161} also demonstrated modest synergy shown in Figure 64 f. These observations demonstrate that direct RNA biosynthesis inhibitors (rifamycins), indirect RNA biosynthesis inhibitors (mupirocin), and protein biosynthesis inhibitors (pleuromutilins and linezolid) can all act synergistically with vancomycin in VREfm. Vancomycin resistance in this strain of VREfm is inducible¹⁶², and the ability of these agents to block RNA and protein biosynthesis likely blocks the ability of this VREfm strain to express high level vancomycin resistance. Rifabutin was the most synergistic of these agents for reasons which are currently unknown. The report of rifampin-

vancomycin in VRE strains, but not in VSE strains¹⁶¹, also supports this conclusion. Figure 63 shows the checkerboard experiment.

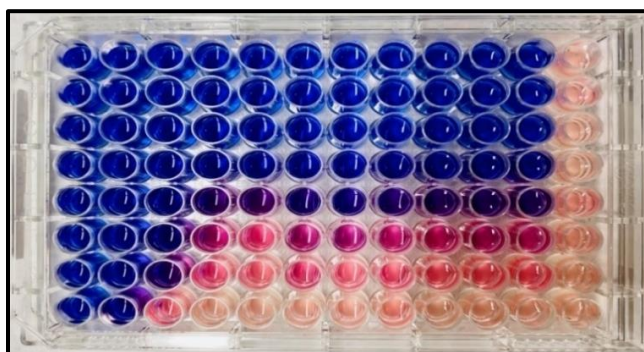


Figure 63 - Checkerboard experiment in 96 well plate.

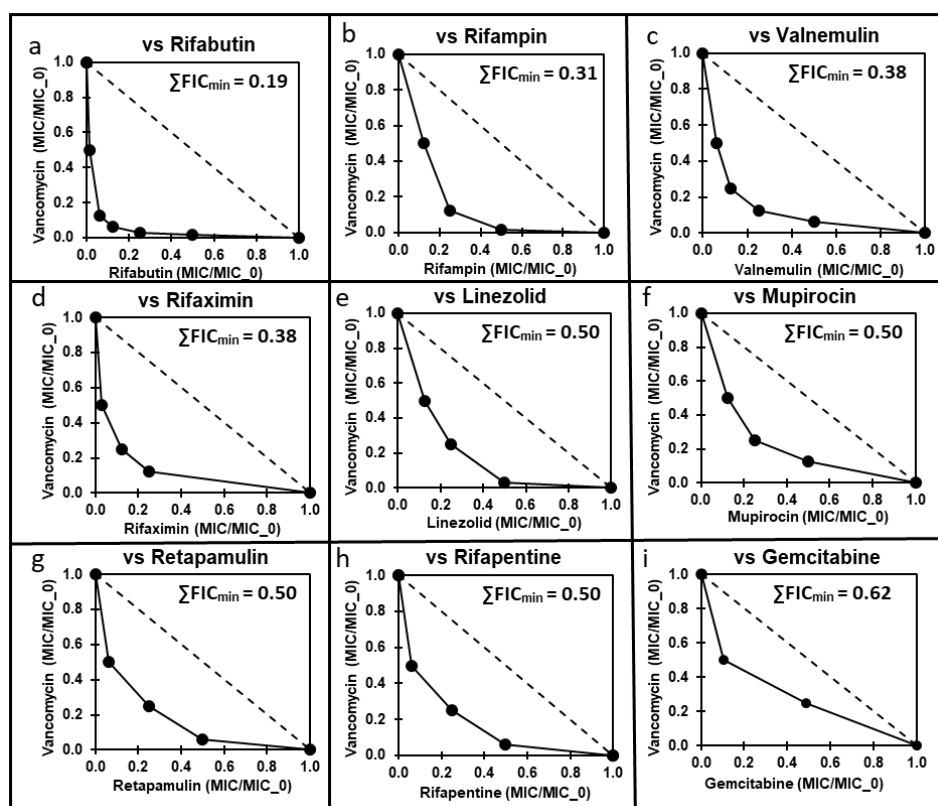


Figure 64 - Checkerboard assay results (isobolograms) for combinations of vancomycin with potentially synergistic agents. Isobolograms for combinations of vancomycin (y-axes) with other agents (x-axes). The dashed line in the isobolograms is for the no interaction (additive MICs) curve.

4.3.7 Optimization of checkerboard experiment

The initial checkerboard assay was done using 8x MIC of vancomycin that is 2048 µg/mL. However, this MIC was high and did not show a diagonal pattern which is observed in a checkerboard experiment. To optimize the pattern, we used a lower MIC of vancomycin at 4x that is 256 µg/mL. With 4x MIC of vancomycin, a diagonal pattern was observed between growth and no growth of VREfm in a 96 well plate. Figures 65 shows the pattern observed in a checkerboard experiment and Figures 66 and 67 shows the difference between the results using 8x and 4x MIC of vancomycin.

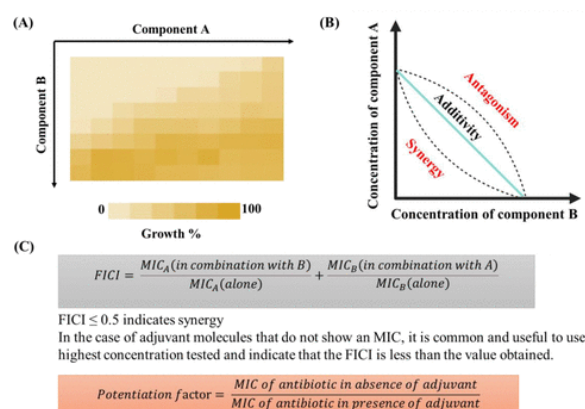


Figure 65 - Checkerboard experiment with a diagonal pattern²⁶⁷

8x MIC of Rifapentine											MIC of Vm		Control	Vancomycin	8x MIC of Vm
Rifapentine	0.78	0.39	0.20	0.10	0.05	0.02	1.2E-02	6.1E-03	3.1E-03	1.5E-03	0				
	1.63	1.59	1.60	1.65	1.64	1.56	1.72	1.61	1.55	1.56	1.62	-0.46		2048	
	1.78	1.80	1.70	1.85	1.76	1.71	1.84	1.84	1.85	1.80	1.81	-0.43		1024	
	1.77	1.81	1.75	1.86	1.82	1.79	1.85	1.88	1.85	1.83	1.83	-0.44		512	
	1.75	1.81	1.81	1.81	1.81	1.65	1.75	1.85	1.84	1.80	1.81	-0.45		256	
	1.78	1.82	1.80	1.81	1.79	1.25	1.03	0.89	1.10	0.83	0.89	-0.45		128	
	1.80	1.80	1.75	1.84	1.10	0.65	0.26	0.07	0.02	-0.07	0.09	-0.45		64	
	1.81	1.84	1.73	1.79	0.50	0.20	-0.10	-0.13	-0.29	-0.23	-0.24	-0.44		32	
MIC of Rifapentine	1.75	1.76	0.60	-0.08	-0.31	-0.46	-0.42	-0.42	-0.41	-0.42	-0.44	-0.44		0	
		1		0.38	0.63	0.56					1				FIC = 0.38

Figure 66 - Checkerboard experiment with 8x MIC of vancomycin (Vm)

8x MIC of Rifapentine											MIC of Vm		4x MIC of Vm
Rifapentine	0.78	0.39	0.20	0.10	0.05	0.02	1.2E-02	6.1E-03	3.1E-03	1.5E-03	0	Control	Vancomycin
	1.74	1.71	1.75	1.72	1.75	1.74	1.73	1.69	1.68	1.64	1.51	-0.44	256
	1.76	1.69	1.78	1.80	1.81	1.76	1.78	1.75	1.75	1.63	1.73	-0.43	128
	1.78	1.78	1.79	1.82	1.81	1.76	1.62	1.35	1.39	1.20	0.93	-0.44	64
	1.78	1.79	1.80	1.84	1.81	1.69	0.88	0.31	0.07	0.27	0.07	-0.43	32
	1.78	1.81	1.83	1.85	1.77	0.92	0.22	0.15	-0.18	-0.22	-0.39	-0.41	16
	1.75	1.80	1.81	1.86	1.41	0.30	-0.32	-0.33	-0.46	-0.41	-0.46	-0.40	8
	1.74	1.79	1.79	1.72	0.58	0.02	-0.48	-0.41	-0.47	-0.46	-0.45	-0.40	4
MIC of Rifapentine	1.73	1.76	1.70	-0.08	-0.06	-0.43	-0.42	-0.41	-0.43	-0.41	-0.42	-0.44	0
			1	0.53	0.31	0.38	0.56				1		0.31

Figure 67 - Checkerboard experiment with 4x MIC of vancomycin (Vm)

The checkerboard experiment was also optimized to check whether water or DMSO works better as a solvent to dissolve the drugs. Plates with DMSO as solvent takes 3 days to dry in a speed vac making it disadvantageous. However, plates with water as solvent takes 1 day to dry in speed vac making it a quick process as compared to DMSO. It was observed that there was no difference in the checkerboard result and pattern when both the solvents were used. Therefore, water was used for further checkerboard experiments. The following figure 68 below shows no difference between DMSO and water when used as a solvent.

DMSO

1.6338	1.5726	1.5694	1.6054	1.59933	1.6078	1.64353	1.64083	1.6684	1.651	1.6041	-0.3716
1.5647	1.54953	1.5623	1.57527	1.57943	1.58917	1.5673	1.59967	1.62327	1.5928	1.5815	-0.3401
1.58333	1.54303	1.5168	1.55573	1.5644	1.55723	1.62183	1.591	1.56517	1.56633	1.58537	-0.3386
1.6133	1.5996	1.57333	1.58523	1.487	1.6021	1.61407	1.61687	1.6145	1.5689	1.51907	-0.3674
1.668	1.5881	1.5216	1.58357	1.60303	1.604	1.63283	1.6015	1.51663	0.90537	-0.0711	-0.3281
1.6419	1.5798	1.48377	1.59647	1.6134	1.60423	1.6215	0.92083	0.16033	-0.1406	-0.298	-0.379
1.55053	1.55747	1.45413	1.57783	1.60443	1.6174	1.5888	-0.0562	-0.2983	-0.3051	-0.4007	-0.3298
1.51477	1.5082	1.32907	1.53773	1.54397	1.50537	-0.3369	-0.3609	-0.374	-0.3374	-0.305	-0.33

Water

1.42617	1.46687	1.4442	1.45237	1.46053	1.44967	1.45007	1.4503	1.46767	1.45327	1.45703	-0.3684
1.45817	1.56853	1.5798	1.88437	1.4754	1.4768	1.46743	1.47813	1.47857	1.47617	1.48033	-0.3921
1.43643	1.86957	1.8749	1.51117	1.45367	1.5065	1.49053	1.47597	1.4872	1.47603	1.47953	-0.3888
1.19863	1.25157	1.21737	1.4626	1.47723	1.4759	1.47033	1.47047	1.24013	1.09473	0.8072	-0.3745
1.4461	1.50577	1.5967	1.48913	1.60353	1.49337	1.16937	0.08947	0.24927	0.13977	-0.2767	-0.4199
1.45283	1.47843	1.48037	1.49043	1.50577	1.5017	0.19133	-0.2697	-0.2427	-0.3619	-0.3789	-0.3795
1.42537	1.52713	1.5037	1.49813	1.49723	1.49257	-0.3678	-0.4422	-0.405	-0.4031	-0.4178	-0.4077
1.34713	1.3909	1.3803	1.4063	1.4205	-0.3527	-0.4017	-0.4304	-0.4043	-0.3901	-0.4137	-0.4462

Figure 68 - No difference in results was observed when water or DMSO were used as a solvent.

4.4 Conclusion

The overall goal of this effort was to further demonstrate the utility of enhanced library screening approaches in which replicate library screens are performed with variation between the replicates. The basic screen (UM-Vm) identified both closantel and gemcitabine as non-typical anti-VRE agents. The spectrum of activity of closantel against several VRE strains has previously been reported¹⁵⁷ Gemcitabine was demonstrated in this study as shown in Table 12 to also have activity against several VRE strains, and this or similar agents may be worth further study. The molecular target of gemcitabine is unknown, but further studies of gemcitabine and homologs seem justified from these observations. No agents with identifiable active metabolites were discovered in this screen, in contrast to the identification of active capecitabine metabolites in MRSA¹⁴³ Screening for synergistic combinations with vancomycin revealed several synergistic agents as seen in Figure 64. These were all either RNA or protein biosynthesis inhibitors, suggesting a common basic mechanistic basis for these synergies. Some of the agents and agent combinations identified in this effort may be suitable candidates for further *in vitro* and *in vivo* studies, and ultimately clinical application.

CHAPTER 5

5. SCREENING THE NCI DIVERSITY SET V FOR ANTI-MRSA ACTIVITY: CEFOXITIN SYNERGY AND LC-MS/MS CONFIRMATION OF FOLATE/THYMIDINE BIOSYNTHESIS INHIBITION

5.1 Introduction and Rationale

Antimicrobial resistance (AMR) in pathogenic bacteria is a major public health threat^{68 89}
^{128 130} Methicillin-resistant *Staphylococcus aureus* (MRSA) causes both nosocomial and
community-acquired infections^{163 164} It is resistant to most β -lactam antibiotics including
methicillin, oxacillin, amoxicillin and cefoxitin, and to many other antibiotic classes and agents¹⁶⁵
Chemical library screening is a popular drug discovery approach where hundreds to many
thousands of compounds are screened in a high throughput fashion to identify novel
pharmacological and biological activities¹⁶⁶ Given that the emergence of resistance to single agents
has so far proven inevitable, methods to reverse or prevent the emergence of resistance, such as
the development of antibacterial agent combinations, seems essential^{149 153 167}

In a prior study, a dimensionally enhanced library screening approach was demonstrated
for screening an FDA approved drug library against MRSA¹⁴³ This approach uses added
dimensions (human liver microsome metabolized library compounds, and +/- cefoxitin screening)
to a standard library screen to provide valuable additional information while also providing a
degree of screening redundancy. In this study, a variation of this approach was applied to MRSA
using a non-FDA approved library to assess the ability of this approach to identify interesting lead
compounds in a general chemical (non-FDA) library screen. The National Cancer Institute
Diversity Set V (NCI) library was used for this effort, which consists of 1593 compounds selected

to cover a wide range of chemical and pharmacophore space. This effort identified agents with good intrinsic anti-MRSA activity, and agents with synergistic activity with ceftazidime. No agents with active metabolites were identified in this screen.

A key bottleneck in whole cell screening for antibacterial activity is the determination of the mechanism of actions (MOAs) of newly identified agents^{168 169} Two of the compounds identified in this screen had obvious similarity to trimethoprim (diaminopyrimidine), a folate reductase inhibitor. Added thymidine, a key metabolite dependent on folate biosynthesis, is known to rescue *S. aureus* from folate/thymidine biosynthesis inhibition¹⁷⁰ A +/- thymidine follow-up screen was therefore implemented, which identified three prospective folate/thymidine biosynthesis inhibitors – two obvious diaminopyrimidine containing candidates plus a fluorinated pyrimidine compound similar to 5-fluorouracil. To provide further confirmation, their effect on bacterial dTTP pool levels was determined by LC-MS/MS analysis. Spectrum of activity data against a panel of MRSA strains was used to identify agents with general activity against MRSA.

5.2 Material and Methods

5.2.1 General

The NCI diversity set V library of 1593 compounds was from the Division of Cancer Treatment and Diagnosis (DCTD) of the National Cancer Institute (NCI). All other materials were as described previously¹⁴³

Library replication, addition of metabolism and antibacterial control compounds. The NCI diversity set V was delivered in 96 well plates in columns 2–11, 20 plates total, with each well containing 20 μ L of a 10 mM solution of a compound in DMSO. Antibiotic controls (20 μ L of 10 mM stock solutions of vancomycin, fosfomycin, ampicillin, doxycycline, or chloramphenicol)

were added to column 1 of each library plate. Microsomal (CYP) substrate controls (20 μ L of 10 mM stock solutions of phenacetin, tolbutamide, dextromethorphan, coumarin, chlorzoxazone or diclofenac) were added to column 12 of each library plate. Aliquots (10 μ L) of library samples were transferred to 96 well plates using a liquid handling workstation (Biomek 3000) and diluted with 90 μ L DMSO to provide UM working plates at 1 mM.

5.2.2 In vitro microsomal metabolism to provide pre metabolized library

For PM library preparation, the remaining 10 μ L of each sample in DMSO was dried by freezing the plates at -80°C and drying under strong vacuum ($<50\text{ }\mu\text{mHg}$) in a Genevac Quatro centrifugal concentrator (DMSO can interfere with microsomal metabolism reactions). The dried library plates were metabolized with human liver microsomes as described previously¹⁴³ To each well was added 10 μ L acetonitrile/water (20/80%, v/v) to redissolve samples. The plates were incubated for 2 h at 35°C , followed by addition of 490 μ L of freshly prepared (on ice) microsomal reaction mixture containing 50 mM potassium phosphate pH 7.4, 3 mM MgCl_2 , 5 mM glucose-6-phosphate, 1 unit mL^{-1} glucose-6-phosphate dehydrogenase, 1 mM NADP^+ and 0.5 mg mL^{-1} total microsomal protein. Reaction mixtures were incubated for 24 h at 35°C with gentle rocking. Library plates were then centrifuged at 4000g for 30 min at 4°C , and 400 μ L of the supernatants then transferred to sterile 96 well plates. To the residues was added 100 μ L DMSO, and the samples mixed thoroughly. Library plates were centrifuged again at 4000g for 30 min, and 150 μ L of the supernatants were removed and combined with the first extracts. The resulting extracts were frozen at -80°C and dried under strong vacuum ($<50\text{ }\mu\text{mHg}$) in a Genevac Quatro centrifugal concentrator. These “pre-met” (PM) library samples were then reconstituted in 100 μ L DMSO to provide a 1 mM PM NCI working library. Both “un-metabolized” (UM) and PM working libraries were stored in U-bottom polypropylene storage plates at -80°C . Samples of wells containing

microsomally metabolized drug controls from PM plates were analyzed by LC-MS/MS to provide a relative measure of metabolism. The percent metabolism of these control drugs was 52%, 55%, 60%, 66%, 95% and 100% for tolbutamide, dextromethorphan, chlorzoxazone, phenacetin, diclofenac and coumarin respectively. These controls demonstrate that the metabolism conditions employed in this study were sufficient to achieve a relatively high degree of metabolism.

5.2.3 UM/PM vs -/+ Cefoxitin library screen against MRSA.

Four sets of library screens were performed (UM-Cef, UM+Cef, PM-Cef, and PM+Cef), as described previously for an FDA approved drug library screen¹⁴³, with the modification that 2 μ L of library samples @ 1 mM were used. During the bacterial incubation step, this provided 100 μ M compound concentrations, rather than 200 μ M as in the previously described study¹⁴³. Plates were frozen at -80 °C and dried as described above. To each well in each set was added 20 μ L cation-adjusted Mueller-Hinton (CAMH) broth containing 4000 cfu MRSA (ATCC 43300) and containing either no cefoxitin for -Cef screens or +8 μ g mL⁻¹ cefoxitin (equal to 1/4x MIC) for +Cef screens. Plates were incubated for 48 h at 35 °C. Fresh CAMH broth (10 μ L) was then added to the wells of these four sets of plates, followed by incubation for 2 h at 35 °C, to restart active cell growth. To the wells of these plates was then added 6 μ L of 100 μ g mL⁻¹ resazurin (sodium salt)^{145 146 147}. The plates were incubated for another 2 h at 35 °C, and the 570/600 fluorescence ratio was measured in a Molecular Devices SpectraMax M5 multimode microplate reader. The resulting data was processed and analyzed using Matlab scripts (The Mathworks, Natick, MA) to identify active wells using a cut-off value between known actives (antibiotic controls) and known inactives (microsomal controls). A merged hit list was generated, in which a compound was included in the merged hit list if it demonstrated activity under any of the four test conditions (UM-Cef, UM+Cef, PM-Cef, or PM+Cef).

5.2.4 Hit picking and minimum inhibitory concentration determination

Follow up MIC determinations for identified hits was performed as described in detail previously¹⁴³ MICs were determined for all actives by hit picking 2 μ L samples from both UM and PM working plates (two sets from each) into the first columns of 384 well plates (four sets total, for UM–Cef, UM+Cef, PM–Cef and PM+Cef MIC determinations). These samples were then serially diluted in steps of two across the plates with DMSO using an Integra Viaflo Assist automated multichannel pipette. The last column was left blank (DMSO only). These plates were frozen at -80°C and dried under strong vacuum as described above. To each well in each set was added 20 μ L cation-adjusted Mueller-Hinton (CAMH) broth containing 4000 cfu MRSA (ATCC 43300) and containing either no ceftiofur for –Cef MICs or 8 $\mu\text{g mL}^{-1}$ Cef for +Cef MICs. (This provided MIC plates with 100 μM as the highest test agent concentration.) Incubation and resazurin treatment were as described above. MICs were determined using a cutoff midway between known active and inactive samples. All MICs were determined at least in triplicate.

5.2.5 Checkerboard assays to confirm synergy with ceftiofur

Several agents showed lower MICs in the presence of ceftiofur as shown in Table 14, indicative of potential synergistic activity. Checkerboard assays¹⁴⁸ were used to confirm and assess synergy for 4-quinazolinediamine, celastrol, teniposide, streptovaricin, porfiromycin and ethyl violet with ceftiofur, as described previously¹⁴³ All checkerboard assays were performed in triplicate. Data were plotted as isobolograms and reported as the minimum sum of fractional inhibitory concentrations ($\Sigma\text{FIC}_{\text{min}}$ values in Figure 69, also referred to as FICI values)¹⁸²

5.2.6 -/+ Thymidine counter screen and LC-MS/MS confirmation for folate/thymidine biosynthesis inhibitors

The effects of folate/thymidine biosynthesis inhibitors on MRSA can be reversed by the addition of thymidine to the culture media¹⁷⁰ This effect was therefore used to assess Table 14 by redetermining the UM-Cef MICs in the absence and presence of 4 μ M (1 μ g/mL) thymidine as shown in Table 17. This identified 3 agents with significant L2(-/+Thy) values.

To further confirm these three agents as thymidine biosynthesis inhibitors, an ion pairing LC-MS/MS assay was developed ATP and dTTP using the same approach as previously described for UDP-linked intermediates in the bacterial cell wall biosynthesis pathway⁵⁷ as shown in Table 18. Antibiotic treated bacterial cultures were prepared as described in detail previously⁵⁷ MRSA cultures were grown in CAMH media to mid-log phase (OD600 = 0.5), and 50 mL of this mid-log phase transferred to baffled 250 mL culture flasks and treated with the test agent at 4x MIC shown in Table 17 -Thy values for 15 min. The tested agents were NSC367428, 4-QDA, and NSC309401, with trimethoprim included as positive control and gemcitabine included as negative control. A no antibiotic control flask was also included. The flasks were incubated at 35 °C with shaking for 15 minutes. Flasks were then rapidly chilled in an ice slush bath, and the samples from individual flasks were collected in quadruplicate and stored on ice for up to 15 min prior to centrifugations and processing for metabolite extraction, as described above. Samples were analyzed for ATP and dTTP using the LC-MS/MS parameters described in Table 18. The results from this experiment are reported in Figure 70.

5.2.7 Spectrum of activity

MICs were determined for many of the Table 14 (UM-Cef) agents against a panel of bacterial strains to assess spectrum of activity as shown in Table 19. The strains tested were MRSA strains F-182 (ATCC 43300), N315 (BEI NR-45898), HI022 (BEI NR-30550), MN8 (BEI NR-45918), TCH70 (BEI HM-139), RN1 (BEI NR-45904), COL (BEI NR-45906), and U9N0, one strain of VRE *faecium* (clinical), one strain of VRE *faecalis* (ATCC 2365) and one strain of *E. coli* K12 (BEI MG1655).

5.3 Results and discussion

5.3.1 Library screening and hit minimal inhibitory concentration determinations

Library screening was performed at 200 μ M (nominal concentration for the PM library screen) as described in detail previously^{143 171} Following library screening, a pooled hit list was made (i.e., any compound that gave a hit (was active in suppressing bacterial growth) in any of the four UM/PM vs $-/+$ Cef screens was added to the list) for follow-up minimum inhibitory concentration (MIC) determinations. MICs for all the compounds in this pooled hit list were then determined by serial dilution in steps of 2 starting at 100 μ M under all four screening conditions (UM–Cef, UM+Cef, PM–Cef, and PM+Cef) to give a final table of MICs. The results from these MIC determinations for minimum MICs of ≤ 12.5 μ M, are summarized in Table 14, and for all screening hits in Table 15. All inactive screened compounds are listed in Table 16. Celastrol is also included in Table 14 even though it had relatively weak activity since it showed significant apparent synergy with cefoxitin as discussed further below.

Table 14 - MICs (μM) for top 14 NCI Diversity Set V compounds against MRSA (ATCC #43300). UM = original unmetabolized library compounds, PM = human liver microsome metabolized compounds (nominal MICs). -Cef = in the absence of cefoxitin, +Cef = in the presence of 8 mg/L cefoxitin

Name	PubChem CID	UM		PM		Min_MIC	L2 (-/ +Cef) ^a	AL2 (-/ +Cef) ^b	L2 (UM/PM) ^c	AL2 (UM/PM) ^d
		-Cef	+Cef	-Cef	+Cef					
Clorobiocin	54677920	0.10	0.10	0.10	0.049	0.049	0	0.5	0	0.5
4-QDA	16682542	0.39	0.10	25	25	0.10	2	1.0	-6	-7.0
Ethyl Violet	16955	1.6	0.78	25	12.5	0.78	1	1.0	-4	-4.0
Bactobolin	54676871	3.1	1.6	12.5	6.25	1.6	1	1.0	-2	-2.0
Hitachimycin	54598584	1.6	1.6	3.1	3.1	1.6	0	0.0	-1	-1.0
NSC53275	9568176	6.25	3.1	50	25	3.1	1	1.0	-3	-3.0
NSC367428	339703	3.1	3.1	50	25	3.1	0	0	-4	-3.5
Porfiromycin	244989	12.5	3.1	25	25	3.1	2	1.0	-1	-2.0
Teniposide	54610154	12.5	3.1	25	12.5	3.1	2	1.5	-1	-1.5
Naphtanilide LB	67238	6.25	6.25	25	12.5	6.25	0	0.5	-2	-1.5
NSC207895	42640	6.25	6.25	200	200	6.25	0	0.0	-5	-5.0
NSC309401	24198955	12.5	6.25	100	100	6.25	1	0.5	-3	-3.5
Streptovaricin C	135431273	6.25	6.25	25	12.5	6.25	0	0.5	-2	-1.5
NSC204262	5216088	12.5	12.5	12.5	25	12.5	0	-0.5	0	-0.5
NSC654260	375121	100	12.5	100	50	12.5	3	2.0	0	-1.0
Chaetochromin	53277	25	25	50	25	25	0	0.5	-2	-0.5
Celastrol	122724	200	50	200	50	50	2	2.0	0	0.0

^a $L2_{(UM-/ +Cef)} = \log_2 \left(\frac{MIC_{UM-Cef}}{MIC_{UM+ Cef}} \right)$.	^b $AL2_{(-/ +Cef)} = \text{Avg} \left[\log_2 \left(\frac{MIC_{UM-Cef}}{MIC_{UM+ Cef}} \right), \log_2 \left(\frac{MIC_{PM-Cef}}{MIC_{PM+ Cef}} \right) \right]$.
^c $L2_{(UM/PM-Cef)} = \log_2 \left(\frac{MIC_{UM-Cef}}{MIC_{PM-Cef}} \right)$.	^d $AL2_{(UM/PM)} = \text{Avg} \left[\log_2 \left(\frac{MIC_{UM-Cef}}{MIC_{PM-Cef}} \right), \log_2 \left(\frac{MIC_{UM+ Cef}}{MIC_{PM+ Cef}} \right) \right]$.

Table 15 - List of active compounds (validated MIC \leq 100 μ M) from NCI Diversity Set V library screening against MRSA (ATCC 43300) (UM/PM vs \pm 8 μ g mL $^{-1}$ Cefoxitin) ranked by lowest minimum MIC

Name/NSC_No	PubChem_CID	UM MICs (μ M)		PM MICs (μ M)		Min_MIC	L2(-/+Cef)
		-Cef	+Cef	-Cef	+Cef		
Clorobiocin	54677920	0.10	0.10	0.10	0.049	0.049	0
(4-QDA)	16682542	0.39	0.10	25	25	0.10	2
Ethyl Violet	16955	1.6	0.78	25	12.5	0.78	1
Bactobolin	54676871	3.13	1.56	12.5	6.25	1.56	1
Hitachimycin	54598584	1.6	1.6	3.1	3.1	1.6	0
NSC53275	9568176	6.25	3.1	50	25	3.1	1
NSC367428	339703	3.1	25	50	25	3.1	-3
Porfiromycine	244989	12.5	3.13	25	25	3.13	2
Teniposide	54610154	12.5	3.13	25	12.5	3.13	2
Naphtanilide LB	67238	6.25	6.25	25	12.5	6.25	0
NSC207895	42640	6.25	6.25	200	200	6.25	0
NSC309401	24198955	12.5	6.25	100	100	6.25	1
Streptovaricin C	135431273	6.25	6.25	25	12.5	6.25	0
NSC654260	375121	100	12.5	100	50	12.5	3
Chaetochromin	53277	25	25	50	25	25	0
Celastrol	122724	200	50	200	50	50	2
NSC204262	5216088	100	100	12.5	25	12.5	
Ellipticine	3213	25	25	25	25	25	
NSC344494	6512428	200	50	200	200	50	
CDDO-Im	9958995	200	50	200	200	50	
CID 319089	319089	50	50	200	100	50	
NSC38090	236065	100	50	100	100	50	
Niazo	96213	200	50	200	200	50	
NSC11667	240350	50	50	100	100	50	
NSC11667	223752	200	200	100	50	50	
NSC11668	54600468	50	50	100	100	50	
NSC11668	223753	200	200	100	50	50	
NSC177407	67275	50	200	200	200	50	
NSC177407	5383615	100	100	100	50	50	
NSC332670	56909	50	50	100	100	50	
NSC332670	332972	200	200	200	50	50	
NSC341196	328773	50	50	200	200	50	
NSC341196	334739	200	200	100	50	50	
NSC369066	339983	100	50	50	50	50	
NSC522131	313619	50	100	200	200	50	
NSC522131	351549	100	100	100	50	50	
Albacarcin V	122815	100	100	100	100	100	

NSC149286	5382674	200	100	200	200	100
NSC186200	5842286	200	100	200	100	100
NSC369070	135493774	100	200	200	200	100
NSC137399	6509134	200	200	200	100	100
NSC33353	40492789	200	100	100	100	100
NSC329249	332429	200	200	200	100	100
NSC33005	95746	200	100	200	200	100
NSC317003	13504751	100	100	100	100	100
NSC133071	280859	200	100	200	200	100
NSC159566	293227	200	100	200	100	100
NSC147358	287384	200	100	200	200	100
NSC177365	5351256	100	200	200	200	100
NSC215721	3967840	200	200	100	200	100
Naphthol AS-OL	67274	200	200	200	100	100
NSC138389	283529	200	100	200	200	100
NSC13156	224574	100	200	100	100	100
NSC30260	232590	100	100	200	200	100
NSC407628	82011	200	100	200	200	100
NSC622689	360560	100	100	200	200	100
NSC311727	100520	100	100	200	200	100
NSC133114	280895	100	200	200	200	100
Benzbromarone	2333	200	200	200	100	100
NSC116339	5381366	200	100	200	200	100
Daunomycin 3-oxime HCl	54606703	200	100	200	200	100
Malonoben	5614	200	200	200	100	100
Mequitazine	4066	200	100	200	200	100
Methiothepin maleate	5358812	200	100	200	200	100
Methyl Streptonigrin	18834	200	200	200	100	100
NSC601359	353380	100	200	200	100	100
Enpiroline	328144	100	100	200	200	100
NSC106208	97205	200	100	200	200	100
NSC302584	163121	200	100	200	200	100
Redoxal	72571	100	100	200	100	100
Sulfaquinoxaline	5338	100	100	100	100	100
Tricinolone acetophenonide	235856	200	100	200	200	100
NSC607097	122737	100	100	200	200	100
Vacquinol-1	224644	200	200	200	100	100
Wander	65558	100	100	200	200	100

Table 16. List of inactive compounds (MIC>100 μ M) from library screening against MRSA (ATCC 43300).

Compound	CAS Number		
Octopamine	770-05-8	Amiloride	17440-83-4
10-Deacetylbaecatin-III	32981-86-5	Aminocaproic	60-32-2
1-Hexadecanol	36653-82-4	Aminogluthimide	125-84-8
2-Methoxyestradiol	362-07-2	Aminophylline	317-34-0
2-Thiouracil	141-90-2	Aminosalicylate	133-10-8
5-Aminolevulinic	106-60-5	Aminothiazole	96-50-4
9-Aminoacridine	90-45-9	Amiodarone	19774-82-4
Abitrexate	59-05-2	Amisulpride	71675-85-9
Acadesine	2627-69-2	Amitriptyline	549-18-8
Acarbose	56180-94-0	Amlodipine	88150-42-9
Acebutolol	34381-68-5	Amlodipine	111470-99-6
Aceclidine	6109-70-2	Glycyrrhizinate	1407-03-0
Acemetacin	53164-05-9	Amorolfine	78613-38-4
Acetanilide	103-84-4	Amphotericin	1397-89-3
Acetarsone	97-44-9	Ampicillin	7177-48-2
Acetylcholine	60-31-1	Ampiroxicam	99464-64-9
Acetylcysteine	616-91-1	Amprenavir	161814-49-9
Acipimox	51037-30-0	Amprolium	137-88-2
Acitretin	55079-83-9	Anagrelide	58579-51-4
Acridinium	320345-99-1	Anastrozole	120511-73-1
Acyclovir	59277-89-3	Aniracetam	72432-10-1
Adapalene	106685-40-9	Anisotropine	80-50-2
Adefovir	142340-99-6	Antazoline	2508-72-7
Adenine	2922-28-3	Antipyrine	60-80-0
Adenosine	58-61-7	Apatinib	811803-05-1
Adiphenine	50-42-0	Apixaban	503612-47-3
Adrenalone	62-13-5	Arbidol	131707-23-8
Afatinib	439081-18-2	Arecoline	300-08-3
Agomelatine	138112-76-2	Argatroban	74863-84-6
Albendazole	54965-21-8	Aripiprazole	129722-12-9
Albendazole	54029-12-8	Artemether	71963-77-4
Alfacalcidol	41294-56-8	Artemisinin	63968-64-9
Alfuzosin	81403-68-1	Articaine	23964-57-0
Alibendol	26750-81-2	Asenapine	65576-45-6
Aliskiren	173334-58-2	Aspartame	22839-47-0
Allopurinol	315-30-0	Aspirin	50-78-2
Allylthiourea	109-57-9	Atazanavir	229975-97-7
Almotriptan	181183-52-8	Atomoxetine	82248-59-7
Alprostadil	745-65-3	Atorvastatin	134523-03-8
Altrenogest	850-52-2	Atovaquone	95233-18-4
Altretamine	645-05-6	Atracurium	64228-81-5
Alverine	5560-59-8	Atropine	5908-99-6
Amantadine	665-66-7	Avanafil	330784-47-9
Ambrisentan	177036-94-1	Avobenzon	70356-09-1
Amfebutamone	31677-93-7	Axitinib	319460-85-0
Amfenac	61618-27-7	Azacitidine	320-67-2
Amidopyrine	58-15-1	Azacyclonol	115-46-8
Amiloride	2016-88-8	Azaguanine-8	134-58-7
		Azaperone	1649-18-9
		Azatadine	3978-86-7
		Azathioprine	446-86-6
		Azelastine	79307-93-0

Azelnidipine	123524-52-7	Bufexamac	2438-72-4
Azilsartan	147403-03-0	Buflomedil	35543-24-9
Azilsartan	863031-21-4	Bumetanide	28395-03-1
Azithromycin	83905-01-5	Bupivacaine	18010-40-7
Azithromycin	117772-70-0	Busulfan	55-98-1
Aztreonam	78110-38-0	Butenafine	101827-46-7
Bazedoxifene	198480-56-7	Cabazitaxel	183133-96-2
Beclomethasone	4419-39-0	Calcitriol	32222-06-3
Bemegride	64-65-3	Calcium	17140-60-2
Benazepril	86541-74-4	Camylofin	54-30-8
Bendamustine	3543-75-7	Candesartan	139481-59-7
Benidipine	91599-74-5	Captopril	62571-86-2
Benserazide	14919-77-8	Carbachol	51-83-2
Benzbromarone	3562-84-3	Carbadox	1791337
Benzocaine	94-09-7	Carbamazepine	298-46-4
Benzoic	65-85-0	Carbazochrome	51460-26-5
Benzthiazide	91-33-8	Carbenicillin	4800-94-6
Benztropine	132-17-2	Carbenoxolone	7421-40-1
Benzydamine	132-69-4	Carbidopa	28860-95-9
Bephenium	3818-50-6	Carbimazole	22232-54-8
Bepotastine	190786-44-8	Carfilzomib	868540-17-4
Bergapten	484-20-8	Carprofen	53716-49-7
Beta	7235-40-7	Carvedilol	72956-09-3
Betahistine	5579-84-0	Catharanthine	2468-21-5
Betamethasone	378-44-9	Ceftazidime	78439-06-2
Betamethasone	5593-20-4	Cephalexin	15686-71-2
Betamethasone	2152-44-5	Cephalomannine	71610-00-9
Betamipron	3440-28-6	Cepharanthine	481-49-2
Betapar	1247-42-3	Cetirizine	83881-52-1
Betaxolol	659-18-7	Chenodeoxycholic	474-25-9
Betaxolol	63659-19-8	Chloramphenicol	56-75-7
Bethanechol	590-63-6	Chlormezanone	80-77-3
Bexarotene	153559-49-0	Chlorocresol	59-50-7
Bextra	181695-72-7	Chlorothiazide	58-94-6
Bezafibrate	41859-67-0	Chloroxine	773-76-2
BIBR-1048	211915-06-9	Chlorpheniramine	113-92-8
Bicalutamide	90357-06-5	Chlorpromazine	69-09-0
Bimatoprost	155206-00-1	Chlorpropamide	94-20-2
Bindarit	130641-38-2	Chlorprothixene	113-59-7
Biotin	58-85-5	Chlorquinaldol	72-80-0
Bisacodyl	30652-11-0	Chlorzoxazone	95-25-0
Bisoprolol	104344-23-2	Choline	67-48-1
Bleomycin	9041-93-4	Chromocarb	4940-39-0
Bortezomib	179324-69-7	Ciclopirox	29342-05-0
Bosentan	147536-97-8	Ciclopirox	41621-49-2
Bosutinib	380843-75-4	Cilnidipine	132203-70-4
Brinzolamide	138890-62-7	Cilostazol	73963-72-1
Bromhexine	611-75-6	Cimetidine	51481-61-9
Brompheniramine	980-71-2	Cinchophen	132-60-5
Broxyquinoline	521-74-4	Cinepazide	26328-04-1
Brucine	652154-10-4	Cisatracurium	96946-42-8
Budesonide	51333-22-3	Cisplatin	15663-27-1

Cladribine	4291-63-8	Dexlansoprazole	138530-94-6
Clarithromycin	81103-11-9	Dexmedetomidine	113775-47-6
Clemastine	14976-57-9	Dexmedetomidine	145108-58-3
Cleviprex	167221-71-8	Dexrazoxane	149003-01-0
Climbazole	38083-17-9	Dextrose	50-99-7
Clindamycin	18323-44-9	Dibenzothiophene	132-65-0
Clindamycin	21462-39-5	Dibucaïne	61-12-1
Clindamycin	25507-04-4	Diclofenac	15307-79-6
Clobetasol	25122-46-7	Diclofenac	78213-16-8
Clofarabine	123318-82-1	Diclofenac	15307-81-0
Clofazimine	2030-63-9	Dicyclomine	67-92-5
Clofibric	882-09-7	Didanosine	69655-05-6
Clofoctol	37693-01-9	Dienogest	65928-58-7
Clomipramine	17321-77-6	Diethylstilbestrol	56-53-1
Clonidine	4205-91-8	Difluprednate	23674-86-4
Clopidogrel	120202-66-6	Diltiazem	33286-22-5
Clorprenaline	6933-90-0	Dimethyl	624-49-7
Clorsulon	60200-06-8	Diminazene	908-54-3
Clozapine	5786-21-0	Diperodon	537-12-2
Cobicistat	1004316-88-4	Diphe-manil	62-97-5
Conivaptan	168626-94-6	Diphenhydramine	147-24-0
Cortisone	50-04-4	Diphenylpyraline	132-18-3
Coumarin	91-64-5	Dipyridamole	58-32-2
Curcumin	458-37-7	Dirithromycin	62013-04-1
Cyclamic	100-88-9	Disopyramide	22059-60-5
Cyclandelate	456-59-7	Disulfiram	97-77-8
Cyclophosphamide	6055-19-2	Divalproex	76584-70-8
Cyclosporine	79217-60-0	DL-Carnitine	461-05-2
Cyproheptadine	969-33-5	D-Mannitol	69-65-8
Cyromazine	66215-27-8	Docetaxel	114977-28-5
Cysteamine	156-57-0	Dofetilide	115256-11-6
Cytidine	65-46-3	Domperidone	57808-66-9
Dabrafenib	1195765-45-7	Dopamine	62-31-7
Dacarbazine	891986	Doripenem	364622-82-2
Daidzein	486-66-8	Doxapram	7081-53-0
Dapoxetine	129938-20-1	Doxazosin	77883-43-3
DAPT	208255-80-5	Doxercalciferol	54573-75-0
Darifenacin	133099-07-7	Doxofylline	69975-86-6
Darunavir	635728-49-3	Doxylamine	562-10-7
Dasatinib	302962-49-8	Droperidol	548-73-2
Decamethonium	541-22-0	Dropropizine	17692-31-8
Decitabine	2353-33-5	Drospirenone	67392-87-4
Deferasirox	201530-41-8	Duloxetine	136434-34-9
Deflazacort	14484-47-0	Dutasteride	164656-23-9
Dehydroepiandrosterone	53-43-0	Dyclonine	536-43-6
Deoxyarbutin	53936-56-4	Dydrogesterone	152-62-5
Deoxycorticosterone	56-47-3	Dyphylline	479-18-5
Desloratadine	100643-71-8	Edaravone	89-25-8
Desonide	638-94-8	Elvitegravir	697761-98-1
Detomidine	90038-01-0	Emtricitabine	143491-57-0
Dexamethasone	50-02-2	Enalapril	76095-16-4
Dexamethasone	1177-87-3	Enalaprilat	84680-54-6

Enoxacin	74011-58-8	Fludarabine	75607-67-9
Entacapone	130929-57-6	Flumazenil	78755-81-4
Entecavir	209216-23-9	Flumethasone	2135-17-3
Epalrestat	82159-09-9	Flunarizine	30484-77-6
Epinephrine	51-42-3	Flunixin	42461-84-7
Eprosartan	144143-96-4	Fluocinolone	67-73-2
Erdosteine	84611-23-4	Fluocinonide	356-12-7
Erlotinib	183319-69-9	Fluorometholone	426-13-1
Erythromycin	114-07-8	Fluoxetine	56296-78-7
Erythromycin	1264-62-6	Flurbiprofen	51543-39-6
Escitalopram	219861-08-2	Flutamide	13311-84-7
Esmolol	81161-17-3	Fluticasone	80474-14-2
Esomeprazole	161973-10-0	Fluvastatin	93957-55-2
Esomeprazole	161796-78-7	Fluvoxamine	61718-82-9
Estradiol	50-28-2	Formoterol	43229-80-7
Estradiol	313-06-4	Fosaprepitant	265121-04-8
Estradiol	979-32-8	Fosfomycin	78964-85-9
Estriol	50-27-1	Fulvestrant	129453-61-8
Estrone	53-16-7	Furosemide	54-31-9
Ethacridine	6402-23-9	Gabexate	56974-61-9
Ethambutol	1070-11-7	Gallamine	65-29-2
Ethamsylate	2624-44-4	Ganciclovir	82410-32-0
Ethinyl	57-63-6	Gefitinib	184475-35-2
Ethionamide	536-33-4	Gemfibrozil	25812-30-0
Ethoxzolamide	452-35-7	Genipin	6902-77-8
Ethynodiol	297-76-7	Geniposide	24512-63-8
Etodolac	41340-25-4	Geniposidic	27741-01-1
Etomidate	33125-97-2	Genistein	446-72-0
Etravirine	269055-15-4	Gestodene	60282-87-3
Everolimus	159351-69-6	Gimeracil	103766-25-2
Evista	82640-04-8	Ginkgolide	15291-75-5
Exemestane	107868-30-4	Glafenine	65513-72-6
Famciclovir	104227-87-4	Gliclazide	21187-98-4
Famotidine	76824-35-6	Glimepiride	93479-97-1
Famprofazone	22881-35-2	Glipizide	29094-61-9
Febuxostat	144060-53-7	Gliquidone	33342-05-1
Felbamate	25451-15-4	Glyburide	10238-21-8
Felodipine	72509-76-3	Guaifenesin	93-14-1
Fenbendazole	43210-67-9	Guanabenz	23256-50-0
Fenofibrate	49562-28-9	Guanidine	50-01-1
Fenoprofen	34597-40-5	Halobetasol	66852-54-8
Fenoprofen	71720-56-4	Haloperidol	52-86-8
Fenspiride	5053-08-7	Homatropine	51-56-9
Fenticonazole	73151-29-8	Homatropine	80-49-9
Fesoterodine	286930-03-8	Hydrochlorothiazide	58-93-5
Fexofenadine	153439-40-8	Hydrocortisone	50-23-7
Finasteride	98319-26-7	Hydroxyurea	127-07-1
FK-506	104987-11-3	Hydroxyzine	2192-20-3
Flavoxate	3717-88-2	Hyoscyamine	101-31-5
Fluconazole	86386-73-4	Ibuprofen	15687-27-1
Flucytosine	2022-85-7	Ibutilide	122647-32-9
Fludarabine	21679-14-1	Idoxuridine	54-42-2

Iloperidone	133454-47-4	Lopinavir	192725-17-0
Imatinib	152459-95-5	Loratadine	79794-75-5
Imatinib	220127-57-1	Lornoxicam	70374-39-9
Imidapril	89371-37-9	Losartan	124750-99-8
Imipramine	113-52-0	Loteprednol	82034-46-6
Indapamide	26807-65-8	Lovastatin	75330-75-5
Indomethacin	53-86-1	Loxapine	27833-64-3
Ipratropium	22254-24-6	L-Thyroxine	51-48-9
Irinotecan	97682-44-5	Malotilate	59937-28-9
Irinotecan	136572-09-3	Manidipine	89226-50-6
Irsogladine	57381-26-7	Maprotiline	10347-81-6
Isoetharine	7279-75-6	Maraviroc	376348-65-1
Isoniazid	54-85-3	Masitinib	790299-79-5
Isoprenaline	51-30-9	MDV3100	915087-33-1
Isosorbide	652-67-5	Mecarbinat	15574-49-9
Isotretinoin	4759-48-2	Meclofenamate	6385-02-0
Isovaleramide	541-46-8	Medetomidine	86347-15-1
Isoxicam	34552-84-6	Medroxyprogesterone	71-58-9
Isradipine	75695-93-1	Mefenamic	61-68-7
Itraconazole	84625-61-6	Megestrol	595-33-5
Ivabradine	148849-67-6	Meglumine	6284-40-8
Ivermectin	70288-86-7	Melatonin	73-31-4
Ketoconazole	65277-42-1	Meloxicam	71125-38-7
Ketoprofen	22071-15-4	Memantine	41100-52-1
Ketorolac	74103-07-4	Menadione	58-27-5
Ketotifen	34580-14-8	Mepenzolate	76-90-4
Lacidipine	103890-78-4	Mepiroxol	6968-72-5
L-Adrenaline	51-43-4	Mepivacaine	1722-62-9
Lafutidine	118288-08-7	Meptazinol	59263-76-2
Lamivudine	134678-17-4	Mequinol	150-76-5
Lamotrigine	84057-84-1	Mercaptopurine	50-44-2
Lansoprazole	103577-45-3	Meropenem	96036-03-2
Lapatinib	231277-92-2	Mesalamine	89-57-6
Lapatinib	388082-77-7	Mesna	19767-45-4
Leflunomide	75706-12-6	Mesoridazine	32672-69-8
Lenalidomide	191732-72-6	Mestranol	72-33-3
Letrozole	112809-51-5	Metaproterenol	5874-97-5
Levetiracetam	102767-28-2	Metaraminol	33402-03-8
Levobetaxolol	116209-55-3	Methazolamide	554-57-4
Levonorgestrel	797-63-7	Methazolastone	85622-93-1
Levosimendan	141505-33-1	Methenamine	100-97-0
Levosulpiride	23672-07-3	Methimazole	60-56-0
Licofelone	156897-06-2	Methocarbamol	532-03-6
Lidocaine	137-58-6	Methoxsalen	298-81-7
Linagliptin	668270-12-0	Methscopolamine	155-41-9
Lincomycin	859-18-7	Methyclothiazide	135-07-9
Liothyronine	55-06-1	Methylprednisolone	83-43-2
Lithocholic	434-13-9	Methylthiouracil	56-04-2
Lomerizine	101477-54-7	Meticrane	1084-65-7
Lomustine	13010-47-4	Metolazone	17560-51-9
Lonidamine	50264-69-2	Metoprolol	392-17-7
Loperamide	34552-83-5	Metronidazole	443-48-1

Mevastatin	73573-88-3	Nisoldipine	63675-72-9
Mexiletine	31828-71-4	Nitazoxanide	55981-09-4
Mianserin	21535-47-7	Nitrendipine	39562-70-4
Mifepristone	84371-65-3	Nitrofurazone	59-87-0
Miglitol	72432-03-2	Nizatidine	76963-41-2
Milnacipran	101152-94-7	Noradrenaline	108341-18-0
Milrinone	78415-72-2	norethindrone	68-22-4
Mirabegron	223673-61-8	Noscapine	912-60-7
Mirtazapine	85650-52-8	Nystatin	1400-61-9
Mitotane	53-19-0	Olanzapine	132539-06-1
Mitoxantrone	70476-82-3	Olmesartan	144689-63-4
Moclobemide	71320-77-9	Olopatadine	140462-76-6
Moexipril	82586-52-5	olsalazine	6054-98-4
Moguisteine	119637-67-1	Omeprazole	73590-58-6
Mometasone	83919-23-7	Ondansetron	99614-01-4
Monobenzene	103-16-2	Orlistat	96829-58-2
Montelukast	151767-02-1	Ornidazole	16773-42-5
Moroxydine	3160-91-6	Orphenadrine	4682-36-4
Mosapride	112885-42-4	OSI-420	183320-51-6
Moxonidine	75438-57-2	Ospemifene	128607-22-7
Mycophenolate	128794-94-5	Ouabain	630-60-4
Mycophenolic	24280-93-1	Oxaliplatin	61825-94-3
Nabumetone	42924-53-8	Oxaprozin	21256-18-8
Nafamostat	82956-11-4	Oxcarbazepine	28721-07-5
Naftopidil	57149-07-2	Oxeladin	52432-72-1
Nalidixic	389-08-2	Oxfendazole	53716-50-0
Nalmefene	58895-64-0	Oxybuprocaine	5987-82-6
Naloxone	357-08-4	Oxybutynin	5633-20-5
Naltrexone	16676-29-2	Oxybutynin	1508-65-2
Naphazoline	550-99-2	Oxymetazoline	1491-59-4
Naproxen	26159-34-2	Oxytetracycline	79-57-2
Naratriptan	143388-64-1	Ozagrel	82571-53-7
Natamycin	7681-93-8	Ozagrel	78712-43-3
Nateglinide	105816-04-4	Paclitaxel	33069-62-4
Nefiracetam	77191-36-7	Paeoniflorin	23180-57-6
Nelarabine	121032-29-9	Pancuronium	15500-66-0
Nelfinavir	159989-65-8	Paroxetine	78246-49-8
Nepafenac	78281-72-8	Pasiniazid	2066-89-9
Nevirapine	129618-40-2	Pazopanib	444731-52-6
Niacin	59-67-6	Pazopanib	635702-64-6
Nialamide	51-12-7	PCI-32765	936563-96-1
Nicardipine	54527-84-3	Penciclovir	39809-25-1
Nicorandil	65141-46-0	Pentamidine	140-64-7
Nicotinamide	98-92-0	Pentoxifylline	1677687
Nicotine	65-31-6	Pergolide	66104-23-2
Nifedipine	21829-25-4	Phenacetin	62-44-2
Nifenazone	2139-47-1	Phenazopyridine	136-40-3
Niflumic	4394-00-7	Phenformin	834-28-6
Nilotinib	641571-10-0	Phenindione	83-12-5
Nilvadipine	75530-68-6	Pheniramine	132-20-7
Nimesulide	51803-78-2	Phenothrin	26002-80-2
Nimodipine	66085-59-4	Phenoxybenzamine	63-92-3

Phentolamine	65-28-1	Protionamide	14222-60-7
Phenylbutazone	50-33-9	Pyrazinamide	98-96-4
Phenylephrine	61-76-7	Pyridostigmine	101-26-8
Phenytoin	57-41-0	Pyridoxine	58-56-0
Phenytoin	630-93-3	Pyrilamine	59-33-6
Phthalylsulfacetamide	131-69-1	Pyrimethamine	58-14-0
Pidotimod	121808-62-6	Quetiapine	111974-72-2
Pilocarpine	54-71-7	Quinapril	82586-55-8
Pimecrolimus	137071-32-0	Quinine	6119-47-7
Pimobendan	74150-27-9	Racecadotril	81110-73-8
Pimozide	2062-78-4	Ractopamine	90274-24-1
Pioglitazone	111025-46-8	Raltegravir	518048-05-0
Pioglitazone	112529-15-4	Ramelteon	196597-26-9
Piromidic	19562-30-2	Ramipril	87333-19-5
Piroxicam	36322-90-4	Ranitidine	66357-59-3
Pitavastatin	147526-32-7	Ranolazine	95635-55-5
Pizotifen	15574-96	Ranolazine	95635-56-6
PMSF	329-98-6	Rapamycin	53123-88-9
Pomalidomide	19171-19-8	Rasagiline	161735-79-1
Ponatinib	943319-70-8	Rebamipide	90098-04-7
Posaconazole	171228-49-2	Reboxetine	98769-84-7
Potassium	7681-11-0	Regorafenib	755037-03-7
Pralatrexate	146464-95-1	Repaglinide	135062-02-1
Pramipexole	104632-26-0	Reserpine	50-55-5
Pramipexole	191217-81-9	Resveratrol	501-36-0
Pramiracetam	68497-62-1	Ribavirin	36791-04-5
Pramoxine	637-58-1	Riluzole	1744-22-5
Pranlukast	103177-37-3	Rimantadine	13392-28-4
Pranoprofen	52549-17-4	Rimonabant	168273-06-1
Prasugrel	150322-43-3	Risperidone	106266-06-2
Pravastatin	81131-70-6	Ritodrine	23239-51-2
Praziquantel	55268-74-1	Ritonavir	155213-67-5
Prednisolone	50-24-8	Rivaroxaban	366789-02-8
Prednisolone	52-21-1	Rivastigmine	129101-54-8
Prednisone	53-03-2	Rizatriptan	145202-66-0
Pregnenolone	145-13-1	Rocuronium	119302-91-9
Pridinol	6856-31-1	Rofecoxib	162011-90-7
Prilocaine	721-50-6	Roflumilast	162401-32-3
Primaquine	63-45-6	Rolipram	61413-54-5
Primidone	125-33-7	Ronidazole	7681-76-7
Proadifen	62-68-0	Ropinirole	91374-20-8
Probenecid	57-66-9	Ropivacaine	98717-15-8
ProbucoI	23288-49-5	Rosiglitazone	122320-73-4
Procaine	51-05-8	Rosiglitazone	302543-62-0
Prochlorperazine	84-02-6	Rosiglitazone	155141-29-0
Procodazole	23249-97-0	Rosuvastatin	147098-20-2
Procyclidine	1508-76-5	Rotigotine	99755-59-6
Progesterone	57-83-0	Roxatidine	93793-83-0
Propafenone	34183-22-7	Roxithromycin	80214-83-1
Proparacaine	499-67-2	Rufinamide	106308-44-5
Propranolol	318-98-9	Ruxolitinib	941678-49-5
Propylthiouracil	51-52-5	Rolipram	85416-73-5

Salicylanilide	87-17-2
Sasapyrine	552-94-3
Saxagliptin	361442-04-8
Scopine	498-45-3
Scopolamine	114-49-8
Secnidazole	3366-95-8
Serotonin	153-98-0
Sertaconazole	99592-39-9
Sertraline	79559-97-0
Sildenafil	171599-83-0
Silodosin	160970-54-7
Simvastatin	79902-63-9
Sodium	94-16-6
Sodium	134-03-2
Sodium	7632-00-0
Sodium	14402-89-2
Picosulfate	10040-45-6
Sodium	54-21-7
Solifenacin	242478-38-2
Sorbitol	50-70-4
Sotalol	959-24-0
Spectinomycin	21736-83-4
Spiramycin	8025-81-8
Spironolactone	52-01-7
Stavudine	3056-17-5
Streptozotocin	18883-66-4
Sucralose	56038-13-2
Sulbactam	68373-14-8
Sulbactam	69388-84-7
sulfacetamide	127-56-0
Sulfadiazine	68-35-9
Sulfaguanidine	57-67-0
Sulfamerazine	127-79-7
Sulfameter	651-06-9
Sulfamethazine	57-68-1
Sulfamethizole	144-82-1
Sulfanilamide	63-74-1
Sulfasalazine	599-79-1
Sulindac	38194-50-2
Sumatriptan	103628-48-4
Sunitinib	341031-54-7
Suplatast	94055-76-2
Suprofen	40828-46-4
Tacrine	1684-40-8
Tadalafil	171596-29-5
TAME	901-47-3
Tazarotene	118292-40-3
Telaprevir	402957-28-2
Telbivudine	3424-98-4
Telmisartan	144701-48-4
Temocapril	110221-44-8
Temsirolimus	162635-04-3

Tenofovir	147127-20-6
Tenofovir	202138-50-9
Tenoxicam	59804-37-4
Terazosin	70024-40-7
Terbinafine	91161-71-6
Terbinafine	78628-80-5
Teriflunomide	108605-62-5
Tetracaine	136-47-0
tetrahydrozoline	522-48-5
Thalidomide	50-35-1
Thiabendazole	148-79-8
Tianeptine	30123-17-2
Tigecycline	220620-09-7
Tilmicosin	108050-54-0
tinidazole	19387-91-8
Tiopronin	19392
Tiotropium	139404-48-1
Tioxolone	4991-65-5
Tiratricol	51-24-1
Tizanidine	64461-82-1
Tofacitinib	540737-29-9
Tolbutamide	64-77-7
Tolfenamic	13710-19-5
Tolmetin	64490-92-2
Tolnaftate	2398-96-1
Tolperisone	3644-61-9
Tolterodine	124937-52-6
toltrazuril	69004-03-1
Tolvaptan	150683-30-0
Topiramate	97240-79-4
Topotecan	119413-54-6
Tranilast	53902-12-8
Tretinoin	302-79-4
Triamcinolone	124-94-7
Triamcinolone	76-25-5
triamterene	396-01-0
Trichlormethiazide	133-67-5
Triclabendazole	68786-66-3
Trifluoperazine	440-17-5
Triflupromazine	1098-60-8
Triflusal	322-79-2
Trilostane	13647-35-3
Trimebutine	39133-31-8
Trimipramine	521-78-8
Tripelennamine	154-69-8
Trometamol	77-86-1
Tropicamide	1508-75-4
Tropisetron	105826-92-4
Trospium	10405-02-4
Troxipide	30751-05-4
Tylosin	74610-55-2
Ulipristal	159811-51-5

Uracil	66-22-8
Urapidil	64887-14-5
Uridine	58-96-8
Ursodiol	128-13-2
Valaciclovir	124832-27-5
valganciclovir	175865-59-5
Valproic	1069-66-5
Valsartan	137862-53-4
Vandetanib	443913-73-3
Vardenafil	330808-88-3
Vecuronium	50700-72-6
Vemurafenib	918504-65-1
Venlafaxine	99300-78-4
Verteporfin	129497-78-5
Vidarabine	5536-17-4
Vildagliptin	274901-16-5
Vinblastine	143-67-9
Vincristine	2068-78-2
Vinorelbine	125317-39-7
Vismodegib	879085-55-9
Vitamin	68-19-9
Vitamin	50-81-7
Vitamin	50-14-6
Vitamin	67-97-0
Voglibose	83480-29-9
Voriconazole	137234-62-9
Vorinostat	149647-78-9
XL-184	849217-68-1
Xylazine	23076-35-9
Xylometazoline	1218-35-5
Xylose	25990-60-7
Zalcitabine	7481-89-2
Zaltoprofen	74711-43-6
Zanamivir	139110-80-8
Zidovudine	30516-87-1
Zileuton	111406-87-2
Ziprasidone	122883-93-6
Zolmitriptan	139264-17-8
Zonisamide	68291-97-4
Zoxazolamine	61-80-3

Several of the identified agents as shown in Table 14 are previously known antibacterial agents. Clorobiocin is an aminocoumarin DNA gyrase inhibitor similar to novobiocin^{172 173} Ethyl violet is a homolog of crystal (methyl) violet which is a well-known antibacterial agent of unknown mechanism¹⁷⁴ Hitachimycin (strobomycin) is a generally cytotoxic agent with gram-positive antibacterial activity isolated from streptomyces cultures^{175 176} Streptovaricin C is a known antibiotic which inhibits mRNA polymerase¹⁷⁷ Several other agents on this list have been identified as having anti-MRSA activity in publicly available library screening databases (ChEMBL CHEMBL4296184¹⁷⁸, and PubChem AIDs 1259311, and 1409573).

5.3.2 Comparative minimum inhibitory concentration analysis to identify agents synergistic with cefoxitin

Comparisons between MIC values are included in Table 14 to highlight the effect of added cefoxitin on compound MICs, and the effect of microsomal metabolism on MICs. The $L2_{(-/+Cef)}$ values represent simple comparisons between UM compound MICs in the absence and presence of cefoxitin:

$$L2_{(-/+Cef)} = \log_2 \left(\frac{MIC_{UM-Cef}}{MIC_{UM+Cef}} \right)$$

This represents the \log_2 -fold change for the UM-Cef/UM+Cef MIC ratio. An $L2$ for UM-Cef vs PM-Cef can be defined similarly ($L2_{(UM/PM)}$), which reflects the change in between the UM-Cef and PM-Cef MIC ratio. The $AL2$ values represent the average effect of added cefoxitin on UM and PM MIC values, or of compound metabolism on both -Cef and +Cef values, as presented previously¹⁴³ and as defined in the footnote to Table 14. Parameter values ≥ 2 (4-fold changes, highlighted in red in Table 14) indicate significantly increased potency (lower MIC), and values ≤ -2 (highlighted in blue in Table 14) indicate significantly decreased potency (higher MIC). Five

compounds demonstrated $L2_{(-/+Cef)} \geq 2$ values, identifying these as likely synergistic agent combinations with cefoxitin, and worthy of follow-up checkerboard analyses. No compounds demonstrated $L2_{(UM/PM)} \geq 2$ values indicative of a substantially more active metabolite, and no further follow-up on active metabolite identification was therefore performed.

5.3.3 Checkerboard analysis

Five compounds in Table 14 showed apparent significant synergy ($L2_{(-/+Cef)} \geq 2$). Follow-up checkerboard assays were performed for all these except NSC654260, which was not available in sufficient amounts for this analysis. This confirmed synergy of cefoxitin with all four of the tested $L2_{(-/+Cef)} \geq 2$ compounds as shown in Figure 69, ranging from relatively strong synergy ($\sum FIC_{min} = 0.19$) for celastrol to relatively weak synergy ($\sum FIC_{min} = 0.5$) for teniposide. There does not appear to be a common mechanistic relationship between these four synergistic-with-cefoxitin compounds.

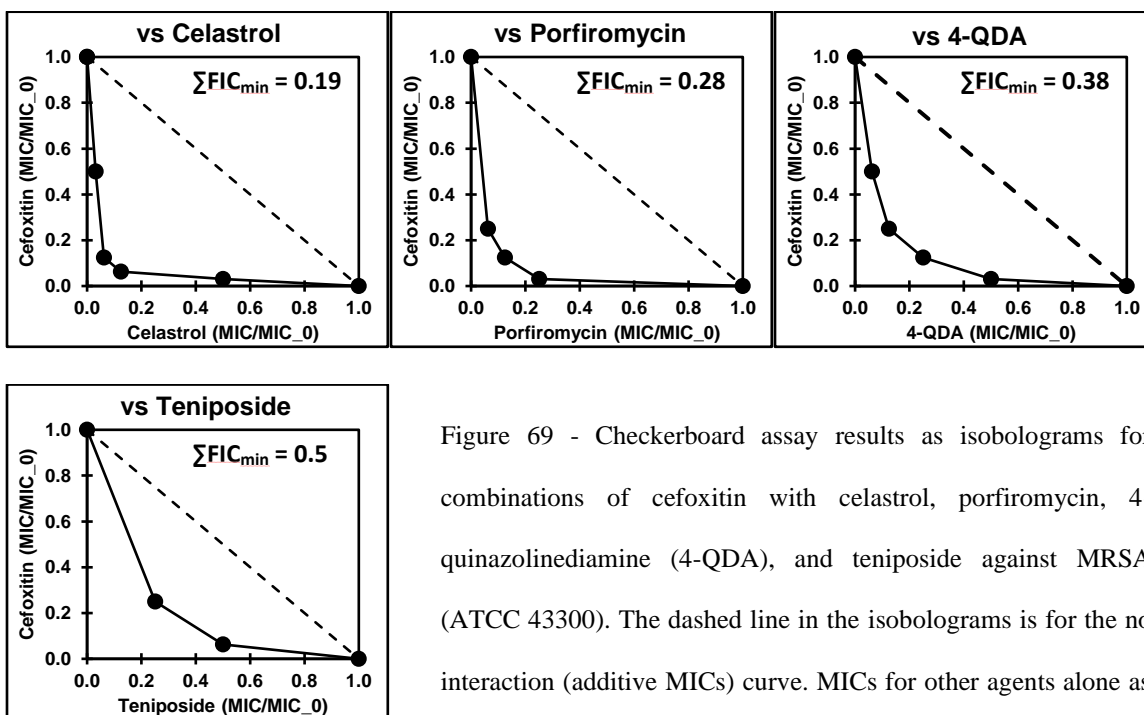


Figure 69 - Checkerboard assay results as isobolograms for combinations of cefoxitin with celastrol, porfiromycin, 4-quinazolinediamine (4-QDA), and teniposide against MRSA (ATCC 43300). The dashed line in the isobolograms is for the no interaction (additive MICs) curve. MICs for other agents alone as given in Table 14.

5.3.4 Identification and confirmation of folate/thymidine biosynthesis inhibitors

Two of the compounds in Table 14 had the diaminopyrimidine pharmacophore associated with folate reductase inhibitors such as trimethoprim (4-QDA and NSC309401 shown in Figure 70). Folate is required for the synthesis of thymidine, and addition of thymidine can be used to reverse the action of folate/thymidine biosynthesis inhibitors¹⁷⁰ It was therefore expected that redetermining the MICs of the compounds in Table 14 in the absence and presence of 4 μ M (1 μ g/mL) thymidine (-/+Thy) could be used to identify folate/thymidine biosynthesis inhibitors within this group as shown in Table 17. This identified 3 compounds with significantly increased MICs in the presence of thymidine ($L2_{(+/-Thy)} \geq 2$); the two diaminopyrimidine compounds (4-QDA and NSC309401) as well as the fluorine substituted pyrimidine analog NSC367428 as shown in Table 17.

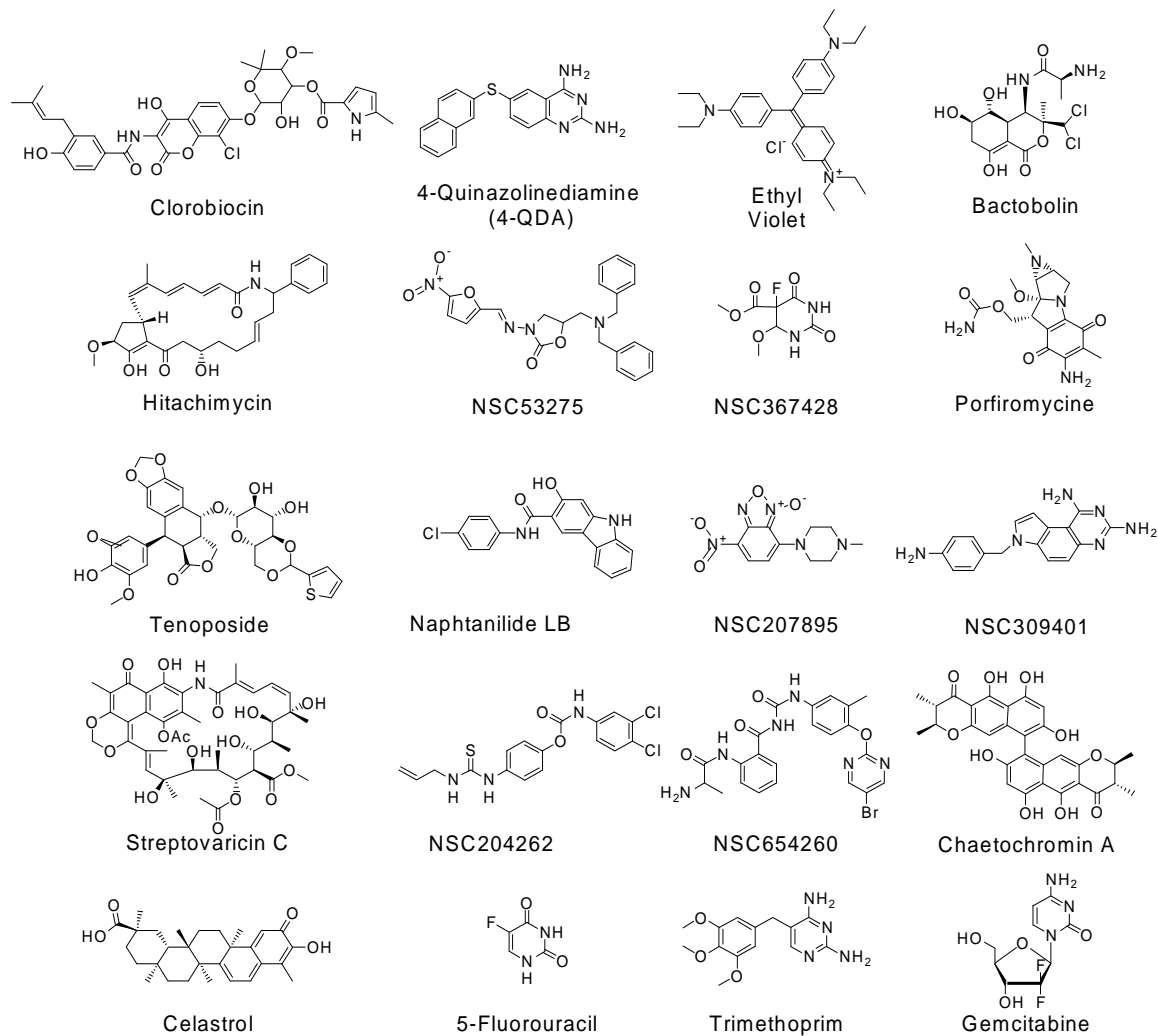


Figure 70 - Structure of active compounds from Table 14

Table 17 - MICs (μM) for the top NCI Diversity Set V compounds against MRSA (ATCC #43300) in the absence and presence of 4 μM of thymidine.			
Name	-Thy	+Thy	L2 _(+/-Thy)
Clorobiocin	0.049	0.049	0
4-QDA	0.78	100	7
Ethyl Violet	3.1	6.25	1
Bactobolin	3.1	6.25	1
Hitachimycin	1.6	1.6	1
NSC53275	100	100	0
Porfiromycin	6.25	6.25	-1
Teniposide	25	25	0
Naphthnilide LB	12.5	12.5	0
NSC207895	6.25	12.5	1
NSC309401	12.5	100	3
Streptovaricin C	3.1	6.25	1
NSC204262	100	100	0
NSC367428	3.1	100	5
NSC654260	100	100	0
Chaetochromin	25	25	0
Celastrol	100	50	-1
^a L2 _(+/-Thy) = log ₂ $\left(\frac{\text{MIC}_{+\text{Thy}}}{\text{MIC}_{-\text{Thy}}}\right)$.			

To further confirm these as thymidine biosynthesis inhibitors, an ion pairing LC-MS/MS method was developed for deoxythymidine triphosphate (dTTP), with ATP as a control nucleotide as shown in Table 18 similarly to the method developed for the UDP-linked intermediates in the bacterial peptidoglycan biosynthesis pathway⁵⁷ This method was used to determine the level of dTTP after MRSA exposure to the putative folate/thymidine biosynthesis inhibitors, with trimethoprim included as a positive control and gemcitabine¹⁴³ included as a negative control. These LC-MS/MS results as shown in Figure 71 clearly demonstrate substantial dTTP level suppression for NSC309401, NSC367428, and 4-QDA. The two diaminopyrimidine containing agents (4-QDA and NSC309401) are likely folate reductase inhibitors. The mechanism of

thymidine biosynthesis inhibition by the fluoropyrimidine NSC367428 is unknown, but it is structurally like 5-fluorouracil as shown in Figure 70. This +/- thymidine approach for quick identification of folate/thymidine biosynthesis inhibitors is a simple extension to the general synergy screening approach used in this and several prior studies. Since folate biosynthesis is an essential bacterial biochemical pathway, this approach could be expanded for the large-scale identification of novel agents targeting this essential and druggable pathway.

Table 18 - Retention time (t_R) and MS/MS parameters for ATP and dTTP quantification.						
	t_R (min)	Q1	Q3	DP (V)	EP (V)	CE (V)
ATP	12.6	506.0	158.9	-60	-3	-44
dTTP	14.3	481.0	158.9	-55	-4	-40

Global method parameters were TEM (source temperature), 300 °C; IS (ion spray voltage), -4500 V; GS1 & GS2 (gas flows), 50 (arbitrary units); CAD gas, medium.

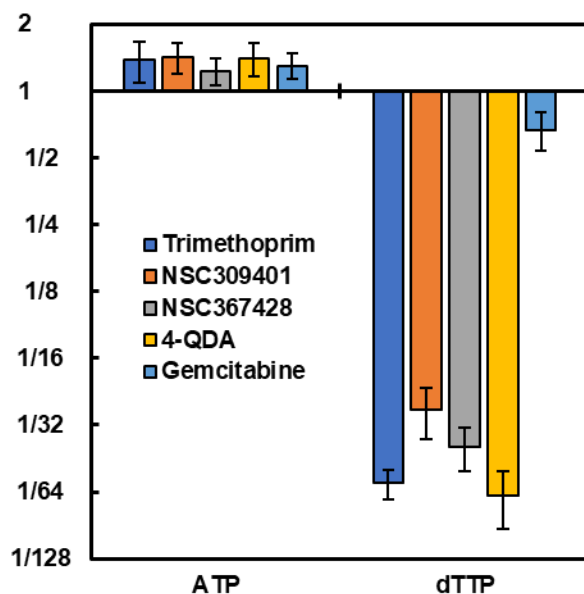


Figure 71- Fold-changes in the levels of ATP and dTTP upon exposure to 4x MIC of different agents for 15 min relative to an untreated control

5.3.5 Spectrum of activity

To further assess the potential of this group of NCI compounds as anti-MRSA and antibacterial agents, spectrum of activity was determined against several MRSA strains, one strain of VRE *faecium*, one strain of VRE *faecalis*, and one strain of *E. coli* (Table 19). Only NSC367428, the fluoropyrimidine derivative (Figure 70), demonstrated appreciable activity against *E. coli*. This contrasts with the structurally similar 5-fluorouracil, which did not show activity against *E. coli*¹⁴³ Clorobiocin showed the best MRSA spectrum of activity, followed by 4-QDA, bactobolin, streptovaricin C, ethyl violet, NSC367428, and hitachimycin, based on average MRSA MIC. Naphtanilide LB and to a lesser degree clorobiocin were unusual in their selectivity's to certain MRSA strains.

Table 19 - Spectrum of activity of NCI compounds (MIC, μ M).

Compound ^a	MRSA (F-182) ^b	MRSA (N315)	MRSA (HI022)	MRSA (MN8)	MRSA (TCH70)	MRSA (RN1)	MRSA (COL)	MRSA (U9N0)	VRE (<i>faecium</i> , clinical)	VRE (<i>faecalis</i> , 2365)	<i>E. coli</i> (K12)
Clorobiocin	0.10	0.10	0.10	NA ^c	0.20	0.20	0.024	NA	6.25	25	NA
4-QDA	0.39	3.1	1.6	0.78	1.6	1.6	6.25	3.1	1.6	NA	50
Ethyl Violet	1.6	6.25	3.1	3.1	6.25	6.25	6.25	6.25	6.25	12.5	50
Bactobolin	3.1	3.1	3.1	3.1	3.1	3.1	3.1	6.25	12.5	NA	50
Hitachimycin	1.6	0.8	12.5	1.6	12.5	3.1	3.1	12.5	1.6	6.25	NA
Porfiromycin	12.5	12.5	12.5	12.5	12.5	12.5	12.5	NA	12.5	12.5	NA
Streptovaricin C	6.25	3.1	6.25	3.1	1.6	3.1	1.6	6.25	25	50	NA
Naphtanilide	6.25	1.6	NA	NA	NA	12.5	NA	NA	NA	NA	NA
NSC207895	12.5	3.1	12.5	50	12.5	12.5	12.5	25	12.5	12.5	NA
NSC309401	12.5	25	50	12.5	25	12.5	50	12.5	NA	NA	6.25
NSC367428	3.1	12.5	6.25	6.25	6.25	6.25	1.56	3.1	NA	NA	NA
Trimethoprim ^d	25	25	12.5	12.5	12.5	25	12.5	12.5	1.6	NA	3.1
Vancomycin ^d	1.6	0.39	1.6	0.39	0.78	0.78	0.78	1.6	NA	NA	NA
Doxycycline ^d	NA	NA	NA	NA	NA	NA	NA	NA	16	3.1	N

^a Structures shown in Figure below.

^b ATCC 43300 MRSA strain used for library screening. Other vendor IDs given in the text.

^c NA – Not active at 50 μ M, the highest concentration used in these MIC determinations.

^d Control antibiotic.

5.4 Conclusion

A library screening effort was performed with the NCI diversity set V against MRSA to both identify novel antibacterial metabolites and synergistic agents with cefoxitin. In contrast to a prior similar screen of an FDA approved drug library against MRSA¹⁴³, human microsome metabolism of the NCI library did not result in the identification of any new active metabolites. However, similarly to this prior FDA screen, screening the NCI library in the absence and presence of cefoxitin allowed for the identification of several synergistic combinations with cefoxitin; celastrol, porfiromycin, 4-QDA, and teniposide. Two of these synergistic agents, celastrol, and porfiromycin, are DNA damaging agents^{179 180}, teniposide is a DNA gyrase inhibitor¹⁸¹, and 4-QDA is a folate/thymidine biosynthesis inhibitor as demonstrated in this study. There does not seem to be an obvious common mechanistic basis for the synergy of these four agents with cefoxitin. The identification of several folate/thymidine biosynthesis inhibitors using a -/+thymidine counter screen identified 3 compounds (4-QDA, NSC367428, and NSC309401) as folate/thymidine biosynthesis inhibitors, and these were confirmed as able to suppress dTTP biosynthesis in MRSA by LC-MS. 4-QDA may provide a lead for further folate biosynthesis inhibitors. Several other agents identified in this screen are of unknown but potentially interesting mechanism including NSC53275, naphtanilide LB, NSC207895, NSC204262, and NSC654260.

CHAPTER 6

6. SCREENING THE NCI DIVERSITY SET V APPROVED DRUGS AND METABOLITES WITH VANCOMYCIN AGAINST VANA-TYPE VANCOMYCIN-RESISTANT *ENTEROCOCCUS FAECIUM*

6.1 Introduction and Rationale

HAIs, are infections acquired in hospitals, pose a significant threat to patient care and result in substantial hospital costs, as treating these infections is no longer reimbursed. Hospitals are under further pressure to decrease their incidence rates due to regulations that require them to report HAIs. Some healthcare systems have had success in reducing MRSA HAIs by screening patients for MRSA at admission, which may also be a useful strategy for controlling other healthcare-associated pathogens such as vancomycin-resistant *Enterococcus* (VRE), *Clostridium difficile*, and carbapenem-resistant *Enterobacteriaceae* (CRE)¹⁸³ However, there is an ongoing debate about the best approach to screening and infection control, which may vary depending on the pathogen in question.

Enterococcus species are well-known pathogens that can cause a range of clinical conditions, such as bacteremia, infective endocarditis, and urinary tract infections^{184 185 186} Vancomycin-resistant *Enterococcus* infections are associated with an increased mortality rate, with patients suffering from VRE bacteremia experiencing a 2.5-fold increase in mortality¹⁸⁷ Vancomycin resistance in *Enterococcus* spp. has been on the rise since its discovery in 1986^{188 189} Presently, 30% of *Enterococcus* species isolates in the US are vancomycin-resistant, and these infections cause an estimated 1,300 deaths per year¹⁹⁰ The majority of VRE cases involve *E. faecium* (77%) and *E. faecalis* (9%), with the remaining 14% of cases involving less frequently implicated species, such as *E. gallinarum*, *E. avium*, *E. casseliflavus*, and *E. raffinosus*¹⁹⁰ To

reduce VRE infections, a multifaceted approach is required, including antimicrobial stewardship to limit the selection of VRE in colonized patients, effective infection control measures to decrease transmission, and reliable and sensitive laboratory methods for the timely detection of VRE. Chemical compound library screening helps discovering new bioactive agents, including antibacterial activity. However, large untargeted (whole cell) and targeted (individual protein) library screening efforts have given overall disappointing results^{136 137} In a prior study, a dimensionally enhanced library screening approach was demonstrated for screening an FDA-approved drug library against VRE faecium¹⁷¹ This approach uses added dimensions (human liver microsome metabolized library compounds, and -/+ vancomycin screening) to a standard library screen to provide valuable additional information while also providing a degree of screening redundancy. In this study, a variation of this approach was applied to VRE using a non-FDA-approved library to assess the ability of this approach to identify interesting lead compounds in a general chemical (non-FDA) library screen. The National Cancer Institute Diversity Set V (NCI) library was used for this effort, which consists of 1593 compounds selected to cover a wide range of chemical and pharmacophore space. This effort identified agents with good intrinsic anti-VRE activity and agents with synergistic activity with vancomycin. No agents with active metabolites were identified in this screen. In this study, this approach was used to screen an NCI library in its original (un-met; UM) and human microsome metabolized (pre-met; PM) versions against VREfm in the absence and presence of sub-MIC levels of vancomycin (-/+Vm) (2x2 library screening design).

6.2 Material and Methods

6.2.1 General

The NCI diversity set V library of 1593 compounds was obtained from the Division of Cancer Treatment and Diagnosis (DCTD) of the National Cancer Institute (NCI). All other materials were as described previously¹⁴³

Library replication, addition of metabolism and antibacterial control compounds. The NCI diversity set V was delivered in 96 well plates in columns 2–11, 20 plates total, with each well containing 20 μ L of a 10 mM solution of a compound in DMSO. Antibiotic controls (20 μ L of 10 mM stock solutions of vancomycin, fosfomycin, ampicillin, doxycycline, or chloramphenicol) were added to column 1 of each library plate. Microsomal (CYP) substrate controls (20 μ L of 10 mM stock solutions of phenacetin, tolbutamide, dextromethorphan, coumarin, chlorzoxazone or diclofenac) were added to column 12 of each library plate. Aliquots (10 μ L) of library samples were transferred to 96 well plates using a liquid handling workstation (Biomek 3000) and diluted with 90 μ L DMSO to provide UM working plates at 1 mM.

6.2.2 In vitro microsomal metabolism to provide Pre-metabolized library

For PM library preparation, the remaining 10 μ L of each sample in DMSO was dried by freezing the plates at -80°C and drying under strong vacuum ($<50\text{ }\mu\text{mHg}$) in a Genevac Quatro centrifugal concentrator (DMSO can interfere with microsomal metabolism reactions). The dried library plates were metabolized with human liver microsomes as described previously¹⁴³ To each well was added 10 μ L acetonitrile/water (20/80%, v/v) to redissolve samples. The plates were incubated for 2 h at 35°C , followed by addition of 490 μ L of freshly prepared (on ice) microsomal reaction mixture containing 50 mM potassium phosphate pH 7.4, 3 mM MgCl_2 , 5 mM glucose-6-

phosphate, 1 unit mL⁻¹ glucose-6-phosphate dehydrogenase, 1 mM NADP⁺ and 0.5 mg mL⁻¹ total microsomal protein. Reaction mixtures were incubated for 24 h at 35 °C with gentle rocking. Library plates were then centrifuged at 4000g for 30 min at 4 °C, and 400 µL of the supernatants then transferred to sterile 96 well plates. To the residues was added 100 µL DMSO, and the samples mixed thoroughly. Library plates were centrifuged again at 4000g for 30 min, and 150 µL of the supernatants were removed and combined with the first extracts. The resulting extracts were frozen at –80 °C and dried under strong vacuum (<50 µmHg) in a Genevac Quatro centrifugal concentrator. These “pre-met” (PM) library samples were then reconstituted in 100 µL DMSO to provide a 1 mM PM NCI working library. Both UM and PM working libraries were stored in U-bottom polypropylene storage plates at –80 °C. Samples of wells containing microsomally metabolized drug controls from PM plates were analyzed by LC-MS/MS to provide a relative measure of metabolism. The percent metabolism of these control drugs was 52%, 55%, 60%, 66%, 95% and 100% for tolbutamide, dextromethorphan, chlorzoxazone, phenacetin, diclofenac and coumarin respectively. These controls demonstrate that the metabolism conditions employed in this study were sufficient to achieve a relatively high degree of metabolism.

6.2.3 UM/PM vs –/+ vancomycin library screen against VRE *faecium*

Four sets of library screens were performed (UM–Vm, UM+Vm, PM–Vm, and PM+Vm), as described previously for an FDA approved drug library screen¹⁴³, with the modification that 2 µL of library samples @ 1 mM were used. During the bacterial incubation step, this provided 100 µM compound concentrations, rather than 200 µM as in the previously described study¹⁴³ Plates were frozen at –80 °C and dried as described above. To each well in each set was added 20 µL brain heart infusion (BHI) broth containing 4000 cfu VRE *faecium* clinical and containing either

no vancomycin for –Vm screens or +16 $\mu\text{g mL}^{-1}$ vancomycin (equal to $\frac{1}{4}\times$ MIC) for +Vm screens. Plates were incubated for 48 h at 35 °C. Fresh BHI broth (10 μL) was then added to the wells of these four sets of plates, followed by incubation for 2 h at 35 °C, to restart active cell growth. To the wells of these plates was then added 10 μL of 100 $\mu\text{g mL}^{-1}$ resazurin (sodium salt)^{145 146 147}. The plates were incubated for another 2 h at 35 °C, and the A610 - A450 absorbance ratio was measured in a Molecular Devices SpectraMax M5 multimode microplate reader. The resulting data was processed and analyzed using Matlab scripts (The Mathworks, Natick, MA) to identify active wells using a cut-off value between known actives (antibiotic controls) and known inactives (microsomal controls). A merged hit list was generated, in which a compound was included in the merged hit list if it demonstrated activity under any of the four test conditions (UM-Vm, UM+Vm, PM-Vm, or PM+Vm).

6.2.4 Hit picking and minimum inhibitory concentration determination.

Follow up MIC determinations for identified hits were performed as described in detail previously¹⁴³. MICs were determined for all actives by hit picking 2 μL samples from both UM and PM working plates (two sets from each) into the first columns of 384 well plates (four sets total, for UM–Vm, UM+Vm, PM–Vm and PM+Vm MIC determinations). These samples were then serially diluted in steps of two across the plates with DMSO using an Integra Viaflo Assist automated multichannel pipette. The last column was left blank (DMSO only). These plates were frozen at –80 °C and dried under strong vacuum as described above. To each well in each set was added 20 μL BHI broth containing 4000 cfu VREfm and containing either no vancomycin for –Vm MICs or 16 $\mu\text{g mL}^{-1}$ Vm for +Vm MICs. (This provided MIC plates with 100 μM as the highest test agent concentration.) Incubation and resazurin treatment were as described above.

MICs were determined using a cutoff midway between known active and inactive samples. All MICs were determined at least in triplicate.

6.2.5 Checkerboard assays to confirm synergy with vancomycin

Several agents showed lower MICs in the presence of vancomycin as shown in Table 20, indicative of potential synergistic activity. Checkerboard assays¹⁴⁸ were used to confirm and assess synergy for 4-quinazolinediamine (4-QDA), celastrol and streptovaricin, with vancomycin, as described previously¹⁴³ All checkerboard assays were performed in triplicate. Data were plotted as isobolograms and reported as the minimum sum of fractional inhibitory concentrations (Σ FICmin values in Figure 72, also referred to as FICI values)¹⁸²

6.2.6 Spectrum of activity against MRSA strains and *E. coli*

MICs were determined for many of the Table 20 (UM-Vm) agents against a panel of bacterial strains to assess spectrum of activity. The strains tested were MRSA strains F-182 (ATCC 43300), N315 (BEI NR-45898), HI022 (BEI NR-30550), MN8 (BEI NR-45918), TCH70 (BEI HM-139), RN1 (BEI NR-45904), COL (BEI NR-45906), and U9N0, and one strain of *E. coli* K12 (BEI MG1655).

6.2.7 Spectrum of activity against VRE strains

MICs were determined for many of the Table 1 (UM-Vm) agents against a panel of ATCC VRE strains including VRE *faecium* and VRE *faecalis* to assess spectrum of activity. The strains tested were VRE *faecium* clinical strain, BAA-2317, BAA-2318, ATCC 51575 and VRE *faecalis* strain BAA-2365, ATCC 700802, BAA-49532, and BAA-49533.

6.2.8 $-/+$ Thymidine counter screen for folate/thymidine biosynthesis inhibitors

The effects of folate/thymidine biosynthesis inhibitors on VRE can be reversed by the addition of thymidine to the culture media¹⁷⁰ This effect was therefore used to assess Table 20 by redetermining the UM-Vm MICs in the absence and presence of 4 μ M (1 μ g/mL) thymidine.

6.3 Results and discussion

6.3.1 Library screening and hit minimum inhibitory concentration determinations

Library screening was performed at 100 μ M (nominal concentration for the PM library screen) as described in detail previously^{143 171} Following library screening, a pooled hit list was made (i.e., any compound that gave a hit (was active in suppressing bacterial growth) in any of the four UM/PM vs $-/+$ Vm screens was added to the list) for follow-up minimum inhibitory concentration (MIC) determinations. MICs for all the compounds in this pooled hit list were then determined by serial dilution in steps of 2 starting at 100 μ M under all four screening conditions (UM-Vm, UM+Vm, PM-Vm, and PM+Vm) to give a final table of MICs. The results from these MIC determinations for minimum MICs of ≤ 25 μ M, are summarized in Table 20.

Table 20- NCI library anti-VREfm hit MICs (Min_MIC ≤ 25 μM).

Compound	UM MICs (μM)		PM MICs (μM)		Min_MIC	L2 (UM-/ +Vm) ^a	AL2 (-/ +Vm) ^b	L2 (UM/PM-Vm)	AL2 (UM/PM) ^d
	-Vm	+Vm	-Vm	+Vm					
4-QDA	1.6	0.39	3.1	12.5	0.39	2	0.0	-1	-3.0
Celastrol	6.3	0.78	100	50	0.78	3	2.0	-4	-5.0
Hitachimycin	0.78	1.6	50	25	0.78	-1	0.0	-6	-5.0
Bactobolin	3.1	1.6	50	50	1.6	1	0.5	-4	-4.5
Chlorobiocin	3.1	1.6	3.1	3.1	1.6	1	0.5	0	-0.5
Streptovaricin C	6.3	1.6	100	50	1.6	2	1.5	-3	4.5
5'-O-Sulfamoyladosine	6.3	3.1	25	12.5	3.1	1	1.0	-2	-2.0
Ethyl Violet	6.3	6.3	100	100	6.3	0	0.0	-4	-4.0

^a $L2_{(UM-/ +Vm)} = \log_2 \left(\frac{UM_{-Vm}}{UM_{+Vm}} \right)$. ^b $AL2_{(-/ +Vm)} = \text{Avg}(\log_2 \left(\frac{UM_{-Vm}}{UM_{+Vm}} \right), \log_2 \left(\frac{PM_{-Vm}}{PM_{+Vm}} \right))$.
^c $L2_{(UM/PM-Vm)} = \log_2 \left(\frac{UM_{-Vm}}{PM_{-Vm}} \right)$. ^d $AL2_{(UM/PM)} = \text{Avg}(\log_2 \left(\frac{UM_{-Vm}}{PM_{-Vm}} \right), \log_2 \left(\frac{UM_{+Vm}}{PM_{+Vm}} \right))$.

Several of the identified agents as shown in Table 20 are previously known antibacterial agents. Chlorobiocin is an aminocoumarin DNA gyrase inhibitor similar to novobiocin^{172 173} In the previous screen of NCI vs MRSA, it was observed that 4-Quinazolinediamine acts as a folate reductase inhibitor. Celastrol is considered as a DNA damaging agent^{179 180} Basic violet is a homolog of crystal (methyl) violet which is a well-known antibacterial agent of unknown mechanism¹⁷⁴ Hitachimycin (strobomycin) is a generally cytotoxic agent with gram-positive antibacterial activity isolated from *streptomyces* cultures^{175 176} Streptovaricin C is a known antibiotic which inhibits mRNA polymerase¹⁷⁷ Several other agents on this list have been identified as having anti-VREfm activity in publicly available library screening databases (ChEMBL ChEMBL¹⁷⁸, and PubChem).

6.3.2 Comparative minimum inhibitory concentration analysis to identify agents synergistic with vancomycin

Comparison between MIC values is included in Table 20 to highlight the effect of added vancomycin on compound MICs, and the effect of microsomal metabolism on MICs. The $L2_{(-/ +Vm)}$

values represent simple comparisons between UM compound MICs in the absence and presence of vancomycin:

$$L2_{(-/+V_m)} = \log_2 \left(\frac{MIC_{UM-V_m}}{MIC_{UM+V_m}} \right)$$

This represents the log₂-fold change for the UM-V_m/UM+V_m MIC ratio. An L2 for UM-V_m vs PM-V_m can be defined similarly (L2_(UM/PM)), which reflects the change in between the UM-V_m and PM-V_m MIC ratio. The AL2 values represent the average effect of added vancomycin on UM and PM MIC values, or of compound metabolism on both -V_m and +V_m values, as presented previously¹⁴³ and as defined in the footnote to Table 20. Parameter values ≥ 2 (4-fold changes, highlighted in red in Table 20) indicate significantly increased potency (lower MIC), and values ≤ -2 (highlighted in blue in Table 20) indicate significantly decreased potency (higher MIC). Three compounds demonstrated L2_(-/+V_m) ≥ 2 values, identifying these as likely synergistic agent combinations with vancomycin, and worthy of follow-up checkerboard analyses. No compounds demonstrated L2_(UM/PM) ≥ 2 values indicative of a substantially more active metabolite, and no further follow-up on active metabolite identification was therefore performed.

6.3.3 Checkerboard analysis

Three compounds in Table 20 showed apparent significant synergy (L2_(-/+V_m) ≥ 2). Follow-up checkerboard assays were performed for all these compounds. This confirmed synergy of vancomycin with all three of the tested L2_(-/+V_m) ≥ 2 compounds as shown in Figure 72, ranging from relatively strong synergy ($\Sigma FIC_{min} = 0.16$) for celastrol to synergy ($\Sigma FIC_{min} = 0.38$) for streptovaricin C. There does not appear to be a common mechanistic relationship between these three synergistic-with-vancomycin compounds.

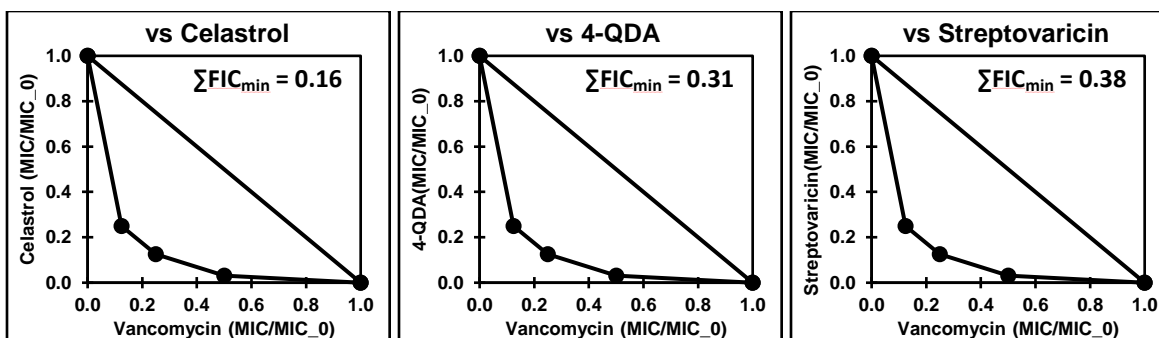


Figure 72 - Checkerboard assay results as isobolograms for combinations of vancomycin with celastrol, 4-quinazolinediamine (4-QDA), and Streptovaricin against VREfm. The dashed line in the isobolograms is for the no interaction (additive MICs) curve. MICs for other agents alone as given in Table 20.

6.3.4 Identification of folate/thymidine biosynthesis inhibitors.

None of the compounds in Table 20 showed activity in presence of thymidine. Doxycycline which was used as control showed slight activity in presence of thymidine (Data not shown).

6.3.5 Spectrum of activity

To further assess the potential of this group of NCI compounds as anti-VREfm and antibacterial agents, spectrum of activity was determined against several MRSA strains, several VRE strains and one strain of *E. coli* (Data not shown). None of the compound demonstrated activity against *E. coli*. Clorobiocin showed the best MRSA and VRE *faecium* spectrum of activity. However, it did not show any activity against VRE *faecalis* strain. 4-Quinazolinediamine showed no activity against MRSA or any VRE strains. 5' sulfamoyladenine showed no activity against MRSA strains and most of VRE *faecalis* strains. However, it did show activity against VRE *faecium* strains. Bactobolin showed activity against MRSA, slight activity towards VRE *faecium*

and no activity against VRE *faecalis*. Ethyl violet showed slight activity against MRSA and VRE strains. Hitachimycin showed good activity against both MRSA and VRE strains.

6.4 Conclusion

The overall goal of this effort was to further demonstrate the utility of enhanced library screening approaches in which replicate library screens were performed with variation between the replicates. However, VRE vs NCI screen did not provide many hits as compared to MRSA-NCI screen. Clorobiocin, hitachimycin and bactobolin were the only compounds that showed spectrum of activity against both MRSA strains and VRE strains (Data not shown). Screening for synergistic combinations with vancomycin revealed three synergistic agents as shown in Figure 72. The synergy of these three compounds with vancomycin was high with very low FICI values. Celastrol which is also known as the DNA damaging agent¹⁷⁹ was synergistic with both vancomycin and cefoxitin in the MRSA vs NCI screens. 4-QDA which is known to act as a folate reductase inhibitor (as mentioned in the previous study) also acted synergistically with both vancomycin and cefoxitin in both VRE and MRSA screen. Some of the agents and agent combinations identified in this effort may be suitable candidates for further *in vitro* and *in vivo* studies, and ultimately clinical application.

PART III: DRUG INTERACTION AND WHOLE GENOME SEQUENCING OF
RESISTANT BACTERIA

CHAPTER 7

7. INTRODUCTION AND LITERATURE REVIEW

7.1 Mechanism of action of antibiotics

During the last few decades, the number of infections caused by gram-positive and gram-negative bacteria has increased tremendously¹⁹¹ Commonly used antibiotics have led to the increased spread of resistance caused by bacteria which are now posing a significant threat in hospitals and community^{192 193} The main reason for bacteria to overcome the action of several antibiotics is through mutagenesis in its DNA and genetic alterations which occurs via exchange of genetic material with other microorganisms¹⁹⁴ Some examples of these resistance causing strains are Vancomycin-resistant *Enterococci*, multiple resistant *Pneumococci*, Methicillin-resistant *Staphylococci*, and *Streptococci*. For over many years, antibacterial drug-target interactions of antibiotics are well known, and these drugs have inhibited cellular function in bacteria like cell wall biosynthesis, transcription, translation, DNA supercoiling, or folate biosynthesis^{195 196} Therefore, the antibiotics used to target these bacteria are classified based on mechanism of action as shown in Figure 73.

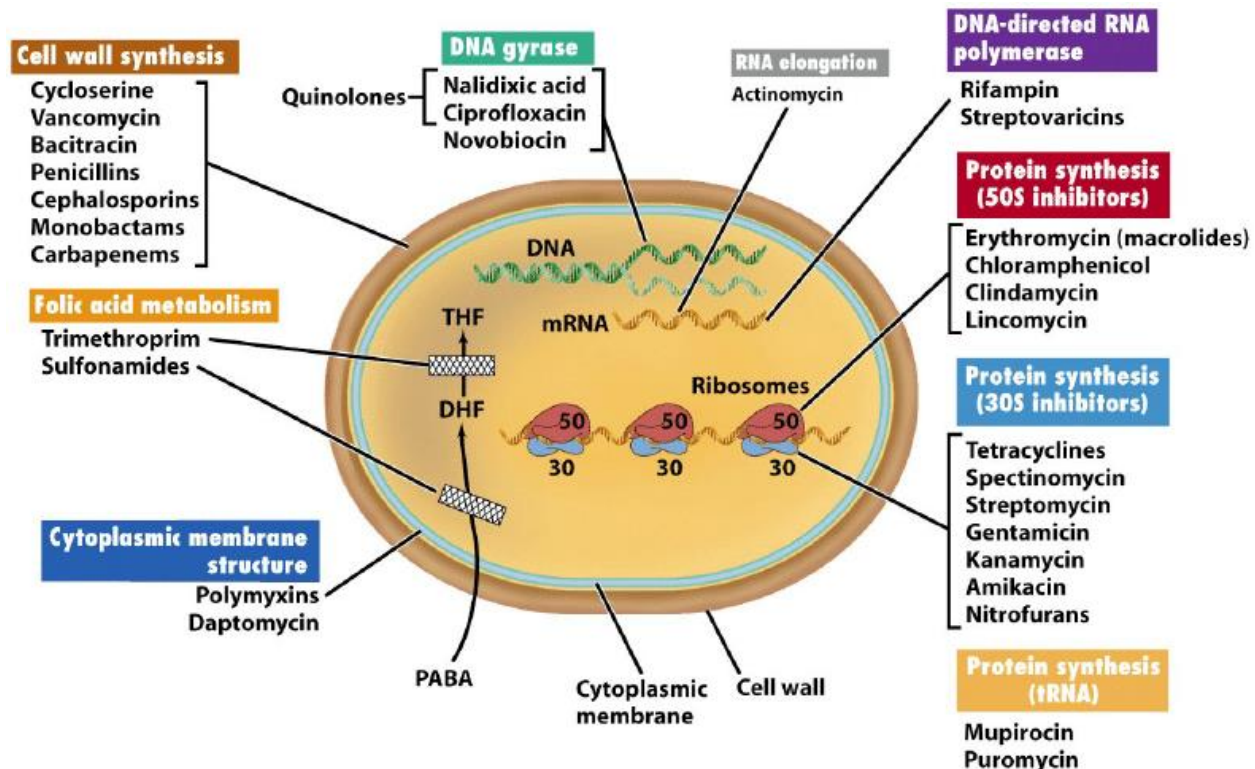


Figure 73 - Mechanism of action of antibiotics²⁰⁰

7.2 Antibiotics targeting bacterial cell wall

Bacterial cells are surrounded by a peptidoglycan layer known as the cell wall consisting of long sugar polymers. This cell wall undergoes cross-linking of the glycan strands, and the peptide chain extends from the sugar moieties to form cross links¹⁹⁷. Penicillin-binding proteins (PBPs) help glycan to cross-link the D-alanyl-D-alanine portion of peptide¹⁹⁸. Beta-lactam antibiotics target the penicillin-binding proteins primarily. Beta-lactam ring mimics D-alanine-D-alanine part of the peptide chain, which is typically bound by penicillin-binding proteins. PBPs interact with the beta-lactam ring and therefore the synthesis of new cell wall stops, which eventually leads to cell death of bacteria¹⁹⁹ as shown in Figure 74. Then comes the glycopeptides, which bind to D-alanyl-D-alanine portion of the peptide chain in the peptidoglycan subunit. One

such example of a glycopeptide is vancomycin which is a large drug molecule and prevents the binding of D-alanyl to PBP thereby inhibiting the cell wall biosynthesis^{199 201}

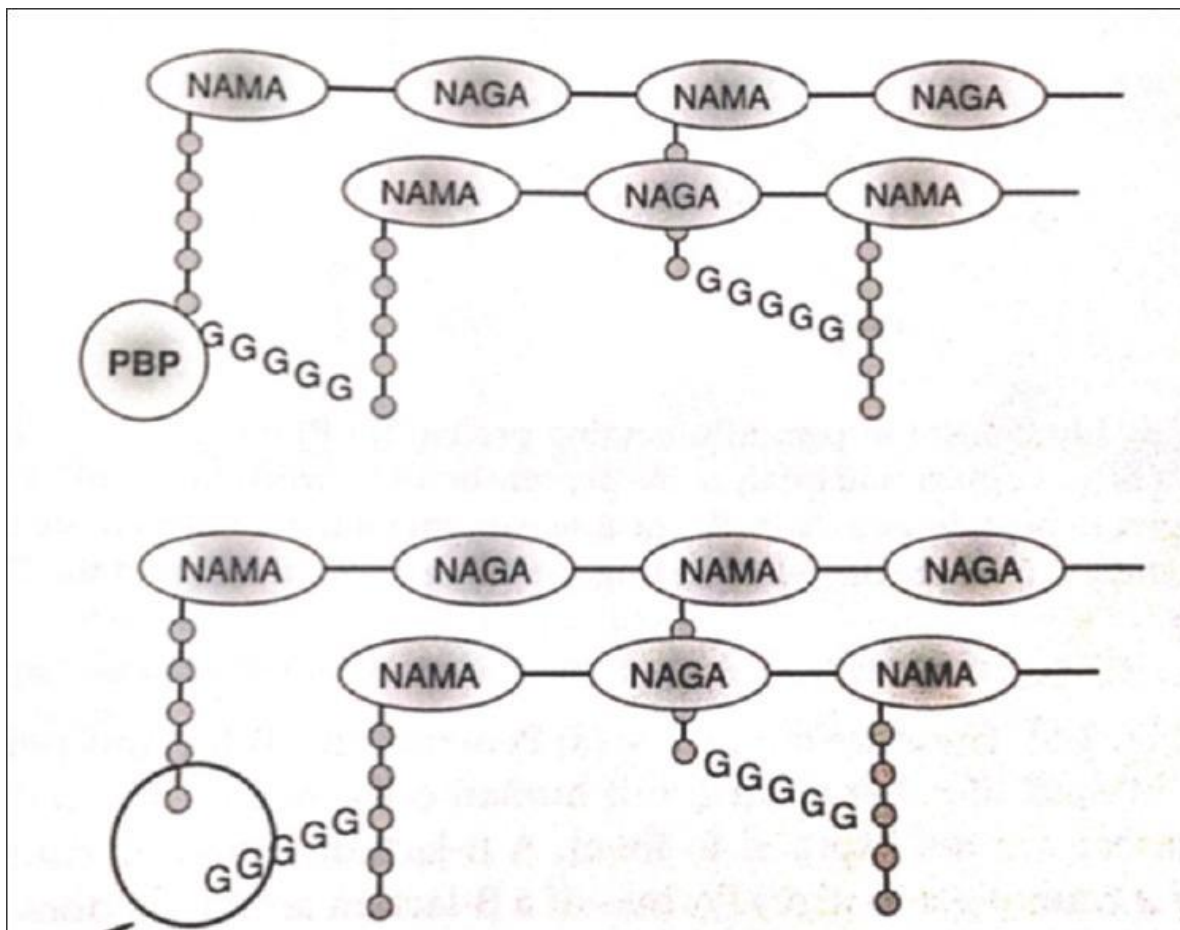


Figure 74 - Mechanism of action of beta-lactams antibiotics²⁰²

7.2.1 Protein biosynthesis inhibitors

Bacterial DNA synthesizes bacterial RNA molecules known as messenger RNA or mRNA, by transcription. This mRNA makes proteins through a process called translation. Cytoplasmic and ribosomal factors catalyze this protein biosynthesis. Bacterial 70S ribosomes comprise two ribonucleoprotein subunits known as the 30S and 50S subunits²⁰² Protein biosynthesis is inhibited

by antibacterial, which targets the 30S and 50S subunits of the bacterial genome as shown in Figure 75.

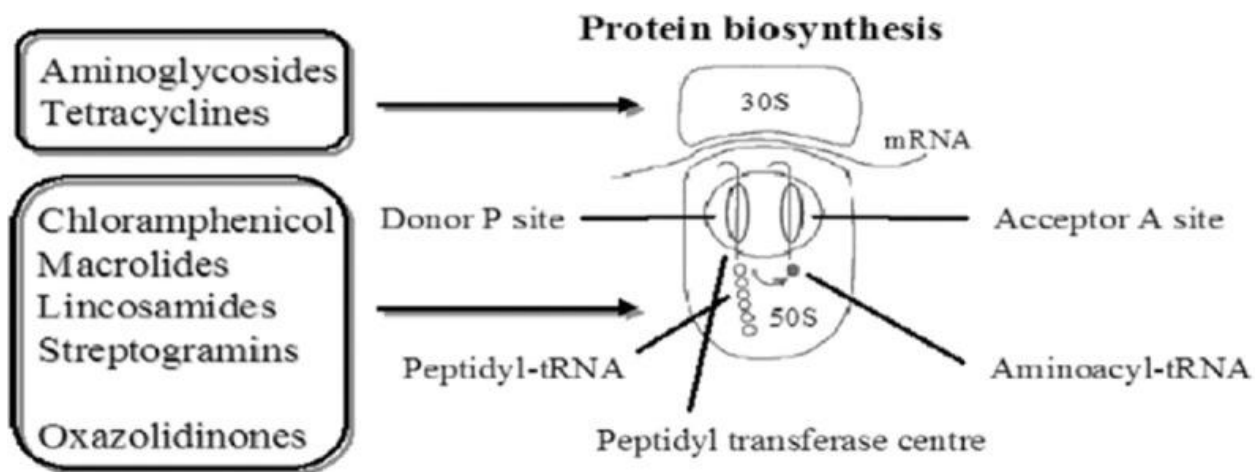


Figure 75 - Protein biosynthesis inhibition with different antibiotics²⁰²

Some inhibitors of 30S subunits are called aminoglycosides which are positively charged molecules that lead to the formation of large pores by attaching to the negatively charged outer membrane of bacteria. These large pores allow the antibiotics to penetrate inside a bacterial cell. However, energy and oxygen are required to pass through the bacterial cell wall, so that the aminoglycosides can work. Therefore, aminoglycosides work in aerobic conditions and have low activity in the absence of oxygen. Aminoglycosides also synergize with other antibiotics inhibiting cell walls, such as glycopeptides and beta-lactams, allowing greater penetration in a bacterial cell at low drug concentration. Aminoglycoside thus interacts with 16S ribosomal RNA of 30S subunit next to the acceptor side via hydrogen bonds and hence causing misreading and termination in translation²⁰⁰ Tetracyclines like doxycycline, minocycline, and tetracyclines kill bacteria by acting

on the conserved sequences of the 16S ribosomal RNA of the 30S subunit and preventing binding of t-RNA to the acceptor site of the bacteria^{202 203} Similarly, inhibitors of 50S subunits interact with the conserved sequences of peptidyl transferase cavity of 23S ribosomal RNA of 50S subunit. An example of such an antibiotic is chloramphenicol, which inhibits the translation process by preventing the binding of t-RNA to the acceptor side of the ribosome^{202 204} Other antibiotics like oxazolidinones or linezolid, a novel class of antibiotic and recently approved chemically synthetic drug. These drugs inhibit protein formation in bacteria by binding to 23S rRNA of the 50S subunit and also suppresses 70S inhibition^{205 206}

7.2.2 DNA replication inhibitors

Quinolones such as fluoroquinolones (FQ) inhibit the DNA gyrase of bacteria by creating a nick in the double-stranded DNA, introducing negative supercoils, and resealing the nick ends. The subunits of DNA gyrase are two A subunits that carry out nicking in the double-stranded DNA. The other is two subunits B which helps introduce negative supercoiling. Finally, subunit A reseals the nicked ends. The FQ has affinity towards Subunit A and binds to it with high an affinity and interferes with its strand cutting and resealing function^{202 203 207}

7.2.3 Inhibitors for folic acid metabolism

Such inhibitors like trimethoprim and sulfonamides inhibit different steps in folic acid synthesis. Sulfonamides inhibit dihydropteroate synthase and trimethoprim act at a later stage of folic acid synthesis by inhibiting dihydrofolate reductase enzyme²⁰²

7.3 Mutation in bacteria

Bacteria were considered too simple to reproduce sexually, undergo mutation or have genes, but now they have become an important tool in the field of biotechnology and genetics. They have been observed to have different colonies, but all these colonies result from mutation. Mutation leads to variation in genes and is very important in the field of biology. The mutation causes variation in genes which can be good or bad. These variations are critical for evolution²⁰⁸
^{209 210} Mutation is a term coined by Hugo de Vries, which means ‘to change’ and causes a heritable change in DNA²¹¹ The mutation process is called mutagenesis. The changes caused in DNA by mutation can drastically affect the product. There are different types of mutations classified based on alterations in the DNA and the mechanism of mutation may include a substitution of a nucleotide which is also known as point mutation involving a change in a single base in the DNA sequence. This mutation change is copied during replication to produce a permanent change. The other mechanism of mutation is a deletion or addition of a nucleotide during replication and occurs when a transposon inserts itself in a gene and leads to disruption of gene^{208 210 211 212 213} The following are the sources of mutation a) Tautomeric shift of bases b) depurination c) deamination d) oxidatively damaged bases e) ultraviolet radiation f) chemical mutagens. Finally, the result of mutation includes 2) missense mutation, which leads to changes in amino acid sequence b) nonsense mutation, where a mutation leads to the formation of a stop codon c) silent mutation, where a single substitution in DNA has result in new codon which codes for the same amino acid d) frameshift mutation where there is either addition or deletion of base pairs causing a shift in reading frames of the genes e) lethal mutation which can affect the vital function and makes the bacterial cell nonviable f) suppressor mutation and g) conditional lethal mutation which causes an

organism to survive under certain conditions only^{208 211} Resistance through chromosomal mutation is depicted in Figure 76.

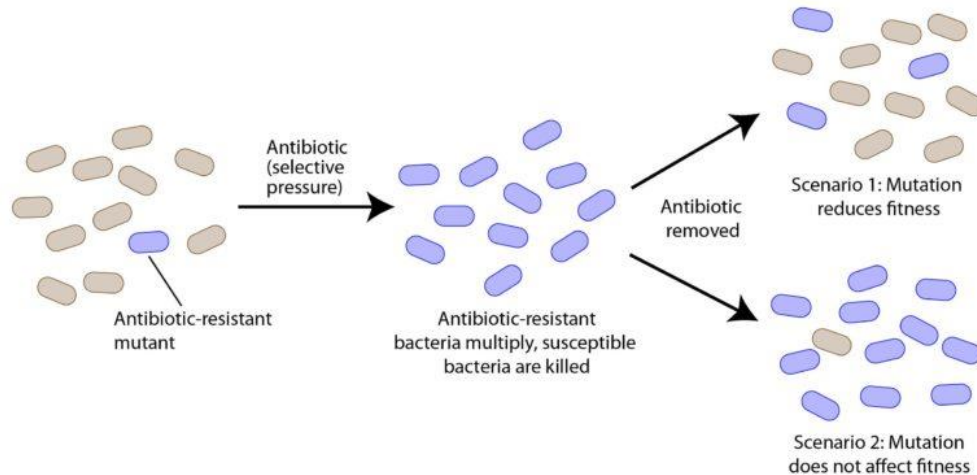


Figure 76 - Resistance in bacteria using antibiotics²¹²

7.4 Frequency of resistance in bacteria

Antibiotic resistance can be achieved in various ways like a mutation in different chromosomes, horizontal gene transfer, and by recombination of foreign DNA into the chromosome²⁵⁶ Frequency of resistance (FOR), also known as the mutation rate, is used when the estimation of the rate of mutation is considered per locus, per nucleotide or even for the whole genome whether it is selectively favorable or unfavorable. FOR is defined as in vitro frequency at which the mutants in a bacterial population arise in the presence of an antibacterial²⁵⁷ FOR is calculated by dividing the resistant colony growing on an antibiotic-containing plate by the total number of colony-forming unit in the initial inoculum and resistant colonies were the ones with MICs ≥ 4 times than the MIC of the wild type bacteria²⁵⁸ A bacterial strain is considered weak mutators when their frequency was $4 \times 10^{-8} \leq f < 4 \times 10^{-7}$, strong when their frequency was $f \geq$

4×10^{-7} , hypomutable when the frequency was $f \leq 8 \times 10^{-9}$ and normutable when the frequency was $8 \times 10^{-9} < f < 4 \times 10^{-8}$ ²⁵⁹ The workflow of FOR is shown in Figure 77.

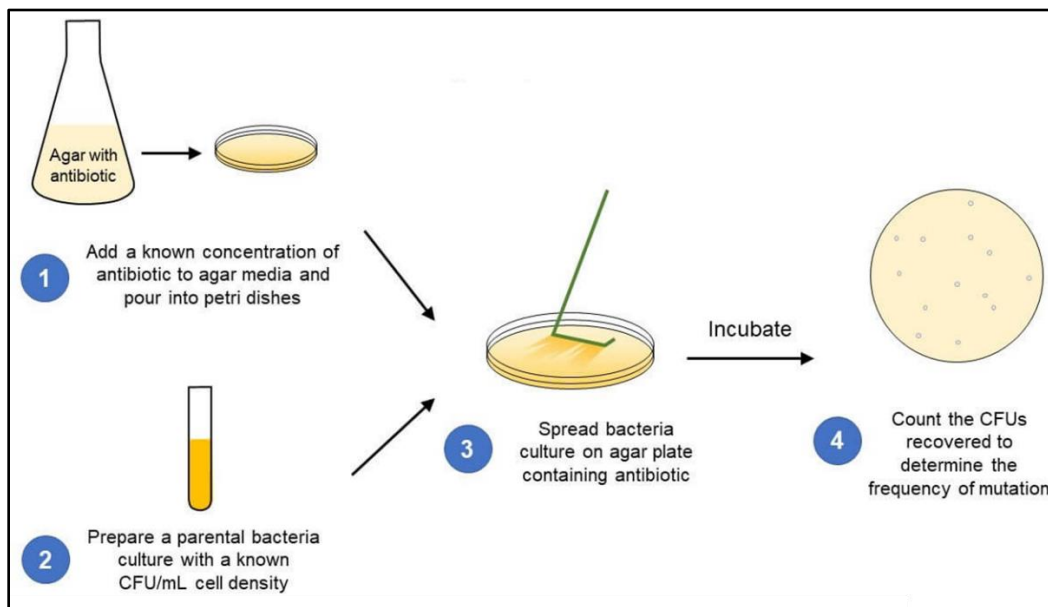


Figure 77 - Frequency of resistance experimental protocol¹¹⁴

7.5 Role of DNA in bacteria

Deoxyribonucleic acid (DNA) is a genetic material found in all living organisms including bacteria. DNA contains important information necessary for an organism's development, reproduction, and function of an organism²¹⁸ In bacterial cells, DNA regulates many physiological processes and synthesizes proteins and other cellular components. Bacterial DNA is a single circular molecule known as the bacterial chromosome and compacted into a nucleoid structure within the cell. DNA replication is crucial for cell division. It occurs via a semi-conservative mechanism where two original strands of DNA serve as a template for synthesizing of a new strand, also known as the complementary strand. After the replication, the two newly made DNA are distributed to the two different bacterial cells during cell division. Bacterial DNA is subjected

to various mutations like insertions, deletions, and base substitution which can lead to new genetic diversity and traits within a bacterial cell. Bacteria can exchange genetic material through horizontal gene transfer, such as conjugation, transduction, and transformation. Exchange in this DNA exchange plays a significant role in the spread of antibiotic resistance among the bacterial species^{219 220}

7.6 Whole genome sequencing in bacteria

Even after huge improvements were made to limit healthcare-associated infections, continuous outbreaks of multi-drug resistant (MDR) bacteria are present as a frequent threat to the patient population in hospitals around the world²¹³ Antibiotic resistance is a complex procedure. If left unchecked, even a minor surgery could become a high-risk procedure²¹⁴ However, there are strategies to combat antibiotic resistance threats, including developing novel antimicrobials. A recent technology known as whole genome sequencing (WGS) has emerged as a tool that can help scientists understand the mechanism of resistance in pathogens. WGS not only elucidates the mechanism of resistance, but also plays an important role in measuring the emergence rate of resistance²¹⁵ WGS is the process of determining the complete DNA sequence of an organism's genome, which can provide useful information like genetic makeup and evolutionary relationships. The techniques used in WGS includes, Next generation sequencing (NGS), which includes Illumina, Ion Torrent, and Pacific Biosciences have reduced the cost of sequencing and increased the speed. Illumina, a widely used platform, relies on sequencing by synthesis, which involves synthesizing DNA strands complementary to the template DNA and detecting the incorporated bases using a fluorescence signal. Some of the applications of WGS include strain typing and epidemiology, which enables high-resolution tracking of outbreaks and transmission events. For

instance, WGS has been used to monitor the spread of antibiotic resistance MRSA and multi-drug resistant *Mycobacterium tuberculosis*. Bacterial WGS also helps in identifying and annotate genes, regulatory elements, and other functional genomic elements, providing data about bacterial physiology and virulence mechanisms. It can also be applied to complex microbial communities to get insights about their function, dynamics and composition, which can help in understanding host-pathogen interaction and the role of pathogens in disease and health²¹⁶ For researchers, it is crucial that they can accurately interpret their results therefore they should have access to reliable genomic information of known provenance. WGS follows a few major steps, including a) DNA shearing, where molecular scissors are used to cut the DNA of many bases into many small pieces so the machine can read it. b) DNA barcoding includes attaching small pieces of DNA tags to the sheared DNA to identify the DNA of a particular organism. c) DNA sequencing includes bar-coded DNA from different organisms that are combined and placed in a DNA sequencer and this sequence identifies the bases that make up the bacterial genome. d) Data analysis includes comparing sequences from multiple organisms to identify their differences. This gives information about how closely related a pathogen is²¹⁷ The workflow for bacterial whole genome sequencing is shown in Figure 78.

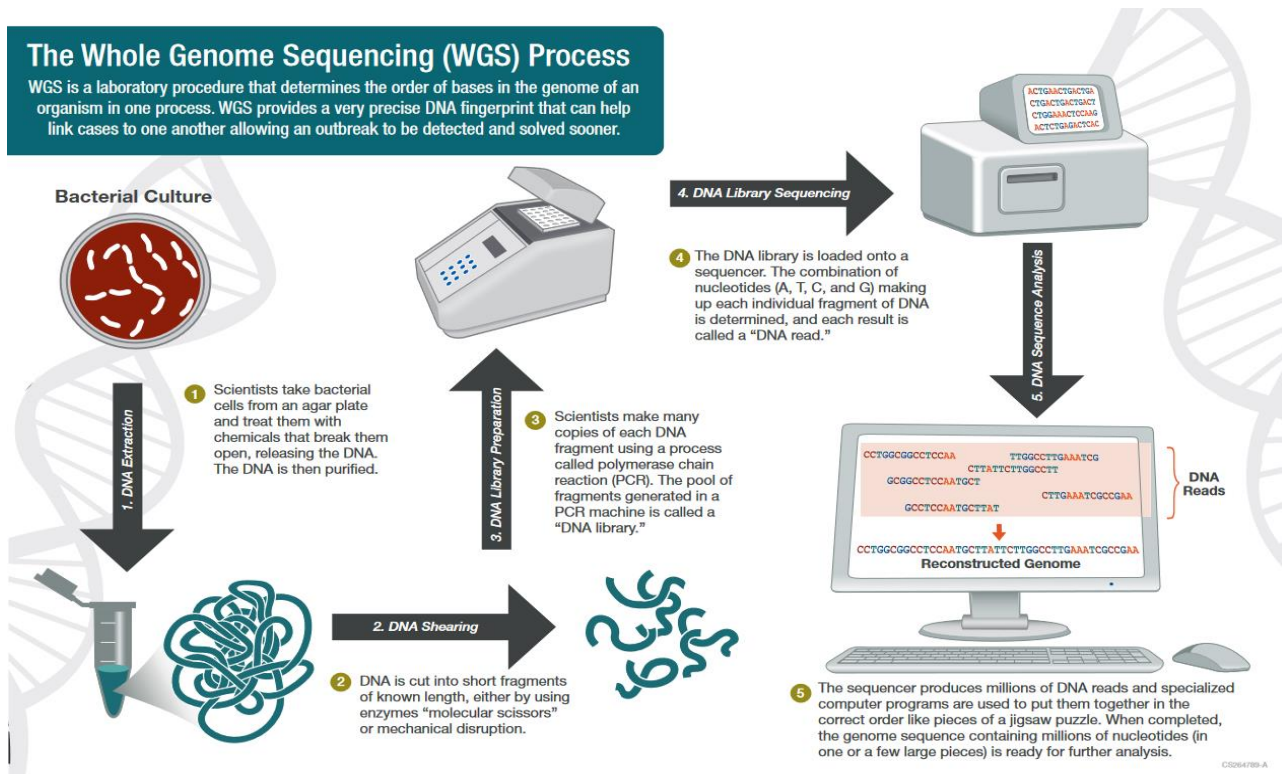


Figure 78 - Workflow for bacterial whole genome sequencing²¹⁷

7.7 RNA induction in bacteria

RNA induction in bacteria refers to synthesizing RNA molecules in bacterial cells in response to various environmental stimuli. The process is crucial for gene expression and regulation allowing bacteria to grow, adapt to changing environments and reproduce. Transcription is a process through which bacteria make the RNA, where DNA or genes are used to make new RNA molecules. There are mainly three types of RNA in bacteria. a) messenger RNA also known as the mRNA, carries genetic information from DNA to ribosomes, where it is further processed to proteins. RNA polymerase enzyme initiates the transcription process, which starts transcription by binding to the specific DNA sequence which is known as the promoter. b) The other type of

RNA is called ribosomal RNA or rRNA, which is a structural and functional component of ribosomes that helps in the protein synthesis. rRNA helps in maintaining the structure of ribosomes and helps in facilitating the correct position of mRNA and tRNA during protein synthesis. c) The third type of RNA is called the transfer RNA, also known as the tRNA, which carries amino acids to the ribosome during translation. The tRNA has a specific anticodon that pairs with a complementary codon on the mRNA. tRNA ensures that the correct amino acid is added to the growing polypeptide chain. RNA induction in bacteria can be regulated at different levels, including transcription, initiation, elongation, and termination. The regulation of RNA synthesis can involve small RNA molecules and regulatory proteins that either activate or repress gene expression depending on specific conditions^{218 221 222 223 224}

CHAPTER 8

8. TWO-DIMENSIONAL SCREEN OF ACTIVE VERSUS ACTIVE

8.1 Introduction and Rationale

The emergence of antibiotic resistance has become a significant public health concern. With this increasing multi-drug resistance in bacteria, there is an urgent need to develop new antibiotics to combat infections caused by them. One potential approach to overcome this resistance is to explore synergy between different antibiotics that can minimize resistance development and enhance efficacy. Synergy between antibiotics refers to the process where two or more antibiotics, when combined, show more significant antimicrobial effects than the sum of their effect²²⁵ This synergistic interaction can enhance antibiotic's therapeutic efficacy, limit antibiotic resistance emergence and reduce their effective doses. Synergism can have the following effect on bacteria a) inhibit the resistant pathway²²⁶ b) enhanced cellular uptake of one or both the drugs in a bacterial cell when they are in synergy²²⁷ c) interference with bacterial metabolic pathways²²⁸ d) some antibiotics can enhance their activity by targeting bacterial virulence factors which can weaken the pathogen and make it more susceptible to other antibiotics²²⁹ Synergy helps in the treatment of multidrug-resistant infections, minimizes side effect by reducing the doses and prevents the resistance development.

This study is an expansion of our completed screening approach of VRE *faecium* against NCI and FDA-approved drug libraries. It provides a rich set of interesting agents that act synergistically and antagonistically. This study also helped us to identify new antibacterial agents and agent combinations. We used a 2-dimensional screening approach where actives can synergize

with other actives. We added $1/4^{\text{th}}$ x MIC of each active compound across the row and then added the same MIC of drug in the column with the diagonal wells in the plate becoming $1/2$ x MIC of each active. Along with synergy, this study also provides information regarding the antagonism between two drug combinations, which is observed when there is bacterial growth in presence of the combinations.

8.2 Materials and Methods

8.2.1 General

The reagents and materials used in this study were as described previously^{143 171} The bacterial strain used for library screening was VanA-type vancomycin-resistant *Enterococcus faecium* (VREfm) clinical strain. FDA and NCI drug libraries were used for active versus active. The NCI drug stocks were obtained from National Cancer Institute and FDA drug stocks were from Millipore Sigma and Alfa Aesar. VRE growth medium consisted of brain heart infusion broth (37.5 g/L), hemin (10 mg/L), and NAD⁺ (10 mg/L).

8.2.2 Determination of minimum inhibitory concentration of all actives from FDA and NCI screen against VRE *faecium* in 384 well plates

Library screening data from both FDA vs VRE *faecium* and NCI vs VRE *faecium* were processed and analyzed using homemade Matlab® scripts (The Mathworks, Natick, MA). Based on the values for known active and inactive antibacterial agent controls, a cut-off value between active and inactive compounds was selected and list of active wells in each screening set (UM-Vm, UM+Vm, PM-Vm, PM+Vm) from both libraries was generated. This list was merged to give a pooled hit list. MICs for all hits from FDA and NCI screen were determined by hit picking 2 μ L samples from both UM and PM working plates (two sets from each) into the first columns of 384

well plates (four sets total, for UM-Vm, UM+Vm, PM-Vm and PM+Vm MIC determinations). These samples were then serially diluted in steps of two across the plates in DMSO using an Integra Viaflo Assist automated multichannel pipettor (Hudson, NH). The last column was left blank (DMSO only). These additions were performed in a Labconco (Kansas City, MO) BSL-2 biosafety cabinet. These plates were frozen at -80 °C and dried under strong vacuum as described above. To each well in each set was added 20 µL VRE growth medium containing 4000 cfu VREfm (This provided MIC plates with 50 µM as the highest test agent concentration.) Plates were incubated for 48 h at 35 °C. Fresh VRE growth medium (10 µL) was added to the wells of plates, followed by incubation for 2 h at 35 °C to restart active cell growth. To the wells of these plates was then added 10 µL of 100 µg mL⁻¹ resazurin^{145 146 147} The plates were incubated for another 2 h at 35 °C, and the A610 - A450 absorbance difference measured in a Molecular Devices SpectraMax M5 multimode microplate reader (San Jose, CA). All MICs were determined at least in triplicate.

8.2.3 Determination of MICS of all actives from FDA and NCI screen against VRE *faecium* in 96 well plates

MICs for all hits from FDA and NCI library screens were determined by adding hits/actives into the first column of 96 well plates. These samples were then serially diluted in steps of two across the plates with DMSO manually using a multichannel pipettor. The last column was left blank (DMSO only). These additions were performed in a Labconco (Kansas City, MO) BSL-2 biosafety cabinet. The plates were frozen at -80 °C and dried under strong vacuum as described above. To each well in each set was added 100 µL VRE growth medium containing 4000 cfu VRE *faecium*. Plates were incubated for 48 h at 35 °C. Fresh VRE growth medium (50 µL) was added to the wells of plates, followed by an incubation of 2 h at 35 °C to restart active cell growth. To

the wells of these plates was then added 50 μ L of 100 μ g mL⁻¹ resazurin^{145 146 147} The plates were incubated for another 2 h at 35 °C, and the A610 - A450 absorbance difference measured in a Molecular Devices SpectraMax M5 multimode microplate reader. All MICs were determined at least in duplicates.

8.2.4 Active vs Active experiment in a 384 well plate

For active vs active experiment in 384 well plate, the bacterial MIC samples from the active (no growth) wells of 96 well plates were used to add in 384 well plate to maintain homogeneity. Therefore, 6 μ L sample (containing no bacterial growth and blue resazurin dye) was added across the row and 6 μ L of the same sample was added in the column of a 384 well plate. Following this, all the actives were added in 384 well plate in each row and column. All the possible combinations between the drugs (actives) were taken into consideration. 8 μ L of fresh BHI media was then added to the wells of 384 well plate. This dilution provided 1/4th x MIC of drugs in each well, with 1/2 x MIC of drugs in the diagonal wells of a 384 well plate. 4x MIC of each active antibiotic was added to the last column of the plate, which served as a control. After the addition of drugs in a 2-dimensional pattern, 20 μ L of VRE growth medium containing 4000 cfu VRE *faecium* was added to each well using integra automated multichannel pipettor. Plates were then incubated for 48 h at 35 °C. Fresh VRE growth medium (10 μ L) was added to the wells of plates, followed by incubation for 2 h at 35 °C to restart active cell growth. To the wells of these plates was then added 10 μ L of 100 μ g mL⁻¹ resazurin^{145 146 147} The plates were incubated for another 2 h at 35 °C, and the A610 - A450 absorbance difference measured in a Molecular Devices SpectraMax M5 multimode microplate reader. This combination was used for FDA vs FDA hits, NCI vs NCI hits and FDA vs NCI hits.

8.3 Results and Discussion

8.3.1 2-dimensional approach of active vs actives for synergy

The synergy workflow consists of adding active samples across the plate and then adding the same drug down each column. This approach was applied to FDA active vs FDA active, NCI active vs NCI active and FDA active vs NCI active.

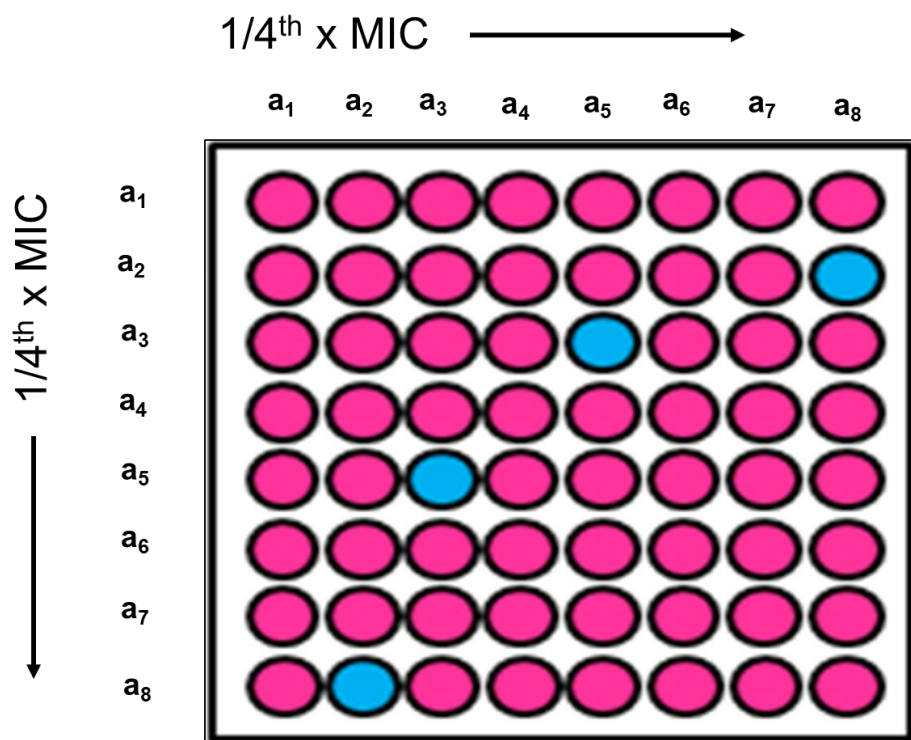


Figure 79 - Workflow for active vs active 2-dimensional screen. The diagonal line gives 1/2x MICs of drugs. The blue wells represent no bacterial growth wells, and the pink well represents bacterial growth. (a = drug)

8.3.2 MICs of all actives in 384 well plate for FDA compounds

Thirteen active hits were obtained after FDA-VRE *faecium* screen. Table 21 shows the FDA-hits and their MICs used for active vs active experiment. Figure 80 shows the FDA active MICs in a 384 well plate.

Table 21- All FDA active hits with MICs in μM

Actives	MICs (μM)
Rifampin	0.1
Rifabutin	0.2
Retapamulin	0.2
Rifapentine	0.2
Rifaximin	0.39
Valnemulin	0.39
Gemcitabine	0.78
Closantel	1.6
Linezolid	3.1
Mupirocin	3.1
Novobiocin	3.1
Fidaxomicin	12.5
Florfenicol	25

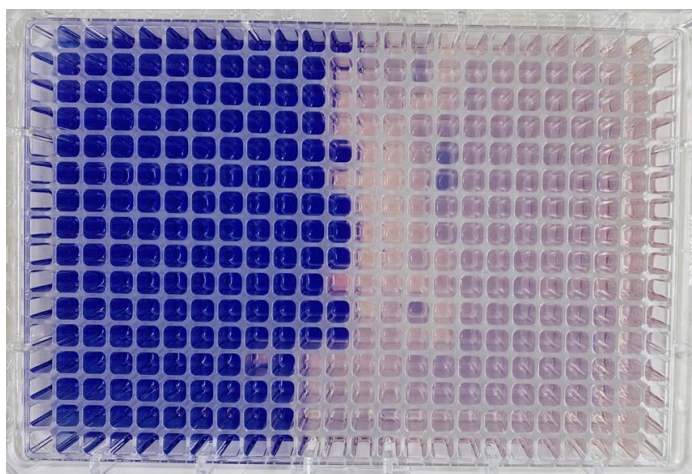


Figure 80 - 384 well plate with FDA actives and MICs

8.3.3 MICs of all the actives in 384 well plate for NCI compounds

Eight actives were obtained as hits after NCI vs VRE *faecium* screen. Table 22 shows the hits with MICs. Figure 81 shows the representation of MICs of all NCI actives in a 384 well plate.

Table 22 - All NCI hits with MICs in μM	
Compounds	MICs (μM)
Hitachimycin	0.78
4-QDA	1.6
Bactobolin	3.1
Clorobiocin	3.1
5'-O-Sulfamoyladenosine	6.3
Ethyl Violet	6.3
Celastrol	6.3
Streptovaricin C	6.3

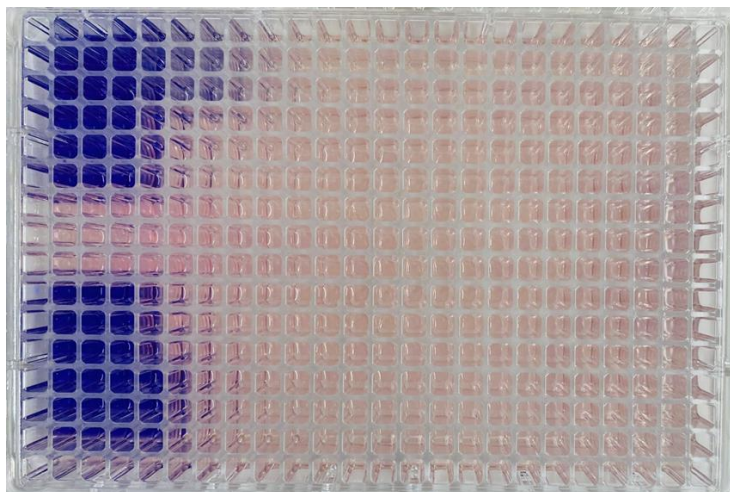


Figure 81 - 384 well plate with NCI actives and MICs

8.3.4 MICs of actives from FDA and NCI screen in 96 well plate

After the addition of 20 μ L drug in the first column of 96 well plate the MICs for all actives were determined. Figures 82 and 83 shows FDA and NCI actives MIC in 96 well plates.

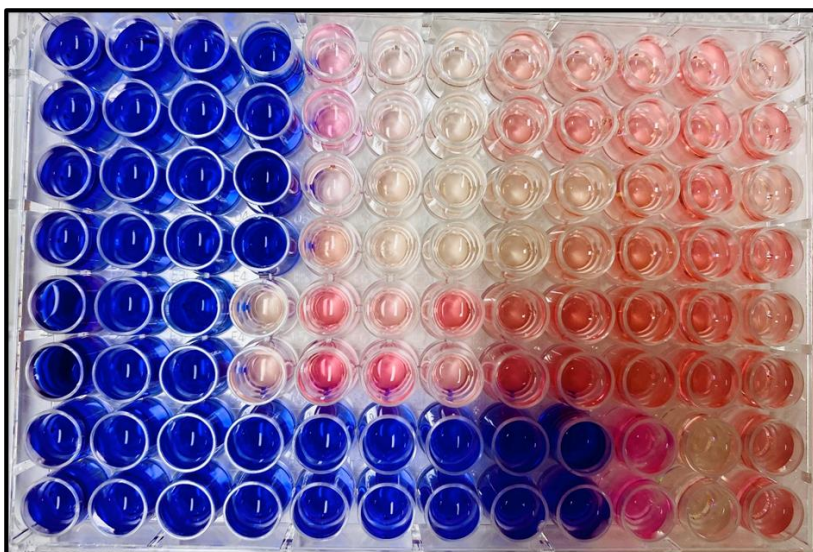


Figure 82 - MICs of FDA actives in duplicates.

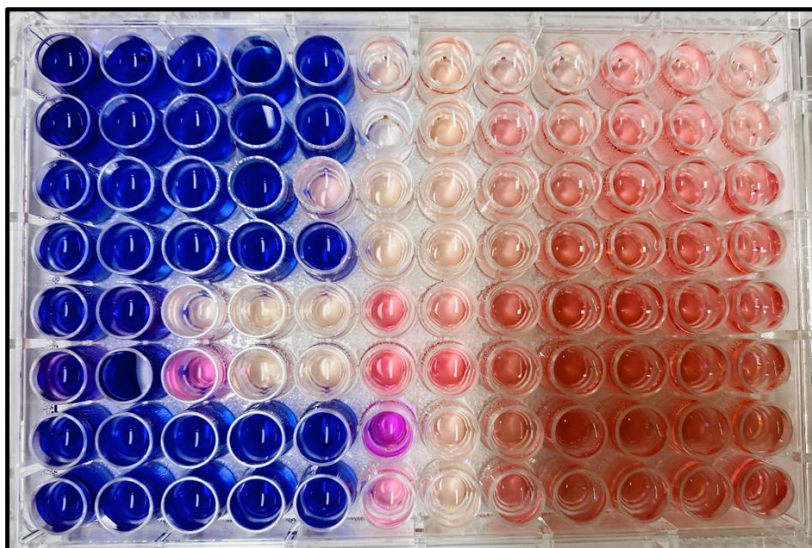
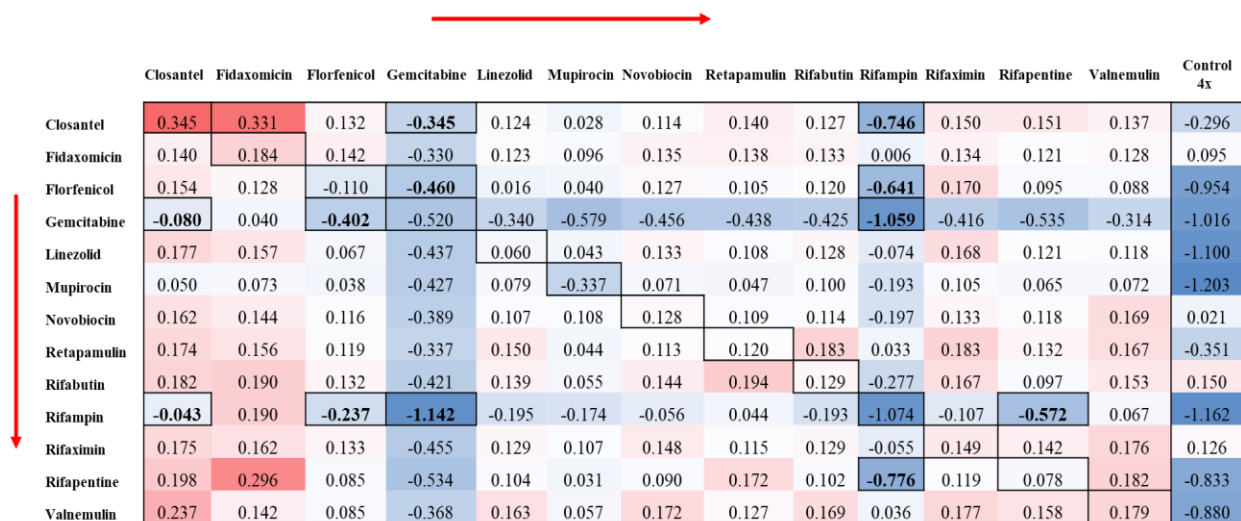


Figure 83 - MICs of NCI actives in duplicates.

8.3.5 FDA active vs FDA active synergistic combinations

After the addition of FDA active drugs in a 2-dimensional pattern in a 384 well plate, some synergistic combinations were observed. Table 23 shows all the FDA synergistic drug combinations. It was observed that gemcitabine which is a synthetic pyrimidine nucleoside prodrug and inhibits DNA synthesis in bacteria shows high synergy with other drugs²³⁰ Rifampin which is an RNA biosynthesis inhibitor and inhibits DNA dependent RNA polymerase shows synergy with drugs like closantel, florfenicol, gemcitabine and rifapentine²³¹ Florfenicol is a protein biosynthesis inhibitor, acts synergistically with both gemcitabine and rifampin²³² Closantel is a veterinary drug used only in animals like cattle sheep and goats also showed synergy with both gemcitabine and rifampin²³³ Figure 84 shows pattern of 2 dimensional FDA active vs FDA active in a 384 well plate.



	Closantel	Fidaxomicin	Florfenicol	Gemcitabine	Linezolid	Mupirocin	Novobiocin	Retapamulin	Rifabutin	Rifampin	Rifaximin	Rifapentine	Valnemulin	Control 4x
Closantel	0.345	0.331	0.132	-0.345	0.124	0.028	0.114	0.140	0.127	-0.746	0.150	0.151	0.137	-0.296
Fidaxomicin	0.140	0.184	0.142	-0.330	0.123	0.096	0.135	0.138	0.133	0.006	0.134	0.121	0.128	0.095
Florfenicol	0.154	0.128	-0.110	-0.460	0.016	0.040	0.127	0.105	0.120	-0.641	0.170	0.095	0.088	-0.954
Gemcitabine	-0.080	0.040	-0.402	-0.520	-0.340	-0.579	-0.456	-0.438	-0.425	-1.059	-0.416	-0.535	-0.314	-1.016
Linezolid	0.177	0.157	0.067	-0.437	0.060	0.043	0.133	0.108	0.128	-0.074	0.168	0.121	0.118	-1.100
Mupirocin	0.050	0.073	0.038	-0.427	0.079	-0.337	0.071	0.047	0.100	-0.193	0.105	0.065	0.072	-1.203
Novobiocin	0.162	0.144	0.116	-0.389	0.107	0.108	0.128	0.109	0.114	-0.197	0.133	0.118	0.169	0.021
Retapamulin	0.174	0.156	0.119	-0.337	0.150	0.044	0.113	0.120	0.183	0.033	0.183	0.132	0.167	-0.351
Rifabutin	0.182	0.190	0.132	-0.421	0.139	0.055	0.144	0.194	0.129	-0.277	0.167	0.097	0.153	0.150
Rifampin	-0.043	0.190	-0.237	-1.142	-0.195	-0.174	-0.056	0.044	-0.193	-1.074	-0.107	-0.572	0.067	-1.162
Rifaximin	0.175	0.162	0.133	-0.455	0.129	0.107	0.148	0.115	0.129	-0.055	0.149	0.142	0.176	0.126
Rifapentine	0.198	0.296	0.085	-0.534	0.104	0.031	0.090	0.172	0.102	-0.776	0.119	0.078	0.182	-0.833
Valnemulin	0.237	0.142	0.085	-0.368	0.163	0.057	0.172	0.127	0.169	0.036	0.177	0.158	0.179	-0.880

Figure 84 - FDA active vs FDA active in a 384 well plate.

Table 23 - FDA active vs FDA active synergistic combinations

Gemcitabine + Closantel
Gemcitabine + Florfenicol
Rifampin + Closantel
Rifampin + Florfenicol
Rifampin + Gemcitabine
Rifampin + Rifapentine

8.3.6 NCI active vs NCI active synergistic combinations

After the addition of NCI active drugs in a 2-dimensional pattern in a 384 well plate, few synergistic combinations were observed. Table 24 shows NCI synergistic drug combinations. Three synergistic combinations were observed. 5' sulfamoyladenine which is a protein biosynthesis inhibitor shows synergy with hitachimycin, streptovaricin C and celastrol²³⁴ Figure 85 shows a pattern of NCI active vs NCI active in a 384 well plate.

	Ethyl violet	5 sulfamoyladosine	4-quinazolinodiamine	Bactobolin	Hitachimycin	Clorobiocin	Streptovaricin	Celastrol	Control (4x)
Ethyl violet	0.386	-0.668	0.313	0.215	0.348	0.155	0.154	0.226	0.129
5 sulfamoyladosine	0.159	-0.997	-0.551	0.139	-0.684	-0.071	-0.770	-0.634	-1.134
4-quinazolinodiamine	0.196	-0.503	0.151	0.225	0.271	0.245	0.163	0.171	-1.014
Bactobolin	0.291	-0.510	0.175	0.368	0.223	0.139	0.248	0.219	-0.227
Hitachimycin	0.250	-0.360	0.202	0.161	0.231	0.142	0.124	0.338	0.164
Clorobiocin	0.212	-0.483	0.173	0.211	0.149	0.151	0.205	0.222	-0.876
Streptovaricin	0.162	-0.862	0.185	0.171	0.182	0.207	0.138	0.190	-1.084
Celastrol	0.281	-0.555	0.180	0.174	0.231	0.228	0.142	0.152	0.210

Figure 85 - NCI active vs NCI actives in a 384 well plate.

Table 24 - NCI active vs NCI active synergistic combinations

5' sulfamoyladosine + Hitachimycin
5' sulfamoyladosine + Streptovaricin C
5' sulfamoyladosine + Celastrol

8.3.7 FDA active vs NCI active synergistic combinations

Actives from FDA library were added across each row in a 384 well plate and the NCI actives were added down the columns of the plate with 4x MIC of drugs as a control in the last column. Four synergistic combinations were observed. Table 25 shows the FDA vs NCI synergistic combination. Gemcitabine shows synergy with both ethyl violet and streptovaricin C. Ethyl violet is a homolog of crystal (methyl) violet which is a well-known antibacterial agent of unknown mechanism¹⁷⁴ Hitachimycin (stubomycin) is a generally cytotoxic agent with gram-positive antibacterial activity isolated from *Streptomyces* cultures^{175 176} Streptovaricin C is a known

antibiotic which inhibits mRNA polymerase¹⁷⁷ Figure 86 shows pattern of FDA active vs NCI active in a 384 well plate.

	Ethyl violet	5' sulfamoyladosine	4-quinazolinediamine	Bactobolin	Hitachimycin	Clorobiocin	Streptovaricin	Celastrol
Closantel	0.320	-0.401	0.221	0.206	0.235	0.242	0.240	0.227
Fidaxomicin	0.281	0.068	0.204	0.185	0.229	0.251	0.302	0.242
Florfenicol	0.210	-0.807	0.165	0.107	0.188	0.073	0.136	0.218
Gemcitabine	-0.312	-1.080	-0.424	-0.372	-0.376	-0.410	-1.136	-0.376
Linezolid	0.252	-0.801	0.157	0.145	0.231	0.199	0.134	0.166
Mupirocin	0.188	-0.747	0.107	0.126	0.120	0.070	0.042	0.127
Novobiocin	0.303	-0.887	0.167	0.099	0.220	0.212	0.241	0.207
Retapamulin	0.210	-0.568	0.162	0.186	0.153	0.174	0.110	0.157
Rifabutin	0.328	-0.837	0.232	0.200	0.203	0.292	0.127	0.175
Rifampin	-0.990	-1.140	-0.817	-1.131	-1.051	-1.130	-1.085	-0.314
Rifaximin	0.210	-1.243	0.198	0.219	0.216	0.240	0.108	0.185
Rifapentine	0.157	-0.692	0.330	0.158	0.149	0.176	0.363	0.141
Valnemulin	0.190	-0.731	0.226	0.248	0.190	0.160	0.220	0.216

Figure 86 - FDA (column) actives vs NCI (row) actives in a 384 well plate.

Table 25 - FDA active vs NCI active synergistic combinations

Gemcitabine + Ethyl violet

Gemcitabine + Streptovaricin C

Closantel + 5' sulfamoyladosine

Rifampin + Ethyl violet

8.4 Conclusion

This approach is a logical extension of our library screening process, and it accelerates our ability to identify both synergistic and antagonistic drug combinations. The development of

effective combinations helps to minimize the emergence of resistance and develop new combinations of drugs with low doses and minimum side effects.

CHAPTER 9

9. MECHANISM OF ACTION OF DIFFERENT ANTIBIOTICS ON VANA-TYPE VANCOMYCIN-RESISTANT *ENTEROCOCCUS FAECIUM*

9.1 Introduction and Rationale

The term antibiotic was coined from the term antibiosis which means ‘against life’. Antibiotics were considered as organic compounds that were produced by one microorganism and used to kill the other microorganism²³⁵ There are two kind of antibiotics one is called bactericidal and are capable of killing bacteria whereas the other antibiotic is called bacteriostatic and are capable to inhibit the growth of bacteria²³⁷ Antibiotics are commonly called as antibacterials and can be differentiated into antifungals, antibacterials and antivirals depending on the microorganism they are targeting^{235 238} It is very crucial to understand the mechanism of action of each drug before introducing them to the health care delivery system and recent molecular biological techniques have played an important role in understanding such mechanisms²³⁶ The classification of antibiotics can be based on their molecular structure, spectrum of activity and mode of action²³⁹ The other type of classification is based on chemical and molecular structures that includes tetracyclines, aminoglycosides, quinolones, beta-lactams, sulphonamides, macrolides, glycopeptides and oxazolidinones^{240 241 242} The primary mechanism of action of antibiotics are a) inhibition of cell wall biosynthesis b) inhibition of protein biosynthesis c) alterations of cell membrane d) inhibition of nucleic acid synthesis e) antimetabolite activity^{243 244 245} A number of studies have explored the effect of cell wall targeting antibacterials on vancomycin-resistant *Enterococci* but the enzyme or transcriptional level remains unexplored. In the previous results, we have seen how the antibacterial effect on VRE *faecium* is based on metabolite level via LC-MS/MS. In this study, the changes in transcriptomic levels of resistant gene involved in the

resistance pathway of VRE is observed in presence of different cell wall targeting antibiotics.

Figure 87 shows the resistance genes involved in the resistance pathway of VRE *faecium*.

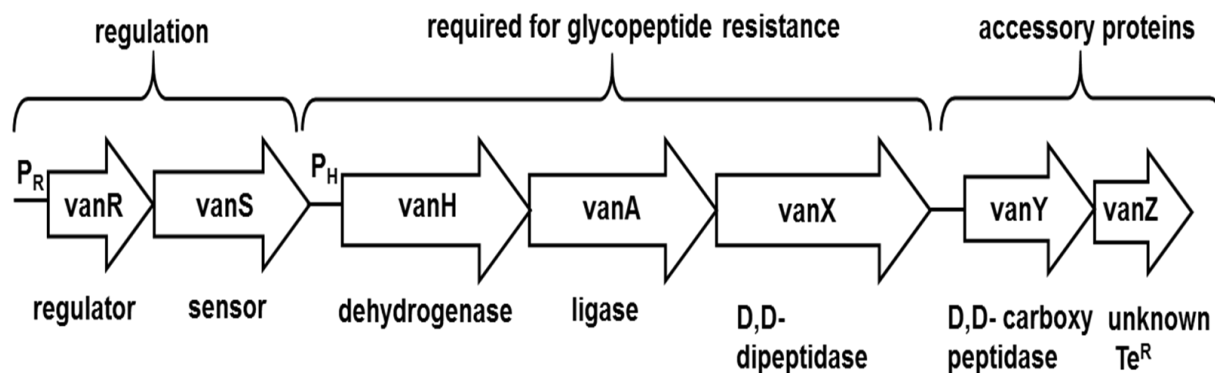


Figure 87 – Resistant genes involved in the resistance pathway of VRE *faecium*

9.2 Materials and Methods

9.2.1 General

All the antibiotics used in this study were obtained from Alfa Aesar and Millipore Sigma. The strains of VRE *faecium* used were VanA type clinical Vancomycin-resistant *Enterococcus faecium* and ATCC 0787. Other materials and reagents were described previously^{20 57 61} VRE growth media – consisting of brain heart infusion (BHI) (37.5 g/L), hemin (10 µg/mL), and NAD (10 µg/mL), was prepared following standard procedures. The forward and reverse primers for the *vanH*, *vanA*, *vanX*, *vanY*, and *vanZ* genes were from Integrated DNA Technologies (IDT) as mentioned in Chapter 4. Two pair of forward and reverse primers for *vanR* and *vanS* genes were made and included in this study as shown in Table 26.

Table 26 - Primers used for RT-qPCR of VanA mRNA transcripts.

Gene	Primer	Sequence (5' – 3')
VanS	F	CTGGAAAAGCGAGAGCAGGA
	R	CATGTCTGGAGCCTCGTCAA
VanR	F	ATGTTATCGTCCACTCCGGC
	R	ATGTTATCGTCCACTCCGGC

F – Forward primer, R – Reverse primer.

9.2.2 Minimal inhibitory Concentrations of various drugs against VanA-type clinical *faecium* strain and ATCC 0787

MICs for antibiotics were determined by adding 2 µl stock (1024 µM/mL) of antibiotics into the first column of 384 well plates. These samples were then serially diluted in steps of two across the plates with DMSO using an Integra Viaflo Assist automated multichannel pipettor. The last column was left blank (DMSO only). These additions were performed in a Labconco (Kansas City, MO) BSL-2 biosafety cabinet. The plates were frozen at -80 °C and dried under strong vacuum as described above. To each well in each set was added 20 µL VRE growth medium containing 4000 cfu VREfm (This provided MIC plates with 512 µM as the highest test agent concentration.) Plates were incubated for 48 h at 35 °C. Fresh VRE growth medium (10 µL) was added to the wells of plates, followed by incubation for 2 h at 35 °C to restart active cell growth. To the wells of these plates was then added 10 µL of 100 µg mL⁻¹ resazurin^{145 146 147} The plates were incubated for another 2 h at 35 °C, and the A610 - A450 absorbance difference measured in a Molecular Devices SpectraMax M5 multimode microplate reader (San Jose, CA). All MICs were determined at least in triplicate.

9.2.3 Effect of different antibiotics on VRE *faecium* mRNA level changes at 1/4th x MIC

A 20 ml saturated overnight VREfm culture was grown in VRE media and was used to inoculate 1000 mL of VRE media to an OD₆₀₀ of 0.05. When the secondary culture reached an OD₆₀₀ 0.5, 50 mL aliquots were transferred to 250 mL baffled flasks and 1/4th x MIC concentrations of each antibiotic were added to the respective flasks. A no vancomycin control flask was also included. The cultures were grown for 15 minutes of shaking at 35°C, and samples of 10 mL were collected in a pre-chilled 250 mL glass flasks and were kept on the ice. mRNA was extracted from these samples using the TRIzol max bacterial RNA isolation kit following the manufacturer's protocol (ThermoFischer Scientific). The quality and concentration of mRNA were determined using a Nanodrop instrument (ThermoFischer Scientific). RNA (100 ng) was then used as the template in quantitative RT-PCR (RT-qPCR) with primer pairs (described in chapter 4) designed to amplify internal regions of vanR, vanS, vanH, vanA, vanX, vanY and vanZ⁷¹. An internal control of 16S primer pair was also used. RT-qPCR was performed with the comparative Ct method. Measurements were performed on a Bio-Rad CFX Connect Real Time system. RT-qPCR reactions cycles were: 10 seconds at 50 °C, 5 minutes at 95 °C, 30 seconds at 94 °C, 30 seconds at 53.2 °C, 30 seconds at 72 °C (for 45 cycles), and 30 seconds at 25 °C. The gene expression was internally normalized to 16S ribosomal gene. After obtaining initial results, mRNA levels were adjusted to give threshold cycle (Ct) values of 18-29. Ct values were used to calculate the fold change (FC) of van gene expression between control and vancomycin treated cultures using the following formula:

$$FC = 2^{-(\Delta\Delta C_T)} \quad \dots \text{(Equation 1)}$$

where,

$$\Delta\Delta C_T = [C_{T(Sample)} - C_{T(16S_Sample)}] - [C_{T(Control)} - C_{T(16S_Control)}] \quad \dots \text{(Equation 2)}$$

The relative fold changes in VanA gene mRNA levels between control and different antibiotic treated samples were determined, and the independent experiment mean, and standard errors reported.

9.2.4 Effect of different antibiotics on VRE *faecium* mRNA level changes at 4 x MIC

A 20 ml saturated overnight VRE *faecium* culture was grown in VRE media and was used to inoculate 1000 mL of VRE media to an OD₆₀₀ of 0.05. When the secondary culture reached an OD₆₀₀ 0.5, 50 mL aliquots were transferred to 250 mL baffled flasks and 4 x MIC concentrations of each antibiotic were added to the respective flasks. A no vancomycin control flask was also included. The cultures were grown for 15 minutes with shaking at 35 °C, and samples of 10 mL were collected in previously chilled 250 mL glass flasks and kept on ice. mRNA was extracted as described previously.

9.3 Results and Discussion

9.3.1 Determination of minimum inhibitory concentration using two different VanA-type strains of VRE i.e.; VRE clinical *faecium* strain and ATCC 0787

MICs were determined for total of nineteen antibiotics. Antibiotics with low MIC values except for moenomycin and vancomycin were selected for the experiments. The new vanA-type strain, VRE ATCC 0787 had high MIC values for various antibiotics as compared to the clinical strain therefore was not used for the study. VRE clinical *faecium* strain provided low MIC values and was used for the study. VRE *faecium* clinical strain provided low MIC against amoxicillin,

bacitracin, chloramphenicol, doxycycline, oritavancin, ramoplanin, teichoplanin except for moenomycin (which is a known cell wall targeting agent) and vancomycin with MIC of 512 and 256 μ M respectively. Table 27 shows MICs for the two VRE *faecium* strains.

Table 27 - Antibiotics and MICs against different VRE strains

Drugs	MIC (μ M)	
	Clinical <i>faecium</i>	ATCC 0787
Amoxicillin	64	512
Ampicillin	512	512
Bacitracin	64	512
Ceftobiprole	256	512
Cefoxitin	512	512
Chloramphenicol	2	25
Ciprofloxacin	512	512
Cycloserine	512	512
Daptomycin	512	512
D-Boro Alanine	512	512
Doxycycline	4	12.5
Fosfomycin	512	512
Moenomycin	512	512
Oritavancin	0.25	12.5
Oxacillin	512	512
Ramoplanin	0.50	1.60
Teicoplanin	8	6.25
Tunicamycin	128	512
Vancomycin	256	512

9.3.2 Effect of antibiotics on mRNA level at 1/4th x MIC

At 1/4th x MIC all genes van (R, S, A, H, X, Y, Z) shows induction effect in presence of teicoplanin and vancomycin. As VanA-type clinical VRE *faecium* is resistant to both vancomycin and teicoplanin, gene induction was observed at low concentrations of both the drugs. This induction of genes shows the presence of resistance pathway in VRE *faecium*. However, no other antibiotic induced resistance genes at 1/4th x MIC.

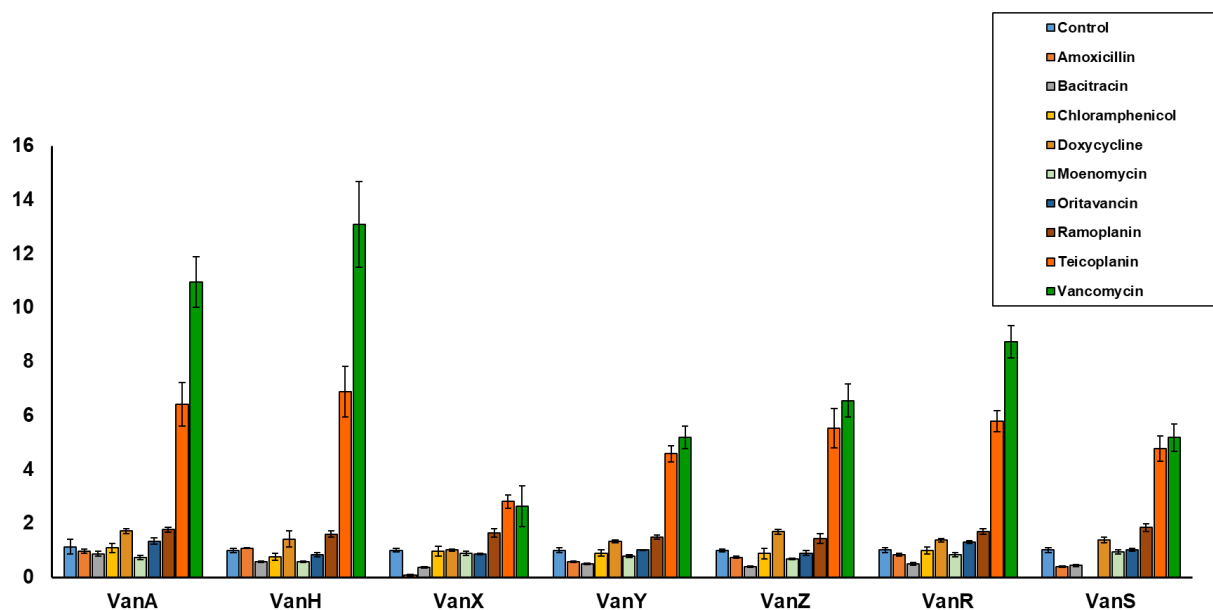


Figure 88 - Fold changes in gene levels showing teicoplanin and vancomycin resistance at 1/4th x MIC.

9.3.3 Effect of antibiotics on mRNA level at 4 x MIC

At 4x MIC all the resistance van (R, S, A, H, X, Y, Z) genes shows an induction effect with doxycycline, oritavancin, teicoplanin and vancomycin. Amoxicillin and bacitracin also showed induction in some of the genes. As VanA-type clinical VRE *faecium* is resistant to both vancomycin and teicoplanin, gene induction was observed at low concentrations of both the drugs.

Doxycycline which is a water-soluble tetracycline is known to kill a wide variety of gram- positive and gram-negative bacteria. Due to its high lipophilicity, doxycycline can easily cross multiple membranes to target bacterial cells. It acts by binding to 30S ribosomal unit during protein biosynthesis^{246 247} Oritavancin is one of the new semisynthetic lipoglycopeptide which is used for the treatment of acute gram-positive skin infections. It is structurally related to vancomycin and inhibits bacterial growth by binding to D-alanine-D-alanine terminus of the peptidoglycan precursor that is linked to the C₅₅-lipid transporter or also known as lipid II^{248 249 250} However, bacitracin is observed to induce vanX gene. Bacitracin is a cyclic peptide that inhibits the bacterial cell wall by preventing the final dephosphorylation step in the phospholipid carrier cycle and interferes with the growing cell wall²⁵¹

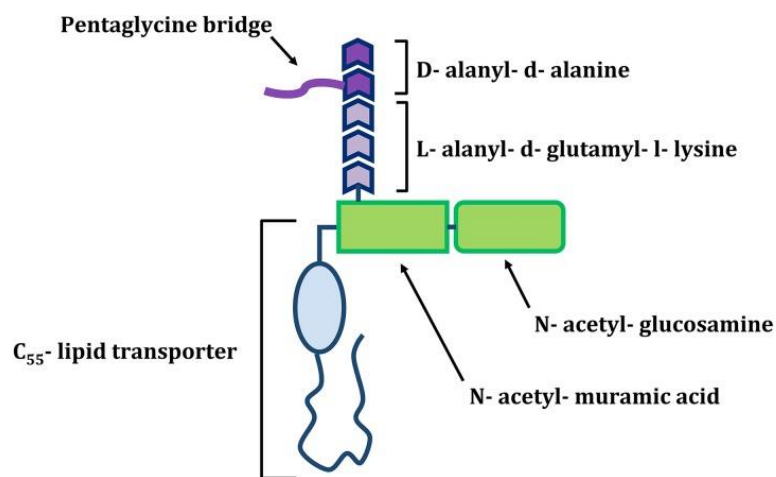


Figure 89 - Action of bacitracin on bacterial peptidoglycan layer²⁵¹

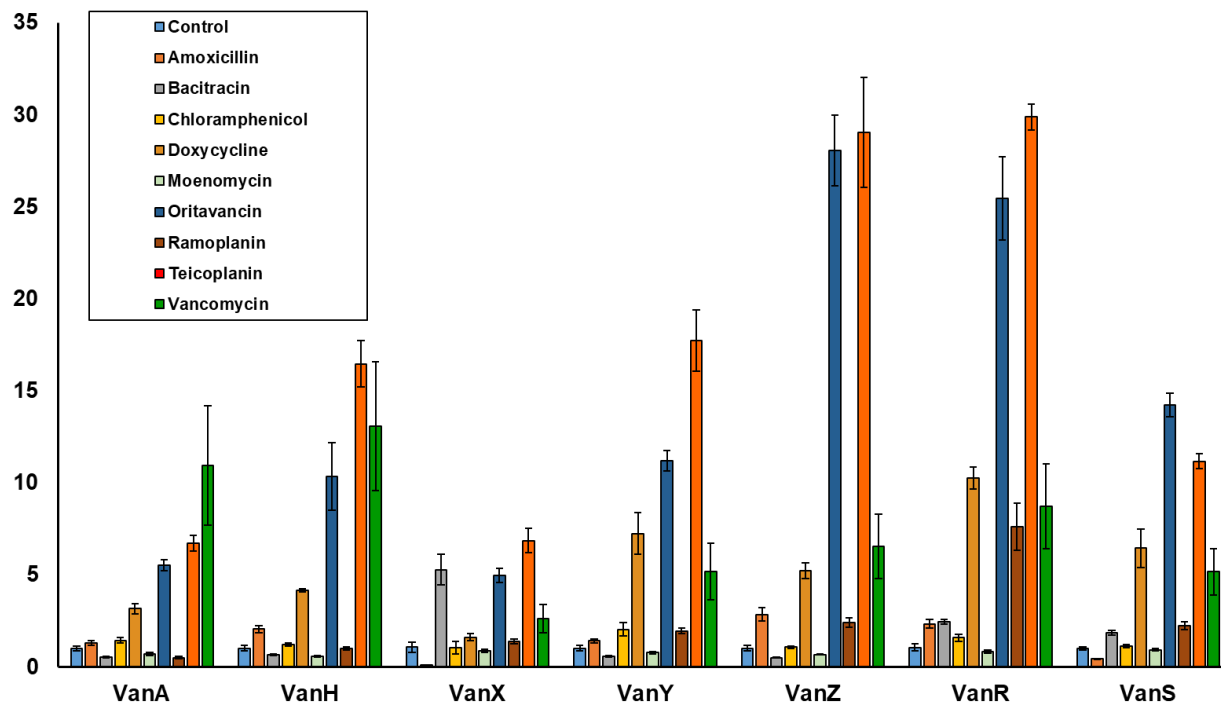


Figure 90 - Fold changes in gene levels showing teicoplanin, vancomycin, doxycycline and oritavancin resistance at 4x MIC

9.4 Conclusion

In the previously described study, we observed that linezolid induces the resistance genes at 4x MIC. In this pilot study, we further investigated the changes in VRE *faecium* transcriptional gene level by inducing them with cell wall targeting antibiotics. Gene level changes were observed with 1/4x MICs of vancomycin and teicoplanin. However, doxycycline, oritavancin, vancomycin and teicoplanin showed changes in the level of gene induction at 4x MIC. Therefore, further study will be done using 4x MIC. Furthermore, a combination of the above-mentioned drugs and vancomycin at 4x MIC will also be used to study the transcriptional levels of these resistant genes.

CHAPTER 10

10. FREQUENCY OF RESISTANCE DETERMINATION AND WHOLE GENOME SEQUENCING OF METHICILLIN-RESISTANT *STAPHYLOCOCCUS AUREUS*

10.1 Introduction and Rationale

Whole genome sequencing (WGS) is a cutting-edge molecular technique used to determine the complete DNA sequence of an organism's genome²⁵² In bacteria, WGS provides identification and characterization of bacterial taxonomy, bacterial strains, antimicrobial resistance pattern, virulence factors, and their genetic relatedness. With bacteria still being a threat to vulnerable patient populations, WGS has helped taxonomy and strain identification allowing higher resolution of bacterial taxonomy compared to traditional methods. The comparison between the genome sequence of two or more strains helps the researchers to determine the phylogenetic relationship and identify novel species or subspecies of bacteria²⁵³ WGS has also helped by comparing genomic sequences of bacterial strains involved in an outbreak by providing epidemiological data that can help identify the source of infection and monitor the evolution of pathogens over time. This information can help control targeted infection and prevent future outbreaks²⁵⁴ WGS also helps in identifying novel virulence factors and their associated genes which could be potential targets for new antimicrobials therapies and vaccines²⁵⁵ Finally, WGS can help identify antimicrobial resistance genes and their genetic context in bacterial genomes providing a useful insight about control of drug-resistant pathogens.

In this study, we developed mutants of ATCC methicillin-resistant *Staphylococcus aureus* 43300 and compared their genome to a wild-type (control) MRSA. This study identified resistant

genes in MRSA. This study also identified key mutations that confirm molecular target of an antibacterial agent and ensures resistance pathways associated with various antibacterial drugs. MRSA was grown in presence of antibiotics to generate mutants. Genomic DNA from the mutant colonies were isolated. DNA was sent to Kansas University Medical Centre for whole genome sequencing. The workflow for whole genome sequencing is depicted in the Figure 91.

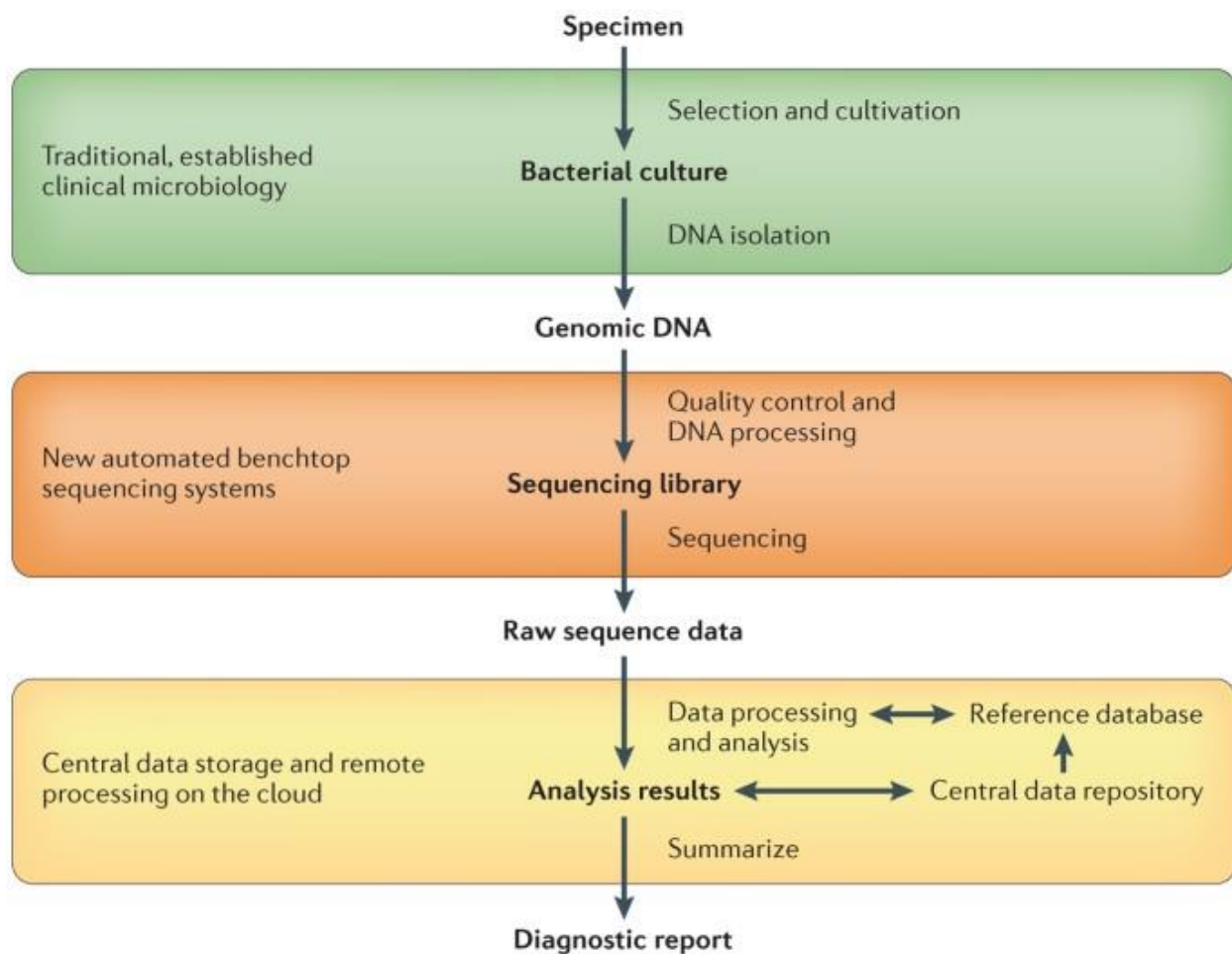


Figure 91 - Workflow for bacterial whole-genome sequencing²⁶⁰

10.2 Materials and Methods

10.2.1 General

The bacterial strain used for preparing mutant colonies was methicillin-resistant *Staphylococcus aureus* (MRSA) strain F-182 (ATCC 43300). The media used to grow MRSA was cation-adjusted Mueller-Hinton (CAMH). Lysozyme used for lysis of bacterial cell was from Millipore Sigma. Bacterial genomic DNA extraction was purchased from Qiagen.

10.2.2 Minimal inhibitory concentration determination of antibiotics to make mutant MRSA

2 μ L of drug samples @ 0.5 mM were added to the first column of 384 well plate. The well was serially diluted in steps of two with DMSO. The last column was control (DMSO only). This provided 50 μ M compound concentrations in the first column. Plates were frozen at -80°C and dried as described above. To each well was then added 20 μ L cation-adjusted Mueller-Hinton (CAMH) broth containing 4000 cfu MRSA (ATCC 43300). Plates were then incubated for 48 h at 35°C . Fresh CAMH broth (10 μ L) was then added to the wells of the plate, followed by incubation for 2 h at 35°C , to restart active cell growth. To the wells of the plate was then added 6 μ L of 100 $\mu\text{g mL}^{-1}$ resazurin (sodium salt)^{145 146 147} The plates were incubated for another 2 h at 35°C , and the 570/600 fluorescence ratio was measured in a Molecular Devices SpectraMax M5 multimode microplate reader.

10.2.3 $-/+$ Thymidine counter screen for folate/thymidine biosynthesis inhibitors

The effects of folate/thymidine biosynthesis inhibitors on MRSA can be reversed by the addition of thymidine to the culture media¹⁷⁰ This effect was therefore used to study the compounds in Table 28 to look for folate biosynthesis inhibitors. The MICs of the compounds were determined in absence and presence of 4 μ M (1 $\mu\text{g/mL}$) thymidine.

10.2.4 Preparation of resistant antibiotic agar plates at 4x MIC of antibiotic

150 mm x 15 mm petri dishes were used to make antibiotic agar plates. 2.2 gm of CAMH media and 1.5 gm of agar were used for every 100 mL of agar media. 3 separate flasks with 350 mL MH agar mixture were autoclaved. Following the autoclave, 4x MIC of antibiotics, floxuridine and gemcitabine were added to each flask respectively. One 350 mL MH agar flask served as no antibiotic control. The MH agar was then poured in petri dishes and the plates were allowed to solidify.

10.2.5 Preparation of different concentrations of resistant antibiotic MH agar plates

150 mm x 15 mm petri dishes were used to make antibiotic agar plates. 2.2 gm of CAMH media and 1.5 gm of agar were used for every 100 mL of agar media. Separate flasks with 350 mL MH agar mixture were autoclaved for different MICs of three antibiotics. Following the autoclave different MICs ($\frac{1}{2}x$, 1x, 2x, 4x, and 8x) of each antibiotic (floxuridine, gemcitabine and trimethoprim) were added to each flask. The MH agar media with each concentration of drug was then poured in petri dishes in quadruplicates and the plates were allowed to solidify as shown in Figure 92. Along with the antibiotic plates, control plates with no antibiotic were also made.

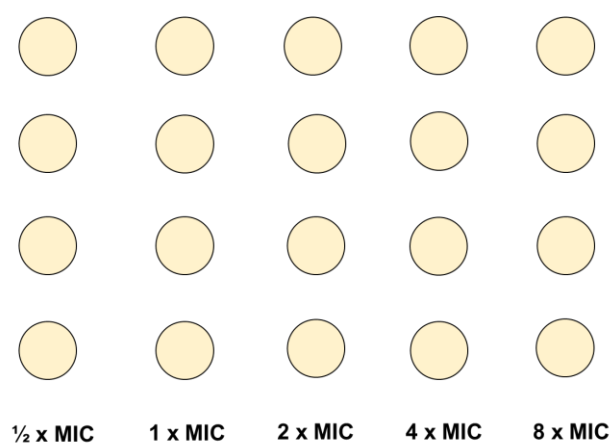


Figure 92 - MH agar plates with different MICs for Trimethoprim, Floxuridine and Gemcitabine

10.2.6 Serial dilution and plating at 4x MIC

An overnight MRSA primary culture was grown. The next day the culture was centrifuged at 4000 rpm for 20 minutes in a 50 mL falcon tube. The supernatant was then discarded and 2.5 mL of fresh CAMH was added to the pellet. This provided a high inoculum of bacteria. This inoculum was serially diluted in steps of 10, and the higher concentration of dilutions were plated on 4x MIC antibiotic MH agar plates and the lower concentration of serially diluted culture was plated on the control MH agar plates.

10.2.7 Serial dilution and plating at various MICs

An overnight primary culture was grown. The next day, this culture was centrifuged at 4000 rpm for 20 minutes in a 50 mL falcon tube. The supernatant was then discarded and 2 mL of fresh CAMH was added to the pellet. This provided a high inoculum of bacteria. This inoculum was serially diluted in steps of 20. The dilution was done as depicted in Figure 93. The dilutions were further plated on the different antibiotic concentrations of the MH agar plates as depicted in Figure 94.

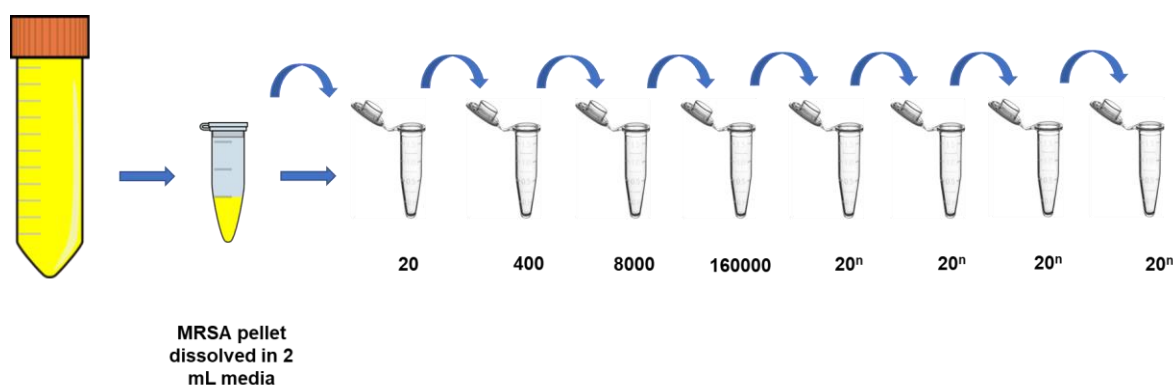


Figure 93 - Serial dilution in steps of 20 from 2 ml of high MRSA cell density.

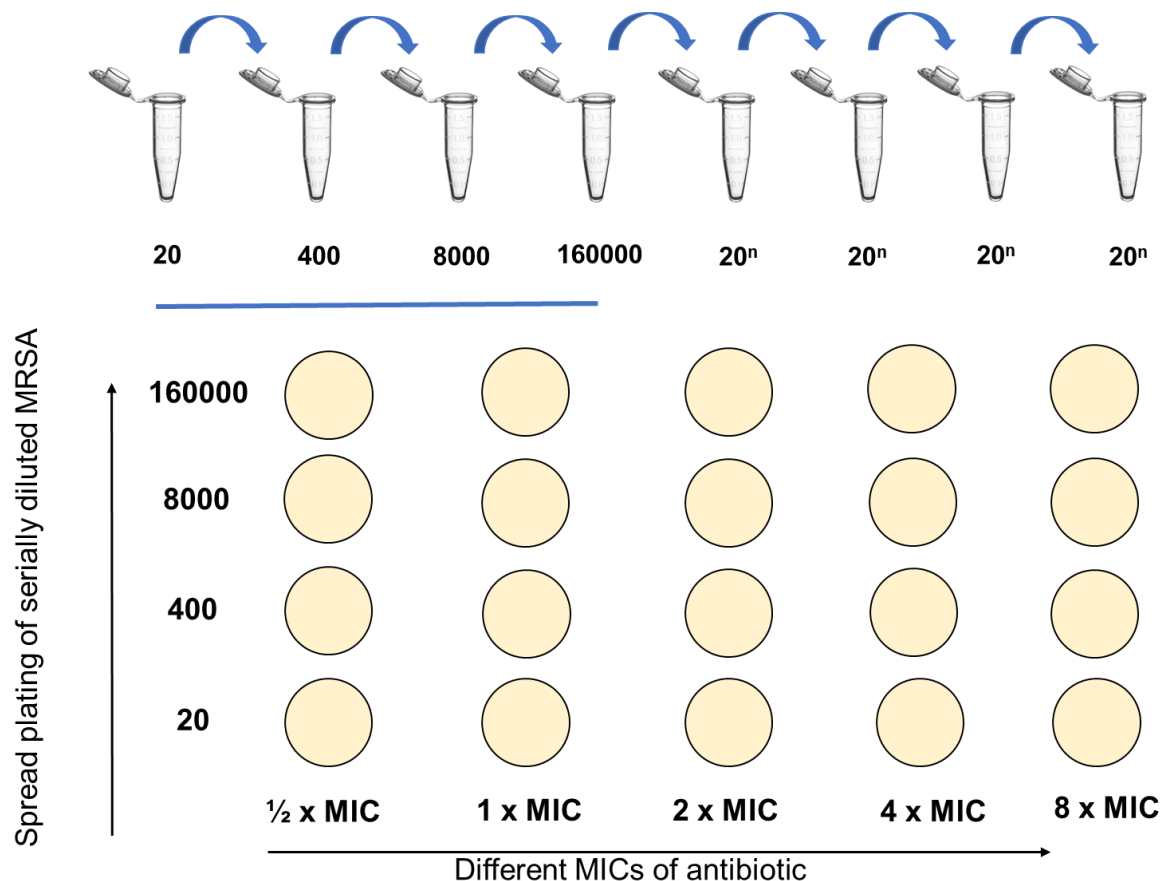


Figure 94 - Various dilutions of MRSA plated on different antibiotic MIC MH agar plates.

10.2.8 Genomic DNA isolation from mutant colonies

Three separate mutant colonies were picked from the same antibiotic MH agar plate and inoculated in three different flasks. These flasks were grown overnight with shaking at 35 °C. The next day, 1.5 mL primary culture was added in 2 mL eppendorf tube. The samples were centrifuged at 14000 rpm for 5 mins and the supernatant was discarded. The pellets were then resuspended in 170 µl of 20 mM tris.HCl pH 8.0, 2 mM EDTA and 1.2% Triton. The tubes were vortexed to resuspend the pellet in the buffer and 30 µl of 25 mg/mL lysozyme was then added to each lysis

tube and mixed well. The tubes were incubated overnight at 37 °C preheated water bath. Genomic DNA was isolated using a Qiagen kit. The purity of the final eluted DNA was checked using nanodrop and 0.8% agarose gel. The DNA was then sent to Kansas University Medical Center for whole genome sequencing. Figure 95 shows the workflow for bacterial whole genome sequencing.

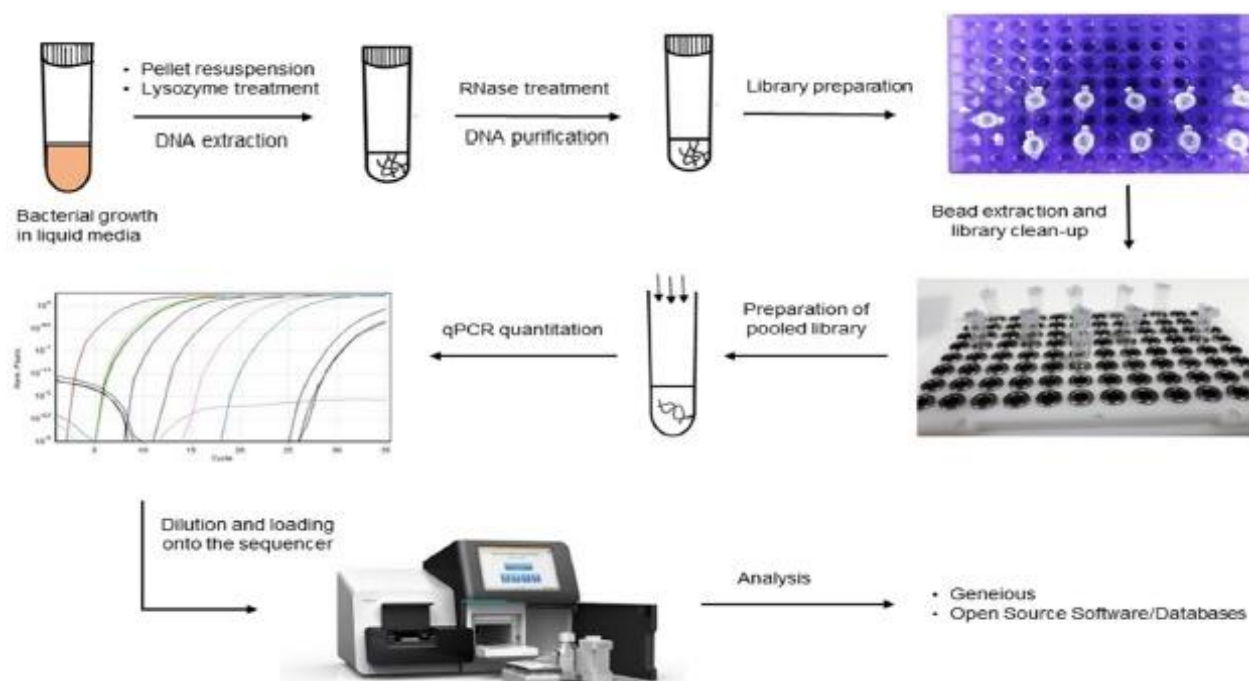


Figure 95 - Workflow of bacterial whole genome sequencing²⁶¹

10.3 Results and Discussion

10.3.1 +/- Thymidine MICs

The MICs were determined in the absence and presence of 4 μ M +/- thymidine. The other aim of this study was to look for folate biosynthesis inhibitors. In a previous study, it was observed that floxuridine acts as a folate biosynthesis inhibitor. Folate biosynthesis inhibition reverses in

presence of thymidine. Table 28 shows the MICs of antibiotics from FDA and NCI library screens in the absence and presence of thymidine. The presence of thymidine shows that many antibiotics like 5-fluorocytidine, Floxuridine, 5-fluorouridine, Carmufur, Doxifluridine, 5-fluorouracil, NSC367428, and DFCR act as folate reductase biosynthesis inhibitors.

Table 28 - Shows MICs of FDA and NCI screened compounds against MRSA.

Compound	MICs (μ M)	
	-Thymidine	+Thymidine
Rifaximin	2.4×10^{-2}	2.4×10^{-2}
Gemcitabine	2.4×10^{-2}	1.2×10^{-2}
5-fluorocytidine	0.20	25
Floxuridine	0.39	50
5-fluorouridine	0.78	50
Carmafur	0.78	12.5
Doxiflurouridine	0.78	100
5-fluorouracil	1.6	50
NSC367428	3.1	100
DFCR	3.1	100
Dicloxacillin	12.5	12.5
Capecitabine	50	100

10.3.2 Preparation of different MICs of antibiotic agar plate and mutation results

Preparation of different MIC plates was done to expand and observe mutation rate of MRSA not only at 4x MIC of an antibiotic but also at 1/2x, 1x, 2x and 8x MICs of antibiotic. This provided a better understanding of antibiotic MIC concentration that can be used to generate mutants. Furthermore, this also provided additional knowledge regarding potent MIC of an antibiotic that can be used to kill MRSA. Floxuridine is potent against resistant bacteria and acts as a folate biosynthesis inhibitor. It has a high frequency of resistant towards MRSA. Gemcitabine has comparatively lower frequency of resistant towards MRSA as seen in Figure 97. Trimethoprim

is a folate biosynthesis inhibitor and was used as a positive control. Floxuridine and trimethoprim both have high frequency of resistance and behave in similar way against MRSA as seen in Figures 96 and 98. One of the control plates is shown in Figure 99.

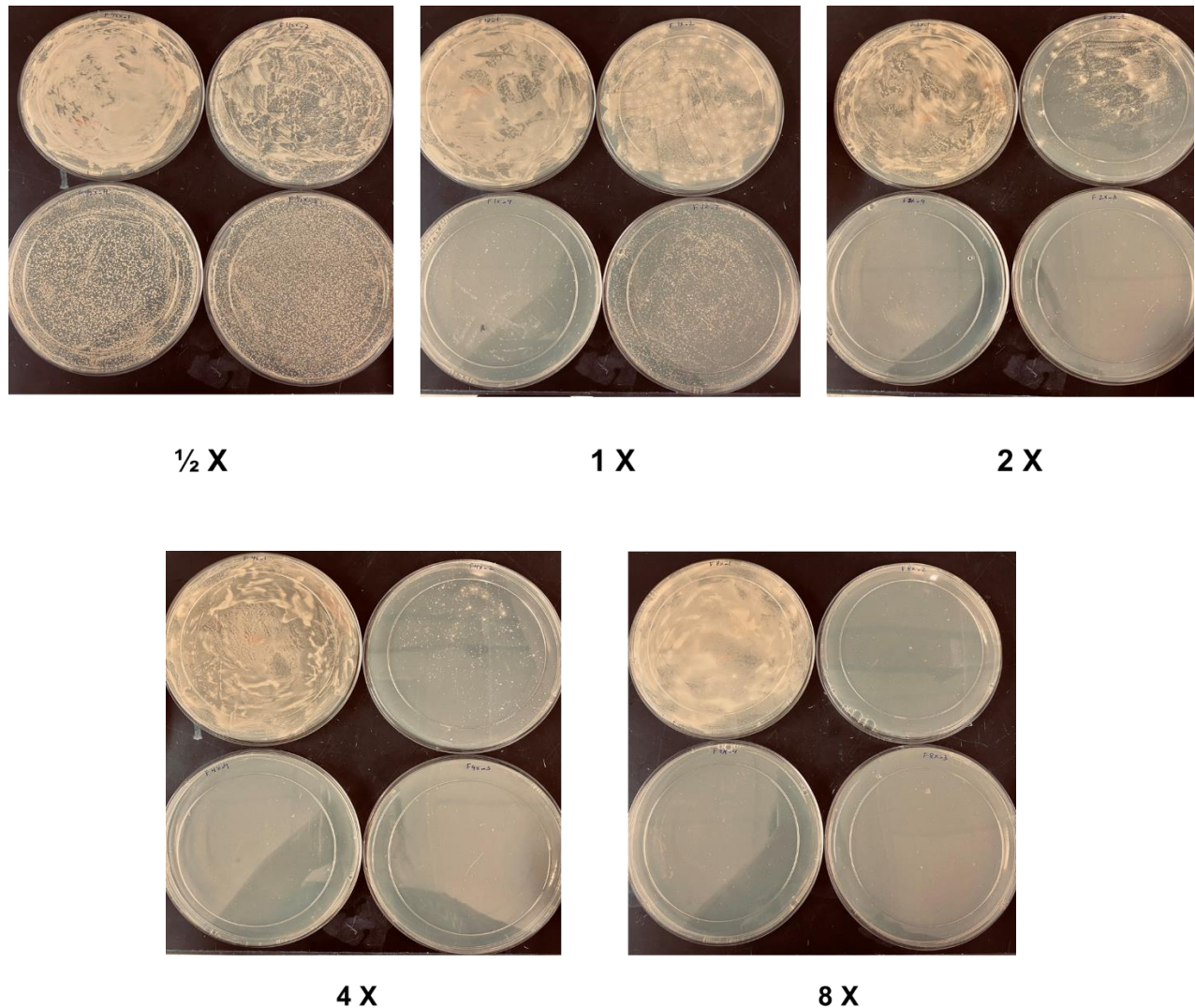


Figure 96 – Various dilutions of MRSA plated on different Floxuridine MIC MH agar plates. Each MIC plate was made in quadruplicates and plated with dilution starting at 20^1 , 20^2 , 20^3 , 20^4 in a clockwise direction (Starting from the highest to the lowest concentration of dilution).

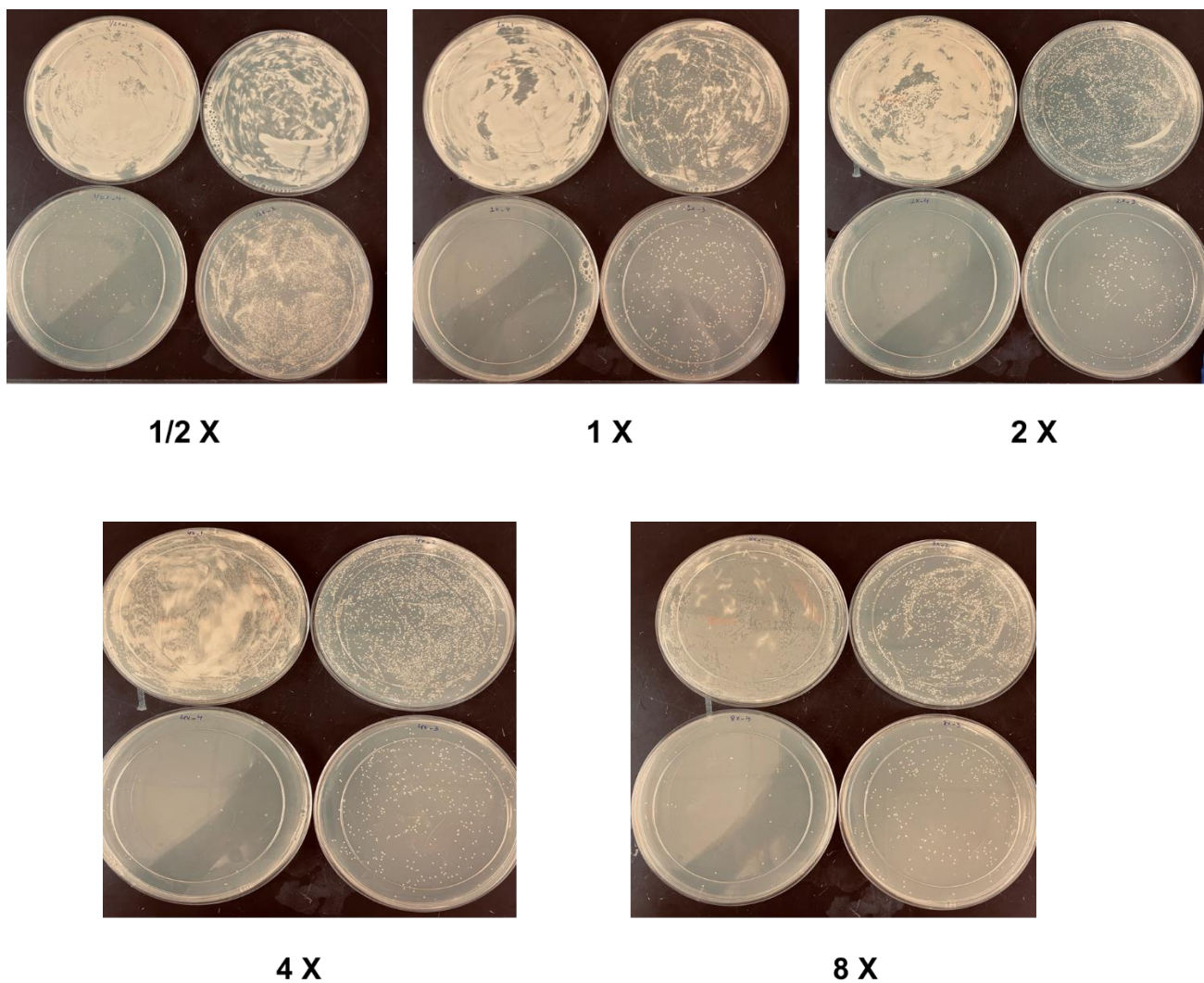


Figure 97 – Various dilutions of MRSA plated on different Gemcitabine MIC MH agar plates. Each MIC plate was made in quadruplicates and plated with dilution starting at 20^1 , 20^2 , 20^3 , 20^4 in a clockwise direction (starting from the highest to the lowest concentration of dilution).

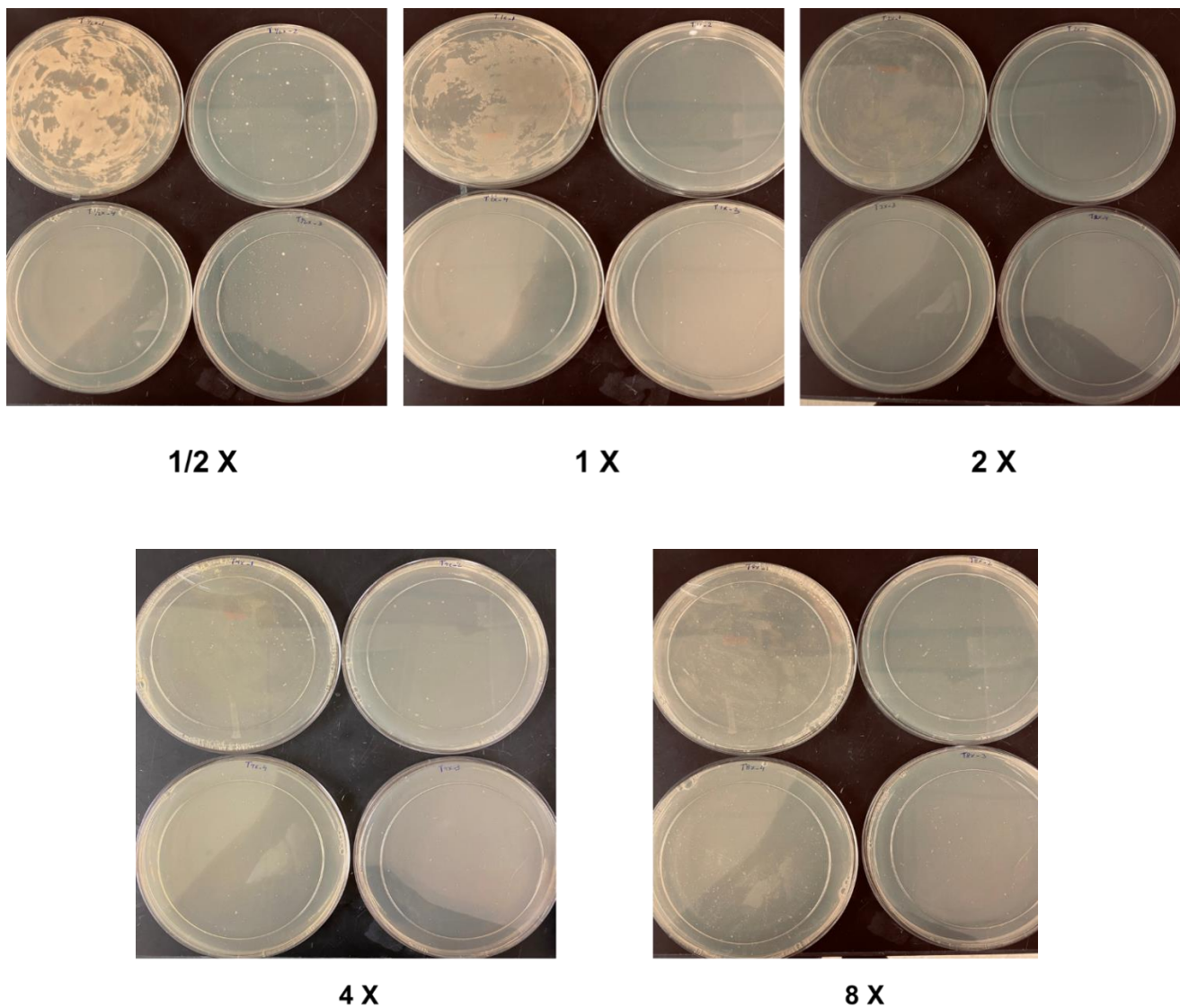


Figure 98 – Various dilutions of MRSA plated on different Trimethoprim MIC MH agar plates. Each MIC plate was made in quadruplicates and plated with dilution starting at 20^1 , 20^2 , 20^3 , 20^4 in a clockwise direction (starting from the highest to the lowest concentration of dilution).

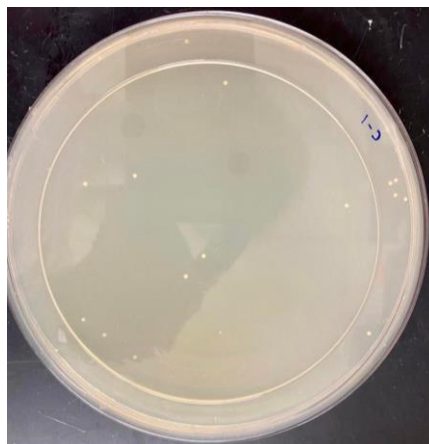


Figure 99 – 7 different control plates were made and plated with 7 dilutions of MRSA. Only one of the control plates with colonies is shown.

10.3.3 Genomic DNA isolation optimization

The cell wall of gram-positive bacteria is thicker than the cell wall of gram-negative bacteria. Therefore, lysis of the cell wall and isolation of genomic DNA from gram-positive becomes difficult. The genomic DNA isolation was optimized using 25 mg/mL lysozyme for the lysis of the cell wall. MRSA was incubated with lysozyme overnight at 37 °C with regular shaking. This optimization yielded a good concentration of genomic DNA.

10.4 Conclusion

Whole genome sequencing is a pilot experiment done to determine mutation in MRSA. Mutant colonies were made, and genomic DNA was isolated. This DNA was sent to Kansas University Medical Center for whole genome sequencing. The analysis of mutant data is done using a program called Snippy. Previously, 4x MIC of antibiotics was used to mutation in MRSA, but this experiment was later expanded to generate mutants at different MIC concentrations of

antibiotics starting from 1/2x to 8x MIC. This optimization provided knowledge about antibiotic MICs that is capable of growing and inhibiting resistant bacteria. It was observed that floxuridine has a higher frequency of resistance and can inhibit the growth of bacteria. Gemcitabine has comparatively lower frequency of resistance than floxuridine. Trimethoprim is a folate biosynthesis inhibitor and is used as a positive control. Furthermore, extraction of DNA from gram-positive bacteria is tedious and becomes difficult as compared to gram-negatives. Lysozyme was thus used to break the cell wall of gram-positive bacteria to isolate DNA. Lysozyme can also be used to isolate RNA and proteins from gram-positives. This technique of whole genome sequencing can be further utilized for vancomycin-resistant *Enterococcus* or gram-negatives to generate mutants and study the genes that provide resistance to the bacteria against antibiotics.

GENERAL CONCLUSION

Vancomycin-resistant *Enterococci* (VRE) are a group of bacteria that have developed resistance to the antibiotic vancomycin. *Enterococci* are naturally found in the human gastrointestinal tract and are typically harmless; however, they can cause infections in certain situations, particularly in healthcare settings. When *Enterococci* develop resistance towards vancomycin, these infections become harder to treat and can lead to more severe complications. The emergence of VRE is a significant public health concern, as it limits the available treatment options for *Enterococcal* infections. In response, efforts are being made to develop new antibiotics that can target VRE effectively and to promote more responsible use of existing antibiotics to slow down the spread of resistance.

Resistance in VanA-type vancomycin-resistant *Enterococcus faecium* (VRE_{fm}) is due to an inducible gene cassette encoding seven proteins (*vanRSHWXYZ*). This provides for an alternative peptidoglycan (PG) biosynthesis pathway whereby D-Alanine-D-Alanine is replaced by D-Alanine-D-Lactate (Lac), to which vancomycin cannot bind effectively. The first part of this dissertation aimed to quantify cytoplasmic levels of normal and alternative pathway PG intermediates in VanA-type VRE_{fm} by liquid chromatography-tandem mass spectrometry before and after vancomycin exposure and to correlate these changes with changes in *vanA* operon mRNA levels measured by real-time quantitative PCR (RT-qPCR). Normal pathway intermediates predominated in the absence of vancomycin, with low levels of alternative pathway intermediates. Extended (18-h) vancomycin exposure resulted in a mixture of the terminal normal (UDP-*N*-acetylmuramic acid [NAM]-l-Ala-D-Glu-l-Lys-D-Ala-D-Ala [UDP-Penta]) and alternative (UDP-NAM-l-Ala- γ -D-Glu-l-Lys-D-Ala-D-Lac [UDP-Pentadepsi]) pathway intermediates (2:3 ratio).

Time course analyses revealed normal pathway intermediates responding rapidly (peaking in 3 to 10 min) and alternative pathway intermediates responding more slowly (peaking in 15 to 45 min). RT-qPCR demonstrated that *vanA* operon mRNA transcript levels increased rapidly after exposure, reaching maximal levels in 15 min. To resolve the effect of increased *van* operon protein expression on PG metabolite levels, linezolid was used to block protein biosynthesis. Surprisingly, linezolid dramatically reduced PG intermediate levels when used alone. When used in combination with vancomycin, linezolid only modestly reduced alternative UDP-linked PG intermediate levels, indicating substantial alternative pathway presence before vancomycin exposure. Comparison of PG intermediate levels between VREfm, vancomycin-sensitive *Enterococcus faecium*, and methicillin-resistant *Staphylococcus aureus* after vancomycin exposure demonstrated substantial differences between *S. aureus* and *E. faecium* PG biosynthesis pathways. The importance of this study is that VREfm is highly resistant to vancomycin due to the presence of a vancomycin resistance gene cassette. Exposure to vancomycin induces the expression of genes in this cassette, which encode enzymes that provide for an alternative PG biosynthesis pathway. In VanA-type resistance, these alternative pathway enzymes replace the D-Alanine-D-Alanine terminus of normal PG intermediates with D-Alanine-D-Lactate terminated intermediates, to which vancomycin cannot bind. While the general features of this resistance mechanism are well known, the details of the choreography between vancomycin exposure, *vanA* gene induction, and changes in the normal and alternative pathway intermediate levels have not been described previously. This study comprehensively explores how VREfm responds to vancomycin exposure at the mRNA and PG intermediate levels.

The second part of this dissertation introduces a 2-dimensional drug library screen against resistant bacteria. Antimicrobial resistance is a major public health threat, and there is an urgent

need for new strategies to address this issue. In this part of thesis, two chemical drug libraries were screened against resistant bacteria. The first library screening strategy consisted of an FDA-approved drug library screen against vancomycin-resistant *Enterococcus faecium* in both its original (un-metabolized [UM]) and its human liver microsome metabolized (pre-metabolized [PM]) forms and in the absence and presence of a resistant-to antibiotic. This allows the identification of agents with active metabolites and agents that can act synergistically with the resistant-to antibiotic. Thirteen drugs with minimum MICs that were $\leq 12.5 \mu\text{M}$ under any tested condition (UM/PM vs. $-/+$ vancomycin) were identified. Seven of these appeared to act synergistically with vancomycin, and follow-up checkerboard analyses confirmed synergy ($\Sigma\text{FIC}_{\text{min}} \leq 0.5$) for six of these. Ultimately, four rifamycins, two pleuromutilins, mupirocin, and linezolid were confirmed as synergistic. The most synergistic agent was rifabutin ($\Sigma\text{FIC}_{\text{min}} = 0.19$). Linezolid, a protein biosynthesis inhibitor, demonstrated relatively weak synergy ($\Sigma\text{FIC}_{\text{min}} = 0.5$). Only mupirocin showed significantly improved activity after microsomal metabolism, indicative of a more active metabolite, but efforts to identify an active metabolite were unsuccessful. Spectra of activity of several hits and related agents were also determined. Gemcitabine showed activity against a number vancomycin-resistant *E. faecium* and *E. faecalis* strains, but this activity was substantially weaker than previously observed in MRSA. The importance of the FDA-approved library screen against vancomycin is that this study reports a complete screen of 1,000 FDA-approved drugs and their metabolites against vancomycin-resistant *Enterococcus faecium* (VREfm) in both the absence and presence of vancomycin. This identified potentially synergistic combinations of FDA-approved drugs with vancomycin, and a number of these were confirmed in follow-up checkerboard assays. Among intrinsically active FDA-approved drugs, gemcitabine was identified as having activity against a panel of VRE strains.

The overall goal of this effort was to further demonstrate the utility of enhanced library screening approaches in which replicate library screens are performed with variation between the replicates. The basic screen (UM-Vm) identified both closantel and gemcitabine as non-typical anti-VRE agents. The spectrum of activity of closantel against several VRE strains has previously been reported¹⁵⁷ Gemcitabine was demonstrated in this study as shown in Table 12 to also have activity against several VRE strains, and this or similar agents may be worth further study. The molecular target of gemcitabine is unknown, but further studies of gemcitabine and homologs seem justified from these observations. No agents with identifiable active metabolites were discovered in this screen, in contrast to the identification of active capecitabine metabolites in MRSA¹⁴³ Screening for synergistic combinations with vancomycin revealed several synergistic agents as shown in Figure 64. These were all either RNA or protein biosynthesis inhibitors, suggesting a common basic mechanistic basis for these synergies. Some of the agents and agent combinations identified in this effort may be suitable candidates for further *in vitro* and *in vivo* studies, and ultimately clinical application.

New antibacterial agents and agent combinations are urgently needed to combat antimicrobial resistance. This dissertation also covers a second multidimensional chemical library screening strategy which is used to identify compounds in the National Cancer Institute (NCI) Diversity Set V library (1593 compounds) with anti-MRSA activity. In this effort, library compounds were screened for anti-MRSA activity in both their original (un-metabolized; UM) and human liver microsome metabolized (post-metabolized, PM) forms, and in the absence and presence of sub-MIC levels of cefoxitin. This strategy allows for the identification of intrinsically active agents, agents with active metabolites, and agents which can act synergistically with cefoxitin. Sixteen UM compounds with MICs $\leq 12.5 \mu\text{M}$ were identified. No agents with

substantially enhanced activity after microsomal metabolism were found. Several agents showed significant apparent synergy with cefoxitin, and checkerboard assays were used to confirm synergy for 4 of these (celastrol, porfiromycin, 4-quinazolinediamine, and teniposide). A follow-up comparative screen in the absence and presence of 4 μ M thymidine was used to identify three agents as likely folate/thymidine biosynthesis inhibitors. An LC-MS/MS assay for deoxythymidine triphosphate (dTTP) (and ATP as a control) was used to confirm these three as suppressing dTTP biosynthesis in MRSA. This study further demonstrates the utility of comparative library screening to identify novel bioactive agents with interesting synergies and biological activities. The identification of several folate/thymidine biosynthesis inhibitors from this small screen indicates that this pathway is a viable target for new drug discovery efforts.

Library screening was also done using NCI diversity set V against VREfm. The goal of the screen was to further demonstrate the utility of enhanced library screening approaches. However, VRE vs NCI screen did not yield many hits as compared to the MRSA-NCI screen. Clorobiocin, hitachimycin and bactobolin were the only compounds that showed a spectrum of activity against both MRSA strains and VRE strains (data not shown). Screening for synergistic combinations with vancomycin revealed three synergistic agents as shown in Figure 72. The synergy of these three compounds with vancomycin was high with very low FICI values. Celastrol which is also known as the DNA damaging agent¹⁷⁹ was synergistic with both vancomycin and cefoxitin in the MRSA vs NCI screen. 4-QDA which is known to act as a folate reductase inhibitor (as mentioned in the previous study) was synergistic with vancomycin and cefoxitin in both VRE and MRSA screens. Some of the agents and agent combinations identified in this effort may be suitable candidates for further *in vitro* and *in vivo* studies, and ultimately clinical application.

The third part of this dissertation contains three different studies which were done to identify potent drugs against resistant bacteria. The first experiment is known as the 2-dimensional active vs active screen. This study expanded our completed screening approach of VREfm against NCI and FDA-approved drug libraries. It provides a rich set of interesting agents acting synergistically and antagonistically. This study helped to identify new antibacterial agents and agent combinations. We used a 2-dimensional screening approach where actives can synergize with other actives. We used $1/4^{\text{th}}$ x MIC of each active compound across each row and then used the same for each column. Apart from synergy, this study provided information regarding antagonism between two drug combinations. This approach is a logical extension of our library screening process, and it accelerates our ability to identify both synergistic and antagonistic drug combinations. The development of effective combinations helps to minimize the emergence of resistance and develop new combinations of drugs with low doses and minimum side effects.

The second study in part three of this dissertation is to look at the mechanism of action of drugs against VRE *faecium* on a transcriptomic level. In the previous study, we have seen how the antibacterial effect on VRE *faecium* is based on metabolite level via LC-MS/MS. However, this study, looks at the mRNA transcript effect when VRE *faecium* is treated with different antibiotics. We looked at how each resistance gene involved in the resistance pathway in VRE behaved in the presence of different antibiotics. In the previously described study, we observed that linezolid induces the resistance genes at 4x MIC. In this pilot study, we further investigated the changes in the gene level of VRE *faecium* transcriptional level by including antibiotics that are bacterial cell wall targeting drugs. Changes in the gene levels at $1/4$ x MIC of antibiotics were only observed with vancomycin and teicoplanin. However, changes in gene induction at 4x MIC was observed with other drugs including vancomycin and teicoplanin. Therefore, further study will be done using

4x MIC. Furthermore, a combination of the drugs mentioned in this study and vancomycin at their 4x MIC combinations will also be used to look at the transcriptional levels of these resistance genes.

The third experiment involved whole genome sequencing of MRSA. Whole genome sequencing (WGS) is a cutting-edge molecular technique used to determine the complete DNA sequence of an organism's genome²⁵². In bacteria, WGS provides identification and characterization of bacterial taxonomy, bacterial strains, antimicrobial resistance pattern, virulence factors, and their genetic relatedness. With bacteria still being a threat to vulnerable patient populations, WGS has helped taxonomy and strain identification allowing higher resolution of bacterial taxonomy compared to traditional methods. In this study, we developed mutants for ATCC Methicillin-resistant *Staphylococcus aureus* 43300 and compared their genome with a wild-type (control) MRSA. This study helped us to identify the genes that cause resistance in MRSA. This study also provides information regarding an antibiotic and whether it can be a potent drug against resistant bacteria. A +/- screen with thymidine was also done to look for potential folate biosynthesis inhibitors. Floxuridine gave a high frequency of resistance and acts similar to trimethoprim which is a folate biosynthesis inhibitor. This +/- thymidine screen would help in finding potent hits against bacteria. MRSA was grown in the presence of antibiotics, and genomic DNA from the mutant colonies were isolated. The DNA were sent to Kansas University Medical Centre for whole genome sequencing. Whole genome sequencing is a pilot experiment done to observe mutation in MRSA. The analysis of mutant data is done using a program called Snippy. In a previous experiment, 4x MIC for antibiotics was used and later different MICs starting from 1/2x to 8x MIC of an antibiotic were used to generate mutants. This will give us a clear idea about the MICs and antibiotics that can grow or kill mutant colonies. Furthermore, extraction of DNA

from gram-positive bacteria is tedious and does not yield us good concentration of DNA as compared to gram-negatives. Lysozyme was thus used to break the cell wall of gram-positives and to isolate DNA. Lysozyme can also be used to isolate RNA and proteins from gram-positives. This technique of whole genome sequencing can be further utilized for Vancomycin-resistant *Enterococcus* or gram-negatives to generate mutants and study the genes that are involved in generating such mutations.

APPENDIX



Dear Shivani Gargvanshi,

American Society for Microbiology - Journals has approved your recent request. Before you can use this content, you must accept the license fee and terms set by the publisher.

Use this [link](#) to accept (or decline) the publisher's fee and terms for this order.

Request Summary:

Submit date: 04-Jun-2023

Request ID: 600124555

Publication: Journal of bacteriology : JB

Title: Effect of vancomycin on cytoplasmic peptidoglycan intermediates and van operon mRNA levels in VanA-type vancomycin resistant *Enterococcus faecium*.

Type of Use: Republish in a thesis/dissertation

Please do not reply to this message.

To speak with a Customer Service Representative, call +1-855-239-3415 toll free or +1-978-846-2600 (24 hours a day), or email your questions and comments to support@copyright.com.

Sincerely,

Copyright Clearance Center

Tel: 1-855-239-3415 / +1-978-846-2600
support@copyright.com
[Manage Account](#)





Copyright Clearance Center

Dear Shivani Gargvanshi,

American Society for Microbiology - Journals has approved your recent request. Before you can use this content, you must accept the license fee and terms set by the publisher.

Use this [link](#) to accept (or decline) the publisher's fee and terms for this order.

Request Summary:

Submit date: 04-Jun-2023

Request ID: 600124555

Publication: Journal of bacteriology : JB

Title: Effect of vancomycin on cytoplasmic peptidoglycan intermediates and van operon mRNA levels in VanA-type vancomycin resistant *Enterococcus faecium*.

Type of Use: Republish in a thesis/dissertation

Please do not reply to this message.

To speak with a Customer Service Representative, call +1-855-239-3415 toll free or +1-978-646-2600 (24 hours a day), or email your questions and comments to support@copyright.com.

Sincerely,

Copyright Clearance Center

REFERENCES

1. Bacteria Medical Microbiology. <https://www.ncbi.nlm.nih.gov/books/NBK8120/>
2. Bacterial classification <https://www.technologynetworks.com/immunology/articles/gram-positive-vs-gram-negative-323007>
3. Pathogens <https://teachmeanatomy.com/immune-system/infections/pathogens/>
4. Cetinkaya, Y.; Falk, P.; Mayhall, CG., Vancomycin-resistant enterococci. *Clin Microbiol Rev* **2000**, 13(4), 686-707.
5. Levitus, M.; Rewane, A.; & Perera, T. B.. Vancomycin-Resistant *Enterococci*. In *StatPearls* **2023**. <https://www.ncbi.nlm.nih.gov/books/NBK513233/>
6. Murray, B. E., Vancomycin-Resistant Enterococcal Infections. *New England Journal of Medicine* **2000**, 342(10), 710-721.
7. Vancomycin resistant *Enterococci* <https://www.cdc.gov/hai/organisms/vre/vre.html>
8. Szakacs, TA.; Kalan, L.; McConnell, MJ.; Eshaghi, A.; Shahinas, D.; McGeer, A.; Wright, GD.; Low, DE.; Patel, SN., Outbreak of vancomycin-susceptible *Enterococcus faecium* containing the wild-type vanA gene. *J Clin Microbiol* **2014**, 52(5), 1682-6
9. Sahm, DF.; Kissinger, J.; Gilmore, MS. et al. In vitro susceptibility studies of vancomycin-resistant *Enterococcus faecalis*. *Antimicrob Agents Chemother* **1989**, 33, 1588-1591
10. Cercenado, E.; García-Leoni, ME.; Díaz, MD.; Sánchez-Carrillo, C.; Catalán, P.; De Quirós, JC.; Bouza, E.; Emergence of teicoplanin-resistant coagulase-negative staphylococci. *J Clin Microbiol* **1996**, 34(7), 1765-8.

11. Clark, NC.; Teixeira, LM.; Facklam, RR.; Tenover, FC.; Detection and differentiation of vanC-1, vanC-2, and vanC-3 glycopeptide resistance genes in enterococci. *J Clin Microbiol* **1998**, 36(8), 2294-7.
12. Linden, PK., Treatment options for vancomycin-resistant enterococcal infections. *Drugs* **2002**, 62(3), 425-41
13. Peptidoglycan (Murein)
<https://www.sciencedirect.com/science/article/pii/B9780123739445003394>
14. Vollmer, W.; Bertsche, U., Murein (peptidoglycan) structure, architecture and biosynthesis in Escherichia coli. *Biochim Biophys Acta* **2008**, 1778(9), 1714-34.
15. Sauvage, E.; Kerff, F.; Terrak, M.; Ayala, JA.; Charlier, P., The penicillin-binding proteins: structure and role in peptidoglycan biosynthesis. *FEMS Microbiol Rev* **2008**, 32(2), 234-58.
16. Typas, A.; Banzhaf, M.; Gross, C. *et al.*, From the regulation of peptidoglycan synthesis to bacterial growth and morphology. *Nat Rev Microbiol* **2012**, 10, 123–136
17. The peptidoglycan cell wall
[https://bio.libretexts.org/Bookshelves/Microbiology/Microbiology_\(Kaiser\)/Unit_1%3A_Introduction_to_Microbiology_and_Prokaryotic_Cell_Anatomy/2%3A_The_Prokaryotic_Cell_-_Bacteria/2.3%3A_The_Peptidoglycan_Cell_Wall](https://bio.libretexts.org/Bookshelves/Microbiology/Microbiology_(Kaiser)/Unit_1%3A_Introduction_to_Microbiology_and_Prokaryotic_Cell_Anatomy/2%3A_The_Prokaryotic_Cell_-_Bacteria/2.3%3A_The_Peptidoglycan_Cell_Wall)
18. Barreteau, H.; Kovac, A.; Boniface, A.; Sova, M.; Gobec, S.; Blanot, D., Cytoplasmic steps of peptidoglycan biosynthesis. *FEMS Microbiol Rev* **2008**, 32(2), 168-207.

19. van Heijenoort, J., Lipid intermediates in the biosynthesis of bacterial peptidoglycan. *Microbiology and Molecular Biology Reviews : MMBR* **2007**, *71* (4), 620-35
20. Vemula, H.; Ayon, N. J.; Gutheil, W. G., Cytoplasmic peptidoglycan intermediate levels in *Staphylococcus aureus*. *Biochimie* **2016**, *121*, 72-8.
21. Bertsche, U.; Breukink, E.; Kast, T.; Vollmer, W., In vitro murein peptidoglycan synthesis by dimers of the bifunctional transglycosylase-transpeptidase PBP1B from *Escherichia coli*. *The Journal of Biological Chemistry* **2005**, *280* (45), 38096-101.
22. Tenover, FC.; McDonald, LC., Vancomycin-resistant staphylococci and enterococci: epidemiology and control. *Curr Opin Infect Dis* **2005**, *18*(4), 300-5.
23. Bugg, TD.; Dutka-Malen, S.; Arthur, M.; Courvalin, P.; Walsh, CT., Identification of vancomycin resistance protein VanA as a D-alanine:D-alanine ligase of altered substrate specificity. *Biochemistry* **1991**, *30*(8), 2017-21.
24. Arthur, M.; Molinas, C.; Dutka-Malen, S.; Courvalin, P., Structural relationship between the vancomycin resistance protein VanH and 2-hydroxycarboxylic acid dehydrogenases. *Gene* **1991**, *103*(1), 133-4.
25. Guffey, AA.; Loll, PJ., Regulation of Resistance in Vancomycin-Resistant Enterococci: The VanRS Two-Component System. *Microorganisms* **2021**, *9*(10), 2026.
26. Périchon, B.; Courvalin, P., VanA-type vancomycin-resistant *Staphylococcus aureus*. *Antimicrob Agents Chemother* **2009**, *53*(11), 4580-7.
27. Li, G.; Walker, MJ.; De Oliveira, DMP., Vancomycin Resistance in *Enterococcus* and *Staphylococcus aureus*. *Microorganisms* **2023**, *11*(1), 24.
28. Thomson, JM.; Lamont, IL., Nucleoside Analogues as Antibacterial Agents. *Front Microbiol* **2019**, *10*, 952.

29. Tsakou, F.; Jersie-Christensen, R.; Jenssen, H.; Mojsoska, B., The Role of Proteomics in Bacterial Response to Antibiotics. *Pharmaceuticals (Basel)* **2020**,13(9), 214.
30. Amato, SM.; Fazen, CH.; Henry, TC.; Mok, WW.; Orman, MA.; Sandvik, EL.; Volzing, KG.; Brynildsen, MP., The role of metabolism in bacterial persistence. *Front Microbiol* **2014** 5, 70.
31. Zhao, YY.; Lin, RC., UPLC-MS(E) application in disease biomarker discovery: the discoveries in proteomics to metabolomics. *Chem Biol Interact* **2014**, 215, 7-16.
32. Wang, JL.; Hsueh, PR., Therapeutic options for infections due to vancomycin-resistant enterococci. *Expert Opin Pharmacother* **2009**, 10, 785-96.
33. Koomanachai, P.; Crandon, JL.; Nicolau, DP., Newer developments in the treatment of Gram-positive infections. *Expert Opin Pharmacother* **2009**, 10, 2829-43.
34. Rivera, AM.; Boucher, HW., Current concepts in antimicrobial therapy against select gram-positive organisms: methicillin-resistant *Staphylococcus aureus*, penicillin-resistant pneumococci, and vancomycin-resistant enterococci. *Mayo Clin Proc* **2011**, 86, 1230-43.
35. Arias, CA.; Murray, BE., The rise of the *Enterococcus*: beyond vancomycin resistance. *Nat Rev Microbiol* **2012**, 10, 266-78.
36. McKenna, M., Antibiotic resistance: the last resort. *Nature* **2013**, 499, 394-6.
37. Nikolaidis, I.; Favini-Stabile, S.; Dessen, A., Resistance to antibiotics targeted to the bacterial cell wall. *Protein Sci* **2014**, 23, 243-59.
38. Van Tyne, D.; Gilmore, MS., Friend turned foe: evolution of enterococcal virulence and antibiotic resistance. *Annu Rev Microbiol* **2014**, 68, 337-56.

39. Miller, WR.; Murray, BE.; Rice, LB.,; Arias, CA., Resistance in Vancomycin-Resistant Enterococci. *Infect Dis Clin North Am* **2020**, 34, 751-771.
40. Nieto, M.; Perkins, HR., Physicochemical properties of vancomycin and iodovancomycin and their complexes with diacetyl-L-lysyl-D-alanyl-D-alanine. *Biochem J* **1971**, 123, 773-87.
41. Barna, JC.; Williams, DH., The structure and mode of action of glycopeptide antibiotics of the vancomycin group. *Annu Rev Microbiol* **1984**, 38, 339-57.
42. Pootoolal, J.; Neu, J.; Wright, GD., Glycopeptide antibiotic resistance. *Annual Review of Pharmacology and Toxicology* **2002**, 42, 381-408.
43. Bugg, TD.; Wright, GD.; Dutka-Malen, S.; Arthur, M.; Courvalin, P.; Walsh, CT., Molecular basis for vancomycin resistance in *Enterococcus faecium* BM4147: biosynthesis of a depsipeptide peptidoglycan precursor by vancomycin resistance proteins VanH and VanA. *Biochemistry* **1991**, 30, 10408-15.
44. Billot-Klein, D.; Gutmann, L.; Collatz, E.; van Heijenoort, J., Analysis of peptidoglycan precursors in vancomycin-resistant enterococci. *Antimicrob Agents Chemother* **1992**, 36, 1487-90.
45. Handwerger, S.; Pucci, MJ.; Volk, KJ.; Liu, J.; Lee, MS., The cytoplasmic peptidoglycan precursor of vancomycin-resistant *Enterococcus faecalis* terminates in lactate. *J Bacteriol* **1992**, 174, 5982-4.
46. Courvalin, P., Vancomycin resistance in gram-positive cocci. *Clin Infect Dis* **2006**, 42 Suppl 1, S25-34.

47. Arthur, M.; Molinas, C.; Courvalin, P., Sequence of the vanY gene required for production of a vancomycin-inducible D,D-carboxypeptidase in *Enterococcus faecium* BM4147. *Gene* **1992**, 120, 111-4.
48. Wu, Z.; Wright, G.D.; Walsh, C.T., Overexpression, purification, and characterization of VanX, a D-, D-dipeptidase which is essential for vancomycin resistance in *Enterococcus faecium* BM4147. *Biochemistry* **1995**, 34, 2455-63.
49. Arthur, M.; Depardieu, F.; Cabanie, L.; Reynolds, P.; Courvalin, P., Requirement of the VanY and VanX D,D-peptidases for glycopeptide resistance in enterococci. *Mol Microbiol* **1998**, 30, 819-30.
50. Arthur, M.; Molinas, C.; Courvalin, P., The VanS-VanR two-component regulatory system controls synthesis of depsipeptide peptidoglycan precursors in *Enterococcus faecium* BM4147. *J Bacteriol* **1992**, 174, 2582-91.
51. Arthur, M.; Depardieu, F.; Molinas, C.; Reynolds, P.; Courvalin, P., The vanZ gene of Tn1546 from *Enterococcus faecium* BM4147 confers resistance to teicoplanin. *Gene* **1995**, 154, 87-92.
52. Arthur, M.; Depardieu, F.; Reynolds, P.; Courvalin, P., Quantitative analysis of the metabolism of soluble cytoplasmic peptidoglycan precursors of glycopeptide-resistant enterococci. *Mol Microbiol* **1996**, 21, 33-44.
53. Billot-Klein, D.; Shlaes, D.; Bryant, D.; Bell, D.; Legrand, R.; Gutmann, L.; van Heijenoort, J., Presence of UDP-N-acetylmuramyl-hexapeptides and -heptapeptides in enterococci and staphylococci after treatment with ramoplanin, tunicamycin, or vancomycin. *Journal of bacteriology* **1997**, 179, 4684-8.

54. Staudenbauer, W.; Strominger, J.L., Activation of D-aspartic acid for incorporation into peptidoglycan. *J Biol Chem* **1972**, 247, 5095-102.
55. Mainardi, J.L.; Legrand, R.; Arthur, M.; Schoot, B.; van Heijenoort, J.; Gutmann, L., Novel mechanism of beta-lactam resistance due to bypass of DD-transpeptidation in *Enterococcus faecium*. *J Biol Chem* **2000**, 275, 16490-6.
56. Ghuysen, J.M.; Bricas, E.; Leyh-Bouille, M.; Lache, M.; Shockman, G.D., The peptide N alpha-(L-alanyl-D-isoglutaminy)-N epsilon-(D-isoasparaginy)-L-lysyl-D-alanine and the disaccharide N-acetylglucosaminy-beta-1,4-N-acetylmuramic acid in cell wall peptidoglycan of *Streptococcus faecalis* strain ATCC 9790. *Biochemistry* **1967**, 6, 2607-19.
57. Vemula, H.; Bobba, S.; Putty, S.; Barbara, J.E.; Gutheil, W.G., Ion-pairing liquid chromatography-tandem mass spectrometry-based quantification of uridine diphosphate-linked intermediates in the *Staphylococcus aureus* cell wall biosynthesis pathway. *Anal Biochem* **2014**, 465, 12-9.
58. Vemula, H.; Ayon, N.J.; Burton, A.; Gutheil, W.G., Antibiotic Effects on Methicillin-Resistant *Staphylococcus aureus* Cytoplasmic Peptidoglycan Intermediate Levels and Evidence for Potential Metabolite Level Regulatory Loops. *Antimicrob Agents Chemother* **2017**, 61.
59. Jamindar, D.; Gutheil, W.G., A liquid chromatography-tandem mass spectrometry assay for Marfey's derivatives of L-Ala, D-Ala, and D-Ala-D-Ala: application to the in vivo confirmation of alanine racemase as the target of cycloserine in *Escherichia coli*. *Anal Biochem* **2010**, 396, 1-7.

60. Ayon, NJ.; Sharma, AD.; Gutheil, WG., LC-MS/MS-Based Separation and Quantification of Marfey's Reagent Derivatized Proteinogenic Amino Acid DL-Stereoisomers. *J Am Soc Mass Spectrom* **2019**, 30, 448-458.
61. Putty, S.; Vemula, H.; Bobba, S.; Gutheil, WG., A liquid chromatography-tandem mass spectrometry assay for D-Ala-D-Lac: a key intermediate for vancomycin resistance in vancomycin-resistant enterococci. *Anal Biochem* **2013**, 442, 166-71.
62. Wright, GD.; Molinas, C.; Arthur, M.; Courvalin, P.; Walsh, CT., Characterization of vanY, a DD-carboxypeptidase from vancomycin-resistant *Enterococcus faecium* BM4147. *Antimicrob Agents Chemother* **1992**, 36, 1514-8.
63. Panesso, D.; Abadia-Patino, L.; Vanegas, N.; Reynolds, PE.; Courvalin, P.; Arias, CA., Transcriptional analysis of the vanC cluster from *Enterococcus gallinarum* strains with constitutive and inducible vancomycin resistance. *Antimicrob Agents Chemother* **2005**, 49, 1060-6.
64. Qureshi, NK.; Yin, S.; Boyle-Vavra, S., The role of the Staphylococcal VraTSR regulatory system on vancomycin resistance and vanA operon expression in vancomycin-resistant *Staphylococcus aureus*. *PLoS One* **2014**, 9, e85873.
65. Bugg, TD.; Braddick, D.; Dowson, CG.; Roper, DI., Bacterial cell wall assembly: still an attractive antibacterial target. *Trends Biotechnol* **2011**, 29, 167-73.
66. Silver, LL., Viable screening targets related to the bacterial cell wall. *Ann N Y Acad Sci* **2013**, 1277, 29-53.

67. Barber, KE.; King, ST.; Stover, KR.; Pogue, JM., Therapeutic options for vancomycin-resistant enterococcal bacteremia. *Expert Rev Anti Infect Ther* **2015**, 13, 363-77.
68. De Oliveira, DMP.; Forde, BM.; Kidd, TJ.; Harris, PNA.; Schembri, MA.; Beatson, SA.; Paterson, DL.; Walker, MJ., Antimicrobial Resistance in ESKAPE Pathogens. *Clin Microbiol Rev* **2020**, 33.
69. Reynolds, PE.; Snaith, HA.; Maguire, AJ.; Dutka-Malen, S.; Courvalin, P., Analysis of peptidoglycan precursors in vancomycin-resistant *Enterococcus gallinarum* BM4174. *Biochem J* **1994**, 301 (Pt 1), 5-8.
70. Patel R, Uhl JR, Kohner P, Hopkins MK, Cockerill FR, Multiplex PCR detection of vanA, vanB, vanC-1, and vanC-2/3 genes in enterococci. *J Clin Microbiol* **1997** 35, 703-7.
71. Wong, ML.; Medrano, JF., Real-time PCR for mRNA quantitation. *Biotechniques* **2005**, 39, 75-85
72. Lee, A.; de Lencastre, H.; Garau, J. et al. Methicillin-resistant *Staphylococcus aureus*. *Nat Rev Dis Primers* **2018**, 4, 18033
73. Wertheim, H. F. et al. The role of nasal carriage in *Staphylococcus aureus* infections. *Lancet Infect. Dis.* **2005**, 5, 751–762
74. Becker, K. et al. *Staphylococcus aureus* from the German general population is highly diverse. *Int. J. Med. Microbiol* **2017**, 307, 21–27
75. Lowy, F. D. *Staphylococcus aureus* infections. *N. Engl J. Med.* **1998**, 339, 520–532
76. MRSA <https://www.cnn.com/2013/06/28/us/mrsa-fast-facts/index.html>

77. Kluytmans, J.; van Belkum, A.; Verbrugh, H., Nasal carriage of *Staphylococcus aureus*: epidemiology, underlying mechanisms, and associated risks. *Clin. Microbiol Rev* **1997**, *10*, 505–520
78. Sim, B. L.; McBryde, E.; Street, A. C.; Marshall, C., Multiple site surveillance cultures as a predictor of methicillin-resistant *Staphylococcus aureus* infections. *Infect. Control Hosp. Epidemiol* **2013**, *34*, 818–824
79. Eriksen, NH.; Espersen, F.; Rosdahl, VT.; Jensen, K., Carriage of *Staphylococcus aureus* among 104 healthy persons during a 19-month period. *Epidemiol. Infect* **1995**, *115*, 51–60
80. Boyle-Vavra, S. et al. USA300 and USA500 clonal lineages of *Staphylococcus aureus* do not produce a capsular polysaccharide due to conserved mutations in the cap5 locus. *mBio* **2015**, *6*, e02585–14
81. Foster, TJ.; Geoghegan, J A.; Ganesh, VK.; Hook, M., Adhesion, invasion and evasion: the many functions of the surface proteins of *Staphylococcus aureus*. *Nat. Rev. Microbiol* **2014**, *12*, 49–62
82. Spaan, AN.; Surewaard, BG.; Nijland, R.; van Strijp, JA., Neutrophils versus *Staphylococcus aureus*: a biological tug of war. *Annu. Rev. Microbiol* **2013**, *67*, 629–650
83. Thomer, L.; Schneewind, O.; Missiakas, D., Pathogenesis of *Staphylococcus aureus* bloodstream infections. *Annu. Rev. Pathol* **2016**, *11*, 343–364
84. Hassanzadeh, S.; Ganjloo, S.; Pourmand, MR.; Mashhadi, R.; Ghazvini, K., Epidemiology of efflux pumps genes mediating resistance among *Staphylococcus aureus*; A systematic review. *Microb Pathog* **2020**, *139*, 103850.
85. Wright, G. D., Q&A: Antibiotic resistance: where does it come from and what can we do about it? *BMC Biol* **2010**, *8*, 123

86. Payne, D.; Gwynn, M.; Holmes, D. et al., Drugs for bad bugs: confronting the challenges of antibacterial discovery. *Nat Rev Drug Discov* **2007**, 6, 29–40
87. Schatz, A.; Bugie, E.; Waksman, SA., Streptomycin reported. *Ann Intern Med* **1973**, 79: 678.
88. Bush, K., Antibacterial drug discovery in the 21st century. *Clin Microbiol Infect* **2004**, 10 Suppl, 4, 10-7.
89. Ventola, CL.; The antibiotic resistance crisis: part 1: causes and threats. *P T*. **2015**, 40(4), 277-83.
90. Drulis-Kawa, Z.; Maciejewska, B. Special Issue: “Bacteriophages and Biofilms”. *Viruses* **2021**, 13, 257.
91. Luepke, KH.; Suda, KJ.; Boucher, H.; Russo, RL.; Bonney, MW.; Hunt, TD.; Mohr, JF., Past, Present, and Future of Antibacterial Economics: Increasing Bacterial Resistance, Limited Antibiotic Pipeline, and Societal Implications. *Pharmacotherapy* **2017**, 37(1), 71-84.
92. Theuretzbacher, U.; Baraldi, E.; Ciabuschi, F.; Callegari, S., Challenges and shortcomings of antibacterial discovery projects. *Clin Microbiol Infect* **2022**, 8, S1198-743X (22)00600-0.
93. Piddock, LJ., The crisis of no new antibiotics—what is the way forward? *Lancet Infect Dis* **2012**, 12(3), 249–253.
94. Gould, IM.; Bal, AM., New antibiotic agents in the pipeline and how they can overcome microbial resistance. *Virulence* **2013**, 4(2), 185–191.
95. Sengupta, S.; Chattopadhyay, MK.; Grossart, HP., The multifaceted roles of antibiotics and antibiotic resistance in nature. *Front Microbiol* **2013**, 4:47.

96. Spellberg, B.; Gilbert, DN., The future of antibiotics and resistance: a tribute to a career of leadership by John Bartlett. *Clin Infect Dis* **2014**, 59 (suppl 2), S71–S75.
97. Brown, E.; Wright, G., Antibacterial drug discovery in the resistance era. *Nature* **2016**, 529, 336–343
98. Finley, RL. et al., The scourge of antibiotic resistance: the important role of the environment. *Clin. Infect. Dis* **2013**, 57, 704–710
99. Forsberg, KJ. et al. The shared antibiotic resistome of soil bacteria and human pathogens. *Science* **2012**, 337, 1107–1111
100. Szymański, P.; Markowicz, M.; Mikiciuk-Olasik, E., Adaptation of high-throughput screening in drug discovery-toxicological screening tests. *Int J Mol Sci* **2012**, 13(1), 427-52.
101. Mayr, LM.; Fuerst, P., The future of high-throughput screening. *J. Biomol. Screen* **2008**, 13, 443–448.
102. High-throughput Screening <https://multispaninc.com/articles/high-throughput-screening-done-right/>
103. Osakwe, O., Chapter 5 - The Significance of Discovery Screening and Structure Optimization Studies. In *Social Aspects of Drug Discovery, Development and Commercialization*, Osakwe, O.; Rizvi, S. A. A., Eds. *Academic Press: Boston* **2016**, pp 109-128.
104. Roberts, SA., Drug metabolism and pharmacokinetics in drug discovery. *Current Opinion in Drug Discovery & Development* **2003**, 6(1), 66-80
105. Eddershaw, Peter J.; Maurice, Dickins., "Advances in in vitro drug metabolism screening." *Pharmaceutical science & technology today* **1999**, 2.1, 13-19.

106. Wang, Disha.; Liu, Wenjun.; Shen, Zihao.; Jiang, Lei.; Wang, Jie.; Li, Shiliang.; Li, Honglin., Deep Learning Based Drug Metabolites Prediction. *Frontiers in Pharmacology* **2020**, 10. 10.3389
107. Dunn, WB.; Bailey, NJ.; Johnson, HE., Measuring the metabolome: current analytical technologies. *Analyst* **2005**, 130(5), 606–625
108. Wishart, DS.; Lewis, MJ.; Morrissey, JA et al., The human cerebrospinal fluid metabolome. *J. Chromatogr. B Analyt. Technol. Biomed. Life Sci* **2008**, 871(2), 164–173
109. Psychogios, N.; Hau, DD.; Peng, J et al., The human serum metabolome. *PLoS One* **2011**, 6(2), e16957
110. Wishart, DS., Advances in metabolite identification. *Bioanalysis* **2011**, 3(15), 1769-82.
111. Chen, Y.; Monshouwer, M.; Fitch, WL., Analytical tools and approaches for metabolite identification in early drug discovery. *Pharm Res* **2007**, 24(2), 248-57.
112. Sofia, Moco.; Jacques, Vervoort.; Sofia, Moco.; Raoul J. Bino.; Ric C.H. De Vos.; Raoul, Bino., Metabolomics technologies and metabolite identification, *TrAC Trends in Analytical Chemistry*, Volume 26, Issue 9, **2007**, Pages 855-866
113. Kowalska-Krochmal, B.; Dudek-Wicher, R., The Minimum Inhibitory Concentration of Antibiotics: Methods, Interpretation, Clinical Relevance. *Pathogens* **2021**, 4 10(2), 165.
114. Minimum inhibitory concentration <https://emerypharma.com/solutions/cell-microbiology-services/minimum-inhibitory-concentration/>
115. Greco, W. R.; Faessel, H.; and Levasseur, L., The search for cytotoxic synergy between anticancer agents: a case of Dorothy and the ruby slippers? *J. Natl. Cancer Inst.* **1996**, 88, 699–700

116. Foucquier, J.; and Guedj, M., Analysis of drug combinations: current methodological landscape. *Pharmacol. Res. Perspect.* **2015**, 3, e00149.
117. Greco, W. R.; Bravo, G.; and Parsons, J. C., The search for synergy: a critical review from a response surface perspective. *Pharmacol. Rev.* **1995**, 47, 331–385.
118. Tallarida, R. J., Drug synergism: its detection and applications. *J. Pharmacol. Exp. Ther* **2001**, 298, 865–872.
119. Caesar, Lindsay K.; Nadja B. Cech., “Synergy and antagonism in natural product extracts: when 1 + 1 does not equal 2.” *Natural product reports* **2019**, 869-888
120. Checkerboard assay <https://emerypharma.com/solutions/cell-microbiology-services/antimicrobial-synergy-study-checkerboard-testing/>
121. Wambaugh, MA.; Brown, JCS., High-throughput Identification of Synergistic Drug Combinations by the Overlap2 Method. *Journal of Visualized Experiments : Jove* **2018**, (135)
122. Grada, A.; Bunick, CG.; Spectrum of Antibiotic Activity and Its Relevance to the Microbiome. *JAMA Netw Open* **2021**, 4(4), e215357.
123. L. Barth Reller.; Melvin, Weinstein.; James H. Jorgensen.; Mary Jane Ferraro.; Antimicrobial Susceptibility Testing: A Review of General Principles and Contemporary Practices, *Clinical Infectious Diseases* **2009**, Pages 1749–1755,
124. Spectrum of activity figure <https://foamid.com/2018/03/26/antimicrobials-spectrum-of-activity/>
125. Qiyuan, Jin.; Xiaolu, Xie.; Yaxuan, Zhai.; Haifang, Zhang., Mechanisms of folate metabolism-related substances affecting *Staphylococcus aureus* infection, *International Journal of Medical Microbiology* **2023**, 151577, ISSN 1438-4221

126. Jin, Q.; Xie, X.; Zhai, Y.; Zhang, H., Mechanisms of folate metabolism-related substances affecting *Staphylococcus aureus* infection. *Int J Med Microbiol* **2023**, 313(2), 151577.
127. Zarou, M.M.; Vazquez, A.; Vignir Helgason, G., Folate metabolism: a re-emerging therapeutic target in haematological cancers. *Leukemia* **2021**, 35, 1539–1551
128. World Health Organization. Antimicrobial resistance: global report on surveillance **2014**, World Health Organization, Geneva, Switzerland.
129. Ventola, CL., The antibiotic resistance crisis: part 1: causes and threats **2015** P T 40, 277-83.
130. CDC. Antibiotic Resistance Threats in the United States, **2019**.
131. Brown, ED.; Wright, GD., Antibacterial drug discovery in the resistance era. *Nature* **2016**, 529, 336-43.
132. Butler, MS.; Blaskovich, MA.; Cooper, MA.; Antibiotics in the clinical pipeline at the end of 2015. *J Antibiot* **2017**, 70:3-24.
133. Teixeira, LM.; Carvalho, MDS.; Facklam, RR., Enterococcus. *Manual of Clinical Microbiology* **2007**, 9th Ed, 430-442.
134. Mancuso, G.; Midiri, A.; Gerace, E.; Biondo, C., Bacterial Antibiotic Resistance: The Most Critical Pathogens. *Pathogens* **2021**, 10.
135. Tacconelli, E.; Carrara, E.; Savoldi, A.; Harbarth, S.; Mendelson, M.; Monnet, DL.; Pulcini, C.; Kahlmeter, G.; Kluytmans, J.; Carmeli, Y.; Ouellette, M.; Outtersen, K.; Patel, J.; Cavaleri, M.; Cox, EM.; Houchens, CR.; Grayson, ML.; Hansen, P.; Singh, N.; Theuretzbacher, U.; Magrini, N., Discovery, research, and development of new antibiotics: the WHO priority list of antibiotic-resistant bacteria and tuberculosis. *Lancet Infect Dis* **2018**, 18, 318-327.

136. Payne, DJ.; Gwynn, MN.; Holmes, DJ.; Pompliano, DL., Drugs for bad bugs: confronting the challenges of antibacterial discovery. *Nat Rev Drug Discov* **2007**, 6, 29-40.
137. Tommasi, R.; Brown, DG.; Walkup, GK.; Manchester, JI.; Miller, AA., ESKAPEing the labyrinth of antibacterial discovery. *Nat Rev Drug Discov* **2015**, 14, 529-42.
138. Miro-Canturri, A.; Ayerbe-Algaba, R.; Smani, Y.; Drug Repurposing for the Treatment of Bacterial and Fungal Infections. *Front Microbiol* **2019**, 10:41.
139. Coates, ARM.; Hu, Y.; Holt, J.; Yeh, P., Antibiotic combination therapy against resistant bacterial infections: synergy, rejuvenation, and resistance reduction. *Expert Rev Anti Infect Ther* **2020**, 18, 5-15.
140. Ejim, L.; Farha, MA.; Falconer, SB.; Wildenhain, J.; Coombes, BK.; Tyers, M.; Brown, ED.; Wright, GD., Combinations of antibiotics and nonantibiotic drugs enhance antimicrobial efficacy. *Nat Chem Biol* **2011**, 7, 348-50.
141. Kang, MJ.; Song, WH.; Shim, BH.; Oh, SY.; Lee, HY.; Chung, EY.; Sohn, Y.; Lee, J., Pharmacologically active metabolites of currently marketed drugs: potential resources for new drug discovery and development. *Yakugaku Zasshi* **2010**, 130, 1325-37.
142. Obach, RS., Pharmacologically active drug metabolites: impact on drug discovery and pharmacotherapy. *Pharmacol Rev* **2013**, 65, 578-640.
143. Ayon, NJ.; Gutheil, WG., Dimensionally Enhanced Antibacterial Library Screening. *ACS Chem Biol* **2019**, 14, 2887-2894.
144. Campanini-Salinas, J.; Andrades-Lagos, J.; Mella-Raipan, J.; Vasquez-Velasquez, D., Novel Classes of Antibacterial Drugs in Clinical Development, a Hope in a Post-antibiotic Era. *Curr Top Med Chem* **2018**, 18, 1188-1202.

145. Baker, CN.; Tenover, FC., Evaluation of Alamar colorimetric broth microdilution susceptibility testing method for staphylococci and enterococci. *Journal of Clinical Microbiology* **1996**, 34, 2654.
146. Rampersad, SN., Multiple applications of Alamar Blue as an indicator of metabolic function and cellular health in cell viability bioassays. *Sensors (Basel)* **2012**, 12, 12347-60.
147. Tyc, O.; Tomás-Menor, L.; Garbeva, P.; Barraón-Catalán, E.; Micol, V., Validation of the AlamarBlue® Assay as a Fast-Screening Method to Determine the Antimicrobial Activity of Botanical Extracts. *PLOS ONE* **2016**, 11, e0169090.
148. Pillai, SK.; Moellering, RCJ.; Eliopoulos, GM., CHAPTER 9: Antimicrobial Combinations, p 365-440. In Lorian V (ed), Antibiotics in Laboratory Medicine Wolters Kluwer Health **2015**, Philadelphia, UNITED STATES.
149. Theuretzbacher, U.; Bush, K.; Harbarth, S.; Paul, M.; Rex, JH.; Tacconelli, E.; Thwaites, GE., Critical analysis of antibacterial agents in clinical development. *Nat Rev Microbiol* **2020**, 18, 286-298.
150. Paulin, S.; Alm, RA.; Beyer, P.; A novel pre-clinical antibacterial pipeline database. *PLoS One* **2020**, 15, e0236604.
151. Burki, TK., Development of new antibacterial agents: a sense of urgency needed. *Lancet Respir Med* **2021**, 9, e54.
152. Roemer, T.; Boone, C., Systems-level antimicrobial drug and drug synergy discovery. *Nat Chem Biol* **2013**, 9, 222-31.
153. Tyers, M.; Wright, GD., Drug combinations: a strategy to extend the life of antibiotics in the 21st century. *Nat Rev Microbiol* **2019**, 17, 141-155.

154. Macielag, MJ.; Demers, JP.; Fraga-Spano, SA.; Hlasta, DJ.; Johnson, SG.; Kanojia, RM.; Russell, RK.; Sui, Z.; Weidner-Wells, MA.; Werblood, H.; Foleno, BD.; Goldschmidt, RM.; Loeloff, MJ.; Webb, GC.; Barrett, JF., Substituted salicylanilides as inhibitors of two-component regulatory systems in bacteria. *J Med Chem* **1998**, 41, 2939-45.
155. Rajamuthiah, R.; Fuchs, BB.; Jayamani, E.; Kim, Y.; Larkins-Ford, J.; Conery, A.; Ausubel, FM.; Mylonakis, E., Whole animal automated platform for drug discovery against multi-drug resistant *Staphylococcus aureus*. *PLoS One* **2014**, 9, e89189.
156. Niu, H.; Yee, R.; Cui, P.; Tian, L.; Zhang, S.; Shi, W.; Sullivan, D.; Zhu, B.; Zhang, W.; Zhang, Y., Identification of Agents Active against Methicillin-Resistant *Staphylococcus aureus* USA300 from a Clinical Compound Library. *Pathogens* **2017**, 6.
157. Mohammad, H.; AbdelKhalek, A.; Abutaleb, NS.; Seleem, MN., Repurposing niclosamide for intestinal decolonization of vancomycin-resistant enterococci. *Int J Antimicrob Agents* **2018**, 51, 897-904.
158. Jordheim, LP.; Ben Larbi, S.; Fendrich, O.; Ducrot, C.; Bergeron, E.; Dumontet, C.; Freney, J.; Doleans-Jordheim, A.; Gemcitabine is active against clinical multiresistant *Staphylococcus aureus* strains and is synergistic with gentamicin. *Int J Antimicrob Agents* **2012**, 39, 444-7.
159. Sandrini, MP.; Shannon, O.; Clausen, AR.; Bjorck, L.; Piskur, J., Deoxyribonucleoside kinases activate nucleoside antibiotics in severely pathogenic bacteria. *Antimicrob Agents Chemother* **2007**, 51, 2726-32.
160. Haseltine, WA.; Block, R.; Synthesis of guanosine tetra- and pentaphosphate requires the presence of a codon-specific, uncharged transfer ribonucleic acid in the acceptor site of ribosomes. *Proc Natl Acad Sci U S A* **1973**, 70, 1564-8.

161. Abranches, J.; Martinez, AR.; Kajfasz, JK.; Chávez, V.; Garsin, DA.; Lemos, JA., The molecular alarmone (p)ppGpp mediates stress responses, vancomycin tolerance, and virulence in *Enterococcus faecalis*. *J Bacteriology* **2009**, 191, 2248-56.
162. Gargvanshi, S.; Vemula, H.; Gutheil, WG., Effect of Vancomycin on Cytoplasmic Peptidoglycan Intermediates and van Operon mRNA Levels in VanA-Type Vancomycin-Resistant *Enterococcus faecium*. *J Bacteriology* **2021**, 203, e0023021.
163. Klein, EY.; Jiang, W.; Mojica, N.; Tseng, KK.; McNeill, R.; Cosgrove, SE.; Perl, TM., National Costs Associated With Methicillin-Susceptible and Methicillin-Resistant *Staphylococcus aureus* Hospitalizations in the United States, 2010-2014. *Clin Infect Dis* **2019**, 68, 22-28.
164. Zhen, X.; Lundborg, CS.; Sun, X.; Hu, X.; Dong, H., Economic burden of antibiotic resistance in ESKAPE organisms: a systematic review. *Antimicrob Resist Infect Control* **2019**, 8, 137.
165. Turner, NA.; Sharma-Kuinkel, BK.; Maskarinec, SA.; Eichenberger, EM.; Shah, PP.; Carugati, M.; Holland, TL.; Fowler, VG, Jr., Methicillin-resistant *Staphylococcus aureus*: an overview of basic and clinical research. *Nat Rev Microbiol* **2019**, 17, 203-218.
166. Dandapani, S.; Rosse, G.; Southall, N.; Salvino, JM.; Thomas, CJ., Selecting, Acquiring, and Using Small Molecule Libraries for High-Throughput Screening. *Curr Protoc Mol Biol* **2012**, 4, 177-191.
167. Worthington, RJ.; Melander, C., Combination approaches to combat multidrug-resistant bacteria. *Trends Biotechnol* 2013, 31, 177-84.
168. Silver, LL., Challenges of antibacterial discovery. *Clin Microbiol Rev* **2011**, 24, 71-109.

169. da Cunha, BR.; Zoio, P.; Fonseca, LP.; Calado, CRC., Technologies for High-Throughput Identification of Antibiotic Mechanism of Action. *Antibiotics* **2021**, (Basel, Switzerland) 10, 565.
170. Stokes, A.; Lacey, RW., Effect of thymidine on activity of trimethoprim and sulphamethoxazole. *J Clin Pathol* **1978**, 31, 165-71.
171. Gargvanshi, S.; Gutheil, WG., Library Screening for Synergistic Combinations of FDA-Approved Drugs and Metabolites with Vancomycin against VanA-Type Vancomycin-Resistant *Enterococcus faecium*. *Microbiol Spectr* **2022**
172. Gormley, NA.; Orphanides, G.; Meyer, A.; Cullis, PM.; Maxwell, A., The interaction of coumarin antibiotics with fragments of DNA gyrase B protein. *Biochemistry* **1996**, 35, 5083-92.
173. Keller, S.; Pojer, F.; Heide, L.; Lawson, DM., Crystallization and preliminary X-ray analysis of the aromatic prenyltransferase CloQ from the clorobiocin biosynthetic cluster of *Streptomyces roseochromogenes*. *Acta Crystallogr Sect F Struct Biol Cryst Commun* **2006**, 62, 1153-5.
174. Maley, AM.; Arbiser, JL., Gentian violet: a 19th century drug re-emerges in the 21st century. *Exp Dermatol* **2013**, 22, 775-80.
175. Komiyama, K.; Edanami, K.; Tanoh, A.; Yamamoto, H.; Umezawa, I., Studies on the biological activity of stubomycin. *J Antibiot* **1983**, 36, 301-11.
176. Umezawa, I.; Takeshima, H.; Komiyama, K.; Koh, Y.; Yamamoto, H.; Kawaguchi, M., A new antitumor antibiotic, stubomycin. *J Antibiot* **1981**, 34, 259-65.
177. Morrow, TO.; Harmon, SA., Genetic analysis of *Staphylococcus aureus* RNA polymerase mutants. *J Bacteriol* **1979**, 137, 374-83.

178. Blaskovich, MA.; Zuegg, J.; Elliott, AG.; Cooper, MA., Helping Chemists Discover New Antibiotics. *ACS Infect Dis* **2015**, 1, 285-7.
179. Padilla-Montaña, N.; de León Guerra, L.; Moujir, L., Antimicrobial Activity and Mode of Action of Celastrol, a Nortriterpen Quinone Isolated from Natural Sources. **2021**, *Foods* 10.
180. Iyer, VN.; Szybalski, W., MITOMYCINS AND PORFIROMYCIN: CHEMICAL MECHANISM OF ACTIVATION AND CROSS-LINKING OF DNA. *Science* **1964**, 145, 55-8.
181. Chan, PF.; Srikanthasan, V.; Huang, J.; Cui, H.; Fosberry, AP.; Gu, M.; Hann, MM.; Hibbs, M.; Homes, P.; Ingraham, K.; Pizzollo, J.; Shen, C.; Shillings, AJ.; Spitzfaden, CE.; Tanner, R.; Theobald, AJ.; Stavenger, RA.; Bax, BD.; Gwynn, MN., Structural basis of DNA gyrase inhibition by antibacterial QPT-1, anticancer drug etoposide and moxifloxacin. *Nat Commun* **2015**, 6, 10048.
182. Spitzer, M.; Robbins, N.; Wright, GD., Combinatorial strategies for combating invasive fungal infections. *Virulence* **2017**, 8, 169-185.
183. Köck, R.; Becker, K.; Cookson, B.; van Gemert-Pijnen, JE.; Harbarth, S.; Kluytmans, J.; Mielke, M.; Peters, G.; Skov, RL.; Struelens, MJ.; Tacconelli, E.; Witte, W.; Friedrich, AW., Systematic literature analysis and review of targeted preventive measures to limit healthcare-associated infections by methicillin-resistant *Staphylococcus aureus*. *Euro Surveill* **2014**, 19, pii20860.
184. Sievert, DM.; Ricks, P.; Edwards, JR.; Schneider, A.; Patel, J.; Srinivasan, A.; Kallen, A.; Limbago, B.; Fridkin, S., National Healthcare Safety Network (NHSN) Team and Participating NHSN Families. Antimicrobial-resistant pathogens associated with

- healthcare-associated infections: summary of data reported to the National Healthcare Safety Network at the Centers for Disease Control and Prevention, 2009–2010. *Infect Control Hosp Epidemiol* **2013**, 34, 1–14.
185. Hill, EE.; Herijgers, P.; Claus, P.; Vanderschueren, S.; Herregods, MC.; Peetermans, WE., Infective endocarditis: changing epidemiology and predictors of 6-month mortality: a prospective cohort study. *Eur Heart J* **2007**, 28, 196–203.
186. Wang, JS.; Muzevich, K.; Edmond, MB.; Bearman, G.; Stevens, MP., Central nervous system infections due to vancomycin-resistant enterococci: case series and review of the literature. *Int J Infect Dis* **2014**, 25, 26–31.
187. DiazGranados, CA.; Zimmer, SM.; Klein, M.; Jernigan, JA., Comparison of mortality associated with vancomycin-resistant and vancomycin-susceptible enterococcal bloodstream infections: a meta-analysis. *Clin Infect Dis* **2005**, 41, 327–333.
188. Leclercq, R.; Derlot, E.; Duval, J.; Courvalin, P., Plasmid-mediated resistance to vancomycin and teicoplanin in *Enterococcus faecium*. *N Engl J Med* **1988**, 319, 157–161.
189. Frieden, TR.; Munsiff, SS.; Low, DE.; Willey, BM.; Williams, G.; Faur, Y.; Eisner, W.; Warren, S.; Kreiswirth, B., Emergence of vancomycin-resistant enterococci in New York City. *Lancet* **1993**, 342, 76–79.
190. Centers for Disease Control and Prevention. Antibiotic resistance threats in the United States, Centers for Disease Control and Prevention **2013**, Atlanta, GA
191. Jones, KE.; Patel, NG.; Levy, MA.; Storeygard, A.; Balk, D.; Gittleman, JL.; Daszak, P., Global trends in emerging infectious diseases. *Nature* **2008**, 451, 990–3

192. Boucher, HW.; Talbot, GH.; Bradley, JS.; Edwards, JE.; Gilbert, D.; Rice, LB.; Scheld, M.; Spellberg, B.; Bartlett, J., Bad bugs, no drugs: no ESKAPE! An update from the Infectious Diseases Society of America. *Clin Infect Dis* **2009**, 48, 1–12.
193. Spellberg, B., The future of antibiotics. *Crit Care*. **2014**, 18, 228–35.
194. Wright, GD., The antibiotic resistome: the nexus of chemical and genetic diversity. *Nat Rev Microbiol* **2007**, 5, 175–86.
195. Walsh, C., Molecular mechanisms that confer antibacterial drug resistance. *Nature* **2000**, 406, 775–81.
196. Kohanski, MA.; Dwyer, DJ.; Hayete, B.; Lawrence, CA.; Collins, JJ., A common mechanism of cellular death induced by bactericidal antibiotics. *Cell* **2007**, 130, 797–810.
197. Kahne, D.; Leimkuhler, C.; Lu, W.; Walsh, C., Glycopeptide and lipoglycopeptide antibiotics. *Chem Rev.* **2005**, 105, 425–48.
198. Reynolds, PE., Structure, biochemistry and mechanism of action of glycopeptide antibiotics. *Eur J Clin Microbiol Infect Dis.* **1989**, 8, 943–50.
199. Džidic, S.; Šuškovc, J.; Kos, B., Antibiotic resistance mechanisms in bacteria: Biochemical and genetic aspects. *Food Technol Biotechnol* **2008**, 46, 11–21
200. Kapoor, G.; Saigal, S.; Elongavan, A., Action and resistance mechanisms of antibiotics: A guide for clinicians. *J Anaesthesiol Clin Pharmacol* **2017**, 33(3), 300-305.
201. Bbosa, G.; Mwebaza, N.; Odda, J.; Kyegombe, D.; Ntale, M.; Antibiotics/antibacterial drug use, their marketing and promotion during the post-antibiotic golden age and their role in emergence of bacterial resistance. *Health* 2014, **6**, 410-425.
202. Yoneyama, H.; Katsumata, R., Antibiotic resistance in bacteria and its future for novel antibiotic development. *Biosci Biotechnol Biochem* **2006**, 70, 1060–75.

203. Wise, R., A review of the mechanisms of action and resistance of antimicrobial agents. *Can Respir J.* **1999**, 6(Suppl A), 20A–2A.
204. Vannuffel, P.; Cocito, C., Mechanism of action of streptogramins and macrolides. *Drugs* **1996**, 51(Suppl 1), 20–30.
205. Lambert, PA., Bacterial resistance to antibiotics: Modified target sites. *Adv Drug Deliv Rev* **2005**, 57, 1471–85.
206. Bozdogan, B.; Appelbaum, PC., Oxazolidinones: Activity, mode of action, and mechanism of resistance. *Int J Antimicrob Agents* **2004**, 23, 113–9.
207. Higgins, PG.; Fluit, AC.; Schmitz, FJ., Fluoroquinolones: Structure and target sites. *Curr Drug Targets* **2003**, 4, 181–90.
- 208.** Jeremy W. Dale.; Simon F. Park., Molecular Genetics of Bacteria, 5 th edition. A John Wiley & Sons, Ltd., Publication **2010**
- 209.** Textbook of Industrial Microbiology, 2nd edition (Biotechnology) by W. Cruger and A. Cruger, Sinauer Associates, Sunderland, US, **2004**
210. Schofield, M.J.; Hsieh, P., DNA mismatch repair: molecular mechanisms and biological function. *Annu Rev Microbiol* **2003**, 57, 579–608
211. Sridhar Rao. PN., *Bacterial genetics* **2006**. <http://www.microrao.com>
212. Resistance through chromosomal mutation
<https://www.futurelearn.com/info/courses/introduction-to-bacterial-genomics/0/steps/45330>
213. Wong, H.; Eso, K.; Ip, A.; Jones, J.; Kwon, Y.; Powelson, S.; de Grood, J.; Geransar, R.; Santana, M.; Joffe, AM.; Taylor, G.; Missaghi, B.; Pearce, C.; Ghali, WA.; Conly, J., Use

- of ward closure to control outbreaks among hospitalized patients in acute care settings: a systematic review. *Syst Rev* **2015**, 4, 152.
214. D, Walker.; T, Fowler (Eds.), Annual Report of the Chief Medical Officer. Volume II: Infections and the Rise of Antibiotic Resistance, *The Stationery Office* **2011**
215. Claudio U, Köser.; Matthew J, Ellington.; Sharon J, Peacock., Whole-genome sequencing to control antimicrobial resistance, *Trends in Genetics*, Volume 30, Issue 9, **2014**, Pages 401-407,
216. Microbial genome databases <https://www.atcc.org/resources/application-notes/microbial-genome-databases#fig1>
217. Whole genome Sequencing <https://www.cdc.gov/pulsenet/pathogens/wgs.html>
218. CHAFFEY N. Alberts, B.; Johnson, A.; Lewis, J.; Raff, M.; Roberts, K.; Walter, P., Molecular biology of the cell. 4th edn. *Ann Bot.* **2003**, 91(3), 401.
219. Barrick, J.; Lenski, R., Genome dynamics during experimental evolution. *Nat Rev Genet* **2013**, 827–839
220. Thomas, CM.; Nielsen, KM., Mechanisms of, and barriers to, horizontal gene transfer between bacteria. *Nat Rev Microbiol.* **2005**, 3(9), 711-21.
221. Browning, D. F.; Busby, SJW., Local and global regulation of transcription initiation in bacteria. *Nature Reviews Microbiology* **2016**, 14(10), 638-650.
222. Storz, G.; Vogel, J.; Wassarman, KM., Regulation by small RNAs in bacteria: Expanding frontiers. *Molecular Cell* **2011**, 43(6), 880-891.
223. Sharma, C. M.; Vogel, J., Differential RNA-seq: The approach behind and the biological insight gained. *Current Opinion in Microbiology* **2014**, 19, 97-105.

224. Gourse, R. L.; Gaal, T.; Bartlett, MS.; Appleman, JA.; Ross, W., rRNA transcription and growth rate-dependent regulation of ribosome synthesis in *Escherichia coli*. *Annual Review of Microbiology* **1996**, 50, 645-677.
225. Pillai, S.K.; Moellering, RC.; Eliopoulos, GM., Antimicrobial Combinations. In: Lorian, V., Ed., *Antibiotics in Laboratory Medicine* **2005**, 5th Edition, the Lippincott Williams & Wilkins Co., Philadelphia, 365-440.
226. Drawz, SM.; Bonomo, RA., Three decades of beta-lactamase inhibitors. *Clin Microbiol Rev* **2010**, (1), 160-201.
227. Eliopoulos, G.; Moellering Jr, RC., Antimicrobial Combinations. In: Lorian, V., Ed., *Antibiotics in Laboratory Medicine* **1996**, the Williams & Wilkins Co., Baltimore, 330-396.
228. Kollef, M., Appropriate empirical antibacterial therapy for nosocomial infections: getting it right the first time. *Drugs* **2003**, 63(20), 2157-68.
229. Rasko, DA.; Sperandio, V., Anti-virulence strategies to combat bacteria-mediated disease. *Nat Rev Drug Discovery* **2010**, 9(2), 117-28.
230. Noble, S.; Goa, KL., Gemcitabine. A review of its pharmacology and clinical potential in non-small cell lung cancer and pancreatic cancer. *Drugs* **1997**, 54(3), 447-72.
231. Beloor, Suresh.; A, Rosani.; A, Wadhwa, R.; Rifampin. Treasure Island (FL): **2023**, PMID: 32491420.
232. Schwarz, S.; Kehrenberg, C.; Doublet, B.; Cloeckaert, A., Molecular basis of bacterial resistance to chloramphenicol and florfenicol. *FEMS Microbiol Rev.* **2004**, 28(5), 519-42.

233. O Leary, E.; Gasior, S.; McElnea, E., Closantel toxicity. *BMJ Case Rep* **2023**, 16(2), e249626.
234. Bloch, A.; Coutso Georgopoulos, C., Inhibition of protein synthesis by 5'-sulfamoyladenine. *Biochemistry* **1971**, 10(24), 4395-8.
235. Russell, AD., Types of antibiotics and synthetic antimicrobial agents. In: Denyer S. P., Hodges N. A. & German S. P. (eds.) *Hugo and Russell's pharmaceutical microbiology*. 7th Ed. Blackwell Science, UK **2004**, Pp. 152-186.
- 236.** Etebu, Ebimiewei.; I. Ariekpar., "Antibiotics: Classification and mechanisms of action with emphasis on molecular perspectives." **2016**
237. Walsh, C., Antibiotics: actions, origins, resistance. 1st Ed. ASM Press, Washington, DC **2003**, 345p.
238. Brooks, GF.; Butel, JS.; Morse, SA., Jawetz, Melnick and Adelberg's Medical Microbiology **2004**, 23rd Edition. McGraw Hill Companies, Singapore.
239. Calderon, CB.; Sabundayo, BP., Antimicrobial classifications: Drugs for bugs. In: Schwalbe R, Steele-Moore L & Goodwin AC (eds). Antimicrobial susceptibility testing protocols. CRC Press, Taylor and Frances group **2007**, ISBN 978-0-8247-4100-6.
240. van Hoek, AHAM.; Mevius, D.; Guerra, B.; Mullany, P.; Roberts, AP.; Aarts, HJM., Acquired antibiotic resistance genes: An overview. *Front. Microbiol* **2011**, 2:203
241. Frank, U.; Tacconelli, E., The Daschner Guide to In-Hospital Antibiotic Therapy. *European standards* **2012**
242. Adzitey, F., Antibiotic classes, and antibiotic susceptibility of bacterial isolates from selected poultry; a mini review. *World Vet. J.* **2015**, 5 (3), 36-41.

243. Talaro, KP.; Chess, B., Foundations in microbiology **2008**, 8th Ed. McGraw Hill, New York.
244. Madigan MT.; Martinko, JM., Brock biology of microorganisms. 11th edition. Pearson Prentice Hall Inc **2006**
245. Wright, G. D., Q & A: Antibiotic resistance: Where does it come from and what can we do about it? *BMC Biol.* **2010**, 8, 123.
246. Chopra, I.; Roberts, M., Tetracycline antibiotics: mode of action, applications, molecular biology, and epidemiology of bacterial resistance. *Microbiol Mol Biol Rev.* **2001**, 65(2), 232-60
247. Patel, RS.; Parmar, M., Doxycycline Hyclate, Treasure Island (FL): StatPearls Publishing; **2023** Jan—. PMID: 32310348.
248. Cooper, RD.; Snyder, NJ.; Zweifel, MJ.; Staszak, MA.; Wilkie, SC.; Nicas, TI., et al. Reductive alkylation of glycopeptide antibiotics: synthesis and antibacterial activity. *J Antibiot.* **1996**, 49(6), 575–581
249. Munch, D., Engels, I.; Muller, A.; Reder-Christ, K.; Falkenstein-Paul, H.; Bierbaum, G.; et al. Structural variations of the cell wall precursor lipid II and their influence on binding and activity of the lipoglycopeptide antibiotic oritavancin. *Antimicrob Agents Chemotherapy* **2015**, 59(2), 772–781
250. Brade, KD.; Rybak, JM.; Rybak, MJ., Oritavancin: A New Lipoglycopeptide Antibiotic in the Treatment of Gram-Positive Infections. *Infect Dis Ther.* **2016**, 5(1), 1-15.
251. Storm, DR., Mechanism of bacitracin action: a specific lipid-peptide interaction. *Ann N Y Acad Sci.* **1974**, 235(0), 387-98.

252. Goodwin, S.; McPherson, J.; McCombie, W., Coming of age: ten years of next-generation sequencing technologies. *Nat Rev Genet* **2016**, 17, 333–351
253. Janda, JM.; Abbott, SL., 16S rRNA gene sequencing for bacterial identification in the diagnostic laboratory: pluses, perils, and pitfalls. *J Clin Microbiol* **2007**, 45(9), 2761-4.
254. Köser, CU.; Ellington, MJ.; Cartwright, EJP.; Gillespie, SH.; Brown, NM.; Farrington, M, et al. Routine Use of Microbial Whole Genome Sequencing in Diagnostic and Public Health Microbiology. *PLoS Pathogens* **2012**, 8(8), e1002824.
255. Deng, W.; Lee, J.; Wang, H.; Miller, J.; Reik, A.; Gregory, PD.; Dean, A.; Blobel, GA., Controlling long-range genomic interactions at a native locus by targeted tethering of a looping factor. *Cell* **2012**, 149(6), 1233-44.
256. Davies, J E., Origins, acquisition and dissemination of antibiotic resistance determinants. *Ciba Found Symp.* **1997**, 207, 15–27.
257. Martinez, JL.; Baquero, F., Mutation frequencies and antibiotic resistance. *Antimicrob Agents Chemother.* **2000**, 44(7), 1771-7.
258. Min, S.; Ingraham, K.; Huang, J.; McCloskey, L.; Rilling, S.; Windau, A.; Pizzollo, J.; Butler, D.; Aubart, K.; Miller, LA.; Zalacain, M.; Holmes, DJ.; O'Dwyer, K., Frequency of Spontaneous Resistance to Peptide Deformylase Inhibitor GSK1322322 in *Haemophilus influenzae*, *Staphylococcus aureus*, *Streptococcus pyogenes*, and *Streptococcus pneumoniae*. *Antimicrob Agents Chemother.* **2015**, 59(8), 4644-52.
259. Baquero, MR.; Nilsson, AI.; Turrientes Mdel, C.; Sandvang, D.; Galán, JC.; Martínez, JL.; Frimodt-Møller, N.; Baquero, F.; Andersson, DI., Polymorphic mutation frequencies in *Escherichia coli*: emergence of weak mutators in clinical isolates. *J Bacteriol.* **2004**, 186(16), 5538-42.

260. Fricke, W.; Rasko, D., Bacterial genome sequencing in the clinic: bioinformatic challenges and solutions. *Nat Rev Genet* **2014**, 15, 49–55
261. Gautam, SS.; Kc, R.; Leong, KW.; Mac Aogáin, M.; O'Toole, RF., A step-by-step beginner's protocol for whole genome sequencing of human bacterial pathogens. *J Biol Methods* **2019**, 15, 6(1), e110.
262. Bacterial morphology <https://microbiologynote.com/structure-of-bacteria/>
263. Bacteria <https://my.clevelandclinic.org/health/articles/24494-bacteria>
264. Malanovic, N.; Lohner, K., Gram-positive bacterial cell envelopes: The impact on the activity of antimicrobial peptides. *Biochim Biophys Acta*. **2016**, 1858(5), 936-46.
265. Choo, EJ., Community-Associated Methicillin-Resistant *Staphylococcus aureus* in Nosocomial Infections. *Infect Chemother*. **2017**, 49(2), 158-159.
266. Di Stefano, A.; Scatà, M.; Vijayakumar, S.; Angione, C.; La Corte, A.; Liò, P., Social dynamics modeling of chrono-nutrition. *PLoS Comput Biol*. **2019**, 15(1), e1006714.
267. Dhanda, G.; Acharya, Y.; Haldar, J., Antibiotic Adjuvants: A Versatile Approach to Combat Antibiotic Resistance. *ACS Omega*. **2023**, 8(12), 10757-10783.

VITA

Shivani Gargvanshi was born on August 1, 1989 in Lucknow, India. She completed her Secondary and Higher Secondary School from Loreto convent (Lucknow, India) and City Montessori School (Lucknow, India) respectively. Later she obtained her Bachelor of Science and Master of Science degree, both from Banasthali University (Rajasthan, India). She worked as Project Fellow at CSIR-Central Drug Research Institute (CDRI) (Lucknow, India) for two and a half years. She also worked as Junior Research Fellow at International Center for Genetic Engineering and Biotechnology (ICGEB) (New-Delhi, India) for a year.

Shivani joined University of Missouri-Kansas City in Spring 2017 to pursue an interdisciplinary doctoral degree in Pharmaceutical Sciences and Chemistry in the laboratory of Professor William G. Gutheil, where she worked on liquid chromatography and mass spectrometry based analytical method development and chemical library screening for antibacterial drug discovery. She won numerous awards during her tenure at the UMKC including prestigious School of Graduate Studies Research Grant Award for academic years (2019, 2020, 2021 and 2022), Judith Hemberger Graduate Scholarship (2018 and 2020), Women's Council Graduate Assistance Fund Fellowship for academic years (2019, 2020, 2021 and 2022) and Somerset Graduate Scholarship (2021).

Shivani has authored/co-authored several peer reviewed research articles in reputed international journals. She has also presented her research in several international and national conferences. She has served as a Secretary and Vice-Chair of American Association of Pharmaceutical Scientists from 2017-2018 and 2018-2019 respectively. She has also served as a Vice-President of Pharmaceutical Sciences Graduate Student Association from 2019-2020. She also served as a President of Controlled Release Society from 2020-2021.

She is also an active member of American Association of Pharmaceutical Scientists and American Chemical Society. She has also been a member of American Society for Mass Spectrometry, American Society for Biochemistry and Molecular Biology, American Society for Microbiology, Pharmaceutical Science Graduate Student Association and Controlled Release Society.